UNIVERSITY OF THE WITWATERSRAND, JOHANNESBURG

School of CHEMISTRY

Design and Synthesis of Antifolates as Potential Antimalarial Agents

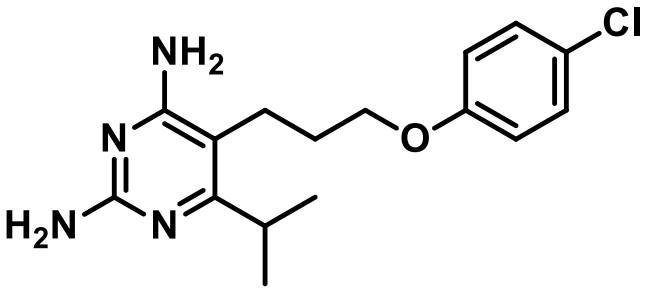

Kamogelo Butsi

A thesis submitted to the Faculty of Science,

University of the Witwatersrand,

Johannesburg

In fulfilment of the requirements of the degree of Doctor of Philosophy

Supervisor: Prof. Amanda Rousseau

Co-supervisor: Prof. Charles DeKoning

21 December 2022

Declaration

I declare that the work presented in this thesis was carried out exclusively by myself under the supervision of Prof. Amanda Rousseau and Prof. Charles DeKoning. It is being submitted for the degree of Doctor of Philosophy at the University of the Witwatersrand, Johannesburg. It has not been submitted before for any degree or examination in any other university.

Kamogelo Butsi

Abstract

Malaria still remains a life threatening disease in many parts of the world. According to the World Health Organisation (WHO) approximately 241 million cases of malaria were reported worldwide in 2020, with Africa being the most affected continent. Prevalence of the disease is attributed to the significant increase in resistance towards currently used chemotherapeutic agents. Therefore, the search for new antimalarial candidates is imperative. In this report, we give progress on the synthesis of novel 2,4-diaminopyrimidine derivatives and their respective activity against *Plasmodium falciparum*.

We have successfully developed a synthetic route towards flexible 2,4-diaminopyrimidine derivatives, which entails the synthesis of these target compounds in five steps starting from commercially available esters. The Sonogashira reaction was the key step employed to functionalise the iodinated pyrimidine ring at the 5-position with a suitable acetylene to form an alkyne intermediate. In this way, a four atom linker was introduced between the heterocyclic ring system and the terminal phenoxy ring. Reduction of the triple bond in the alkyne intermediate by a hydrogenation reaction afforded a library of the desired flexible 2,4-diaminopyrimidine analogues. Of the synthesised compounds, 15 were sent for activity assessment against both wild type and mutant *Pf*DHFR enzymes. They inhibited both *Pf*DHFR enzymes at low nanomolar concentrations. Additionally, these compounds were also tested against the human DHFR to evaluate their selectivity. All tested compounds were selective for *Pf*DHFR over human DHFR.

Further assessment on the antiplasmodial activity of these compounds were conducted *in vitro* in a whole cell *P*. *falciparum* assay against the drug sensitive TM4/8.2 strain and the multidrug resistant strain V1S. The tested compounds displayed moderate antiplasmodial activity in the micromolar range with IC_{50} values of 0.28 – 23.4 µM and 17.`6 – 64.0 µM against the drug sensitive strain and multidrug resistant strain, respectively. Unfortunately, they were mild to highly cytotoxic towards VERO cells. Further interrogation of the selectivity index (SI) indicated that the tested compounds did not display any selectivity for the plasmodial parasite over VERO cells.

Therefore, inhibition of the *Plasmodium* strains is not only due to compounds interacting with the parasite but also cytotoxicity of the compounds on the viability of erythrocyte.

Acknowledgements

I would like to extend my deepest gratitude to my Supervisor Prof. Amanda Rousseau. Your profound knowledge in the field of Medicinal Chemistry saw me through the toughest concepts of Biology to the tricky reactions of Organic Chemistry. Thank you for your immense faith in me; I would not have made it this far without your support and encouragement.

Secondly, I am most grateful to my co-supervisor Prof. Charles deKoning for the technical advices shared and financial support. I was truly privileged to have worked under your supervision.

I am grateful to have had the opportunity to work with an awesome team of supervisors in the organic group; Prof. Jo Michael, Prof. Dean Brady, Prof. Moira Bode, Dr. Kennedy Ngwira, and Dr. Memory Zimuwandeyi.

I am mostly indebted to Matthew Maree for joining in the research during the developmental stages of the synthetic route. Thank you for your hard work and diligence, I know for sure that your presence accelerated completion of this research.

I would also like to thank our collaborators at Biotech, Thailand, for conducting the enzymatic inhibitory tests and the antiplasmodial screening. A huge thank you to Eric Morifi and Refilwe Moepya for running the HRMS analysis.

A special thank you to Songeziwe Ntsimango, Nompumelelo Mathebula, Mudzuli Maphupha, dear friends I encountered during the course of this journey. Thank you for your support and input especially during times when reactions were not working. Thank you for your encouragement, I drew a lot of inspiration from you guys.

Thank you to the entire organic group, more especially Sandile, Alex, Bianca, Ntombi, Khonzi, Josephine, Bongi, Lebo and Kabelo it was pleasure working with you guys.

To my dear friends, Nomawabo Lolwana, Evah Phago, Malitsatsi Mnguni, Sivuyisiwe Jikele, Lebogang Mogaoatlhe, William Mokone, Rinae Tshikalake, Okuhle Dweba and Boitumelo Tshose, I am deeply grateful for your presence. Thank you for being there

during tough times and celebrating with me during my wins. Thank you all for your support and abundant love for me.

To my dear parents Josephine and Jacob Butsi, thank you for your unwavering love. I am greatly blessed to have been raised under your guidance and teachings. I am because of the many values you instilled in me. I love and appreciate you.

I would like to acknowledge my sisters, Otshepeng Butsi and Ikageng Butsi, thank you for always being there especially during times when I had to put in extra hours towards my research. It is because of your constant support that I get to relish in this achievement. Thank you so much for being my eternal best friends.

To my lovely kids Atlegang Machaba and Kopano Machaba, I love you so much. I hope this work inspires you to go after your wildest dreams.

To my dear husband Sello Machaba thank you so much for your constant and continued support. This was definitely a testing journey. I appreciate the compromises and sacrifices you made during this season. I am deeply grateful that I had you to remind me of my own strength, to inspire me during the lows of life, to cheer on during small victories and to hold my hand when I doubted myself. Thank you for your patience, for loving me through my mess, and for the constant affirmations of my greatness. I love you.

Psalm 107:1

Give thanks to the Lord for he is good! His faithful love endures forever.

Dedications

This Thesis is dedicated to my late aunt Julia Kgomotso Botsi and late grandmother Basadi Dorothy Moatshe.

To all the women who came before me, thank you!
You have crawled so I could fly.

Ke dikgakganthane tsa mmamasela
Kwena magadima ntweng ga ba ja ga ba gadimane.
Ke motho wa bophedi bokone ka borethe o tshwana le kgomo basadi b aka be ba bolawa.
Mmasisinyi lo seka la mmolaya
Go nne o re tsalla basadi ba matsele a kgapakgapa.
Ke gobane w abo kentse, a re ga gaatlala metsi, o tletse lefulo, banthelli ba ba ntshwara ba siya
Matlakala ke morothi a kgaka mebala ya serokane sa borena.
Ba Botsi ba re ga ba fitlha ntweng ba re iyo bag a etsho b aka.
Ba re phokwanen belebetsa re o lebele noka o kgaotse
Ke baja book ba potsane

Table of contents

Table of Abbreviations

2-Me THF	2-Methyltetrahydrofuran
ACT	Artemisinin-based combination therapy
ATP	Adenosine triphosphate
DHF	Dihydrofolate
DHFR	Dihydrofolate reductase
DHFS	Dihydrofolate synthase
DHNA	Dihydroneopterin aldose
DHNP	Dihydroneopterin triphosphate
DHPP	Dihydropterin pyrophosphine
DHPS	Dihydropteroate synthase
DIIPA	Diisopropylamine
DIPEA	Diisopropylethylamine
dTMP	Deoxythymidine monophosphate
dUMP	Deoxyuridine monophosphate
FPGS	Folypolyglutamate synthase
GTP	Guanosine triphosphate
GTPC	Guanosine triphosphate cyclohydrolase I
HMDP	2-Amino-4-hydroxy-6-hydroxymethyldihydropterin
HPPK	Hydroxymethyldihydropterin pyrophosphate

HRP2	Histidine-rich protein 2
IRS	Indoor residual spraying
ITNS	Insecticide treated mosquito nets
MTX	Methotrexate
pABA	*p*-Aminobenzoic acid
PCR	Polymerase chain reactions
Pf	*Plasmodium falciparum*
PfCRT	*P. falciparum* chloroquine resistance transporter
pLDH	Plasmodial lactate dehydrogenase
RDT	Rapid diagnostic tests
SMC	Seasonal malaria chemoprevention
TEA	Triethylamine
THF	Tetrahydrofolate
TMS acetylene	Trimethylsilylacetylene
TMT	Trimetrexate
TS	Thymidylase synthase

Table of Figures

Table of Schemes

1 CHAPTER 1: Introduction

Antifolates have sparked interest in medicinal chemistry due to their antiplasmodial activity. This class of chemotherapeutic agents act by inhibiting folate metabolism. Folate metabolism is a cascade of enzyme catalysed reactions that give rise to folate co-factors. These folate derivatives are essential for biosynthesis of amino acids and participate in one-carbon transfer reactions during DNA replication.[1] Inhibition of key enzymes in the "folate cycle" could potentially halt DNA replication, thereby causing cell arrest. Understanding the role of folate derivatives in living systems allows organic chemists to take advantage of their functional properties to identify key enzyme targets in biological systems and subsequently develop pharmaceutical drug candidates.[2]

1.1 Folate Metabolism

Folate cofactors are essential for cell survival. They are required for the biosynthesis of amino acids such as methionine and glycine.[1,3,4] They also play an essential role in the synthesis of nucleotides required for DNA replication. During DNA replication the folate cofactor tetrahydrofolate (THF) is involved in the transfer of a one-carbon methyl group that converts deoxyuridine monophosphate (dUMP) to deoxythymidine monophosphate (dTMP) by the enzyme thymidylate synthase.[5] The triphosphate derivative is utilised by DNA polymerase to add thymine ('T') nucleotides to growing DNA chains.[5] Furthermore, these folates play a fundamental role in the initiation of protein synthesis through formylation of methionine.[4] Rapidly growing cells such as the malaria causing parasite, *Plasmodium*, rely on the availability of folate derivatives for cell replication.

The purpose of the folate pathway is to provide folate cofactors for cellular metabolic processes mentioned above. Methods for obtaining these reduced folates differ between prokaryotes and eukaryotes. Plants and most microorganisms synthesise folates using the *de novo* pathway, whereas mammals cannot synthesise folates *de novo*.[6] Mammals obtain folate derivatives from their diet; and are able to recycle them *in vivo* via the folate salvage pathway. By comparison, the *protozoa* causing malaria synthesises reduced folates *de novo* from the simple precursors guanosine triphosphate (GTP), *p*-aminobenzoic acid (pABA) and L-glutamate which are

assembled into a structural conformation characteristic of folates (**Figure 1**). Folate cofactors are refered to as “conjugated” pterins because of the pterin moiety linked to *p*-aminobenzoate and glutamate. In addition to the *de novo* pathway, the parasite can exploit the host folate pathway and salvage folic acid from the host *in vivo*.[7,8]

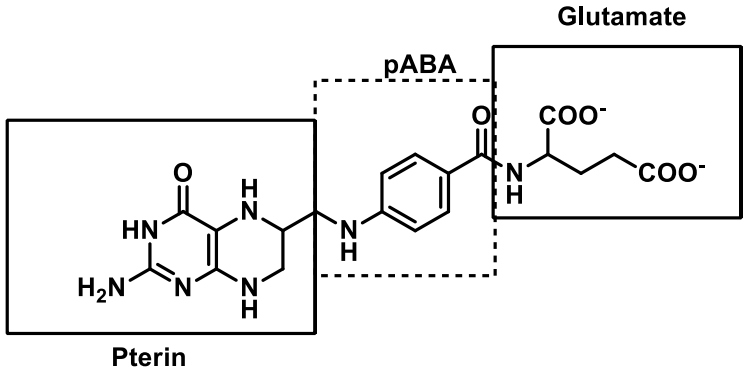

Figure 1. *Chemical structure of folate moiety*

The *de novo* synthesis of folates is initiated from GTP as depicted in **Figure 2**.[9] Conversion of GTP to dihydroneopterin triphosphate (DHNP) is facilitated by GTP cyclohydrolase I (GTPC), the first enzyme of the folate synthesis pathway,[6] which is available in both mammalian and microbial cells. Because of the absence of the necessary subsequent enzymes in the pathway, DHNP is not particularly used for folate production in mammalian cells but it serves as a precursor for the synthesis of neopterin and biopterin derivatives.[6,9] The triphosphate product of the GTPC reaction, DHNP, is then hydrolysed to the free hydroxyl form. This hydrolysis reaction has been postulated to involve a non-enzymatic loss of pyrophosphate followed by non-specific phosphatase activity that removes the third phosphate group.[6] The resulting substrate is converted to 2-amino-4-hydroxy-6-hydroxymethyldihydropterin (HMDP) in the presence of dihydroneopterin aldolase (DHNA).[6] Hydroxymethyldihydropterin pyrophosphokinase (HPPK) then catalyses the diphosphorylation of HMDP using adenosine triphosphate (ATP).[6,9] The activated pterin ring product of HPPK undergoes a condensation reaction with pABA to give dihydropteroate (DHP), catalysed by dihydropteroate synthase (DHPS). In turn, DHP is converted to DHF by adding an L-glutamate residue by dihydrofolate synthase (DHFS).[7] The final step is the NADPH-dependent reduction of DHF to THF, catalysed by dihydrofolate reductase (DHFR).[7] Production of each molecule of dTMP results in the oxidation of the THF molecule to DHF, which must be recycled by DHFR back to the THF form.[5]

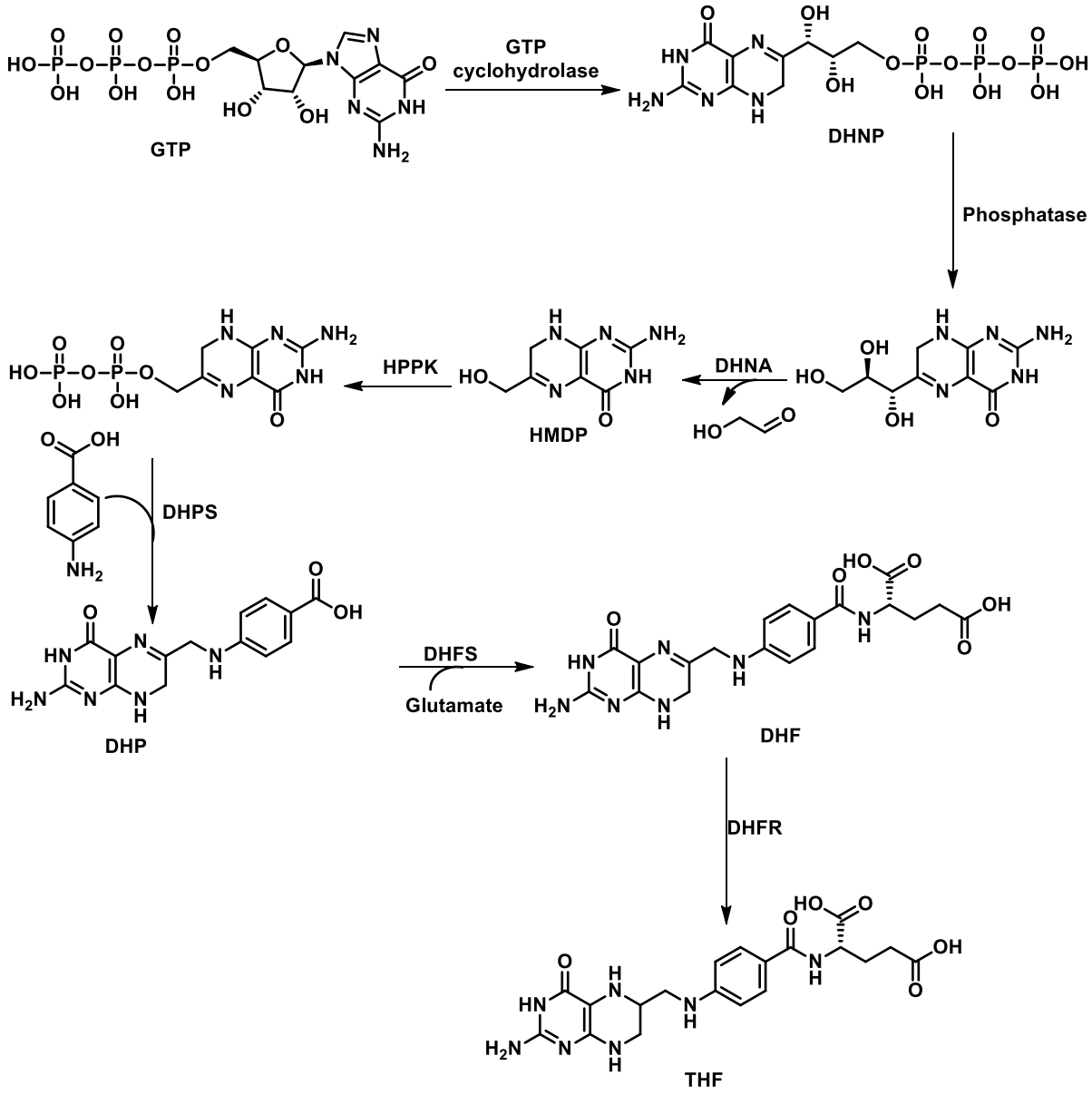

Figure 2. *Biosynthesis of THF from GTP via the de novo pathway*

Disruption of this pathway leads to critical deficiency of these key methyl activated folate cofactors, which subsequently impairs DNA replication and leads to cell death.[10] Several enzymes involved in folate metabolism have been explored as drug targets for chemotherapy purposes.[11] However, DHFR and DHPS are the only two enzymes validated as chemotherapeutic drug targets for malaria.[8,9]

1.1.1 Reasons why DHFR and DHPS are good drug targets for malaria

1.1.1.1 Dihydrofolate reductase

Fundamental metabolic roles played by DHFR, such as the synthesis of THF via the *de novo* pathway, have rendered the enzyme a desirable and successful drug target.[9] Inhibition of the enzyme leads to a deficiency in THF and therefore halts DNA synthesis, thereby arresting cell replication.[8] Not only does the enzyme catalyse the reduction of DHF to THF, but it also participates in the recycling of DHF resulting from the synthesis of dTMP and oxidised forms of folates salvaged from the host. Therefore, the enzyme is central to both the *de novo* and folate salvage pathways. Protein crystallography has provided vast information on the structure of DHFRs from human and protozoa. In comparison to microbial DHFRs, mammalian DHFRs are highly conserved and they have relatively larger active sites.[8,12,13] These structural differences in the microbial and host DHFR allows for the development of antifolates that selectively target the plasmodial DHFR. For instance, in the host both DHFR and thymidylase synthase (TS) are coded by separate genes, whereas the malaria parasites express a bifunctional DHFR-TS enzyme coded by a single gene.[5] The thymidylate cycle is the sole *de novo* pathway for the synthesis of dTMP. TS catalyses the reductive methylation of dUMP to dTMP, using N^5,N^{10}-methylene tetrahydrofolate as the one-carbon methyl donor.[4] TS is the only enzyme that causes oxidation of THF to DHF as its one-carbon fragment is lost. The DHF generated is then recycled and reduced by DHFR. Complete inhibition of TS leads to thymineless death.[5] Limited data is available on parasite TS as a potential drug target. However, plasmodial DHFR is a good target because it is limited in its mutational capacity, owing to loss in enzyme function.

1.1.1.2 Dihydropteroate synthase

DHPS is one of the key enzymes essential in the *de novo* pathway due to the role it plays in the production of reduced THF. It catalyses the condensation of pABA with dihydropterin pyrophosphate (DHPP) to afford DHP (**Figure 2**).[6] DHP is produced from a nucleophilic substitution reaction resulting in the formation of a C-N bond between the amino nitrogen of pABA and the carbon atom of DHPP. This condensation reaction has been shown to abide by the S_N1 reaction mechanism,[14] where the leaving group dissociates first from a molecule followed by a nucleophilic attack on the remaining

carbocation intermediate. During the enzyme-catalysed reaction to produce DHP, DHPP loses its pyrophosphate group, leaving a dihydropterin core as a cationic intermediate in the pterin-binding pocket. The cation-intermediate is susceptible to nucleophilic attack by pABA to produce DHP. As described, the plasmodium parasite can synthesise DHPP and pABA *de novo*. DHPP is synthesised via the diphosphorylation reaction catalysed by HPPK as shown in **Figure 2** and pABA is acquired from the shikimate pathway.[15] Analogous to folates, the parasite can also salvage pABA from the host plasma *in vivo*.[5] Understanding the mechanism of this metabolic reaction at a molecular level and how the substrates involved are obtained is essential for the development of chemotherapeutic drug targets. Currently used sulfa antifolates are structural analogues of pABA utilised to inhibit DHPS. Due to their structural similarities to pABA, the parasite utilises the salvage pathway to take up sulfa drugs from the host *in vivo*, which inhibits the S_N1 reaction from taking place, ultimately hindering the function of DHPS. The human host does not produce folate cofactors *de novo*, therefore, it does not have the enzyme DHPS, DHPS is unique to the parasitic cells. This feature makes it desirable as a drug target because it allows development of chemotherapeutic agents that are selective to the parasite and not the human host.

1.2 Malaria

Development of chemotherapeutic agents against malaria is important because it still remains a life threatening disease in many parts of the world. According to the World Health Organisation (WHO) approximately 241 million cases of malaria were reported worldwide in 2020, with Africa being the most affected continent, contributing 95% of the reported cases.[16] An estimated 627 000 deaths caused by the disease were reported globally, of which 602 000 (96%) deaths were accounted for in the WHO African regions. Since 2000 there has been a gradual decline in malaria deaths from an estimated 896 000 to 558 000 in 2019. The current malaria report indicates a 12% increment in the total number of estimated deaths observed from 2019 to 2020 in 85 malaria endemic countries.[16] The increase in mortality is partly due to the challenges imposed by the Covid-19 pandemic. Covid-19 is a disease caused by a novel coronavirus named severe acute respiratory syndrome coronavirus-2 (SARS-CoV-2, 2019-nCoV) as the virus primarily affects the respiratory system.[17] Since its first

detection in China (2019), the virus has rapidly spread worldwide and the WHO declared the disease a pandemic. To curb the transmission of the virus, many countries imposed strict Covid-19 regulations, some of which included a lockdown restricting movement of the general population and some economic activities. For the past three years, the health care system has been under enormous pressure to manage and mitigate the threat imposed by Covid-19 to the general well-being being of humanity. In malaria endemic countries the demands needed to treat and detect *Plasmodium* infection add to the burden caused by the disease. The imposed regulations have made it challenging to import and supply medications from manufacturing companies into endemic countries. One can appreciate the difficulties people had to endure to access treatment for malaria in their local health care facilities during this period.

The annual implementation of strategies employed to control the spread of the malaria parasite, such as insecticide-treated mosquito nets and indoor residual spraying, have also been significantly disturbed during the last two years.[16] Delivery and distribution of these services to many African endemic countries was not as effective in 2020 and this can be seen by the sharp increase in reported mortality rate. The financial burden that the public health care system of endemic countries has to carry also contribute to limitations in distribution and supply of medical services to treat and detect malaria. Medications to treat malaria are expensive for these countries,[18] particularly as the price of shipping and distribution has increased considerably due to increases in oil prices. It is clear that the pandemic disrupted strategies put in place to detect, control, treat and halt the spread of malaria, particularly in impoverished communities.

Although efforts made to eradicate malaria might currently seem bleak, there is still hope that the fight against the disease can be won. Between the year 2000 and 2020, 23 countries had achieved three consecutive years of zero indigenous malaria cases; 12 of the countries were certified malaria free by WHO.[16] China was certified malaria free in 2021 following 70 years of investment in the fight against malaria. From a country that reported 30 million cases annually in the 1940s; this is a great achievement.[19]

1.2.1 Life cycle of the malaria parasite

1.2.1.1 Transmission to man and human liver stage

Malaria is an infectious disease caused by parasitic protists of the genus *Plasmodium*. Currently the *Plasmodium* species known to cause malaria in humans include: *Plasmodium falciparum*, *P. vivax*, *P. malariae*, *P. knowlesi* and *P. ovale*. A female mosquito vector of the genus *Anopheles* facilitates transmission of human malaria. The complex lifecycle of the *Plasmodium* parasite involves two hosts, mosquito host (primary host), in which the parasite reproduce sexually, and the human host, in which the asexual stage takes place as shown in **Figure 3**.[20] Though the female *Anopheles* mosquito is considered the primary host by definition, in the context of this report it will be referred to as the vector, while the human host will be referred to as the host. There are three key stages in the parasite's life cycle: human liver stage, human blood stage and the mosquito stage. The human host acquires the parasite in the form of sporozoites from an infected mosquito while feeding.[21] The sporozoites enter the skin through inoculation and circulate the host bloodstream for approximately an hour before migrating to the liver where they invade hepatocytes and multiply into merozoites enclosed in a schizont.[22] The asexual multiplication of sporozoites in the liver stage is specifically known as exoerythrocytic schizogony.[23] The mechanism in which sporozoites invade hepatocytes is not clear and is still under investigation. From the multiple studies conducted to investigate the invasion, it is apparent that depending on the species, different modes of invasion are possible.[24] It has been suggested that a sporozoite glycoprotein, thrombospondin, binds to specific receptors on liver cells, i.e. the thrombospondin domain of the parasite binds to hepanan sulfate proteoglycans on hepatocytes.[24] This protein-receptor interaction facilitates the ultimate invasion of hepatocytes. The mature schizonts rupture hepatocytes and merozoites are released into the bloodstream. On the other hand, some *P. vivax* and *P.ovale* schizonts turn into hypnozoites, a form that can remain dormant in the liver for months or years. [22] The dormant hypnozoite liver stage can cause relapse in infected people.

1.2.1.2 Human blood cell stage

The merozoites released into the blood stream quickly invade erythrocytes. Masamichi Alkawa and colleagues investigated the mechanism of erythrocyte invasion by the *Plasmodium* parasite using electron microscopy.[25] The merozoites make contact with

the erythrocyte cell membranes at their apical end, and then create a junction with the cell membrane. They invade the erythrocyte cell membrane by inward budding into the cell enveloped in a vacuole. The vacuole originates from the host plasma membrane and it is formed as the merozoite enters the cell.[24] Once inside the erythrocytes, the merozoites undergo asexual multiplication to produce many individual merozoites. Asexual multiplication of merozoites in the blood stage is known as erythrocytic schizogony.[26] Upon rupture of the erythrocytes, merozoites are released into the blood stream where they infect other erythrocytes and can repeat the cycle indefinitely. This stage is responsible for the manifestation of malaria and coincide with malaria symptoms in the host.[27] During progression of the disease, other merozoites develop into female and male gametocytes taken up by the mosquito while feeding.

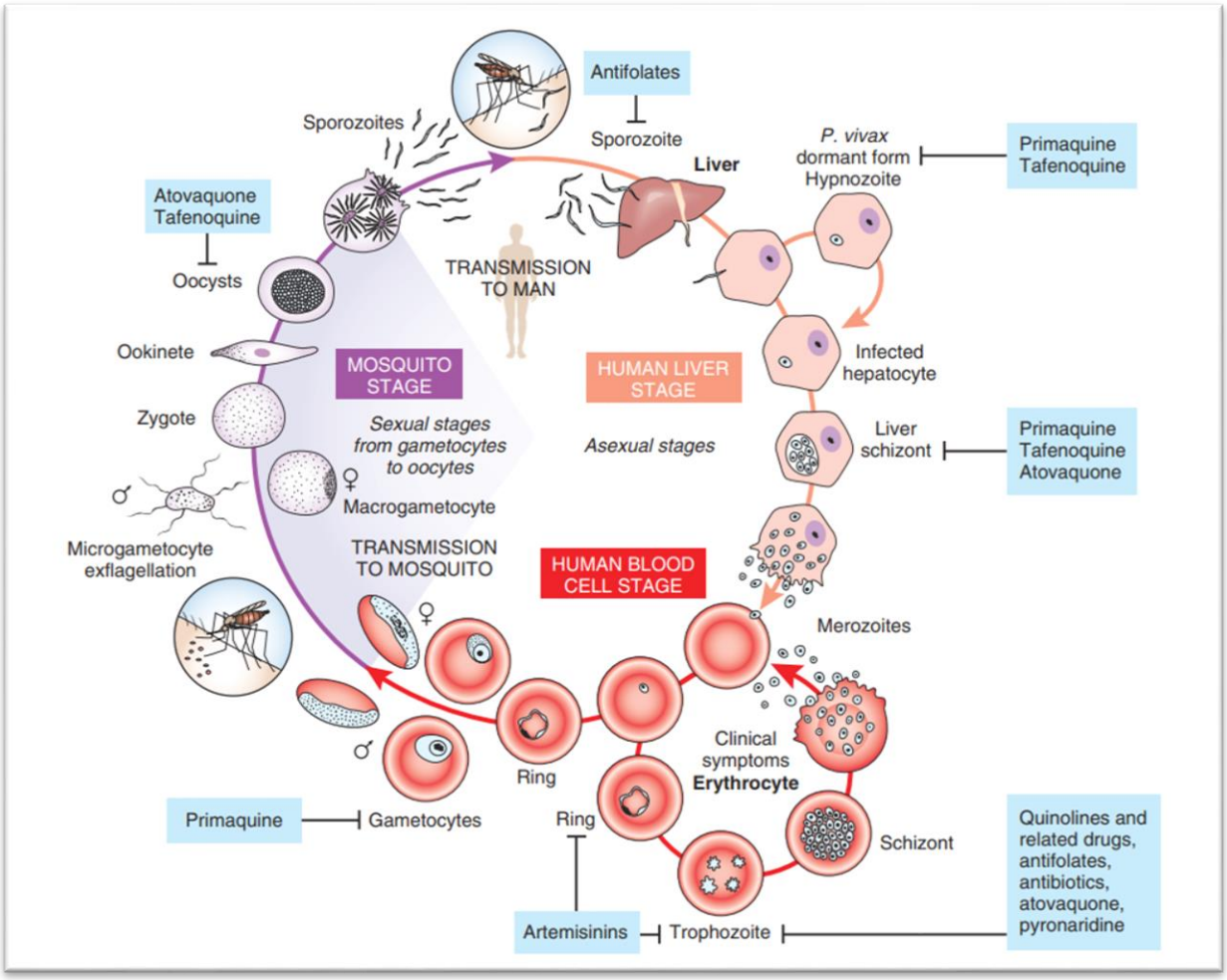

Figure 3. *Life cycle of Plasmodium falciparum and available antimalarial drugs currently used to target certain stages in the life cycle.*[28]

1.2.1.3 Mosquito stage

The gametocytes develop into mature gametes inside the midgut lumen of the insect. In fact, ingestion of gametocytes activates maturation of male and female gametogenesis. The male gametocytes undergo exflagellation, and fertilise mature female gametes, macrogametocytes, to produce a zygote.[29] Ookinetes develop from the zygote and transform into oocyst. The oocysts is the only developmental stage of the parasite that occurs extracellularly and results in the formation of sporozoites.[29] Mature sporozoites are released from the midgut into the body cavity of the mosquito and invade the salivary glands of the insect vector, and are therefore transmitted back to the human host during the next mosquito blood feed to continue the cycle.

1.3 Forms of human malaria

1.3.1 *Plasmodium malariae*

Malariae was the first *Plasmodium* species to be recognised as a cause of human malaria. A French army physician, Charles Louis Alphonse, described it in 1880 and it was named by Grassi and Feletti in 1890.[30,31] *P. malariae* has a worldwide distribution, with clinical cases detected in malaria endemic regions such as sub-Saharan Africa and Southwest Pacific.[32] However, low-level infections seem to be common especially in areas such as Asia, South America and Central America with detected infections hardly ever exceeding 1-2%.[32] Moreover, *P. malariae* prevalence in West Africa has been reported to peak in children under ten years of age. Although considered to cause mild infections, *P. malariae* causes quartan malaria in humans, a form of malaria where an onset of fever occurs at 3 day periods.[33] It is unique in that it establishes blood stage parasitemia at concentrations below the level of detection by light microscopy.[34] Without treatment, the parasite can go undetected in the host for extremely long periods before it manifests into malaria symptoms. Chronic *P. malariae* parasitemia can cause nephrotic syndrome, a kidney disorder that causes the body to excrete high protein content in urine.[35] The syndrome often occurs because of damage to microvasculature in the kidney that filters waste and excess water from the blood. Nephropathy syndrome associated with prolonged *P. malariae* parasitemia may be difficult to diagnose because of the low parasitemia giving negative rapid diagnostic test results.[34]

1.3.2 *Plasmodium vivax*

P. falciparum and *P. vivax* account for the majority of reported cases of malaria. *P. falciparum* is responsible for the high mortality rate, whereas *P. vivax* is the most wide spread of the malaria species and can cause severe and fatal infection.[36] *P. vivax* is the dominant species with relatively high prevalence in South East Asia and the Western Pacific region. The wide geographic distribution of this species of protozoa is due to its dormant liver stage, called the hypnozoite,[27] which allows *P. vivax* to survive for longer periods during cold climates where mosquito vectors are scarce for transmission and propagation of the parasite. Activation of the dormant liver stage weeks or months later following the initial infection can cause clinical relapse episodes.[37] Activation of hypnozoite reservoirs release new blood-stage infections that cannot be distinguished clinically from the primary infections, simultaneously increasing the chances of parasite transmission and wide distribution. Significantly, the prevalence of *P. vivax* infections in the WHO African region is very low owing to the Duffy negative trait in African populations.[36] The parasite requires the Duffy antigen on the surface of red blood cells to invade them. Populations without the antigen are immune from the parasite.

1.3.3 *Plasmodium knowlesi*

P. knowlesi is a malarian parasite first isolated in the early 1930s at the Kolkata School of Tropical medicine in India.[38] Until recently, this *Plasmodium* species was known to cause malaria among its natural simian hosts, long-tailed and pig tailed macaques as well as the band leaf-monkey,[39] and natural acquired human infections were thought to be rare. Even though it was known from experimental infections that the *Plasmodium* parasite could potentially infect human beings, naturally acquired infections were only reported in 2004 during a study conducted at Sarawak focusing on malaria human infections.[40] Since the report, *P. knowlesi* has been recognised as the 5th human malaria causing parasite and cases of malaria caused by the parasite are reported throughout Southeast Asia.[38] Human infections were probably undiagnosed due to morphological similarities between *P. knowlesi* and *P. malariae*. The golden standard laboratory diagnostic technique used to detect malaria parasites is a light microscope, which highly depends primarily on the morphological characteristics of the parasite. [41] Therefore similarities in morphology could have led

to the inability to distinguish between *P. knowlesi* and *P. malariae*, subsequently resulting in misdiagnosis.

Transmission of *P. knowlesi* is zoonotic, mosquito vector infected with parasite from simian host passes on the malaria disease to the human host while feeding. Mosquito vectors of *knowlesi* malaria belong to the *Anopheles leaucosphyrus* group that are found only in South-western India, Southern China, Taiwan, South-east Asia, Indonesia and Philippines.[42] The geographical distribution of the vector is limited to South-east Asia and corresponds to that of long-tailed and pig tailed macaques (**Figure 4**).[38] Because of the vector, geographical distribution of *P. knowlesi* is restricted to South-east Asia.

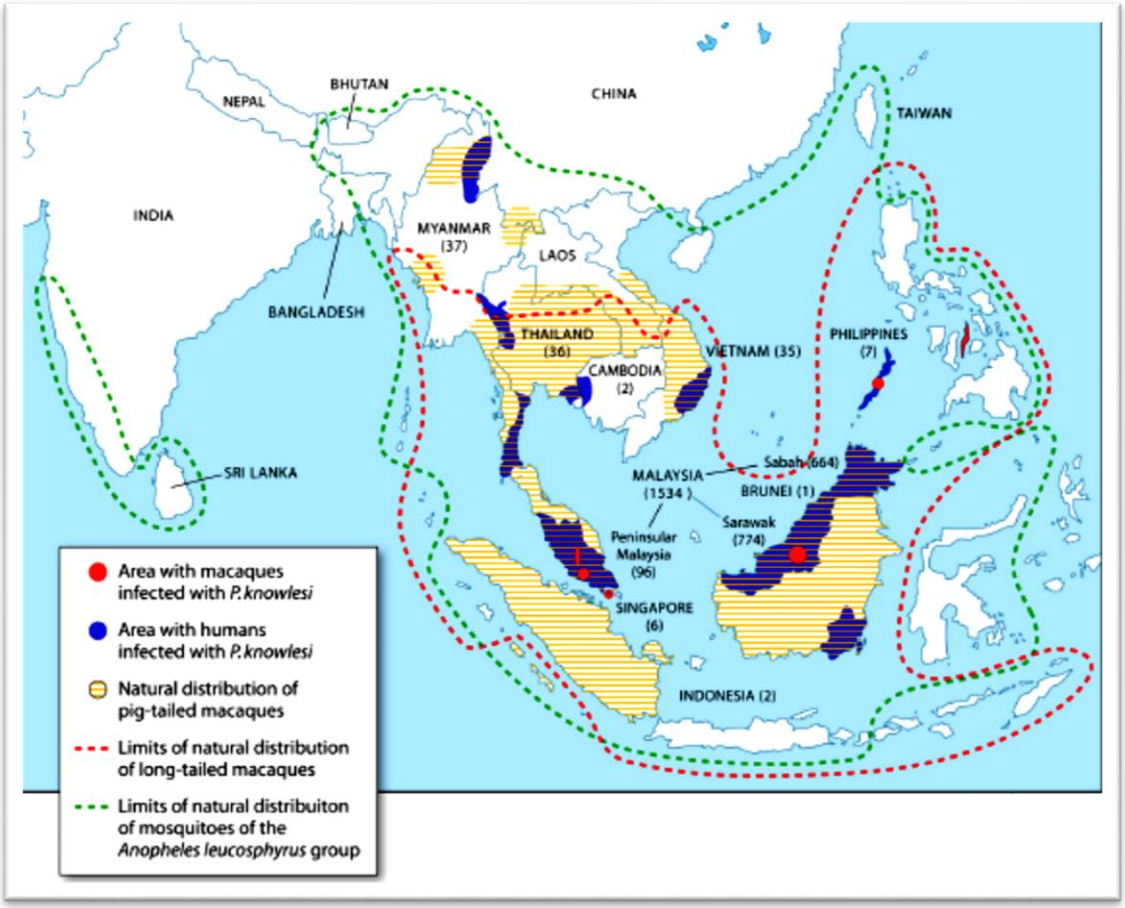

Figure 4. *Geographical distribution of Anopheles leucosphyrus group, limits of natural distribution of long tailed macaques and area with P. Knowlesi infected humans.*[38]

1.3.4 *Plasmodium ovale*

P. ovale is one of the least virulent malaria causing species in humans. It rarely causes severe illness or death. *P. ovale* may comprise of two species because of dimorphism in defined genes.[43] These two species are *P. ovale curtisi* and *P. ovale wallikeri*. The plasmodial parasite is endemic to tropic sites of the world such as tropical Western Africa.[44] *P. ovale* causes similar clinical effects as *P. vivax*. It has a dormant human blood stage that can cause relapse of symptoms.[27]

1.3.5 *Plasmodium falciparum*

P. falciparum causes the most severe cases and the vast majority of deaths from malaria worldwide. It is the predominant malaria causing species in the WHO Africa regions causing ~ 99.7% of reported cases.[45] Due to the prevalence of the species in Africa, this continent contains the highest levels of morbidity and mortality, 80% of the deaths are among children aged under 5 years.[16] Complications of *P. falciparum* infections include cerebral malaria, severe anaemia, respiratory stress and multi-organ failure to name a few.[33] These clinical complications of severe malaria are thought to occur because of high parasite load resulting from the blood stage and sequestration of parasite-infected mature erythrocytes in microvasculature throughout the body.[46] Sequestration occurs during the blood stage of *P. falciparum* life cycle, when adhesions expressed on the surface of mature infected erythrocytes bind to receptors on human cells.[47] These adhesions are derived by the parasite. There are three adhesion processes that promote sequestration as illustrated in **Figure 5**:[33,46]

- Adherence of infected erythrocytes to endothelial cells.
- Rosetting, binding of infected erythrocytes to uninfected erythrocytes.
- Platelet-mediated clumping of infected erythrocytes.

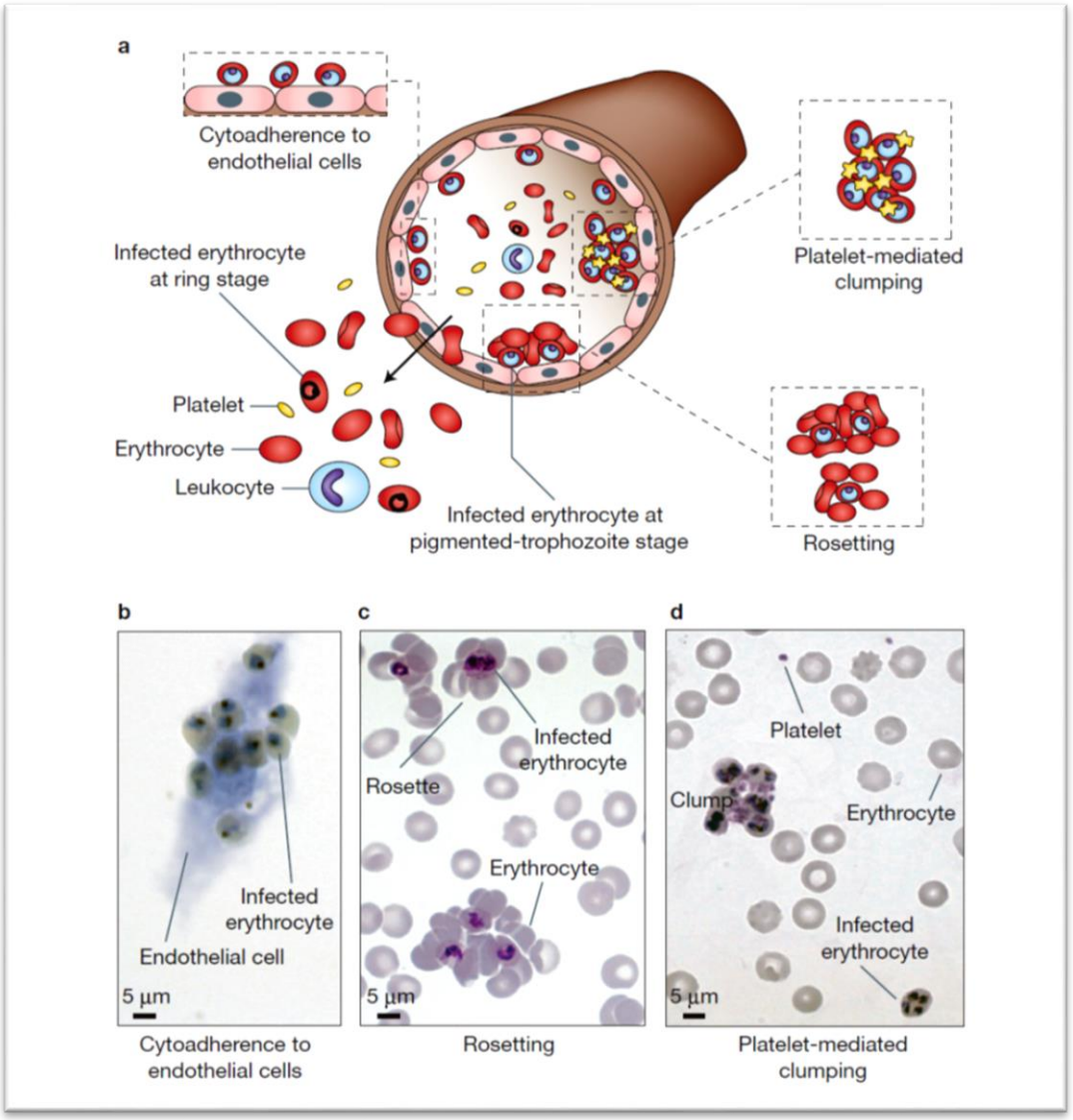

Figure 5. *Adhesion of P. falciparum infected erythrocytes to human cells.*[46]

In addition, a special type of adhesion occurs during manifestation of malaria during pregnancy.[46] Parasite-infected erythrocytes bind to syncytiotrophoblasts to bring about placental sequestration.[46] Sequestration leads to microvascular obstruction, therefore, blocking the microvascular system results in a decrease in supply of oxygen and nutrients needed by the internal organs or tissues. Deficiency in oxygen leads to the conversion of glucose to lactate, and the build-up of lactate results in acidosis. Fatal *P. falciparum* infections are often associated with the failure of multiple organ systems. Sequestration primarily benefits the parasite. The host's splenic clearance mechanism is meant for the removal of aged or damaged erythrocytes. Sequestration helps the parasite avoid removal of disease-damaged erythrocytes by the spleen.[33]

1.4 Strategies employed to eradicate malaria

The gradual decrease in malaria infections reported in the period of 2000 to 2019 was the result of many strategies recommended by WHO to detect, treat, control and eradicate malaria.[16] Major malaria intervention strategies include rapid diagnostic tests (RDT) to rapidly detect fever caused by plasmodial species, insecticide treated mosquito nets (ITNS), indoor residual spraying (IRS) of insecticide, artemisinin-based combination therapy (ACT) and the recently added intervention, seasonal malaria chemoprevention (SMC).

1.4.1 Diagnostic methods

Early diagnosis of malaria is important for early intervention of chemotherapy to increase the likelihood of patient survival and decrease mortality rates. Light microscopy is the golden standard technique used for detecting plasmodia species.[22] The technique is popular because it is cost-effective and only requires experience of a trained technician. It can therefore be utilised in local clinics. Giemsa-stained peripheral blood smears made from patient's blood samples are used to diagnose malaria infections.[22] The technique depends on the morphological differences of the species for confirmation of infection. For instance, the distinguishing feature between *P. falciparum* and *P. malariae* to other *Plasmodium* species is that they do not cause enlargement of erythrocytes. This could generally be because they invade mature erythrocytes instead of reticulocytes, like *P. vivax* and *P. ovale*.[27] In the case of *P. malariae*, all developmental stages in the liver cycle can be observed from blood films.[22] However, in *P. falciparum* only ring forms and crescent-shaped gametocytes are usually observed using microscopy.[38] Certain developmental stages of *P. falciparum* go undetected due to sequestration of trophozoites and schizonts of *P. falciparum* infected erythrocytes.[38] Although the technique is widely used to identify plasmodia species in infected patients, misidentifications do occur and this limits microscopy as a diagnostic tool. As mentioned before, it is impossible to distinguish between *P. knowlesi* and *P. malariae* by microscopy because the morphological features of the two species during the blood stage are closely similar. Additionally, *P. malariae* at low parasitemia can go undetected by microscopy. The accuracy of microscopy depends on variables that cannot be controlled such as the quality of the

blood smears and the experience of the technician conducting the test. This makes results obtained from the technique debatable.

Ideally, blood tests should be done on patients presenting malaria signs and symptoms for more sensitive and accurate diagnosis. However, molecular detection methods such as polymerase chain reactions (PCR) are more available in research settings and are rarely available in rural areas.[27] RDTs have been developed and employed to improve accuracy of malaria detection for clinical use. They are immune-chromatographic devices that detect specific antigens from the parasite using antibodies.[48] RDTs which contain antibodies targeting histidine-rich protein 2 (HRP2) and plasmodial lactate dehydrogenase (pLDH) are specific to *P. falciparum*; the latter can be specific for *P. vivax*. They have also developed RDTs that detect antigens common to all *Plasmodium* species; these make use of pan-pLDH and aldolase monoclonal antibodies.

1.4.2 Vector control

ITNS and IRS are preventative measures put in place to control the mosquito vector. They are used in combination to improve efficacy of insecticides employed to either kill or repel the mosquito vector. Pyrroles and pyrethroids are the two insecticides currently approved for use. Synthetic pyrethroids were introduced in the 1990s to minimise the threat of a potential increase in malarial infections brought about by the development of resistance gained by some *Anopheles* mosquito species against insecticides used at the time.[49] Pyrethroids are neurotoxins that act by interacting with voltage-gated sodium channels in neurons.[50,51] This interaction triggers sodium channels located on the membrane of axons to open, allowing an influx of sodium cations inside the cells. The prolonged influx of sodium results in depolarisation, where the potential charge of the membrane changes from negative to positive inside the cell. Depolarisation leads to repetitive nerve activity that can result in hyperexcitation and death.[50]

Pyrroles offer a different mode of action to pyrethroids. They affect the insect's ability to produce energy in the form adenosine triphosphate (ATP) by targeting its' mitochondrial oxidative pathways.[52] Oxidative phosphorylation is an enzyme-

catalysed metabolic pathway made of two important components: the electron transport chain and chemiosmosis. The electron transport chain forms a proton electrochemical gradient across the inner mitochondrial membrane, the energy-rich intermediate of oxidative phosphorylation.[53] The chemical energy produced by the electron transport chain is utilised in chemiosmosis by ATP synthase. ATP synthase utilises the energy to make ATP from adenosine diphosphate (ADP) and phosphate. Pyrrole insecticides uncouple oxidative phosphorylation.[54] They inhibit the coupling between the electron transport chain and chemiosmosis (i.e. phosphorylation reaction), therefore disrupting synthesis of ATP.[55] Loss of energy production leads to cell dysfunction and subsequent death of the insect.[54]

1.4.3 Vaccine

RTS,S/AS01 is the first malaria vaccine to be approved for widespread use primarily in children as of October 2021.[56] Its purpose is to inhibit the liver stage of *P. falciparum*. During the liver stage, *P. falciparum* expresses a protein called circumsporozoite that plays an important role in the invasion of hepatocytes by sporozoites.[57] Parts of circumsporozoite sequences are co-expressed with fused and free hepatitis B surface antigen and formulated with the AS01 adjuvant.[57] The vaccine's mode of action is to trigger the hosts' immune response to identify circumsporozoite antigens and inhibit infection of hepatocytes. Inhibition of the liver stage subsequently results in the disruption of the parasitic lifecycle.[56] The vaccine offers immunity against *P. falciparum* especially to countries with high to moderate transmission. This is particularly important in endemic countries in the WHO African region where *P. falciparum* infections greatly affect children under the age of five.

From March 2009 to January 2011, infants (6-12 weeks) and children under 5 from Burkina Faso, Gabon, Ghana, Kenya, Malawi, Mozambique and Tanzania were enrolled for phase 3 RTS,S/AS01 malaria vaccine trials.[57] Results from the trials indicate that RTS,S/AS01 efficacy against clinical malaria was 28% in children and 18% in young infants during the conclusion of the 3 year study.[57] Furthermore, protection against the disease was prolonged with administration of a booster dose. However, efficacy of the vaccine remained lower even after the booster dose. Despite the decrease in vaccine efficacy against clinical and severe malaria overtime, overall

the vaccine can prevent a significant number of severe malaria cases for children under 5 years of age and infants administered with or without a booster dose. The vaccine can be utilised in combination with other implemented malaria strategies to control and prevent malaria infections. It was shown that a combination of the vaccine with chemoprevention, such as sulfadoxine-pyrimethamine and amodiaquine, greatly improved protection against uncomplicated clinical malaria.[58] As observed, in combination with chemoprevention, the vaccine can decrease mortality rates from malaria by over 70% in children under 5 years of age. Discovery of a potential vaccine is a monumental milestone in the fight against malaria and adds to the tremendous efforts put towards eradication of the disease.

1.4.4 Treatment

Antimalarials are antagonists of the life cycle of *Plasmodium* species and form the basis of chemotherapeutic agents designed to treat malaria. They are an essential tool utilised either for treatment of clinical cases or inhibiting continuous transmission of the parasite. Most chemotherapeutic agents are designed to target the blood stages, which result in parasitemia. Their purpose is to clear parasitic particles and prevent disease progression to severe malaria and death. Chemotherapeutic agents with activity against the gametocytes have potential to reduce the onward transmission of the parasite to the mosquito. The liver stage is the least explored developmental stage of the parasite. Chemotherapeutic agents designed to target the liver stage could potentially disrupt the entire life cycle of the parasite. **Figure 3** shows the lifecycle stages targeted by available antimalarial drugs.

1.4.4.1 Quinolines

Quinolines are essential drug agents in the treatment of malaria. There are a wide variety of quinolones that have been explored as antimalarials (**Figure 6**). They mostly target trophozoites in the blood stage of the parasite, with exception to primaquine, which can be used in all stages of the parasite's lifecycle within the human host.

1.4.4.1.1 Quinine

During a visit to Peru, the Spanish Countess of Chinchon presented a fever. Natives of Peru gave her a bark of a tree to cure the fever. Now the tree is commonly known as *Cinchona*, named in her honour. She introduced the tree bark to Europeans upon

her return to Spain in 1638.[59] Almost two centuries later, the active compound in the *Cinchona* tree was isolated and named quinine by Pierre Pelletier and Joseph Caventon.[59] Quinine has since replaced the tree bark in the treatment of malaria. Although the mechanism of action of the alkaloid is not known, quinine has a rapid schizonticidal activity in the blood stage.[28]

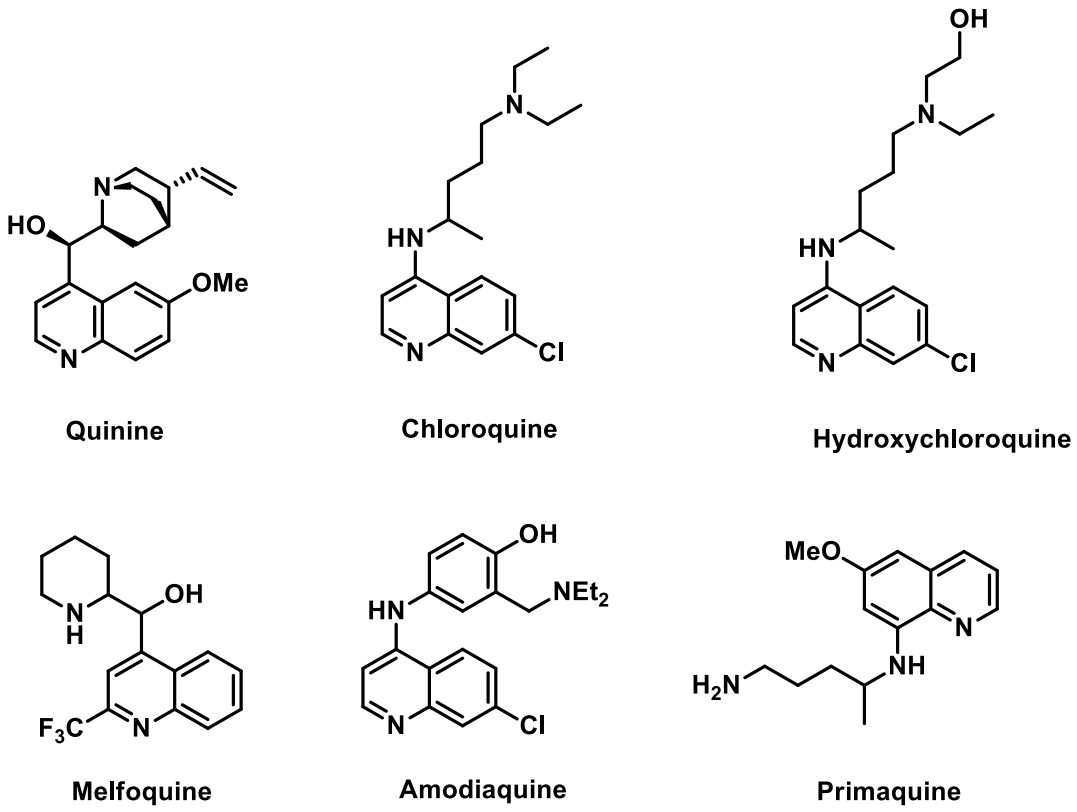

Figure 6. *Chemical structures of antimalarial including quinolines. quinine, chloroquine, hydroxychloroquine, melfoquine, amodiaquine and primaquine.*

After all these years quinine is still used as a chemotherapeutic drug against malaria. Quinine is currently used in combination with doxycycline as a second line treatment to artesunate for uncomplicated malaria. The prominent activity of quinine against malaria has led to development of derivatives of this aryl amino alcohol drug such as chloroquine, melfoquine, amodiaquine and primaquine **Figure 6**.

1.4.4.1.2 Chloroquine

Chloroquine is a structural derivative of quinine and was first synthesised in Germany In 1934. It became the predominant quinoline used to treat malaria in the late 1940s. Chloroquine, like quinine, exerts its antimalarial effect during the blood stages of the parasite. During the blood stage, within the hosts' erythrocytes, the *Plasmodium*

parasite degrades haemoglobin in an acidic food vacuole **Figure 7**.[60] Haemoglobin degradation is an enzyme catalysed metabolic process that releases peptides and amino acids important for *Plasmodium* development in the host.[61] Degradation of haemoglobin produces haem (Ferroprotoporphyrin IX) which is quickly oxidised to the toxic monomer haematin (Ferriprotoporphyrin IX).[62]The parasite protects itself from haematin by detoxifying the monomer and polymerising it into inert biocrystals of haemozoin.[60] Chloroquine is a weak base; it concentrates in the acidic food vacuole of the parasite due to a pH gradient between the vacuole and the parasite cytoplasm. Once inside the acidic medium, it picks up a proton. The protonated chloroquine cannot permeate the parasite membrane so therefore it is locked inside the vacuole.[28]

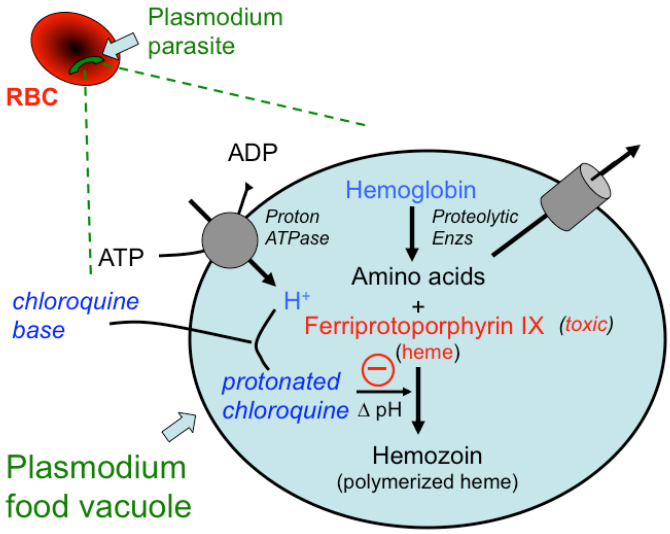

Figure 7. *Mode of action of chloroquine inside the parasites acidic food vacuole*.[63]

Chloroquine acts by binding to the haem monomer released during degradation of haemoglobin, preventing its conversion to haemozoin. The accumulation of toxic haem monomers ultimately causes parasite death.

Unfortunately, as evolution would have it, the parasite has gained resistance against chloroquine. A reduction in drug accumulation in the food vacuole is believed to be the main reason for resistance. Mutations in the genome expressing transmembrane proteins located on the parasite's food vacuole membrane could be the reason why resistant strains of *Plasmodium* accumulate lower concentrations of the drug.[60] *P. falciparum* chloroquine resistance transporter (*Pf*CRT) is one of the transmembrane

genes that have been implicated in development of resistance by the parasite to chloroquine. Reports indicate that *P. falciparum* strains expressing mutant *Pf*CRT accumulate less chloroquine in the food vacuole in comparison to *Plasmodium* strains expressing wild type *Pf*CRT.[60]

1.4.4.2 Artemisinin

Artemisinin is an active compound extracted from *Artemisia annua*, a plant long used in China to treat fever-presenting illness. Artemisinin was introduced in the 1970s after a significant drug search in China for new antimalarials with novel mode of action against the malaria parasite prompted by the discovery of multi-drug resistant *P. falciparum* strains. Development of resistance by *Plasmodium* against currently used drugs poses a threat to the enormous efforts made to control malaria and reduce the burden it causes to endemic countries.

Artemisinin and its derivatives are active against multi-drug resistant *P. falciparum* and they target both the gametocyte and asexual blood stage of the *Plasmodium* life cycle.[64] Its ability to target gametocytes is vital for the inhibition of further transmission of the parasite to mosquito vectors. Clinical studies have indicated that artemisinins are potent compounds and act faster to clear fever in comparison to other antimalarials. They typically clear fever within 20 hours and parasitemia within 48 hours.[28] Because of their effectiveness, artemisinins are used as the frontline treatment of severe malarial infections for quick resolution of symptoms.[64] Artemisinins are quickly eliminated, as a result, the WHO has recommended for the compounds to be used in combination with another blood-stage targeting drug as part of artemisinin-based combination treatment (ACT).[65] ACT's are now the main line of malaria treatment.

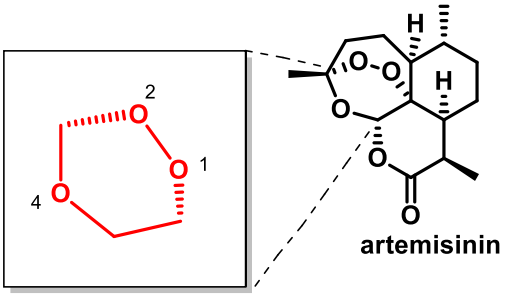

Figure 8. *Chemical structure of artemisinin and its 1,2,4-trioxane core.*

The unique sesquiterpene trioxane lactone configuration (**Figure 8**) is responsible for the novel activity of artemisinin.[28,64] Mode of action begins with artemisinin activation, resulting from interaction of artemisinin with divalent iron (Fe II), which ultimately leads to cleavage of the endoperoxide bridge releasing free radicals.[66] The source of Fe II was initially thought to be haem, as this monomer is released in abundance during degradation of haemoglobin within the parasite's food vacuole. However, reports indicate that artemisinin and its derivatives are bioactivated by non-haem iron sources.[67] Ferrous ions (Fe^{2+}) reduces the endoperoxide bridge to form oxyradicals, which further rearrange to carbon centred radical intermediates. These carbon centred radicals are believed to kill the parasite by alkylating vital parasite macromolecules and haem.[67] Furthermore, artemisinin helps clear parasitemia by increasing cellular oxidative stress. Within the parasite, artemisinin accumulates in the food vacuole forming reactive oxygen species that induce membrane damage and ultimately parasite death.[68]

1.4.4.3 Antifolates

Antifolates are extensively used in the treatment of malaria. Their ability to disrupt folate metabolism has gained them popularity as inhibitors of fast growing cells such as tumours and bacteria. Several antifolates are used in the treatment of cancer and bacterial infections.

1.4.4.3.1 Antifolates in the treatment of cancer

Antifolate drugs mimic one or more of the folate cofactors, and bind to the active site of the target enzymes to inhibit their function. Due to the importance of folates in fast growing cells, enzymes of the folate metabolic pathway were identified as anticancer drug targets in the 1940s.[69] DHFR and TS are crucial for the synthesis of dTMP in dividing cells, and hence inhibition of either leads to thymineless death. Thus both of these enzymes are attractive targets for developing antitumour agents. Several TS and DHFR inhibitors, as separate entities, have found clinical utility as anitumour agents. Methotrexate (MTX, displayed in **Figure 9**) was first introduced into the clinic in the early 1950s and remains a long standing anticancer agent.[69,70] It is commonly used to treat cancers such as acute lymphocytic leukemia, choriocarcinoma, osteosarcoma and breast cancer.[71–73] It targets DHFR in folate metabolism of tumour

cells by binding to the active site of the enzyme. Its structural similarity with DHF allows it to compete for the active site.

Despite its potency against DHFR, MTX has limitations in clinical use because of its cytotoxicity in cancer patients. Inhibition of DHFR suppresses molecular synthesis of dTMP and purine precursors required for DNA biosynthesis. Ultimately, DHFR inhibition leads to cell death. The mode of action, although excellent for halting replication of fast growing cells, does not exclusively select tumour cells over healthy cells. Additionally, MTX has a narrow solid tumour spectrum and it fails to penetrate the blood-brain barrier efficiently, therefore cannot be used systemically to treat brain tumours.[73] MTX requires a cell membrane carrier protein for cellular uptake; mutations of this transport protein often results in resistance towards the drug.[74]

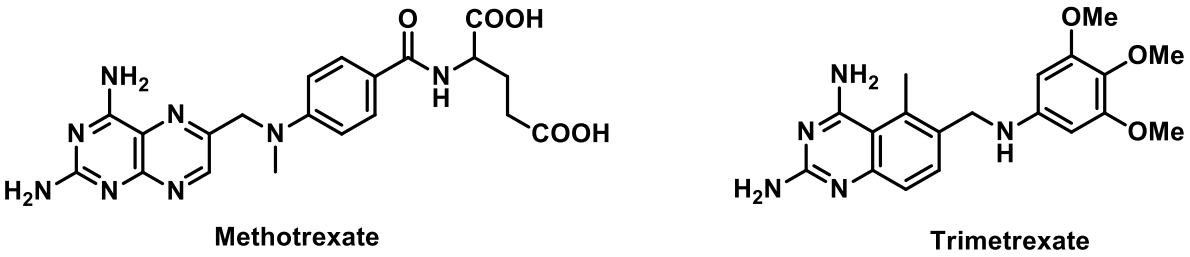

Figure 9. *Methotrexate and structural analogue trimetrexate, clinically used antifolates which target DHFR in cancer chemotherapy.*

To combat the disadvantages posed by the use of MTX, other antifolates have been developed and successfully introduced as anticancer agents. Trimetrexate (TMT) is a structural analogue of MTX (**Figure 9**). It contains a quinazoline ring and lacks the glutamic acid residue, making it lipophilic in comparison to MTX.[74] TMT was first described in 1979, it formed part of a large screening of compounds originally developed as potential antimalarials. TMT is a potent inhibitor of DHFR. Studies show that TMT inhibits the growth of a range of murine tumour models both *in vivo* and *in vitro*.[74] Further preclinical studies indicate that TMT could overcome some types of natural MTX resistance and therefore extend the tumour range of antifolates.

Thymidylase synthase (TS) is slowly gaining prominence as a drug target in the folate metabolic pathway. The enzyme catalyses the reductive methylation of uridine to thymidine, methylene THF acting as a source of the one-carbon unit. **Figure 10** illustrates clinically used TS inhibitors licensed for cancer treatment, such as raltitrexed

and pemetrexed.[69] Raltitrexed is a quinazoline analogue containing a 6-6 ring-fused system similar to natural nucleotides, whereas pemetrexed contains a 6-5 ring-fused pyrrolo[2,3-*d*]pyrimidine system.

Pemetrexed is a multi-targeted antifolate.[75] The antifolate and its polyglutamylated metabolites are inhibitors of several important enzymes in folate metabolism. Pemetrexed targets TS, DHFR, and glycinamideribo-nucleotide formyltransferase.[70,75] The antifolate enters the cells via a reduced folate carrier and is polyglutamated by folylpolyglutamate synthase (FPGS) to the pentaglutamate metabolite which is 60 times more potent than the parent compound and has enhanced intracellular retention.[70] It then inhibits at least three enzymes in the purine and pyrimidine synthesis pathway.

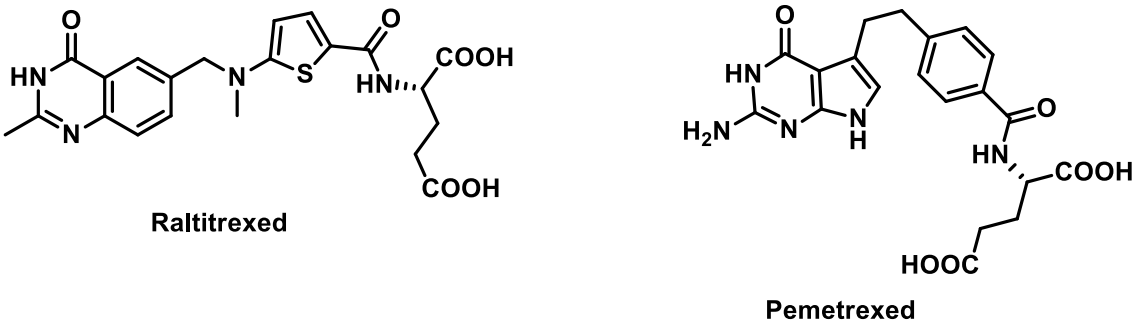

Figure 10. *Raltitrexed and pemetrexed, clinically accepted TS inhibitors.*

1.4.4.3.2 Antifolates in the treatment of bacterial infections

We currently live in an era where resistance to currently used antibiotics has increased at an alarming rate. Multi-drug resistant organisms render therapy more costly and sometimes unsuccessful. Individuals may succumb to drug resistant infections because all available drugs are inactive. Global drug-resistant bacteria species include *Mycobacterium tuberculosis*, *Enterococcus faecium*, *Enterobacter cloacae*, *Klebsiella pneumoniae*, *Staphylococcus aureus*, *Acinetobacter baumanii* and *Pseudomonas aeruginosa*.[76] Some of these bacterial species can manifest into severe clinical conditions such as tuberculosis, pneumonia and neonatal meningitis. Discovery and development of new chemotherapeutic agents is important to mitigate potential health threats in the event of infection outbreaks.

Antifolates that target folate metabolism offer a different mode of action to commonly used antibiotics. Illustrated in **Figure 11** are some of the widely used antifolates used

in the treatment of bacterial infections. Prontosil was introduced during the early 1930s as one of the azo dyes examined for possible antibacterial activity (**Figure 11**).[77] Soon after, it was discovered that prontosil was a pro-drug converted to sulfanilamide in the body, which led to the development of sulfonamides as a drug class. Prontosil, like many related sulfonamides, is a structural analogue of pABA and has been found to competitively inhibit DHPS.[78] Sulfonamides are still currently used as antimicrobial agents; sulfamethoxazole is used in combination with trimethoprim to treat multiple infections such as pneumonia and urinary tract infections.[77]

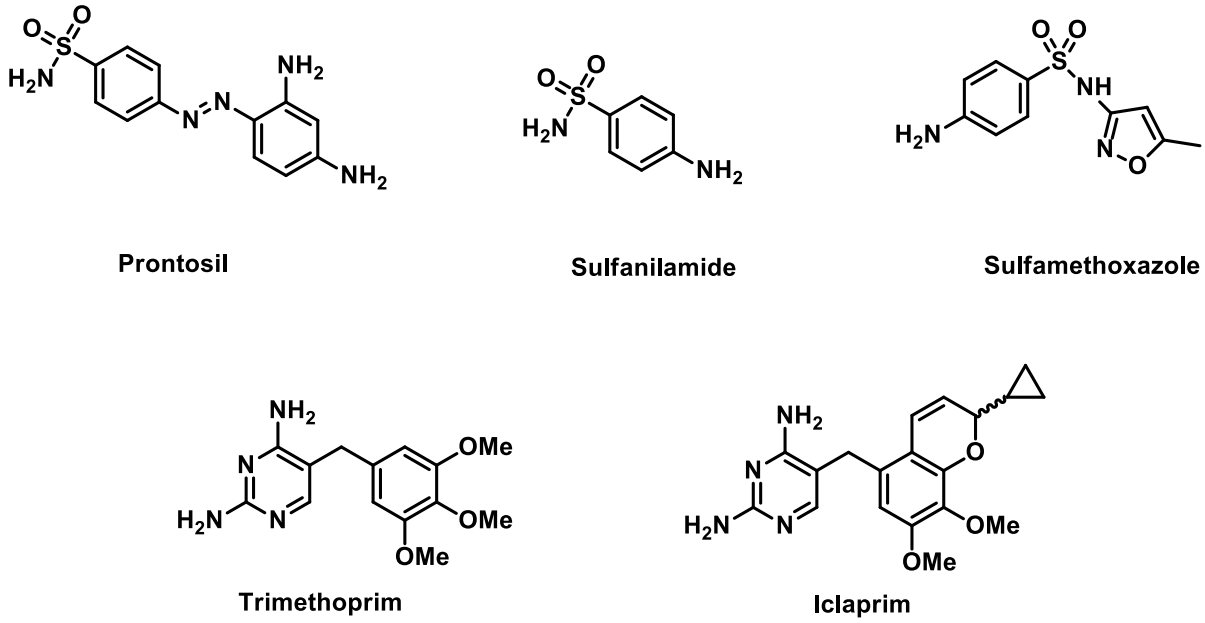

Figure 11. *Chemical structure of antifolates used in the treatment of bacterial infections: prontosil, sulfanilamide, sulfamethoxazole, trimethoprim and iclaprim.*

Trimethoprim (**Figure 11**) is a 2,4-diaminopyrimidine antibacterial agent that effectively inhibits DHFR in various bacterial species.[78] The antibiotic is frequently used together with sulfonamides because of the synergistic impact on the disruption of folate metabolism. Unlike trimethoprim, iclaprim is an antibiotic utilised as a monotherapy for serious hospital infections. The novel diaminopyrimidine analogue is potent against DHFR. It exhibits excellent activity against staphylococci, including most of the trimethoprim-resistant strains,[79] and respiratory track pathogens, such as pneumococci.[8] In 2003, it successfully completed Phase II clinical trials for complicated skin and skin structure infections in hospitalised patients.[79]

1.4.4.3.3 Antifolates in the treatment of malaria

Antifolates targeting specific enzymes in the *de novo* folate pathway behave in a similar manner as the innate folate co-factor at the molecular level. Their sole mode of action is to mimic the natural folate co-factor and compete for the active site of the enzyme. Their affinity for the enzyme determines potency against the *Plasmodium* parasite. Antifolates used in the treatment of malaria infections are subdivided into two classes: inhibitors of DHPS, known as class I, and inhibitors of DHFR, the class II antifolates. DHPS and DHFR inhibitors work synergistically; hence they are often used in combination therapy to combat malaria.

1.4.4.3.3.1 Class I Inhibitors

Class I inhibitors are commonly referred to as sulfa-drugs, they are structural analogues of pABA. They mimic pABA and compete for the active site of DHPS. Inhibition of DHPS by sulfa-drugs interrupts catabolic activity further downstream of the *de novo* pathway,[6,7] i.e., inhibition of the enzyme halts synthesis of DHF *de novo*. DHPS is one of the enzymes in the folate metabolic pathway exclusive to the parasite; the human host salvages its folates, it does not utilise DHPS to acquire folates. Sulfa-drugs block the synthesis of folates *de novo*, which makes them attractive for selective inhibition of parasite growth.[2] Previous, attempts were made to use these drugs as monotherapeutic agents for malarial. However, this approach was abandoned because of their low potency and toxic nature.[80] This class of compounds belong to two families: sulfonamides and sulfones (**Figure 12**). Dapsone is a sulfone based agent that shows potency against DHPS of malaria.

Dapsone was synthesised at the beginning of the 20th century as a result of a massive search for molecules to produce azo dyes.[77] It was only tested for antimicrobial activity during the late 1930s, where it was assessed for its biological activity against bacterial cells.[2] This antifolate agent was found to inhihit the growth of various pathogenic agents including the malaria causing parasite, *Plasmodium*.[2] It was used for the treatment of clinical infections caused by both malaria parasites *P. falciparum* and *P. vivax*. Development of the drug for chemotherapeutic use was abandoned due to its limited efficacy and high toxicity.[2]

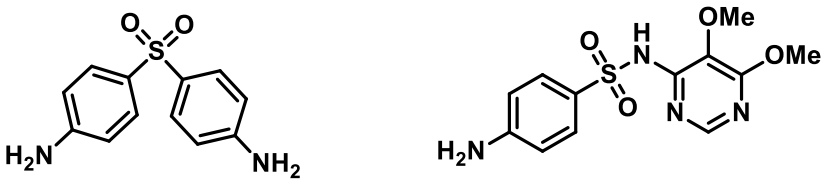

Dapsone Sulfadoxine

Figure 12. *Chemical structures of class I inhibitors: Dapsone and Sulfadoxine.*

Sulfadoxine is a sulfonamide which has demonstrated remarkable promise as a prophylactic agent against *P. falciparum*, such drugs can be utilised for as chemopreventative measures against the parasite.[81] Furthermore, the drug has shown efficacy against *P. falciparum*. Several early trials confirmed that a single 1.00 g dose of sulfadoxine was effective, although slow, schizontocide.[82]

1.4.4.3.3.2Class II Inhibitors

In 1945, proguanil was first reported as an antimalarial agent. The drug was found to be more active than quinine, the first of the antimalarial agents to be used against avian malaria and to have a better therapeutic index in animal models, this encouraged its use in humans.[2] After this discovery, studies demonstrated that in fact, proguanil is a prodrug and metabolises to its triazine form, cycloguanil (**Figure 13**), an inhibitor of the parasite DHFR.[2] This pro-drug can be used alone as a chemoprevention agent against malaria or in combination with chloroquine. The effectiveness of proguanil prompted the search for its derivatives such as chlorproguanil, a DHFR inhibitor generated by the chlorination of proguanil on the phenyl ring. Similar to proguanil, chlorproguanil is metabolised to its active metabolite chlorcycloguanil (**Figure 14**). Currently chlorproguanil is utilised in combination with dapsone for prophylaxis.

Proguanil Cycloguanil

Figure 13. *Conversion of proguanil to its respective metabolite cycloguanil.*

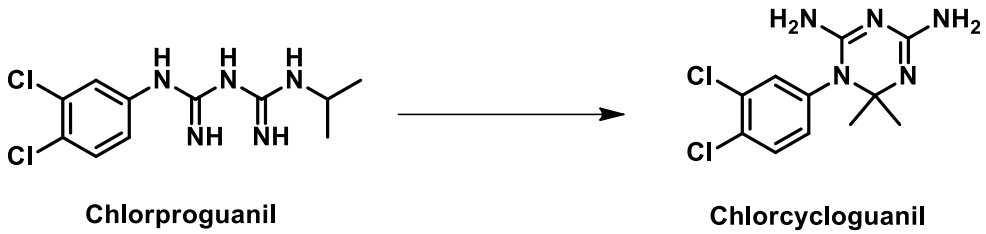

Chlorproguanil Chlorcycloguanil

Figure 14. *Conversion of chlorproguani to its respective metabolite chlorcycloguanil.*

Pyrimethamine (**Figure 15**) was developed shortly after proguanil; it belongs to the 2,4-diaminopyrimidine family. Pyrimethamine is a structural analogue of cycloguanil with a fully aromatic pyrimidine ring. Pyrimethamine and cycloguanil have a high affinity for DHFR and therefore can facilitate inhibition of the enzyme.[83] They inhibit the reduction of DHF to THF; essentially, they inhibit one of the most important metabolic reactions in DNA synthesis. The structures of these antifolates is a key factor in their mode of action. Pyrimethamine contains a 2,4-diaminopyrimidine ring and cycloguanil is made of a triazine-ring system. The ring systems allows these antifolates to mimic the pterin-ring of DHF and compete with it for the active site of DHFR. The bi-aryl bond present in the structure of pyrimethamine and cycloguanil fits the hydrophobic pocket of the active site.[83] Pyrimethamine has been the most widely used antimalarial agent in both prophylaxis and the treatment of malaria to date. However, concerns about the rapid development of parasite resistance to pyrimethamine and its slow schizontocidal activity were raised shortly after its introduction.[84]

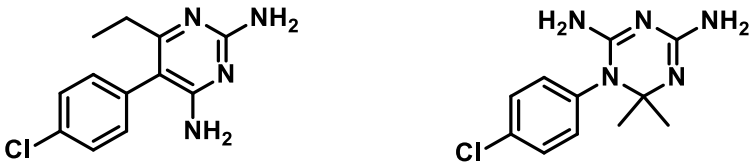

Pyrimethamine Cycloguanil

Figure 15. *Chemical structure of pyrimethamine, structural analogue of cycloguanil.*

Point mutations occurring in the genome encoding for parasitic DHFR are culpable for the increased emergence of resistance against cycloguanil and pyrimethamine. DHFR mutations occur in a progressive, stepwise fashion. Mutations build up in response to pressure brought about by the drug; hence, there is broad correlation between increased frequency of mutations and resistance to anti-DHFR agents across the world. Resistance resulting from point mutation highlights the challenge of developing

new antifolates with prolonged useful therapeutic life, since new mutations could possibly arise to compromise the new antifolates. Since the parasites needs to maintain the biological function of the enzyme, the parasite has limited mutational possibilities.[85] Therefore DHFR remains a viable enzyme target for the development of new drug candidates.

Point mutations probably occur because of deletion, addition or substitution of genes encoding for specific amino acids in the active site, changing the configuration of the active site. If a drug cannot conform to the new configuration of the active site it loses its potency against the enzyme. Studies involving crystal structures and homology models of DHFR-TS have highlighted a number of features concerning the basis of drug resistance.[85] Pyrimethamine and cycloguanil experience steric effects between *para*-substituted chlorine atoms on the phenyl ring with the side chain of Asparagine108 in mutant enzymes. In the case of cycloguanil, steric clashes occuring between one of the 2,2-dimethyl groups and the side chain of Valine16 have been implicated in drug resistance.[84,85] Pyrimethamine and cycloguanil are rigid, they contain a bi-aryl ring system covalently bonded by a rigid single bond that does not allow for torsional freedom. The rigid geometric conformation of these two antifolates does not allow the flexibility to overcome point mutations imposed by the parasite. In light of these observations, a number of investigations were carried out to develop new antifolates with structural similarities to pyrimethamine and cycloguanil, with the intention to overcome resistance.[85] The results from these studies suggest that the resistance can be reversed by:

1. Modifying the aromatic ring, by changing substituents on the aryl-ring.
2. Use of a flexible side chain, instead of the rigid bi-aryl bond, which will provide conformational freedom to fit in the active site.
3. Elimination of one of the bulky alkyl groups in cycloguanil, to avoid steric clashes with amino acids in the active site.

To combat development of resistance towards pyrimethamine, a study demonstrated that sulfadoxine potentiates pyrimethamine in human *falciparum* infections.[86] The combination of pyrimethamine and sulfadoxine was more effective than either drug alone; additionally, faster schizontocidal activity and improved clinical response were observed.[87] When multidrug-resistant infections were increasing in Southeast Asia in

the mid to late 1960s, sulfadoxine-pyrimethamine was a logical first-line drug replacement for chloroquine in Thailand.[88] Despite the largely successful field trials, reports of clinical failure from Southeast Asia, South America, Africa and USA indicated that the sulfadoxine-pyrimethamine combination might prove to be an ineffective long-term solution.[89,90]

In a quest to develop new antifolates by modification of existing drugs, compounds such as WR99210 and its metabolic precursor PS-15 (**Figure 16**) were identified as promising DHFR inhibitors. WR99210 is a triazine structural analogue of the antimalarial drug cycloguanil with a flexible aliphatic linker.[91] It was advanced as an antifolate-based antimalarial with high activity against both wild-type and drug-resistant DHFR.[92] In cell proliferation assays, WR99210 inhibits *P. falciparum* with an IC_{50} value of 0.1 nM.[93] However, WR99210 could not be developed as an antimalarial agent because of its poor bioavailability and gastrointestinal intolerance.[2] Similar to the conversion of proguanil to cycloguanil, a biguanide prodrug of WR99210, PS-15, was developed (**Figure 16**); this compound has better bioavailability properties and showed more potency than WR99210 in an *in vivo* model.[2] One of the key aspects of the prodrug that makes it even more interesting is the potency it displays in a variety of different pathogens. The pro-drug has displayed activity against other opportunistic pathogens, such as *Pneumocystis carinii*, *Toxoplasma gondii* and *mycobacterium avium*.[94]

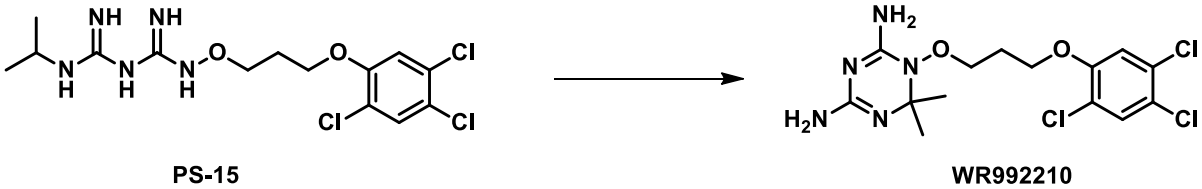

PS-15 WR992210

Figure 16. *WR99210 and its precursor PS-15.*

The precursor was not further explored due to cross resistance with cycloguanil and pyrimethamine.[95] However, this is evidence that antifolates with structural flexibility such as WR22910 and PS-15 are potent against drug resistant strains of *P. falciparum*. WR992210 contains a 5-atom flexible linker between the triazine ring system and the substituted phenoxy, and it is proposed that the flexible linker allows WR992210 torsional freedom, which in turn is responsible for the antifolate to overcome point mutations imposed by the drug resistant *P. falciparum* strain.

1.5 Dihydrotriazines

In a previous study, Prof. Rousseau and co-workers at the CSIR were responsible for a project entailing the design and synthesis of flexible dihydrotriazines.[96] The novel 6-aryl-1,6-dihydro-1,3,5-triazine-2,4-diamines **1** are structural derivatives of cycloguanil. They contain a dihydro-1,3,5-triazine heterocycle with an aryl ring at position 6 and a flexible linker attached to the endocyclic N-5 (**Figure 17**), as opposed to the dimethyl groups at C-6 and the rigid single bond connecting the triazine and the phenyl rings of cycloguanil. The length of the flexible linker was varied from 1 to 6 atoms between the triazine and substituted aromatic ring.

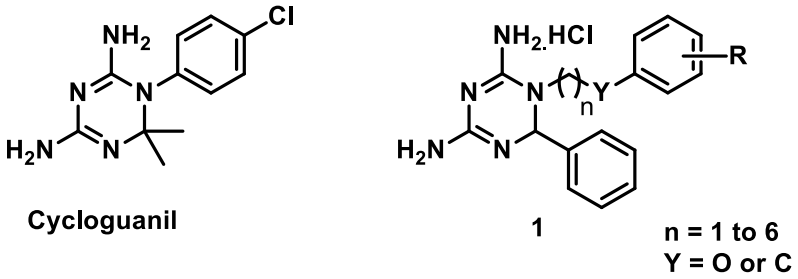

Figure 17. *Cycloguanil and experimental proposed 6-aryl-1,6-dihydro-1,3,5-triazine-2,4-diamines **1** from CSIR research group.*

These dihydrotriazines were synthesised in a two-step reaction sequence from amines **2** with dicyandiamide **3** under acidic conditions to produce arylbiguanides **4** (**Scheme 1**).[97] The amines **2** were either synthesised from phenols or obtained from commercial sources. The arylbiguanides **4** were further reacted with benzaldehyde **5** to form a Schiff-base intermediate **6** in the presence of an acid catalyst, which further cyclizes *in situ* to give the 1,2-dihydro-triazine-4,6-diamine **1**.

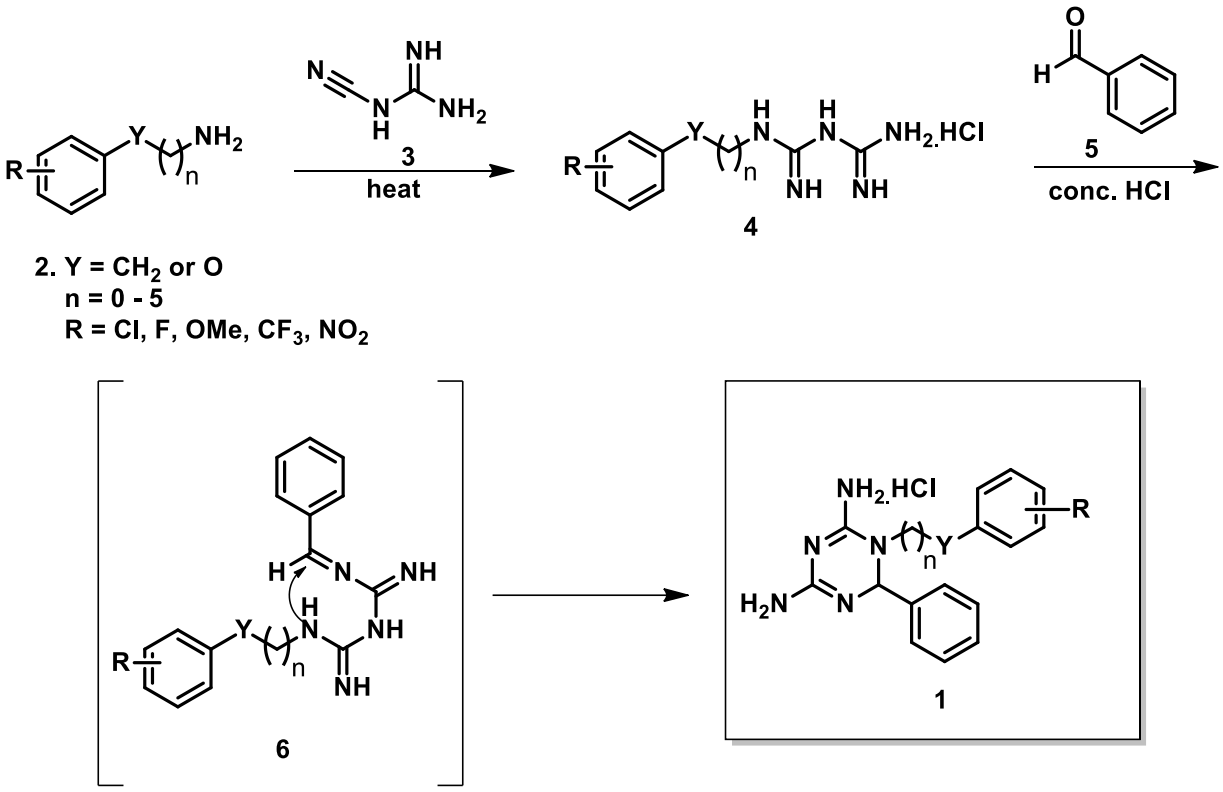

***Scheme 1**. Synthetic procedure towards 1,2-dihydro-triazine-4,6-diamines **1**.*

These compounds exhibited *in vitro* antiplasmodial activity in the low nanomolar range against both drug sensitive and resistant strains of *P. falciparum*.[96] The most potent compound from this series displayed activity with an IC_{50} value of 2.66 nM against the cycloguanil resistant Gambian FCR-3 strain (**Figure 18**).[96] These compounds were found to be non-toxic to mammalian cells at therapeutic concentrations and inhibited parasitic DHFR. From the study, a key structure-activity relationship was evident, see **Figure 18**.[96] The most potent compounds contained a flexible linker of 4-atoms between the triazine ring system and the phenoxy ring, which could accommodate a variety of substituents. Additionally, compounds with unsubstituted phenyl rings attached to C-6 of the triazine displayed high activity in comparison to those bearing substituents on the phenyl ring. The loss in activity from substrates with substituted phenyls is most likely due to steric clashes in the active site of the enzyme.

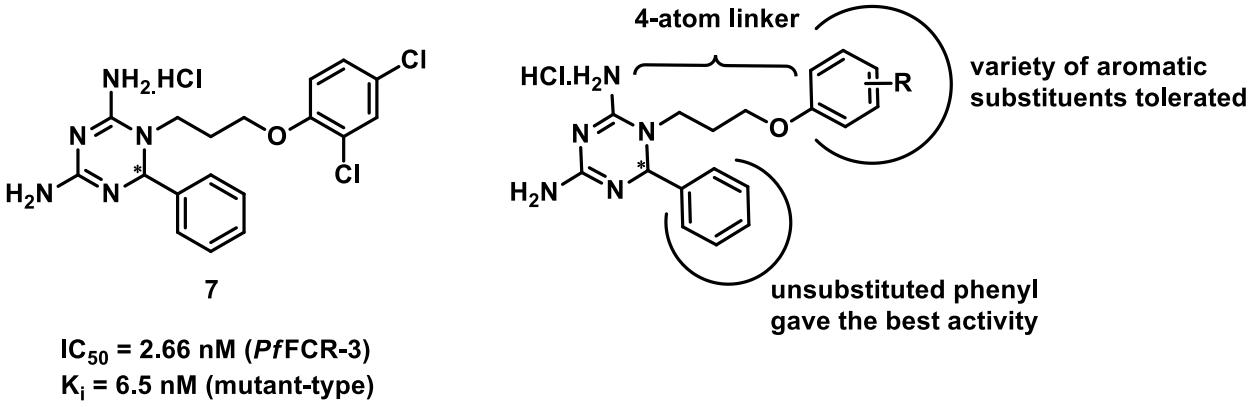

Figure 18. *Chemical structure of the hit compound **7** and key structure-activity relationships identified for the potent compounds.*

Despite the promising results *in vitro*, the synthesis of these flexible dihydrotriazines was not trivial and target compounds were isolated as a racemic mixture. Enantiomers are not favourable as chemotherapeutic agents because each enantiomer may behave differently in biological systems. One enantiomer may have the desired beneficial activity against *Plasmodium* species, while the other may cause negative side effects. An enantioselective approach could be developed for these types of compounds; however, it would most likely be too expensive to carry out for commercial application. This led to the development of the first generation of pyrimidines synthesised in our laboratory.

1.6 Pyrimidines

Prof Rousseau continued the work initiated at the CSIR at the University of the Wiwatersrand, and the first generation of pyrimidines **8** were synthesised in the School of Chemistry.[98] The pyrimidines are structural analogues of the dihydrotriazines previously synthesised at CSIR. They contain a heterocyclic ring bonded to a phenyl ring at position 6 and a flexible chain connected at C-5 (**Figure 19**). Unlike the triazine, they do not harbour a chiral carbon within the heterocyclic ring but contain a fully aromatised pyrimidine heterocycle. The purpose of designing analogues with an aromatic pyrimidine ring was to evade complications associated with isolating a racemate for use as a chemotherapeutic agent.

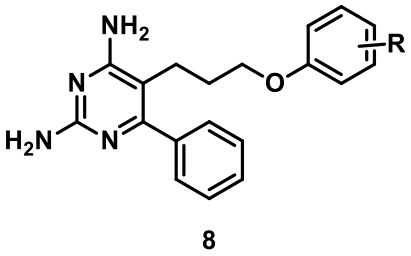

8

Figure 19. *Chemical structure of the 1st generation pyrimidines **8**.*

The first generation of 2,4-diaminopyrimidines were successfully synthesised in a 5- step synthetic route (**Scheme 2**) initiated by alkylating substituted phenols **9** using 1,4-dibromobutane. This reagent introduced the 4-atom linker to the molecule. After a functional group interconversion from the alkylbromide **10** to a suitable nitrile **11** using potassium cyanide as the nucleophile, the nitrile reacted with ethyl benzoate under basic conditions to give the β-ketonitrile product **12**. Alkylation of compound **12** using diazomethane afforded the enol ether **13**. Despite its effectiveness to alkylate ketones at the carbonyl-oxygen, diazomethane is a toxic, carcinogenic and explosive gas.[99] The use of the reagent even at laboratory scale is problematic owing to the safety concerns associated with its preparation. The last step in the synthesis was the ring closure using guanidine hydrochloride to form the desired 2,4-diaminopyrimidine **8**.

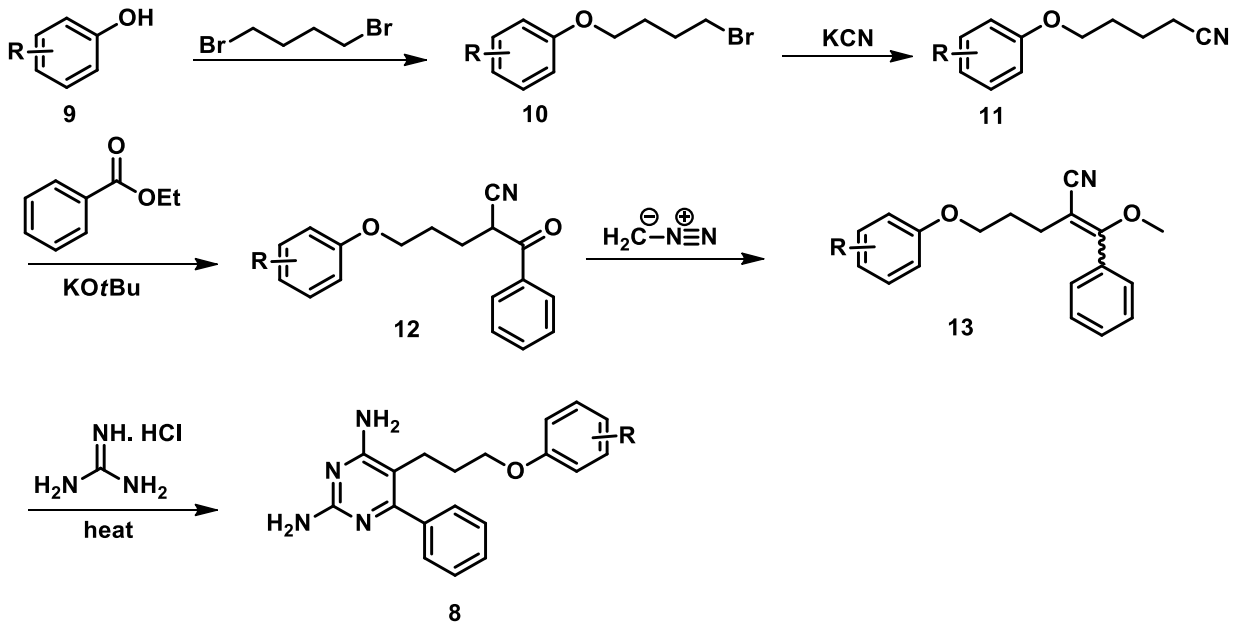

Scheme 2. *Schematic representation of the synthetic route towards first generation of 2,4-diaminopyrimidines.*[98]

The novel synthesised compounds were tested for antimalarial activity *in vitro* against the drug resistant Gambian FCR-3 strain in a *P. falciparum* assay. Of the tested compounds, the hit compound **14** displayed activity against the drug resistant *P. falciparum* with an IC_{50} of 90 nM (**Figure 20**). The rest of the compounds in this series displayed activity in the micromolar range. In comparison to the dihydrotriazines synthesised previously, which displayed antimalarial activity in the low nanomolar range, the pyrimidines seemed to have lost activity against *P. falciparum in vitro*. The loss in activity was thought to be due to the introduction of a rigid bi-aryl bond between the 2,4-diaminopyrimidine ring and the phenyl ring at position 6, as highlighted in **Figure 20**.

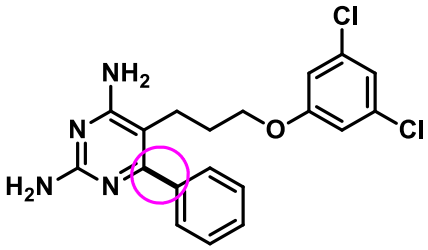

14
IC_{50} = 90 nM

Figure 20. *Most active compound from the 1st generation of pyrimidines **14**. Illustration of the rigid single bond between the 2,4-diaminopyrimidine ring system and the phenyl ring at position 6.*

Many challenges were encountered during the synthesis of the 1st generation of pyrimidine analogues. Their antimalarial activity was significantly lower in comparison to the dihydrotriazines synthesised previously. Additionally, formation of the pyrimidine ring from enol ether intermediates was low yielding, with the highest reported yield of 11%. Although execution of the synthetic route towards novel 2,4-diaminopyrimidine analogues was successful, the yields for the last step were disappointingly low for a medicinal chemistry project. The organic compounds are synthesised with intent to be commercialised as pharmaceutical agents, therefore, the synthetic route should take into consideration development of drug-candidates at industrial scale. Low yields make production of synthetic drug actives costly and not financially viable for pharmaceutical companies.

The use of toxic reagents such as potassium cyanide and diazomethane during the synthetic procedure is a huge health and environmental concern. Ideally, pharmaceutical actives should be synthesised from environmentally friendly and non-toxic chemical reagents or solvents to minimize health risks associated with utilising such lethal chemicals and the negative impact toxic waste could have on global ecosystems. Potassium cyanide is a potent inhibitor of the respiratory system and can be fatal if ingested or inhaled, whereas, diazomethane gas is toxic and carcinogenic, and the formation of the reagent could potentially be explosive when exposed to moisture. Working with such chemicals could cause tragic incidences that are fatal. For future purposes, risks profiles of the reagents will be evaluated in order to find alternatives that are not explosive or as toxic as the ones used previously.

To improve biological activity of the pyrimidines, a molecular modelling campaign was conducted in the search for structural derivatives of the 1st generation analogues with optimal affinity to *Pf*DHFR. This study did not form part of this PhD, but was done by a colleague in our laboratories. The data generated from the molecular modelling was used to inform the design of compounds that are the focus of this PhD. We selected four wild type[92,100–102] and four quadruple mutant [100–103] enzyme crystal structures of *Pf*DHFR as biological drug targets for the virtual screening. Numerous flexible pyrimidine analogues were designed for molecular docking against the selected enzymes, varying the aliphatic groups attached to C-atom at position 6 and substituents on the aryl ring (**Figure 21**). From the simulated interaction between designed pyrimidine ligands with the crystal structures of the enzymes, pyrimidine analogues containing an isopropyl group or a cyclopropyl ring at C-6 on the 2,4-diaminopyrimidine ring scored the highest during molecular docking. Although molecular modelling results may not translate in actual biological systems, the results are a good indicator as to which structural analogues can be further developed as potential drug targets against *Pf*DHFR.

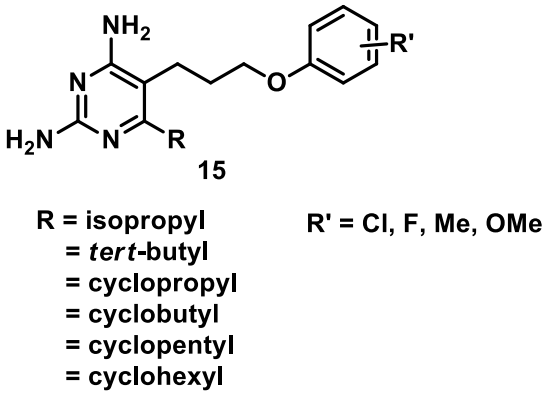

Figure 21. *Illustration of pyrimidine analogues designed for molecular docking against the selected enzymes with aliphatic alkyl groups or cycloalkyl rings.*

Previously in our laboratories, an attempt was made to use the experimental procedure employed to synthesise 1st generation pyrimidines to make analogues **15** with aliphatic substituent at C-6.[98] Unfortunately, the synthetic procedure was not robust enough to accommodate the use of aliphatic esters. From the schematic representation below (**Scheme 3**), it is illustrated that the β-ketonitriles utilised were formed by acylating nitriles with benzoate in the presence of a base. Efforts made to produce β-ketonitrile derivatives using aliphatic cyclohexyl and cyclopropylesters were unsuccessful. To synthesise second-generation pyrimidines with aliphatic groups bonded at C-6, development of a different synthetic procedure was required.

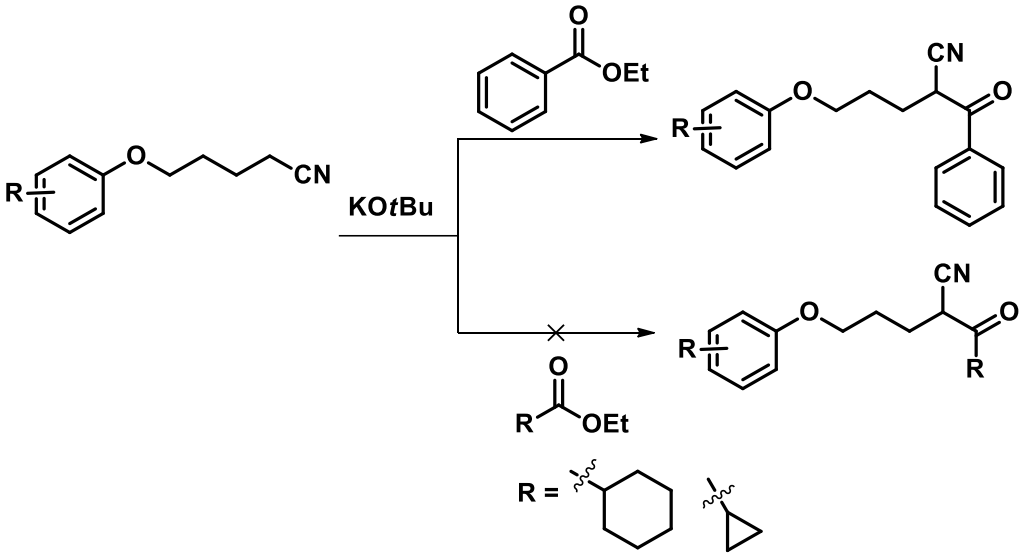

Scheme 3. *Acylation of nitriles by benzoate vs. aliphatic cyclic esters in the presence of t-BuOK.*

In a different research project aimed at synthesising flexible 2,4,6-triaminopyrimidine derivatives, Tebogo Molatsane (MSc student, Wits University) attempted the Sonogashira cross-coupling reaction as a key step to couple the 2,4,6-triaminopyrimidine ring with the flexible alkyl chain (**Scheme 4**).[104] The pyrimidine ring system **16** was successfully synthesised in two reaction steps starting from commercially available 4,6-dichloropyrimidin-2-amine **17**, which was further iodinated in the presence of K_2CO_3 to give compound **18**. The iodinated pyrimidine substrate was subjected to Sonogashira cross-coupling reaction conditions with an acetylene prepared from a commercially available 4-fluorophenol. Unfortunately, formation of the desired product **19** was unsuccessful and the iodinated starting material was isolated. It was postulated that the two amino groups were coordinating to Pd in the reaction, hence, the reaction did not take place.

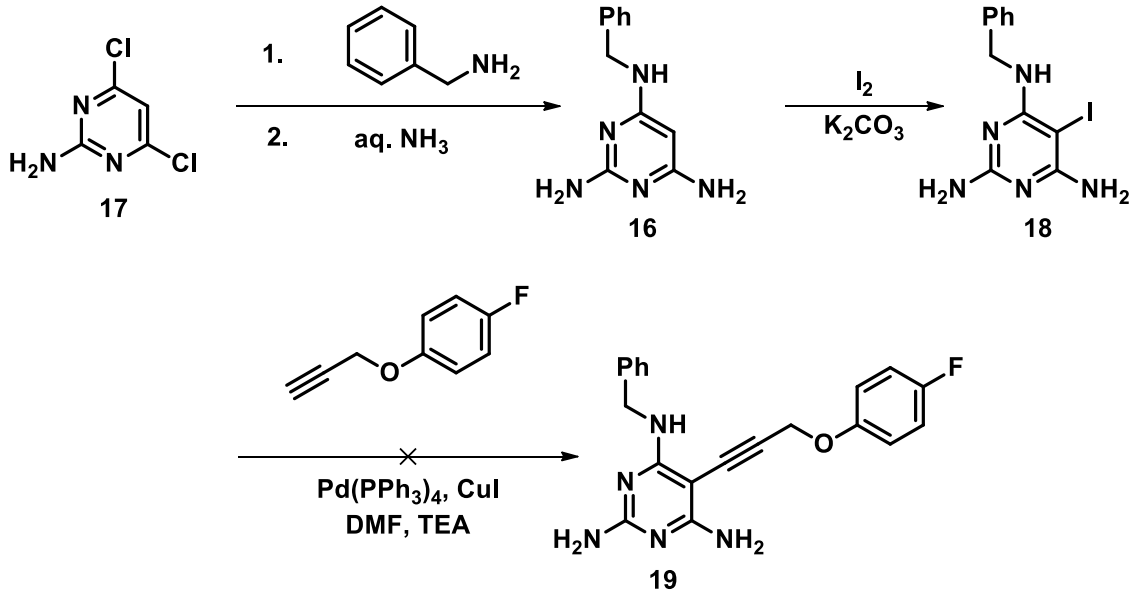

Scheme 4. *Schematic representation of the Sonogashira reaction towards synthesis of compound **19**.*[104]

Failure of the Sonogashira reaction, prompted an attempt of the Sonogashira reaction on a simple acetylene as illustrated in **Scheme 5**. The iodinated 4,6-diaminopyrimidine **18** was coupled with trimethylsilyl acetate (TMS acetylene) in the presence of a Pd-catalyst resulting in formation of compound **20** in 45% yield. Having successfully coupled acetylene TMS with the pyrimidine ring, the protecting group was deprotected with TBAF to afford compound **21,** which was further subjected to a copper mediated coupling reaction with ethynylbenzene to give the 1,3-diyne **22** in 14% yield. The 1,3-

diyne intermediate was further reduced to the desired 2,4,6-triaminopyrimidine derivative **23**. Although, the method suffers from setbacks including low yields and difficulty purifying certain key intermediates,[104] at this point this methodology has been proven to be a viable alternative to the methodology outlined for the 1st generation of 2,4-diaminopyrimidines.

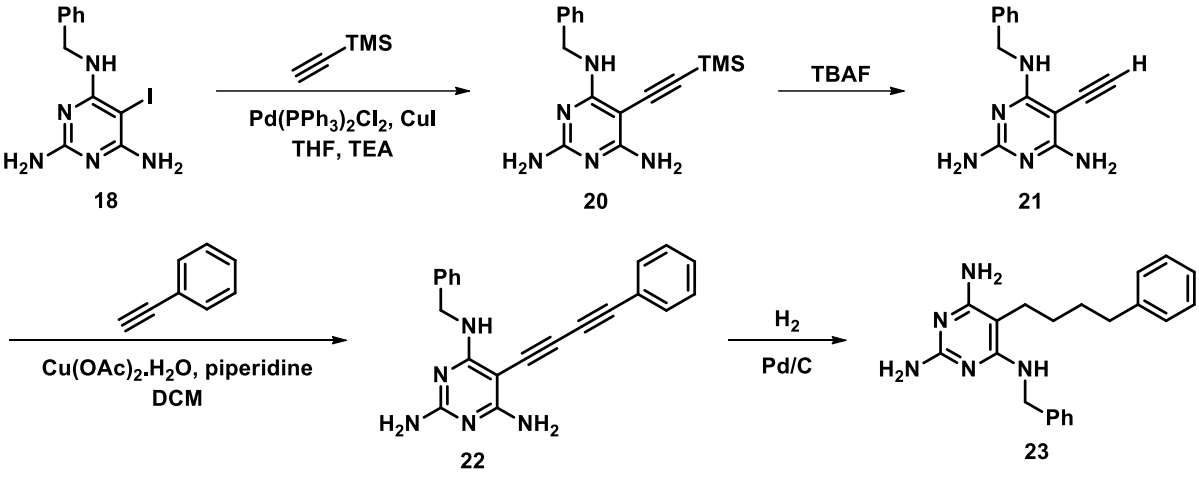

Scheme 5. *Transition metal-mediated coupling reactions for the synthesis of the desired 4,6-diaminopyrimidine **23**.*[104]

1.7 Aims

In this project, we intend to synthesise novel second generation 2,4-diamino-pyrimidines **24** as potential antimalarial agents (**Figure 22**). Ideally, we would prefer to synthesise analogues were Y = O mainly due to the high molecular modelling scores observed for these analogues. However, due to the structural similarities between the two derivatives, we are optimistic about the potential biological activity of both the Y = O and Y = C analogues against *Pf*DHRF. Considering that the Sonogashira reaction was unsuccessful when the pre-functionalised acetylene substrate was utilised to couple with compound **18** (**Scheme 4**), we plan to utilise the transition metal-mediated coupling reaction methodology outlined for the synthesis of 2,4,6-triaminopyrimidine **23**, to synthesise 2,4-diamino-pyrimidines **24**, where Y = C. We plan to design and develop a synthetic route towards oxygen-containing analogues during the course of the research project. Similar to the synthetic approach illustrated in **Scheme 5**, perhaps this series of analogues could potentially be synthesised from a simple oxygen containing acetylene such as propargyl alcohol.

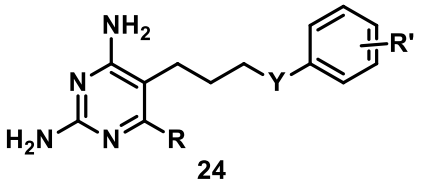

24

R = isopropyl
= *tert*-butyl
= cyclopropyl
= cyclobutyl
= cyclopentyl
= cyclohexyl

R' = Cl, F, Me, OMe

Y = C or O

Figure 22. *Illustration of the proposed pyrimidine analogues with aliphatic alkyl groups or cycloalkyl rings.*

The proposed pyrimidine analogues are intended to target *P. falciparum* DHFR. Based on the knowledge attained from the 1st generation of pyrimidines, we plan to synthesise pyrimidines with an aliphatic group at position 6 instead of the phenyl ring to improve activity against drug resistant *P. falciparum* strains. The target compounds will maintain the structural features of the active dihydrotriazine, i.e, a heteroatomic ring system bonded to a 4-atom linker at C-5, which separates the heteroatomic ring system from a substituted phenyl ring (**Figure 22**). However, the heteroatomic ring will be a fully aromatic pyrimidine ring. In light of the failure to produce β-ketonitrile substituted with the 4-atom linker chain, from derivatives using aliphatic cyclohexyl and cyclopropyl esters, the second-generation pyrimidines will be synthesised by a different synthetic. We aim to design a synthetic procedure that applies basic concepts of green chemistry where possible, such as the use of environmentally friendly reagents and solvents. The synthesised analogues will be tested for activity against wild type and mutant *Pf*DHFR enzymes. Moreover, their antiplasmodial activity will be tested in a whole cell assay against drug sensitive and resistant *P. falciparum* strains.

1.7.1 Proposed Methodology

Our proposed synthetic route as outlined in **Scheme 6** will be initiated by formation of the 2,4-diaminopyrimidine ring system **25** in two steps from commercially available aliphatic esters **26**. These esters will be utilised to acylate acetonitrile in the presence of a base to afford the β-ketonitrile products **27**. The variety in the esters will provide a library of different analogues that can be synthesised from the proposed synthetic route. The nitrile products will undergo a further chemical reaction with guanidine

hydrochloride to give the aromatic pyrimidine ring **25**, followed by an iodination reaction of the pyrimidine ring. Coupling of compound **28** with ethynyltrimethylsilane using palladium catalysis will give compound **29**. This type of reaction is commonly known as a Sonogashira cross-coupling reaction, utilised in preparation of arylalkynes.[105] Usually, the Sonogashira coupling is carried out in the presence of catalytic amounts of a palladium (II) complex as well as copper (I) iodide in an amine solvent.[105] Deprotection of TMS will be carried out in the presence of TBAF to give compound **30**, a precursor which undergo a second transition metal-coupling reaction with **31** to give 1,3-diyne **32**, which further undergoes reduction to give the 2,4-diaminopyrimidine derivative **24.**

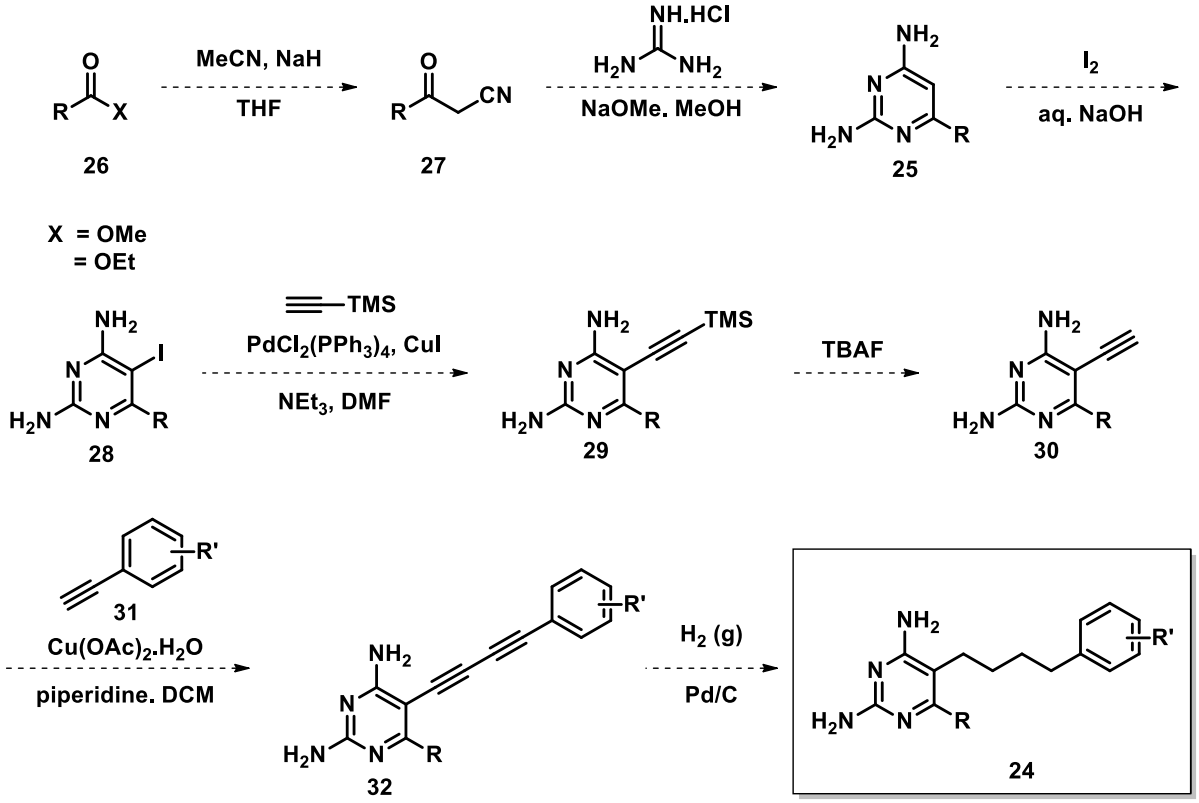

Scheme 6. *Proposed synthesis towards synthesis of second generation pyrimidines.*

2 CHAPTER 2: Results & Discussion

2.1 Development of synthetic procedure

The aim of this project is to develop a synthetic procedure for the formation of novel 2,4-diaminopyrimidine derivatives **24** bearing aliphatic groups at the C-6 position (R= cyclopropyl, *tert*-butyl, isopropyl, cyclopentyl and cyclohexyl) (**Scheme 6**). In this chapter we discuss the development of the synthetic procedure starting with the synthesis of β-ketonitriles **27** from commercially available aliphatic esters **26**.

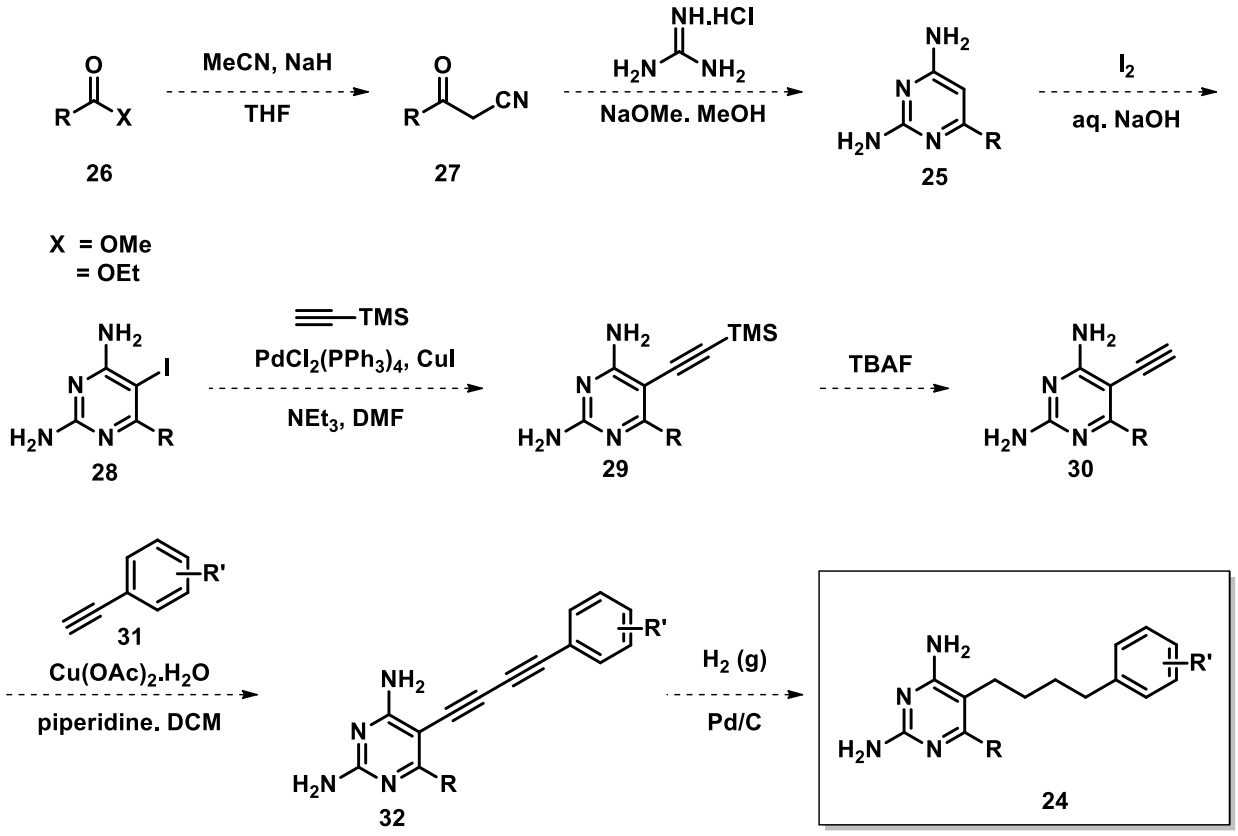

Scheme 6. *Proposed synthesis towards synthesis of second generation pyrimidines.*

In summary, the β-ketonitrile synthons **27** we hoped would undergo a condensation reaction with the nucleophilic guanine to form a heteroatomic aromatic ring system **25**. Successful formation of this 2,4-diaminopyrimidine ring scaffold we believed would give rise to the halogenated-aryl ring essential for coupling with trimethylsilylacetylene (TMS-acetylene) via the Sonogashira reaction, a Pd-catalysed cross coupling reaction. The transition-metal catalysed reactions serve as key steps in the synthetic

route. They introduce C≡C bonds which can further be reduced to the desired novel 2,4-diaminopyrimidine derivatives **24** via a Pd/C catalysed hydrogenation reaction.

2.1.1 Introduction to β-Ketonitriles

β-Ketonitriles are versatile building blocks that are highly exploited in the synthesis of various complex heterocycles such as pyrimidines,[106] pyrazoles,[107] pyrans[108] and thiazolidines.[109] These heterocycles are important structural components of biologically active compounds utilised as pharmaceuticals. Development of efficient synthetic procedures for the formation of β-ketonitriles remains an ongoing area of interest due to their applications in organic synthesis. There are several strategies employed for the synthesis of these intermediates such as (i) the ring opening of isoxazole, (ii) electrophilic cyanation, (iii) nucleophilic cyanation, (iv) metal-catalysed carbonylative coupling, and (v) acylation of nitriles by esters under basic conditions, a strategy we are particularly interested in applying (**Figure 23**).[110] Ring opening of isoxazoles is an indirect approach to making β-ketonitriles. The method requires breaking of the O-N bond in the isoxazole ring, which can be facilitated by electron attachment.[111] Electron attachment is a chemical process where an electron attaches to a neutral molecule, in this case isoxazole. Cleavage of the bond results in formation of an anion with a conjugated π-system, which undergoes a base-promoted elimination reaction to form the nitrile functional group.[112] The resulting hydroxyl-alkene-nitrile can tautomerise from the enol to the keto form affording the desired β-ketonitrile intermediates.

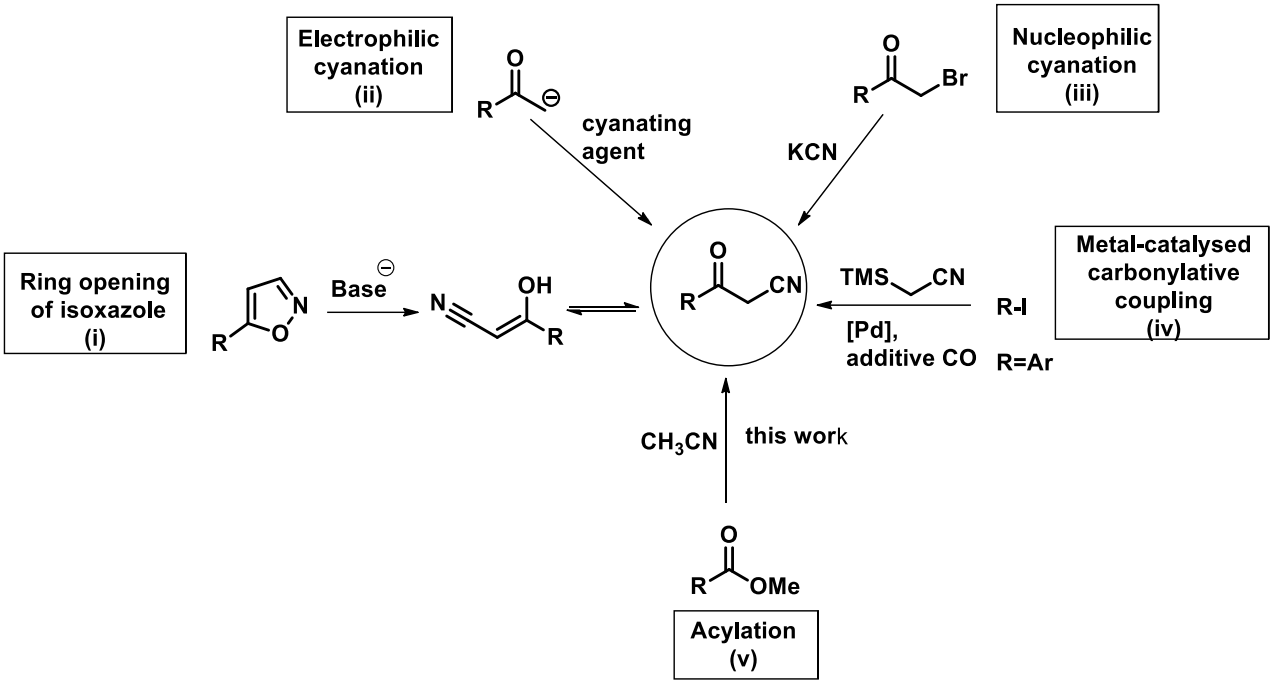

Figure 23. *Protocols applied to synthesise β-ketonitriles such as (i) the ring opening of isoxazole, (ii) electrophilic cyanation, (iii) nucleophilic cyanation, (iv) metal-catalysed carbonylative coupling, and (v) acylation of nitriles.*

Electrophilic cyanation is a more direct β-ketonitrile forming strategy in comparison to the ring-opening of isoxazole, where ketone derived enolates or enolate equivalents are cyanated by reagents such as *p*-toluenesulfonyl cyanide, cyanogen chloride and 1-cyano-3,3-dimethyl-1,2-benziodoxole.[110] Although the cyanating reagents are good sources of electrophilic cyanates, some are also highly toxic and hazardous. For instance, cyanogen chloride is a volatile and toxic chemical that reduces the concentration of oxygen. When inhaled, it hinders the body's ability to use oxygen. During oxidative phosphorylation in the mitochondria, the cyanide disrupts the electron transport chain by binding to cytochrome C oxidase, a terminal enzyme in the mitochondrial oxidative pathway that catalyses the transfer of electrons from reduced cytochrome C to oxygen.[113] Inhibition of the enzyme prevents electron transfer to oxygen and hinders ATP production.[114] This results in cellular hypoxia and metabolic acidosis leading to death.[114] The use of toxic cyanating reagents has limited the use of the method in organic synthesis.

Nucleophilic cyanation relies on the acylation of metalated nitriles by α-haloketones.[110] In this strategy, α-haloketones are electrophiles containing a halogen-atom that serves

as a leaving group upon nucleophilic attack by nitrile anions. The method offers the most effective approach in synthesis of β-ketonitriles, however, it suffers from setbacks concerning the use of hazardous and toxic reagents as well as harsh reaction conditions.[10] The harsh anionic conditions are incompatible with electrophilic functional groups, and therefore limits the substrate scope of the procedure. Transition metal-catalysed carbonylative coupling reactions were developed as an alternative approach to increase electrophilic substrate scope when synthesising β-ketonitriles.[115]

Schoenberg and Heck were the first to report a palladium-catalysed carbonylation coupling of aryl halides with carbon monoxide (CO) and amine nucleophiles in 1974.[116] Since then, the procedure has been utilised to synthesise carboxylic acids, aryl ketones and aryl aldehydes.[117] The direct synthesis of β-ketonitriles using the procedure was only reported in 2012.[117] Benzoylacetonitriles were successfully synthesised from a palladium-catalysed carbonylation coupling reaction of substituted aryl iodides and trimethylsilylacetonitrile under CO atmosphere. The reaction procedure has a broad substrate scope as it can accommodate various substituents on the iodinated aryl starting material.

In a quest to find an alternative approach to synthesise benzoyl acetic esters other than the use of the Claisen condensation reaction, Dorsch and McElvain reported the synthesis of β-ketonitriles using acylation protocols in their experimental methodology.[118] The α-benzoyl alkyl cyanide derivatives were synthesised by condensation of ethyl benzoate with alkyl-nitriles by means of an ethoxide anion and the yields varied from 53 to 60%. Even though the yields were not exceptionally high, they were acceptable bearing in mind the mild reaction conditions. The reaction proceeded more efficiently when using a stronger base, sodium amide, with yields ranging between 54 and 94% (**Scheme 7**).[119] Under these strongly basic conditions, aliphatic nitriles bearing an α-hydrogen atom such as acetonitrile can undergo two different types of reactions: (i) the desired acylation of the nitrile by the ester or (ii) addition of the amide anion to the nitrile C-atom to yield an amidine side product.[120] Although amidine formation was possible, the reaction conditions are believed to favour the former type of reaction because of the high yields obtained from acylations.[119] The harsh basic conditions did not negatively affect acylation reactions but promoted efficient production of the desired β-ketonitriles. This is a positive

outcome for future development of acylating procedures using strong bases in the presence of acetonitrile as a reagent.

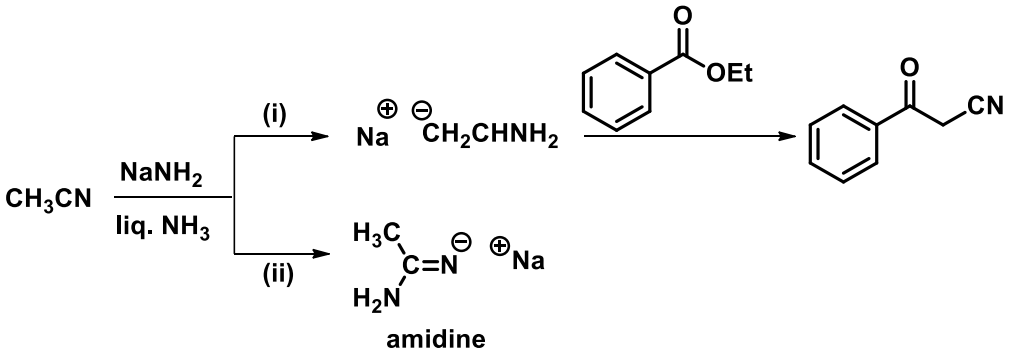

Scheme 7. *(i) Acylation of aliphatic nitriles with esters and (ii) amidine formation in the presence of sodium amide.*

When the 1st generation of 2,4-diaminopyrimidines **8** were synthesised in our laboratory, acylations of alkyl-nitriles were successfully achieved by reaction with ethyl benzoate (**Scheme 2**, **Chapter 1**).[98] The reaction was conducted in the presence of potassium *tert*. butoxide (*t*-BuOK) as a base and tetrahydrofuran (THF) at room temperature for 18 hours. The products were isolated in exceptionally high yields ranging from 63% to 94%. Regrettably, these reaction conditions were not feasible when applied to aliphatic esters as illustrated in **Scheme 3** of the previous chapter. Therefore, development of a new synthetic approach using aliphatic esters was required. *t*-BuOK is a relatively mild base, and it was speculated that replacing it with a stronger base could improve the feasibility of the acylation reaction by aliphatic esters. Various research groups have reported acylation of acetonitrile by both cyclic and linear aliphatic esters in the presence of sodium hydride (NaH) as a base.[121–124] NaH is a strong base and a good source of hydride (H^-) nucleophile. However, the harsh nucleophilic conditions are of concern in relation to the use electrophilic esters. Under such conditions, the esters can undergo hydride reduction and form alcohols. This side reaction could negatively affect yields for the acylation reaction. Similarly, harsh basic conditions are favourable for acetonitrile to undergo deprotonation of the α-hydrogen giving the desired nitrile anion, which is the reactive species in acylation or self-condensation.[120] Due to the competitive nature of the side reactions, the order in which the reagents were added to the reaction pot was important. From the reports, NaH was heated to 70 °C in tetrahydrofuran THF followed by the dropwise addition of

the appropriate ester and acetonitrile mixture. Reported yields were high, ranging from 70% to quantitative.[121–124] One can deduce that the simultaneous slow addition of acetonitrile and the ester minimises formation of the competing side products. It is worth noting that the β-ketonitriles were isolated without any further purification. We plan to adopt this approach to synthesise the desired aliphatic β-ketonitriles required for the preparation of the proposed 2nd generation pyrimidines **24**.

2.1.1.1 Formation of β-ketonitriles using NaH

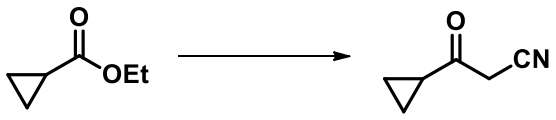

33a **34a**

Scheme 8. *Reagents and conditions; CH_3CN, NaH, THF, 70 °C, 16 h.*

We began the synthesis of β-ketonitriles starting from commercially available ethyl cyclopropane carboxylate **33a**. The choice of the ester was informed by the molecular modelling results, which showed that 2,4-diaminopyrimidines bearing a cyclopropyl ring at C-6 displayed the highest activity against both the wild type and quadruple mutant *Pf*DHFR model. As expected, we sought to develop a synthetic procedure for this class of analogues. To prepare 3-cyclopropyl-3-oxopropanenitrile **34a**, we followed the synthetic procedure reported by Getlik in 2012.[122] They synthesised compound **34a** by means of a condensation reaction between acetonitrile and methyl cyclopropane carboxylate in the presence of NaH at 70 °C, to afford 96% of the desired β-ketonitrile product as an orange solid. Unfortunately, attempts to reproduce their results were unsuccessful. Under the described reaction conditions, we recovered 24 % of the product as a yellow oil. Although the significant difference in the physical description of the product was questionable, high yields reported by other research groups for the condensation reactions of acetonitrile with aliphatic esters affirmed the feasibility and effectiveness of the reaction. [121,123,124] Additionally, the low yields came as no surprise considering the side reactions that can compete with formation of the β-ketonitrile product. For instance, NaH does promote reduction of the electrophilic ester to form its' alcohol equivalent by-product. Therefore, complications associated with side reactions could not be overlooked. It is worth noting that the product was not isolated crude, it contained impurities that were removed after purification by silica gel

column chromatography. The characterisation NMR spectra of the isolated by-products were inadequate to make a conclusive identification; however, some of the by-products contain the distinct cyclopropyl moiety.

To optimise the yields and minimize formation of the by-products, the reaction was set at reduced concentration, i.e. double the amount of solvent was utilised in an attempt to minimise formation of the by-products. This was in accordance with the collision model, which illustrates that in order for a reaction to occur, molecular components such as atoms and ions have to collide.[125] When these components are in close proximity to each other, they are more likely to come into contact and undergo a chemical reaction. The more dilute a reaction mixture, the more disperse the substances are from each other, consequently reducing the likelihood to collide. Unfortunately, the diluted concentration also affected the desired condensation reaction between the ester and acetonitrile. The product was isolated in 10% yield.

2.1.1.2 Formation of β-ketonitriles using *t*-BuOK in 2-Me THF

Failure to optimise yields for the condensation reaction led to the development of a green approach towards the synthesis of β-ketonitriles from esters.[126] The approach entails preparation of β-ketonitriles from acylation of acetonitrile by means of 2 mole equivalents of *t*-BuOK and 1 mole equivalent of the esters. The reaction was conducted at room temperature in the presence of a catalytic amount of isopropanol and 2-Me THF as a solvent. This approach follows a typical Claisen condensation reaction mechanism, initiated by deprotonation of acetonitrile facilitated by a base. The resulting anion undergoes a nucleophilic addition to the ester, followed by elimination of the alkyl-oxide group to give the desired products.

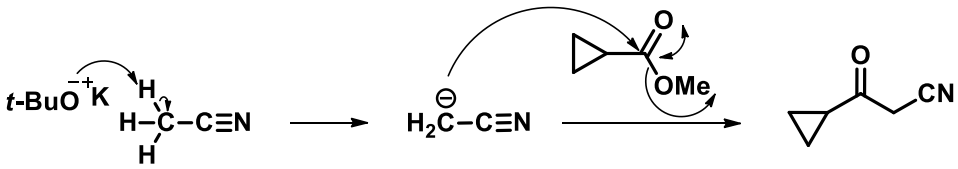

***Scheme 9**. Mechanism of the condensation reaction.*

Although the role IPA plays to facilitate formation of the β-ketonitriles is not conclusively determined, the presence of the alcohol does seem to promote feasibility of the reaction. Previous unsuccessful acylation reactions of alkyl-nitriles with aliphatic esters were conducted in the absence of IPA. We propose that catalytic amounts of

IPA increase the dielectric constant of the solvent, thereby increasing solubility of *t*-BuOk in the solvent system. Accessibility of *t*-BuOk promotes deprotonation of acetonitrile giving the nucleophilic $\bar{C}H_2CN$ anion that attacks the ester. Furthermore, IPA might be protonating the anion of the product to minimize side products.

There are several environmental benefits to the present methodology such as the use of a green solvent. 2-Methyl THF is a green solvent produced from direct reduction of furfural,[127] a furan aldehyde derived from lignocellulose biomass of corncobs. The use of biomass is an important principle in green chemistry. Currently, the majority of raw materials used in organic chemistry are derived from petroleum feedstock.[128] High demand in petroleum energy sources pose serious threats to the depletion of natural fossil fuel reservoirs. Exhaustion of these resources will have a negative impact on accessibility of many raw materials and the economy. The need for sustainable resources for both raw materials and energy has never been more crucial. Biomass is carbon rich and the major source of sustainable feedstock available.[129] The residues of corncobs are good sources of bio-based chemicals and their exploitation do not add to the concerns of utilising limited resources as opposed to the use of fossil-fuel based chemicals.[130] Additionally, since furfural is derived from non-edible waste residues, production of 2-Me THF does not compete with present food sources. For these reasons, 2-Me THF has the potential to replace THF in organic synthesis.[131]

THF is one of the most commonly used solvents in organic synthesis and its application as a solvent is broad, ranging from reactions such as the Sonogashira or Suzuki-cross- coupling reaction, to organometallic reactions such as the Grignard reaction. 2-Me THF has a boiling point of 80 °C which is higher than that of THF, and a freezing point of -136 °C, which is than THF. By virtue, it can be utilised in reactions that require higher or lower temperatures than THF.[131] Moreover, THF is partially miscible in water, a characteristic that makes 2-Me THF favourable over THF in water sensitive reactions.

The present synthetic method to from β-ketonitriles takes presidence over the preceding approach. In addition to the use of a green solvent, *t*-BuOK serves as a strong enough base to abstract an α-hydrogen atom from acetonitrile while providing mild conditions compatible with the electrophilic ester. Fortunately, for reactions with electrophilic functional groups susceptible to nucleophilic attack, *t*-BuOK does not

display the dual nature observed in NaH, thereby limiting formation of competing by-products. The relatively weak nucleophilic nature of *t*-BuOK is predominantly due to its bulky geometry. The bulky structural configuration does not favour nucleophilic substitution reactions because of the high possibility of steric hindrance. Therefore, *t*-BuOK is a better base than NaH in relation to the acylation reaction under these conditions. Unlike the previous method set at 70 °C, the current method is conducted at room temperature. This is particularly beneficial because the reaction consumes very little electrical energy to achieve and the set reaction temperature is compatible with a wide spectrum of reagents, especially those that are temperature sensitive. To top it all, the significant reduction in the reaction time from 16 hours to 2 hours, makes the new approach even more attractive because it is less time consuming.

In hindsight, the newly developed procedure is similar to the method used for the 1st generation pyrimidines **8**. Similar to our methodology, they synthesised β-ketonitriles using ethyl benzoate and *t*-BuOK as a base in the presence of THF at room temperature. Although they did not use IPA, reasons to why the acylation reaction did not work when ethyl cyclohexanecarboxylate and ethyl cyclopentanecarboxylate where used as esters are not clear. There are several reasons that could possibly account to failure of the acylation reaction; Geometric configuration of cyclic aliphatic esters, electrophilicity of the carbonyl-carbon or the methoxide leaving group. Although methoxides are good leaving group, replacing it with a better leaving group such as halogens could potentially improve feasibility of the reaction Taking into account that the esters were subjected to an acylation reaction with a secondary nitrile, whereas in our case, we utilised acetonitrile which is a primary nitrile. Possibly, steric hindrance could be contributing to the failure of the acylation reaction. Considering that the employed aliphatic esters have a “chair” 3D-geometric configurations. Perhaps their 3-D structures are too bulky thereby exerting steric effects when in contact with their respective coupling nitriles.

Subjecting acetonitrile to an acylation reaction with ethyl cyclopropane carboxylate **33a** facilitated by *t*-BuOk in the presence 20 mol % isopropanol and 2-Me THF as a solvent resulted in formation of the desired β-ketonitrile **34a** in 48% yield. Since both the starting material and the product are aliphatic, a potassium permanganate stain was utilised to assist when monitoring

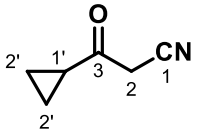

34a

the reaction progress by thin layer chromatography (TLC). The TLC did confirm the presence of starting material and the product after completion of the set time. The β-ketonitrile product was isolated from the starting material by silica gel column chromatography. Successful acylation of acetonitrile was confirmed by the presence of the distinct CH_2 peak at δ 3.65 ppm in the ^1H NMR spectrum. The peak is an important indicator that deprotonation of an α-hydrogen atom of acetonitrile took effect, giving the anion that attacks the electrophilic ester to form the β-ketonitrile. The methylene carbon corresponds to a peak appearing at δ 33.0 ppm on the ^{13}C NMR spectrum. Presence of the nitrile carbon was confirmed by a signal appearing at δ 114.5 ppm on the ^{13}C NMR spectrum, giving further evidence to the successful acylation of acetonitrile by the ester **33a**.

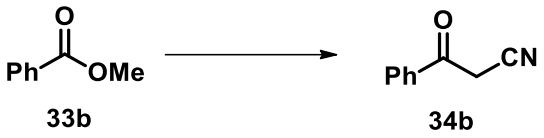

33b **34b**

Scheme 10. *Reagents and conditions; CH_3CN, t-BuOK, THF/ 2-Me THF, rt.*

In an attempt to optimise the yield of the reaction, we utilised an aromatic ester **33b** to probe the reaction conditions. The ester was selected because it does not contain an enolisable hydrogen atom α to the carbonyl carbon, which are prone to deprotonate under basic conditions, consequently promoting self-condensation of the ester. Using an ester without the α-hydrogen atom could potentially limit formation of by-products and favour the desired acylation reaction. Additionally, working with aromatic substrates makes it easier to monitor the progress of the reaction via TLC since they are UV-active, in comparison with monitoring the condensation reaction of an aliphatic ester as a starting material, which required the use of a permanganate stain. Methyl benzoate **33b** was subjected to similar reaction conditions as compound **33a**. We initially treated the ester with 1 eq. of *t*-BuOK and 1 eq. of acetonitrile in the presence of 20 % isopropanol and THF as a solvent for 2 hours (**Table 1**, entry 1). This afforded a low yield of 11 % of the product. Increasing molecular equivalents of the base and acetonitrile from 1 mol equivalent to 2 mol equivalents, increased the yield of the reaction from 11% to 23 % (entry 2). Changing the solvent from THF to 2-Me THF increased the reaction yield significantly to 49 % (entry 4). The remarkable increased yields due to change in solvent could be due to low water miscibility of 2-Me THF, in

comparison to THF, resulting in more product extraction during the work up stage. It is worth noting that upon monitoring the reaction by TLC, both the ester and the desired β-ketonitrile were observed and almost all the unreacted starting material was recovered. If we base the yield of the condensation reaction solely on the reacted starting material, then the yield of the reaction is calculated to 99%. Since only half of the starting material was consumed in the set 2 hours, we decided to carry out the reaction for an extended 16 hour duration. After this time, no significant difference was observed between the amounts of reacted and unreacted starting material, as compared to the 2 hour duration (entry 5).

Table 1. *Summary of reaction conditions applied to optimise the green, t-BuOK approach for the formation of* ***34b*** *from* ***33b****.*

Entry	MeCN	*t*-BuOK	Solvent	Dosing	Duration (h)	Yield (%) 34b
1	1.0 eq.	1.0 eq.	THF	no	2	11
2	2.0 eq.	2.0 eq.	THF	no	2	23
3	1.0 eq.	1.0 eq.	2-Me THF	no	2	46
4	2.0 eq.	2.0 eq.	2-Me THF	no	2	49
5	2.0 eq.	2.0 eq.	2-Me THF	no	16	50
6	2.0 eq.	2.0 eq.	2-Me THF	yes	2	47 - 59
7	3.0 eq.	1.0 eq.	2-Me THF	yes	2	48

Isolation of the starting material indicated that the reaction did not fully go to completion; at some point, the reaction reaches equilibrium. Using the Le Châtelier's principle to drive the equilibrium towards formation of the β ketonitrile product **34b**, [132] an equivalent of *t*-BuOK and of acetonitrile was added at the beginning of the reaction, and an additional equivalent was added an hour after the reaction had commenced (entry 6). Subjecting the reaction to an additional mole equivalent of the reagents was intended to disturb the equilibrium, which in response will utilise the added reagents to re-establish equilibrium by formation of the desire β ketonitrile. In this attempt; a yield of 47 % product was isolated from the reaction. Upon repeating the methodology to build enough material for subsequent synthetic steps, the yields were improved to 59% as a result of continuous extraction of the product during the workup stage. With

frequent repeats of the reaction we noticed that the β-ketonitrile products are polar and therefore were likely to remain in the aqeous layer. We therefore did multiple extraction of the organic layer to ensure optimum isolation of the product. Utilisation of higher equivalents of acetonitrile did not have significant effect on the yield (entry 7).

The method was applied to several other aliphatic and aromatic esters to test the spectrum of substrates that can be converted to β-ketonitriles using the approach. A summary of all the ester substrates tested was reported in 2019.[126] **Scheme 11** below summarises the aliphatic esters that we particularly were interested in exploring. In addition, **Tables 2** and **3** below provide evidence of the formation of the β-ketonitriles from their respective esters.

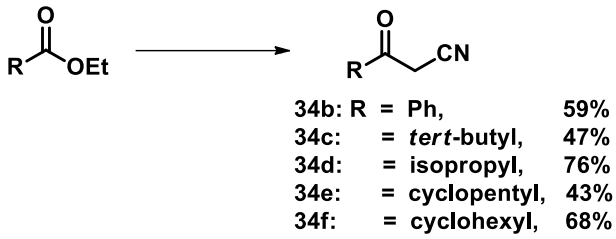

Scheme 11. *Reagents and conditions; CH_3CN, t-BuOK, IPA, 2-MeTHF, rt, 2 h.*

Table 2. *Key signals in the ^1H NMR spectra of the β-ketonitriles **34b-f**.*

Entry	Prod. #	-CH_2-CN (ppm)
1	**34b**	4.10
2	**34c**	3.63
3	**34d**	3.56
4	**34e**	3.53
5	**34f**	3.53

Table 3. *Key signals in the ^{13}C NMR spectra of the β-ketonitriles **34b-f**.*

Entry	Prod. #	C=O (ppm)	CN (ppm)	CH_2-CN (ppm)
1	**34b**	187.3	113.9	29.5
2	**34c**	202.8	114.2	27.5
3	**34d**	201.7	114.2	30.1
4	**34e**	200.2	114.2	31.2
5	**34f**	200.7	114.2	30.4

With the β-ketonitriles in hand; we now set about utilising these key intermediates in the formation of the suitably substituted pyrimidine rings.

2.1.2 Introduction to pyrimidine ring systems

Pyrimidines are six-membered aromatic systems containing two nitrogen-atoms. They are characterised by the 1,3-position the N-atoms hold in the aromatic ring (**Figure 24**). The pyrimidine core is an important structural feature found abundantly in nature. Many natural molecules such as DNA nucleoside bases, vitamins and alkaloids harbour the pyrimidine ring, as illustrated in **Figure 24**.[133]

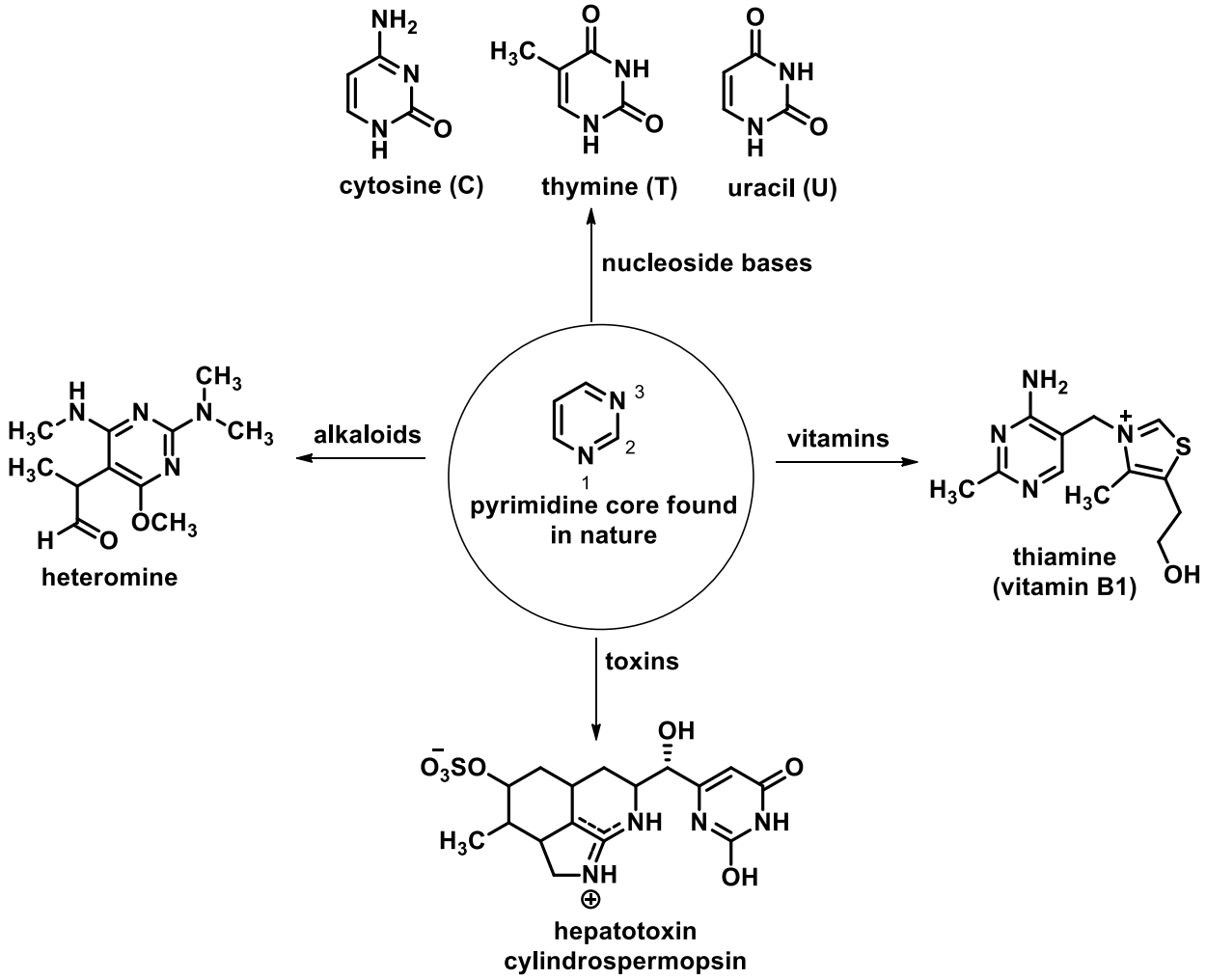

Figure 24. *Illustration of 1,3-diazine ring and structural pyrimidine derivatives found in nature.*

Additionally, the pyrimidine ring is a pharmacophore found in many biologically active compounds used in the treatment of malaria,[7,83] cancer,[134] bacterial infections,[78,79,135] and AIDS caused by the human immunodeficiency virus (HIV).[136] Pyrimethamine and

sulfadoxine (**Figure 25**) are antimalarial chemotherapeutic agents that target folate metabolism. These chemotherapeutic compounds have a common mode of action; they target key enzymes in folate metabolism and inhibit their metabolic catalytic function. Inhibition of folate metabolism halts DNA replication, and ultimately leads to cell death. Pyrimethamine is an antifolate that targets DHFR in the folate metabolic pathway, an enzyme that catalyses the reduction of DHF to THF, an important co-factor in DNA synthesis. Pyrimethamine is used in combination with cycloguanil as the first line treatment for uncomplicated malaria cases. Sulfadoxine is an antifolate that targets the *de novo* enzyme, DHPS, an enzyme exclusive to the parasite. Therefore, antifolates that target DHPS selectively function against the *Plasmodium* parasite. Trimethoprim and iclaprim are antifolates used to treat bacterial infections. They act by inhibiting the catabolic reaction facilitated by DHFR.

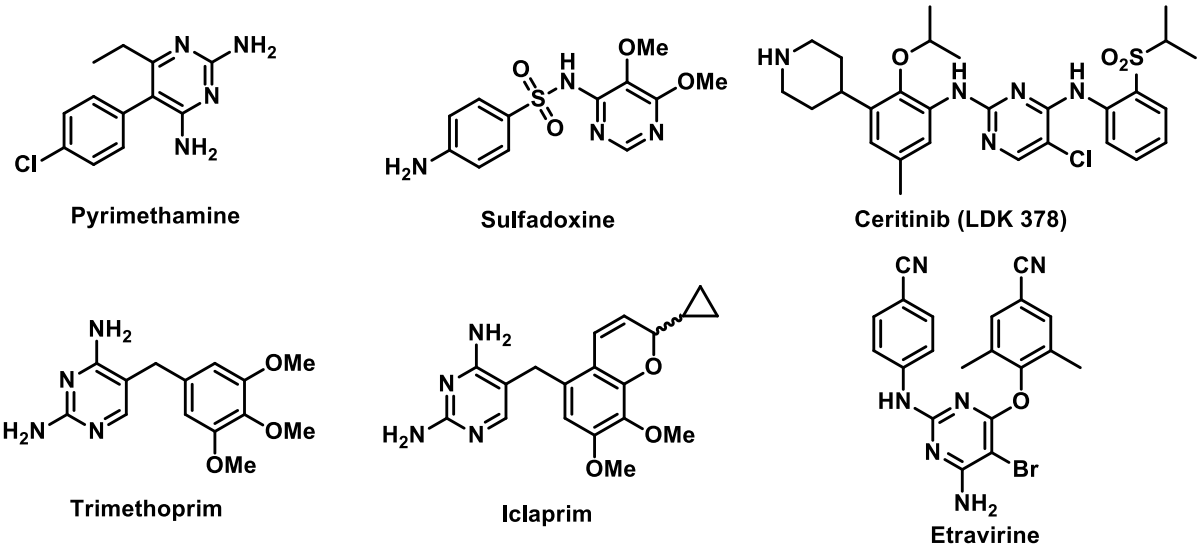

Figure 25. *Chemical structures of biological actives bearing the pyrimidine core such as pyrimethamine, sulfadoxine, ceritinib, trimethoprim, Iclaprim and etravirine.*

Ceritinib is an anaplastic lymphoma kinase (ALK) inhibitor approved to treat non-small cell lung cancer (NSCLC).[137] ALK is an enzyme-linked receptor encoded by the human genome, commonly activated when a ligand binds to its extracellular ligand-binding domain. Ligand-receptor interactions result in homo-dimerization leading to conformational changes required for the expression of enzymatic activity.[138] In the absence of the ligand, ALK is inactivated by means of de-phosphorylation. [138] ALK activates multiple pathways that are important for cell growth, transformation and anti-apoptotic signalling. [138] Many forms of human cancers seem to involve genetically

altered ALK variants in their pathogenesis.[139] These genetic alterations can occur as a result of mutations in the gene encoding ALK, gene amplification or chromosome rearrangement. Genetic alteration of ALK leads to continuous activation of the receptor. The aberrant continuous activation of ALK is thought to drive carcinogenesis. Ceritinib displayed high potency against NSCLC harbouring the ALK gene rearrangements.[139] It acts by inhibiting ALK autophosphorylation.

Etravirine is a diarylpyrimidine analogue used in the treatment of HIV-infected patients. It falls under the umbrella of chemotherapeutic agents commonly known as non-nucleoside reverse transcriptase inhibitors (NNRTIs). They inhibit HIV by binding to the enzyme reverse transcriptase.[140] The diarylpyrimidine-enzyme interaction is non-competitive because the NNRTI binds to the hydrophobic allosteric binding site instead of the catalytic active site.[136] Binding of the ligand induces a change in enzyme configuration, preventing the viral single-stranded RNA genome from binding to the enzyme, thereby preventing viral RNA transcription to DNA.[140]

2.1.2.1 Formation of pyrimidine-ring systems

Synthesis of pyrimidine ring scaffolds dates back to 1818, when the Italian chemist Luigi Brugnatell prepared alloxan by oxidation of uric acid using nitric acid (**Scheme 12** (a)).[133] Alloxan is synthesised by the degradation of another heteroatomic ring. The protocol is different to the principal synthetic method that involves a condensation reaction between C-C-C fragments with N-C-N fragments.[141] Formation of pyrimidine scaffolds using the principal synthetic method generally entails building the heterocyclic ring with most of its substituents already in place, where the heteroatom fragment is ordinarily the nucleophile while the carbon atoms serve as electrophiles. Following the synthesis of alloxan, one of the early pyrimidines, Edouard Grimaux pioneered a synthetic procedure to afford a pyrimidine scaffold using a condensation reaction. This synthetic procedure is currently utilised as the principal synthetic method for making pyrimidine ring systems. In 1879, he reported synthesising barbituric acid from a condensation reaction between malonic acid and urea in the presence of phosphoryl chloride (**Scheme 12** (b)).[142] The reaction mechanism is similar to that of the Claisen-condensation, where the nucleophile attacks the electrophilic carbonyl-carbon. The methodology was extensively explored using 1,3-dicarbonyl compounds as C-C-C synthons.[141] Linking unsymmetrical C-C-C

with unsymmetrical N-C-N fragments brings about variation in the development of pyrimidine derivatives.

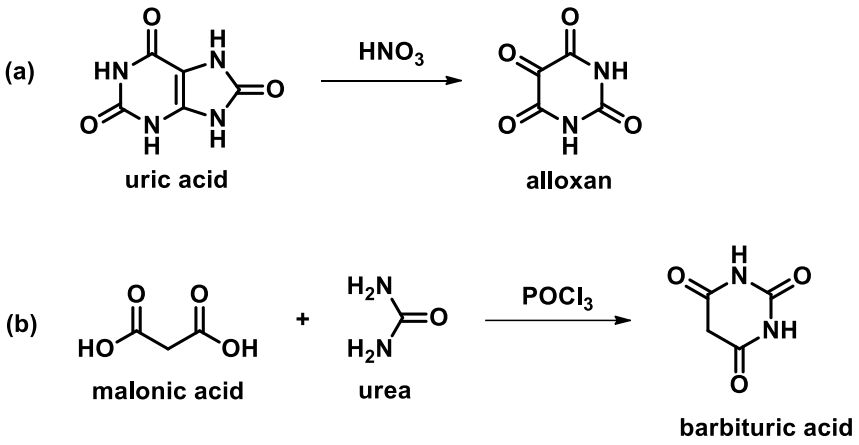

Scheme 12. *(a) Nitric acid oxidative degradation of uric acid to form alloxan. (b) Condensation reaction of malonic acid and urea in the presence of $POCl_3$ to form barbituric acid.*

In the quest to synthesise 2,4-diaminopyrimidine derivatives as antimalarials, George Hitchings and colleagues (1951) followed a 3-step synthetic procedure towards the formation of 2,4-diaminopyrimidines initiated by condensation of dicarbonyl synthons such as β-ketoesters with guanidine.[143] Condensation of α-benzyl-β-ketoesters **35** with guanidine in basic conditions resulted in the formation of aminohydroxypyrimidines **36**, which further underwent chlorination by treatment with $POCl_3$, then amination (**Scheme 13**). Formation of the pyrimidine scaffold was not feasible through condensation of β-ketoester analogues with ortho-substituents (R') on the benzyl-ring.[144] Ineffectiveness of the condensation step was also observed in the use of β-ketoester analogues with electron donating groups such as methoxy-group.[144] Limitations in the substrate scope of the condensation of dicarbonyl synthons with guanidine prompted the search for alternative methods to make the pyrimidine scaffold.

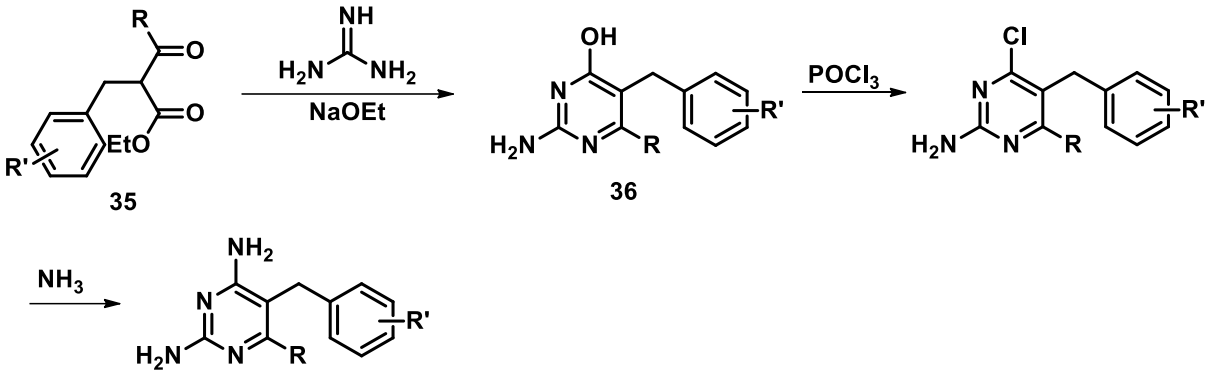

Scheme 13. *Three-step synthetic procedure towards formation of 2,4-diamino-pyrimidines.*

After consideration of several alternative methods, condensation of guanidine with enol ethers in a similar fashion to the principal methodology of synthesising pyrimidine scaffolds seemed promising. Rupe developed the method in 1927,[144] where guanidine was condensed with hydroxymethylenephenacetaldehyde **37**, an enol ether, to form 2-amino-5-phenylpyrimidine **38** (**Scheme 14** (a)). Grewe also confirmed the effectiveness of using an enol-ether as the C-C-C substrate in 1936, by the condensation reaction between ethoxymethylenemalononitrile **39** with acetamidine to give 4-amino-5-cyano-2-methylpyrimidine **40** (**Scheme 14** (b)).[144]

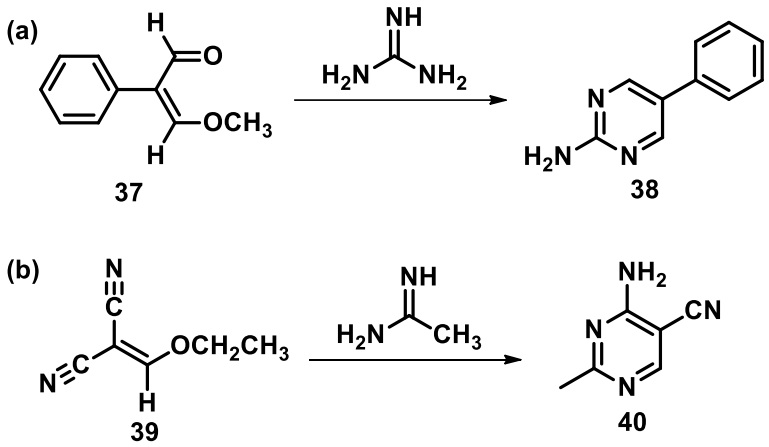

Scheme 14. *Use of enol ethers to synthesise pyrimidines*

With this information in hand, Hitchings *et al.* subjected guanidine to a condensation reaction with β-alkoxy-α-arylcrylonitriles **41** to give 5-aryl-2,4-diaminopyrimidines **42** isolated in high yields (**Scheme 15**). Replication of 2,4-diaminopyrimidine derivatives prepared by functionalisation of the pyrimidine ring (**Scheme 15**) were carried out using the enol ether condensation reaction, it was reported that the yields were greatly

improved. The synthetic procedure is robust enough to allow for various substituents on the phenyl ring, this allows for a wider substrate scope. These enol ethers were prepared from α-acylphenylacetonitrile **43** by reaction with diazomethane. Hitchings and co-workers were the first group to report the synthesis of 2,4-diaminopyrimidines using these types of enol ethers **41**.[144] Since then, many reported synthetic procedures utilised the enol ether intermediate to synthesise the pyrimidine ring scaffold.[145–147]

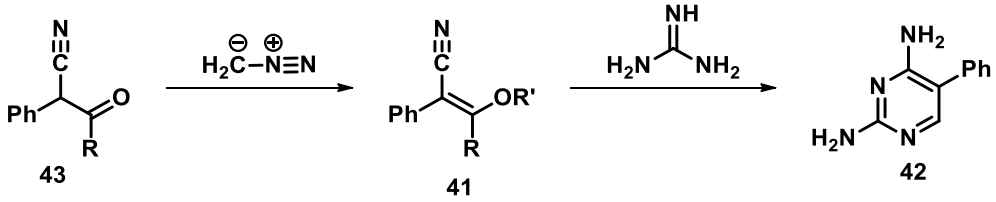

Scheme 15. *Development of the enol ether synthetic method towards synthesis of 2,4-diaminopyrimidine derivatives.*

The first generation pyrimidine derivatives **8** (**Figure 19, Chapter 1**) synthesised in our laboratories were prepared using the enol ether condensation approach, where formation of the enol ethers was achieved via the diazomethane reaction. Due to the risks associated with diazomethane, a safer alternative method to synthesise these heterocyclic ring systems is desirable. In 1975, Ito *et al.* reported the synthesis of 2,4-diamino-6-methylpyrimidine **44** from a condensation reaction between acetoacetonitrile **45** and guanidine in the presence of sodium methoxide (NaOMe) (**Scheme 16** (a)).[148] The reaction mixture set in methanol was heated at reflux for 1.5 hours and afforded the product in 75 % yield. Usually formation of pyrimidines require harsh reaction conditions, set at very high temperatures over extended periods. Therefore, this approach offers synthesis of pyrimidine ring systems with mild reaction conditions over a short period of time. A variety of C-C-C synthons have been utilised in this classic condensation reaction to form pyrimidine ring systems, however, very little has been reported about the synthesis of such scaffolds using β-ketonitriles. We plan to utilise the synthetic method to synthesise our desired 2,4-diaminopyrimidines from the previously synthesised β-ketonitriles (**Scheme 16** (b)).

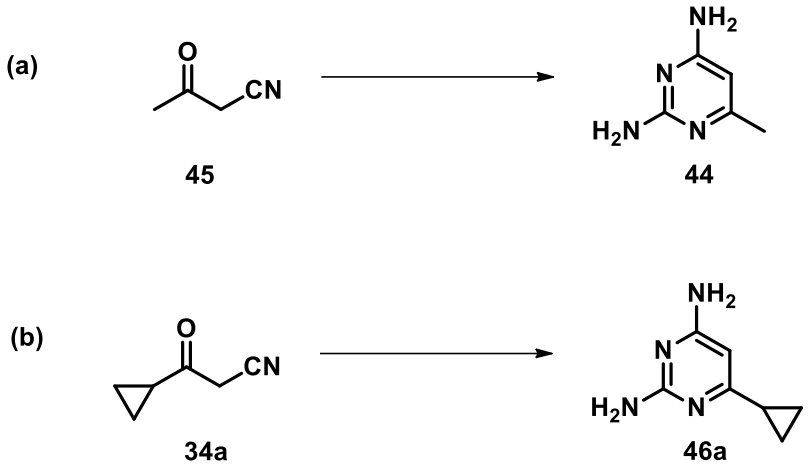

Scheme 16. *Reagents and conditions; guanidine.HCl, NaOMe, MeOH, reflux, 1.5 h.*

With a synthetic approach in hand, we were ready to test the synthesis of 2,4-diamino-6-cyclopropylpyrimidine **46a** from the previously prepared β-ketonitrile **34a** (**Scheme 16** (**b**)). Compound **34a** was subjected to reaction conditions described by Ito *et al.* and the desired pyrimidine ring system was regrettably not isolated.[148] Increasing the reaction time did not improve the feasibility of the reaction. After various failed attempts to synthesise the desired pyrimidine scaffold using conventional heating, we developed an alternative microwave facilitated synthetic procedure inspired by Goswami *et al*.[149] They synthesised a series of functionalised pyrimidines under microwave irradiation from various nucleophilic N-C-N synthons and C-C-C electrophilic sources such as β-dicarbonyl compounds, ethyl cyanoacetate and malonitrile. The reagents, in the presence of potassium carbonate (K_2CO_3) as a base, were subjected to irradiation at 450 W in a domestic microwave oven for 10 minutes and the products were isolated in good yields.

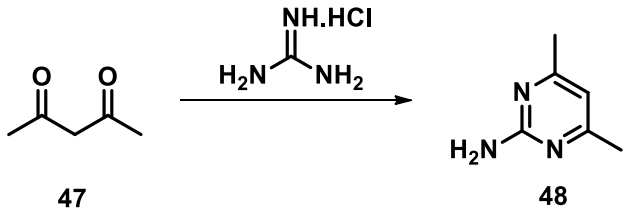

Scheme 17. *Reagents and conditions; K_2CO_3, MW 80 °C, 300 W, 10 min, 42%.*

In a similar fashion, we attempted to reproduce these results using the described microwave conditions to facilitate formation of the pyrimidine ring system using the microwave reactor in our laboratory.[149] We utilised acetylacetone **47** as the electrophilic C-C-C synthon to prepare compound **48** which were isolated as a light brown solid in 42% yield (**Scheme 17**). The obtained yield was significantly lower compared to the one reported by Goswami *et al,* of 96%, for this particular product **48**. Since this was a trial for the feasibility of the cyclisation reaction using our microwave reactor, the reaction was not optimised to further improve the yield. The three signals appearing in the ^{1}H NMR spectrum confirms formation of the pyrimidine ring. The H-atom at position 5 of the pyrimidine ring is responsible for the singlet observed δ 6.29 ppm, whereas the amine group and the two methyl groups are observed at δ 5.70 and 2.22 ppm respectively. The peak appearing at δ 110.3 ppm in the ^{13}C NMR spectrum is for C-5, which is one the key characteristic peaks indicative of the formation of the pyrimidine ring. Since the ring system is symmetrical, the peak for C-4 and C-6 appears at δ 167.7 ppm on the ^{13}C NMR spectrum, and that of C-2 appears at δ 163.2. This was an indication of the successful formation of the pyrimidine ring using the microwave reactor.

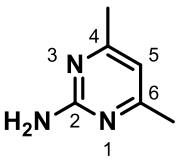

48

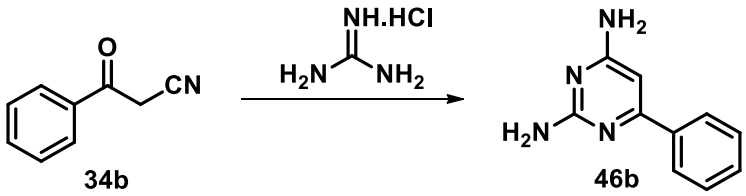

34b **46b**

Scheme 18*. Development of the microwave irradiation approach to synthesise pyrimidine ring systems.*

Having successfully tested the microwave reaction conditions, we were optimistic about formation of pyrimidines from β-ketonitriles via the microwave irradiation technique. We began to explore development of a synthetic approach towards pyrimidine ring systems using the β-ketonitrile we had in abundance, **34b** to afford substituted 2,4-diaminopyrimidine **46b** (**Scheme 18**). One of the many advantages associated with using microwave irradiation in organic synthesis is reduced reaction time.[150] Traditionally, such complex heterocyclic ring systems are formed through conventional heating at high temperatures over extended periods of time. The requirement for high temperatures over extended periods is an ineffective method for

transferring adequate heat energy for the synthesis of heteroaromatic systems. In contrast, microwave irradiation provides efficient internal heat energy by direct coupling of microwave energy with the polar molecules that are present in the reaction mixture. The microwave-assisted synthetic approach offers reduction of the reaction time from 24 hours to less than 30 minutes in some instances.

Table 4. *Summary of reaction conditions applied to achieve and optimise the microwave approach.*

Entry	Base	Solvent	MW conditions	Time (min)	Yield %
1	K_2CO_3	-	ov, 300 W, 80° C	30	No reaction
2	K_2CO_3	Dioxane	ov, 300 W, 80° C	30	No reaction
3	K_2CO_3	Dioxane	cv, 150 W, 150° C	60	No reaction
4	*t*-BuOK	Dioxane	cv, 150 W, 150° C	60	52
5	*t*-BuOK	2-Me THF	cv, 150 W, 150° C	60	41 - 57

MW= microwave, ov= open vessel, cv= closed vessel.

3-Oxo-3-phenylpropanenitrile **34b** was therefore subjected to the solvent-free microwave conditions described by Goswami *et al*.[149] in an attempt to produce 6-phenylpyrimidine-2,4-diamine **46b**, in the presence of guanidine hydrochloride and K_2CO_3. The reaction mixture was irradiated in an open vessel microwave reactor at 300W, at 80 °C for 10 minutes. Unfortunately, no reaction was detected (**Table 4**, entry 1). After several failed attempts to get the reaction to work varying the temperature, power and time, we discovered that a change of base facilitated formation of 6-phenyl-2,4-diaminopyrimidine **46b** (entry 4). The starting material, **34b**, dissolved in dioxane was irradiated with *t*-BuOK as a base in a closed vessel microwave reactor at 150 W, 150 °C for 30 minutes. After this time, a new product spot was evident by TLC, but a significant amount of the starting material was still present. The reaction mixture was subjected to microwave irradiation for an additional 30 minutes. To our delight, the product was isolated as a cream white solid in 52% yield. Dioxane is an ethereal solvent, however the use of dioxane is not recommended owing to the environmental risks associated with it.[151] As an alternative, we tested the feasibility using 2-Me THF in the reaction and 41 % of the product was initially isolated (entry 5). Optimisation of the work up and purification procedure slightly improved the yields to 57%.

Formation of the 2,4-diaminopyrimidine ring system **46b** was confirmed by the presence of the two singlets appearing at δ 6.37 and 6.00 ppm in the ^{1}H NMR spectrum accounting for the newly formed primary amine (NH_2) groups bonded to C2 and C4 on the pyrimidine ring. The distinct appearance of an aromatic proton signal at δ 6.22 ppm was assigned to H5, which further confirmed formation of the aromatic heterocycle. The ^{13}C NMR spectrum provided additional evidence to prove the success of the cyclisation reaction. Key signals owing to C2, C4, C5 and C6, which are characteristic carbon-atoms of the pyrimidine ring, were observed at δ 163.7, 165.2, 90.6 and 162.3 ppm respectively on the analysed ^{13}C NMR spectrum. The presence of the NH_2 groups was further verified by FTIR spectroscopy with two visible peaks at approximately 3293 and 3169 cm^{-1} signalling for an N-H stretch. A molecular ion peak observed at 187.0967 amu upon examination of the HRMS was in agreement with the expected mass of 187.0978 for $C_{10}H_{10}N_4$ $[M + H]^+$.

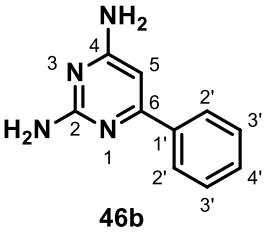

46b

Successful formation of compound **46b** led to the application of the microwave conditions to the previously synthesised aliphatic β-ketonitriles (**Scheme 19**). The yields from this reaction ranged from 29% to 97% depending on the β-ketonitrile used (**Table 5**). Compound **46a**, the lowest yielding product, was synthesised during the early developmental stages of the synthetic procedure. It was therefore synthesised without optimisation strategies employed during the work-up stage and purification of the pyrimidines. HRMS of the scaffolds, as seen in **Table 5**, was in agreement with what was expected in each case. Furthermore, characteristic signals in both ^{1}H NMR and ^{13}C NMR spectra were present (**Tabled 6,7**) Formation of these heteroaromatic scaffolds. In each case, signals for the distinct R groups were also evident.

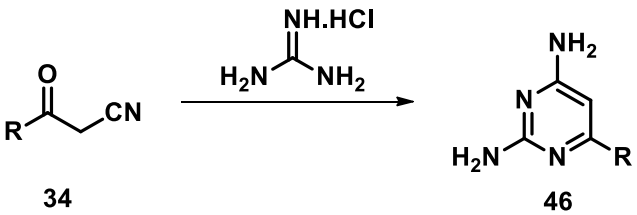

34 **46**

Scheme 19. *Reagents and conditions; t-BuOK, 2-Me THF, MW 150 °C, 150 W, 1 hr.*

Table 5. *Results for Microwave-assisted pyrimidine rings* ***46a-d****.*

Entry	Prod. #	R=	Yield (%)	Mp. (°C)	HRMS cal.	HRMS (found)
1	**46a**	cyclopropyl	29	148	151.0978	151.0996
2	**46b**	Ph	57	153	187.0978	187.0967
3	**46c**	*tert*-butyl	61	130	167.1291	167.1290
4	**46d**	isopropyl	97	130	153.1135	153.1132

Table 6*. Key signals in the ^{1}H NMR spectra of the pyrimidine ring scaffolds* ***46a-d****.*

Entry	Prod. #	NH_2 (ppm)	NH_2 (ppm)	H5 (ppm)
1	**46a**	6.04	5.66	5.61
2	**46b**	6.37	6.00	6.22
3	**46c**	6.17	5.80	5.71
4	**46d**	5.20	5.00	5.69

Table 7*. Key signals in the ^{13}C NMR spectra of the pyrimidine ring scaffolds* ***46a-d****.*

Entry	Prod. #	C2 (ppm)	C4 (ppm)	C5 (ppm)	C6 (ppm)
1	**46a**	163.4	164.1	91.8	169.0
2	**46b**	163.7	165.2	90.6	162.3
3	**46c**	163.0	164.9	89.5	175.6
4	**46d**	163.0	164.6	92.0	176.0

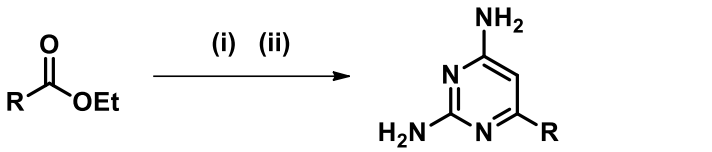

33a
33c

46a R = cyclopropyl, 20%
c R = tert-butyl, 43%

Scheme 20*. Reagents and conditions;(i) CH_3CN, t-BuOK, 2-Me THF, isopropanol, 2hr, rt. (ii) guanidine HCl. MW 150 °C, 150 W, 1 hr.*

The optimised reaction conditions for, both the acylation reaction and the cyclisation reaction were carried out in the presence of *t*-BuOK as a base and 2-Me THF as a solvent. With this in mind, we decided to attempt formation of the pyrimidine ring from commercially available esters in a one-pot-two-step reaction, where the β-ketonitrile intermediate is not isolated. Following the general synthetic procedure described for the condensation reaction of esters to form β-ketonitriles, commercially available ethyl

cyclopropane carboxylate **33a** was subjected to nucleophilic attack by the anion derived from deprotonation of acetonitrile by means of 2 mole equivalents of *t*-BuOK (**Scheme 20**). The reaction was conducted at room temperature in the presence of a catalytic amount of isopropanol and 2-Me THF as a solvent in a round bottom flask. After 2 hours, the reaction mixture was transferred into a microwave tube, followed by the addition of 2 mol equivalence of guanidine hydrochloride. The reaction mixture was then irradiated at 150 W and150 °C for an hour in a microwave reactor. Upon purification by silica gel column chromatography, the product was isolated in 20% yield. The overall yield for compound **46a** prepared by the condensation and the cyclisation steps separately is 39%. Though the overall yield is significantly low, it is still better in comparison to the 20% obtained from the one pot-two step reaction. In a similar fashion, methyl pivalate **43c** was tested under the reaction conditions described for the one pot-two step approach, and the product **46c** was isolated in 43% yield. Similarly to **46a**, the two steps taken to synthesise **46c** gave a better overall yield of 54% in comparison to the one-pot-two-step approach. Although in our case the approach was not favourable, the idea of a one-pot-two steps is beneficial under industrial setting. It minimises the number of steps for the total synthesis of a product. Additionally, it cut costs and time taken to purify both individual products. As the one-pot approach did not offer any improvement in yield at this scale, preparation of the desired pyrimidines were carried out over two steps.

2.1.3 C-5 Functionalisation of the pyrimidine ring systems

Pyrimidine derivatives bearing a C-5 substituent, such as compound **38** (**Scheme 14** (a)), were synthesised from functionalised C-C-C fragments with the desired substituent already present. In contrast, we opted to functionalise the pyrimidine ring system at C-5 after the cyclisation reaction. We intended to utilise the Sonogashira-cross coupling reaction as the key step to introduce the alkyl chain at the 5-position of the pyrimidine ring. The reaction is well known for coupling halogenated phenyl rings with alkynes, forming new C-C bonds.[152] Similarly, halogenated pyrimidine rings can be coupled to alkynes using palladium-catalysis. Here we report halogenation of our pyrimidines using available conventional methods.

2.1.3.1 Iodination of pyrimidine-ring systems

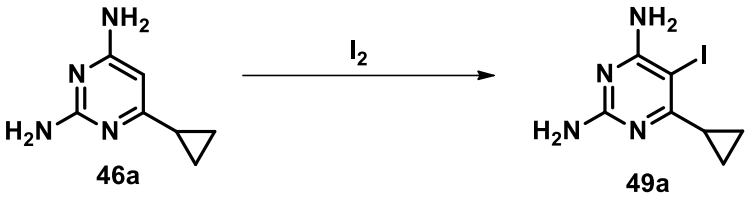

Scheme 21. *Reagents and conditions;HIO_3, AcOH, H_2O, H_2SO_4, 80 °C, 8 hr.*

With the successful preparation of the pyrimidine rings, we were now ready to introduce an iodo-substituent at C5. Under harsh acidic conditions, previously prepared 2,4-diaminopyrimidine **46a** was iodinated with iodine in the presence of iodic acid (**Scheme 21**). The reaction was conducted in a mixture of acetic acid, water and sulfuric acid. After heating at 80 °C for 8 hrs, TLC confirmed complete consumption of the pyrimidine starting material. The crude product **49a** was isolated pure in moderate yields of 57% without requirement for further purification.

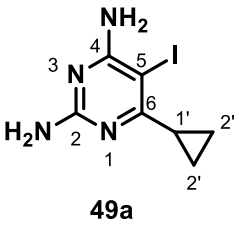

Upon examination of the ^{1}H NMR spectrum, the signal due to the aromatic proton previously observed at δ 5.61 ppm and assigned to H5 of the starting material **46a**, was absent. This indicated successful substitution of iodine at C5. Although the reaction was carried out under harsh acidic conditions, the presence of the two primary amine groups confirmed the preservation of the heteroatomic aromatic ring's integrity. The amino groups were observed as singlets in the ^{1}H NMR spectrum of the iodinated pyrimidine, appearing at δ 6.34 and 5.91 ppm respectively. Preservation of the integrity of the pyrimidine ring system was further confirmed by observation of the four key characteristic carbon-peaks of the 2,4-diaminopyrimidine ring system on the ^{13}C NMR spectrum. Peaks for C2, C4, C5 and C6 were observed at δ 162.5, 162.5, 64.3 and 169.2 respectively. It is worth noting that substitution of the 2,4-diaminopyrimidine ring **46a** with an iodine atom at position 5 significantly changed the chemical shift of the C5 peak from 91.8 ppm to 64.3 ppm in the ^{13}C NMR spectrum. Substitution of H5 on the pyrimidine ring with iodine, which has an atomic weight of 126.9045 g/mol, explains the significant difference in the mass unit of the starting material **46a** (151.0996 amu) and that of the iodinated pyrimidine **49a** (276.9930 amu)

observed on the HRMS. The difference in molecular weight provides irrefutable evidence to the success of the iodination reaction

The reaction was repeated using **46b**,**c** and **d**, to afford iodinated pyrimidines **49b-d** in good yields (60-77%; **Table 8**). In each case, the expected mass of the desired product was observed using HRMS. Key signals in the ^{1}H and ^{13}C NMR spectra were also evident for each product (**Tables 9** and **10**). In particular, the observed shift in the chemical shift of C5 observed for **49a** was common with the other iodinated pyrimidine analogues with these signals appearing at 62.5 - 66.1 ppm (**Table 10**).

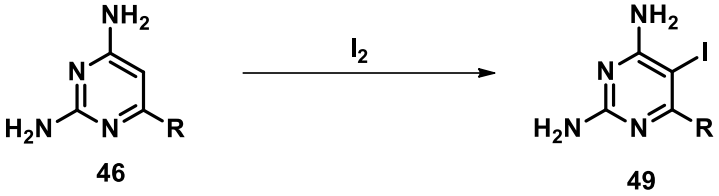

Scheme 22. *Reagents and conditions;HIO_3, AcOH, H_2O, H_2SO_4, 80 °C, 8 hr.*

Table 8. *Results of the Iodinated of 2,4-diaminopyrimidines **49b-d**.*

Entry	Prod. #	R =	Yield (%)	Mp. (°C)	HRMS cal.	HRMS (found)
1	**49b**	Ph	69	190	312.9945	312.9931
2	**49c**	*tert*-butyl	77	117	293.0258	293.0250
3	**49d**	isopropyl	60	115	279.0101	297.0079

Table 9. *Key signals in the ^{1}H NMR spectra for the formation of iodinated pyrimidine **49b-d**.*

Entry	Prod. #	NH_2 (ppm)	NH_2 (ppm)
1	**49b**	6.51	6.17
2	**49c**	5.77	5.15
3	**49d**	5.33	4.95

Table 10. *Key signals in the 13C NMR spectra for the formation of iodinated pyrimidine **49b-d**.*

Entry	Prod. #	C2 (ppm)	C4 (ppm)	C5 (ppm)	C6 (ppm)
1	**49b**	162.5	163.7	62.5	168.4
2	**49c**	161.4	163.7	62.2	175.6
3	**49d**	162.7	162.9	66.1	175.6

2.1.3.2 Synthesis of 5-substituted 2,4-diaminopyrimidines using Sonogashira reaction

Having successfully synthesised the iodinated pyrimidines, we were now ready to focus on the palladium-catalysed cross-coupling reaction, which entails coupling of the pyrimidine ring with a suitable alkyne to form a new carbon-carbon bond. This type of a coupling reaction can be achieved by palladium catalysis. Synthetic chemists have extensively studied such transition metal-mediated cross coupling reactions due to their ability to allow for the formation of carbon-carbon bonds. Formation of carbon bonds is an important feature in organic chemistry because it allows access to highly complex and functionalised synthetic compounds. The use of transition metals to mediate coupling reactions dates back to 1869 when Gaser reported the oxidative dimerization of metallic acetylides,[153] a homocoupling reaction where oxidation of a metallic acetylide such as copper phenylacetylide gives the diphenyldiacetylene dimer (**Scheme 23**(a)).

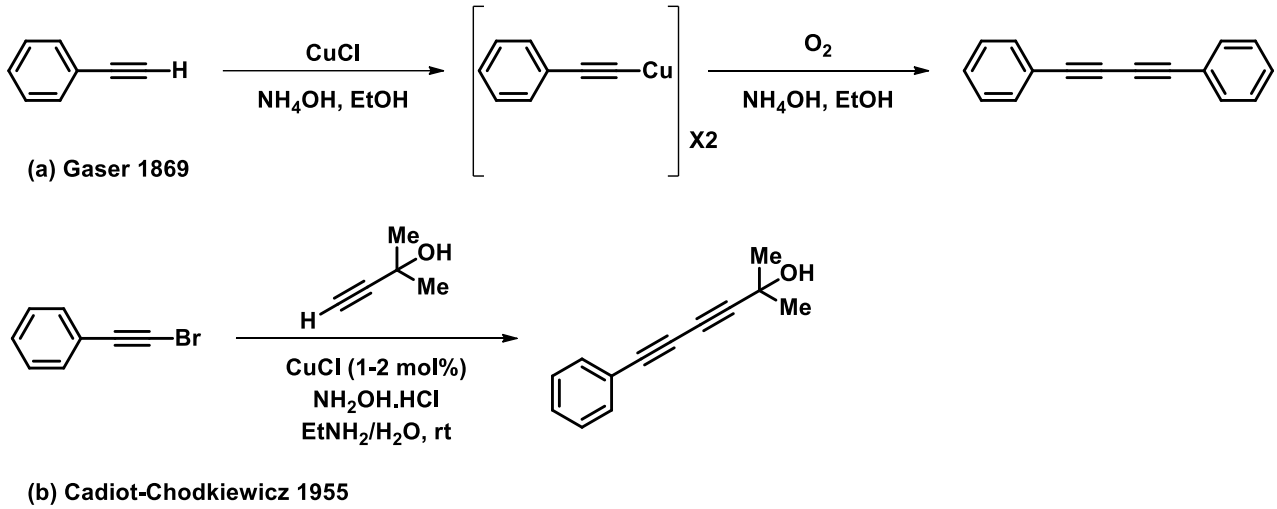

Scheme 23. *(a) The Gaser homocoupling of copper phenylacetylide and (b) The first cross-coupling reaction.* [153]

However, it was not until 1955 when the first selective cross-coupling reaction was reported by Cadiot-Codkiewicz. They successfully coupled alkynes with bromoalkynes using copper catalysis (**Scheme 23** (b)).[154] At this point in the history of coupling reactions, it was apparent that in order for a selective coupling reaction to take effect, three important components were a requirement; the two coupling partners i.e., an organohalide and an organometallic reagent, and a transition metal catalyst. The organometallic agent can either be prepared prior or *in situ* to prevent the

homocoupling reaction.[153] The work done by Cadiot-Chodkiewicz and other chemists involved in early cross-coupling reactions and metal-catalysed reactions laid the foundation of what would become Pd-catalysed cross-coupling reactions.

Since its discovery by Wollaston in 1802, the use of palladium was very limited. The first industrial use of palladium was the Wacker process in 1956, a Pd-catalysed process that involves oxidation of ethylene to acetaldehyde.[154] In a quest to study the reaction mechanism of this particular process, Richard Heck successfully achieved an arylation of alkenes with an organomercury arylating reagent and a catalytic amount of palladium catalyst (**Scheme 24** (a)).[153]

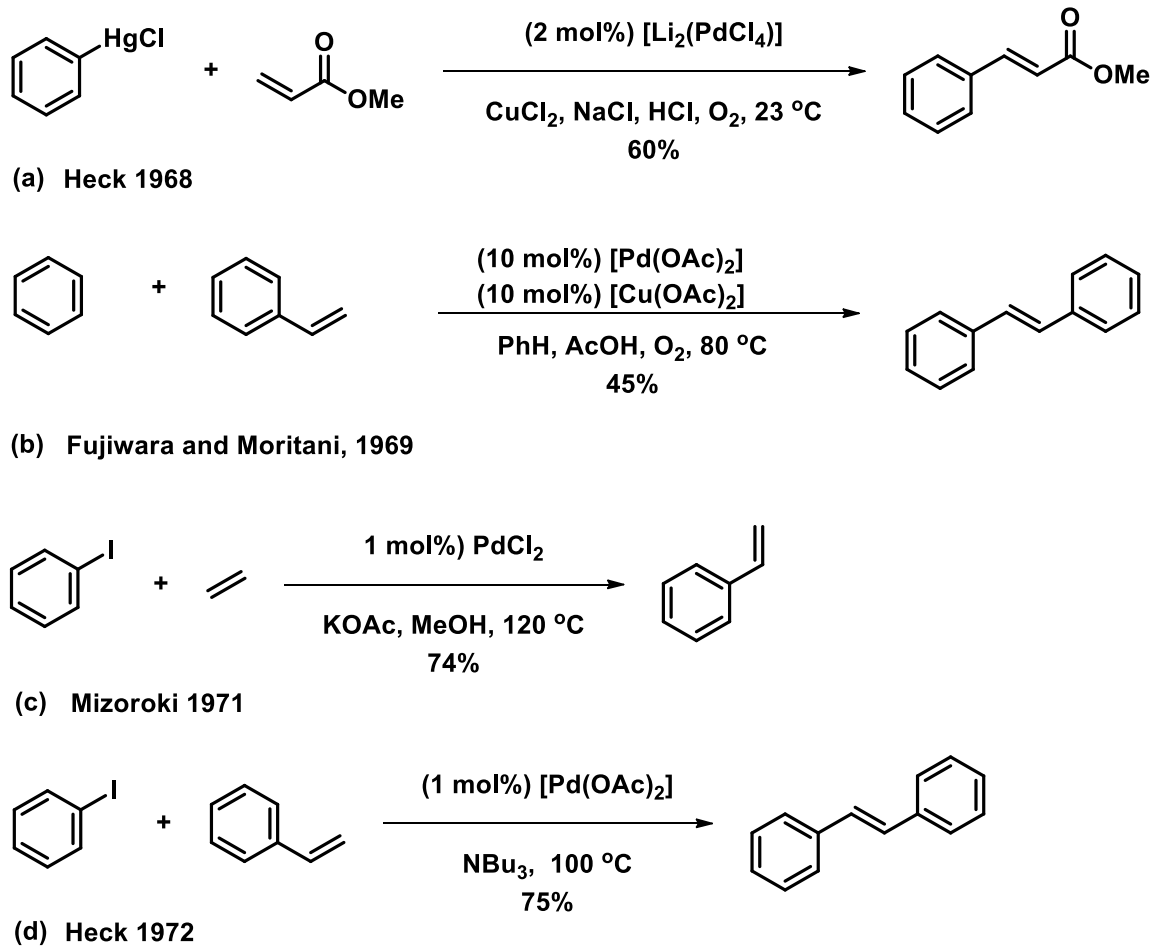

Scheme 24. *The first palladium catalysed cross-coupling reactions.*[155]

Subsequent to Heck's coupling reaction, Fujiwara and Moritani published an improved approach to the Pd-catalysed reaction. They directly coupled arenes to alkenes in a fashion that did not require the use of a toxic organomercury reagent as a nucleophilic coupling partner (**Scheme 24** (b)).[156] This observation can be considered one of the

early direct C-C bond formations via C-H activation,[155] a transition metal-mediated transition state in which C-H bonds from an arene are broken and new C-C bonds are formed. In the early 1970s, Mizoroki and Heck independently reported coupling of aryl-halides to alkenes employing Pd-catalysis almost concurrently (**Scheme 24** (c &d).[153,155] Heck's contribution towards aryl and vinyl halide substrates led to the cross-coupling reaction currently appreciated by many organic chemists as the Mizoroki-Heck reaction.[156]

Shortly after the establishment of palladium as an alkenophile, three independent groups discovered palladium cross-coupling reactions of alkynes with halogenated aryls or vinyls: Sonogashira,[152] Heck[157] and Cassar (**Scheme 25**).[158] In comparison, the reaction conditions proposed by Sonogashira were superior over the high temperature conditions required by Cassar and Heck. Application of a copper co-catalyst enabled the Sonogashira reaction to proceed efficiently at room temperature. The reaction conditions are therefore suitable for temperature sensitive reagents.

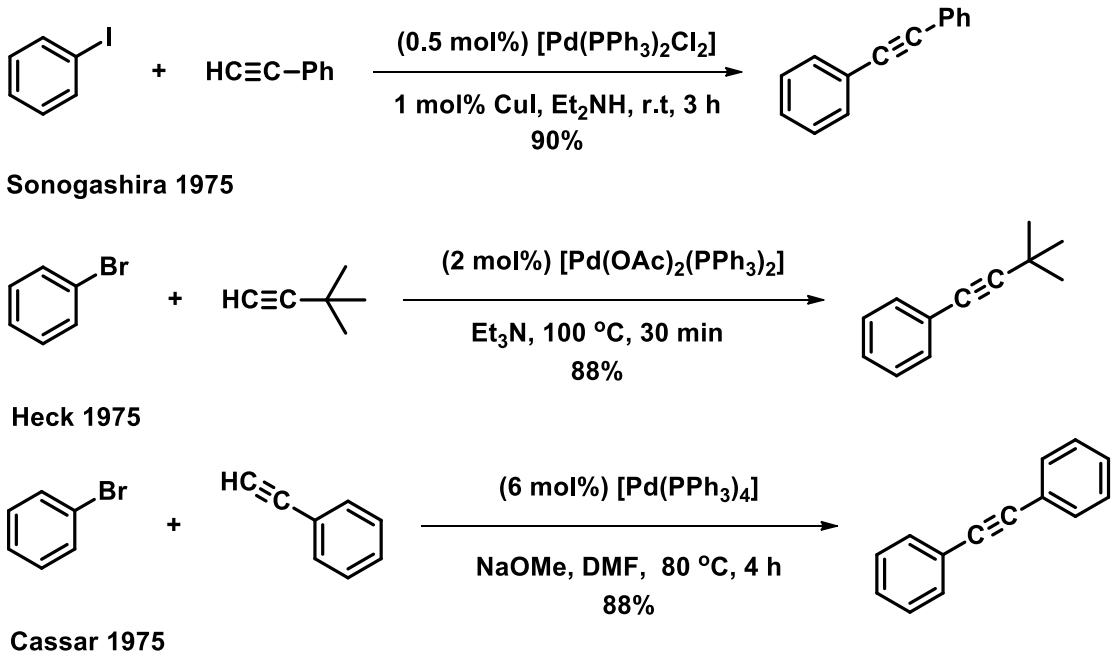

***Scheme 25**. Sonogashira reaction discovery in 1975.*[153]

The Sonogashira cross-coupling reaction offers a different mechanism for the synthesis of 2,4-diaminopyrimidine derivatives functionalised at C-5. As stated previously, the method is well known to couple halogenated aryl rings with alkynes, forming new C-C bonds. Similarly, iodinated pyrimidines can be coupled to alkynes using palladium catalysis. Recent reports have proven the feasibility of functionalising

iodinated 2,4-diaminopyrimidines using the Sonogashira reaction.[159,160] Iodinated pyrimidines were subjected to Sonogashira reaction conditions using $Pd(PPh_3)_2Cl_2$ as a catalyst and the co-catalyst CuI in the presence of basic trimethylamine to give highly functionalised pyrimidine derivatives (**Scheme 26**), and the products were isolated in exceptionally high yields.[159] The success of the palladium catalysed cross-coupling reactions to generate functionalised 2,4-diaminopyrimidine derivatives from iodinated pyrimidine scaffolds speaks to the robust nature of the methodology to accommodate diverse reagents and functionalities. We intend to employ this key reaction in the synthesis of our 2nd generation analogues (**Scheme 6, ch. 1**)

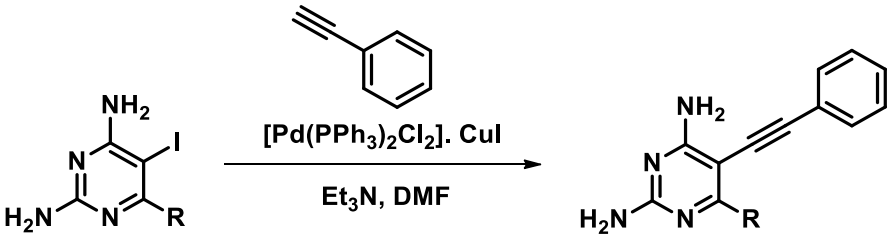

***Scheme 26**. Synthesis of 5-substituted 2,4-diaminopyrimidines using the Sonogashira reaction.*

The Sonogashira-copper co-catalysed reaction follows the general mechanism for palladium catalysed cross-coupling reactions (Pd-catalytic cycle) connected to an independent copper cycle (Cu cycle) (**Figure 26**). Pd-catalytic cycle is initiated by an oxidative addition of the organic halide, iodinated pyrimidine (pyr-I), to the catalytic active Pd(0) complex $[Pd(0)L_2]$ giving a Pd(II) intermediate.[155,161] Notably, the $[Pd(0)L_2]$ is formed by reduction of the employed Pd(II)-complex such as $Pd(PPh_3)_2Cl_2$ under the set reaction conditions.[161] The next step marries the Pd-catalytic cycle with the Cu cycle. Pd(II) intermediate undergoes a transmetallation with a copper alkynyl, formed in the Cu cycle, to generate a pyr-Pd(-C≡ C-Ph)L_2 species, which gives the coupled pyr-alkyne product in a reductive elimination reaction resulting in the regeneration of the active catalyst Pd(0).[155]

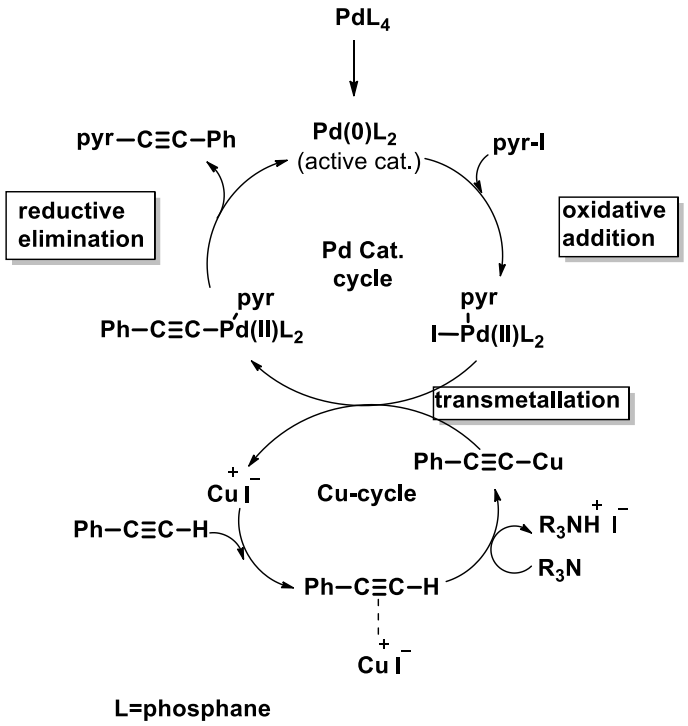

Figure 26. *Schematic representation of the Sonogashira cross-coupling mechanism.*

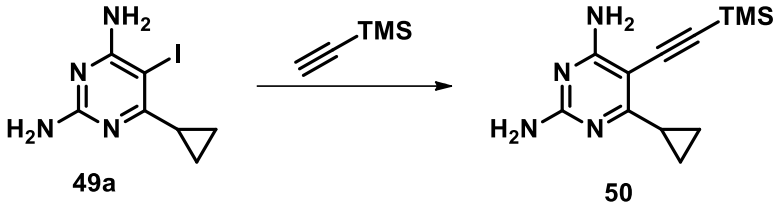

Scheme 27. *Reagents and conditions; (a)Pd(PPh$_3$)$_2$Cl$_2$, CuI, TEA, DMF, rt, 18 hr, 0%. (b) Pd(PPh$_3$)$_2$Cl$_2$, CuI, DIIPA, THF, Δ, 18 hr, 38%.*

In 1999 Jones *et. al.* reported the Sonogashira cross-coupling reaction conditions they used to couple an iodinated 2,4-diaminopyrimidine ring to various terminal acetylenes in the presence of triethylamine and DMF at room temperature.[162] The reported yields range from 27% to 78%. Although not exceptionally high, the yields gave realistic results on the effectiveness of coupling 2,4-diaminopyrimidine ring systems to terminal acetylenes via the Sonogashira cross-coupling reaction. Following the described reaction conditions, an attempt to couple the starting material **49a** with TMS acetylene was performed (**Scheme 27**). Unfortunately, the coupling reaction did not take effect in the presence of triethylamine and DMF as a solvent. We therefore utilised THF and DIIPA as alternatives at reflux. These changes to the reaction conditions improved the results of the reaction, giving the product **50** in 38% yield.

Formation of the product was confirmed by NMR spectroscopy. Upon analysis of the ^{13}C NMR spectrum, a notable shift of the peak assigned to C5 was observed. On the iodinated starting material **49a**, the peak for C-5 appears at δ 64.3 ppm in the^{13}C NMR spectrum, whereas the peak appears at 88.0 ppm for the product **50**. The significant shift of the C-5 peak from δ 64.3 ppm to 88.0 ppm indicates that a chemical conversion took place at this position, and this comes as a result of the newly formed C-C bond at position 5 of the 2,4-diaminopyrimidine ring. The nine signals present on the ^{13}C NMR spectrum of the product explicitly support success of the carbon-carbon coupling reaction. Furthermore, the new alkyne carbon peaks observed at δ 101.9 and 100.4 ppm confirmed the presence of structural features from the acetylene reagent. The presence of the new peak at δ 0.3 ppm in the ^{13}C NMR spectrum is due to the three methyl groups from the trimethylsilyl group, which corresponds to a singlet at δ 0.21 ppm integrating for 9 protons on the ^{1}H NMR spectrum.

Although the success of the Sonogashira reaction was a positive result, the low yield was rather discouraging as there are three more reaction steps towards our desired final product, one of which includes a copper catalyzed coupling reaction between the resulting deprotected acetylene and commercially available substituted ethynylbenzenes to produce diyne intermediates **31** (refer to **Scheme 6**). From the previous study conducted in our laboratories, production of these diynes using copper catalysis was rather low yielding, with the highest yield reported as 26%.[104] The disappointing low yields are not favourable for a medicinal chemistry project because production of a library of adequate analogues is a requirement in order to identify a hit compound. It was at this point that we decided to explore an alternative synthetic route towards the desired 2,4-diaminopyrimidine derivatives. Preserving the idea of introducing the flexible alkyl chain to the pyrimidine ring via the Sonogashira cross-coupling reaction, we revisited the idea of coupling halogenated pyrimidine ring systems to pre-functionalised acetylene nucleophiles. Although in previous work, the Pd-catalysed coupling reaction between 4,6-diamino-pyrimidine **18** and the alkyne substrate to produce compound **19** was unsuccessful (**Scheme 28**), the feasibility of the Sonogashira reaction to couple pyrimidine systems (including our pyrimidines) with acetylene has been proven. [104,159,160] It is worth noting that the iodinated 4,6-diaminopyrimine starting material was recovered from the failed reaction.

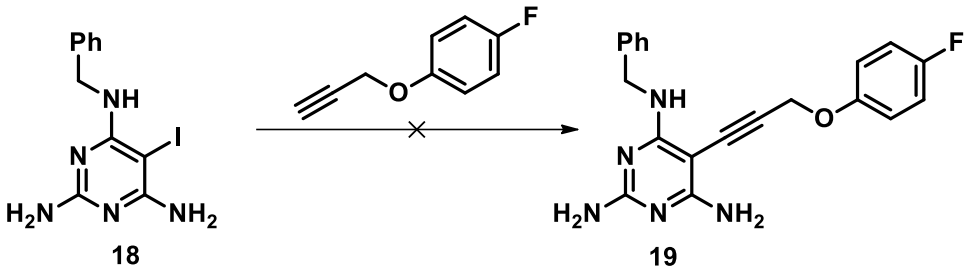

***Scheme 28**. Reagents and conditions; Pd(PPh$_3$)$_4$, CuI, TEA, DMF, rt.*

Failure of the Sonogashira reaction using a complex acetylene led to the success of the reaction using a simple TMS acetylene (**Scheme 28**). In hindsight, this result supported the idea that the pre-functionalised terminal alkyne substrate was responsible for the failed reaction. However, it is worth noting that our halogenated pyrimidines 49 are 2,4-diaminosubstituted pyrimidines, while those considered previously has an additional 6-amino substituent, which could also have negatively impacted the success of the Sonogashira reaction. Looking at the copper cycle in **Figure 25**, the amine base is responsible for deprotonating the acidic proton of the terminal alkyne.[161] Terminal alkynes are considered weakly acidic because the σ electron pair of C-H bond are positioned closer to the C-atom, which render the alkyne H-atom more positive and therefore more easily removed by strong bases.[163] Generally, amines employed as bases in Sonogashira cross-coupling reactions to form the anionic nucleophile resulting from abstraction of the acetylenic protons are not strong enough. In order to make copper acetylide resulting from deprotonation of the terminal alkyne, a π alkyne-Cu complex as shown in **Figure 26** could be involved in the cycle, consequently making the alkyne H-atom more acidic for easier deprotonation.[161] Since deprotonation of acetylenic H-atoms is dependent on the copper cycle, we can deduce that the nature and electronics associated with the alkyne substrate should have little effect on the success of the Sonogashira reaction. Furthermore, the Sonogashira reaction should be able to accommodate a vast variety of acetylene substrates, and these claims are supported by a review reported by Chinchilla and Nájera in 2007.[161] They highlighted various examples of the Sonogashira reaction using different acetylene substrates such as the complex ethynylestradiol, or propargyl alcohol containing an electron-withdrawing atom. In 2017, Beesu *et al*. reported the coupling of various terminal alkynes using the Sonogashira reaction to 2,4-diaminopyrimidine **51** (**Scheme 29**).[160] The report was of

particular interest because the alkyne substrates utilised were similar in structure to the pre-functionalised acetylene substrate used in **Scheme 28**. Moreover, the resulting Sonogashira alkyne intermediates **52** were isolated in high yields ranging from 55 – 80%. Considering these positive results, we were interested to try the Sonogashira reaction using a pre-functionalised acetylene substrate on our iodinated pyrimidines.

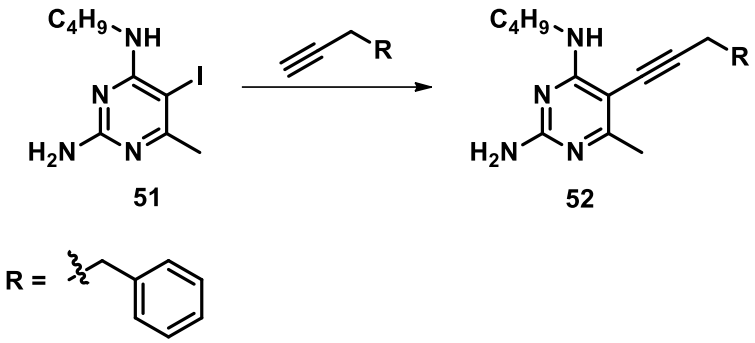

Scheme 29. *Reagents and conditions; alkyne, Pd(PPh$_3$)$_4$, CuI, DIPEA/DMF (1;2), 12 h, rt.*[160]

Test reaction using conditions described by Beesu *et al*. (**Scheme 28**).[160]

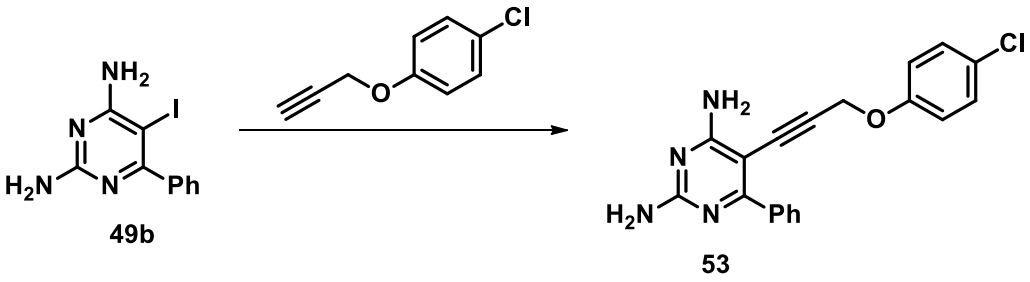

Scheme 30. *Reagents and conditions; alkyne, Pd(PPh$_3$)$_2$Cl$_2$, CuI, DIIPA/DMF (1;2), 12 h, rt.*

To our delight, iodinated 6-phenyl-2,4-diaminopyrimidine **49b** was successfully coupled to an acetylene substrate in a reaction medium catalysed by Pd(PPh$_3$)$_2$Cl$_2$ in the presence of CuI and DIIPA to yield compound **53** in 54% yield. Formation of the product was confirmed by NMR spectroscopy. The two additional signals in the ^{1}H NMR spectrum observed at the aromatic region confirmed the success of the coupling reaction. These signals integrated for two protons respectively and were assigned to protons found on the 4-chlorophenoxy ring. Additionally, the singlet appearing at δ 4.85 ppm integrating for two protons was due to the CH$_2$ denoted 3'. It is evident that due

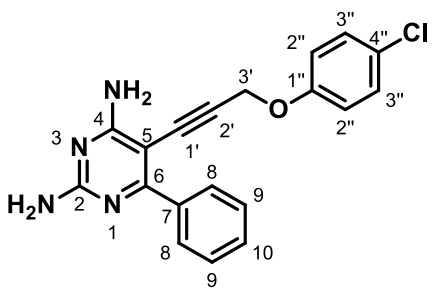

to the electronegative oxygen covalently bonded to the CH_2 group; the signal has significantly shifted from a shielded aliphatic region to a more deshielded region. The ^{13}C NMR spectrum showed 15 non-equivalent carbon peaks, which further confirmed the success of coupling the pyrimidine ring to the pre-functionalised acetylene substrate. In the aromatic region 12 signals were observed belonging to the heterocyclic ring system, the phenyl ring and the 4-chlorophenoxy ring. The four newly added signals of the 4-chlorophenoxy ring were observed at δ 156.2, 116.5, 129.5 and 126.5 ppm for C1'', C2'', C3'' and C4'' respectively. Peaks associated with the acetylenic carbon atoms were observed at δ 92.3 and 82.3 ppm, and the CH_2 group was distinctively identified using DEPT at 57.1 ppm. HRMS data showed a molecular ion peak of 351.0961 amu which is in agreement with the mass calculated for $C_{19}H_{15}ClN_4O$ $[M + H]^+$ of 351.1007 amu.

Successful formation of compound **53** led to the interrogation of why the reaction in **Scheme 28** failed. In accordance with the Pd catalytic cycle, active Pd-catalyst species have to insert in between the iodine-atom and the 4,6-diaminopyrimidine ring forming a pyr-Pd(II)L_2-I complex. Possibly, the utilised Pd-catalyst coordinates to the two amino groups bonded at C-4 and C-6 of the pyrimidine as illustrated in **Figure 27**, instead of inserting between the carbon and iodine bond. This is supported by the recovery of the starting material, which indicate that the important oxidative addition step in the Pd-cycle did not take place. In our case, the amino groups are bonded to C-2 and C-4, i.e., the iodine-atom is not situated in between the two amino groups. Configuration of the 2,4-diaminopyrimidine ring system **49** eliminates the possibility of coordination of the Pd-metal to groups attached at positions 4 and 6, consequently promoting the likelihood of an oxidative addition at position 5. In accordance, these could be the reason for the successful result.

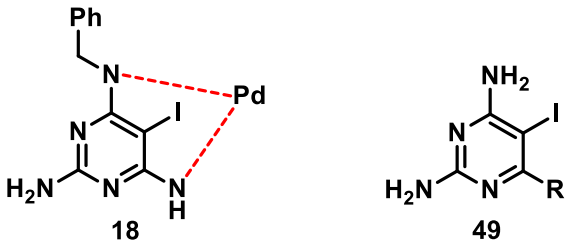

Figure 27. *Illustration of Pd interaction with amino groups of 4,6-diaminopyrimidine ring system.*

Even though the yield for the reaction was not exceptionally high, we have successfully coupled a pre-functionalised acetylene substrate to a 2,4-diaminopyrimidine ring system. Reduction of the Sonogashira alkyne intermediate **53** will yield one of the 1st generation 2,4-diaminopyrimine analogues **8** (**Scheme 2**, **Chapter 1**). This result indicates the successful development of a new alternative and relatively safe procedure towards previously synthesised pyrimidines, eliminating the need for hazardous reagents such as diazomethane. Application of the pre-functionalised acetylenes as nucleophiles coupling to our 2,4-diaminopyrimidine ring system containing aliphatic groups bonded at position 6, can potentially lead to production of the desired 2nd generation 2,4-diaminopyrimine derivatives **15** (**Scheme 31**). Additionally, introduction of the pre-functionalised acetylene substrate in the Sonogashira reaction has significantly reduced the number of reaction steps. The initial proposed synthetic route consisted of seven steps towards the desired products, whereas the newly improved synthetic route contains five steps.

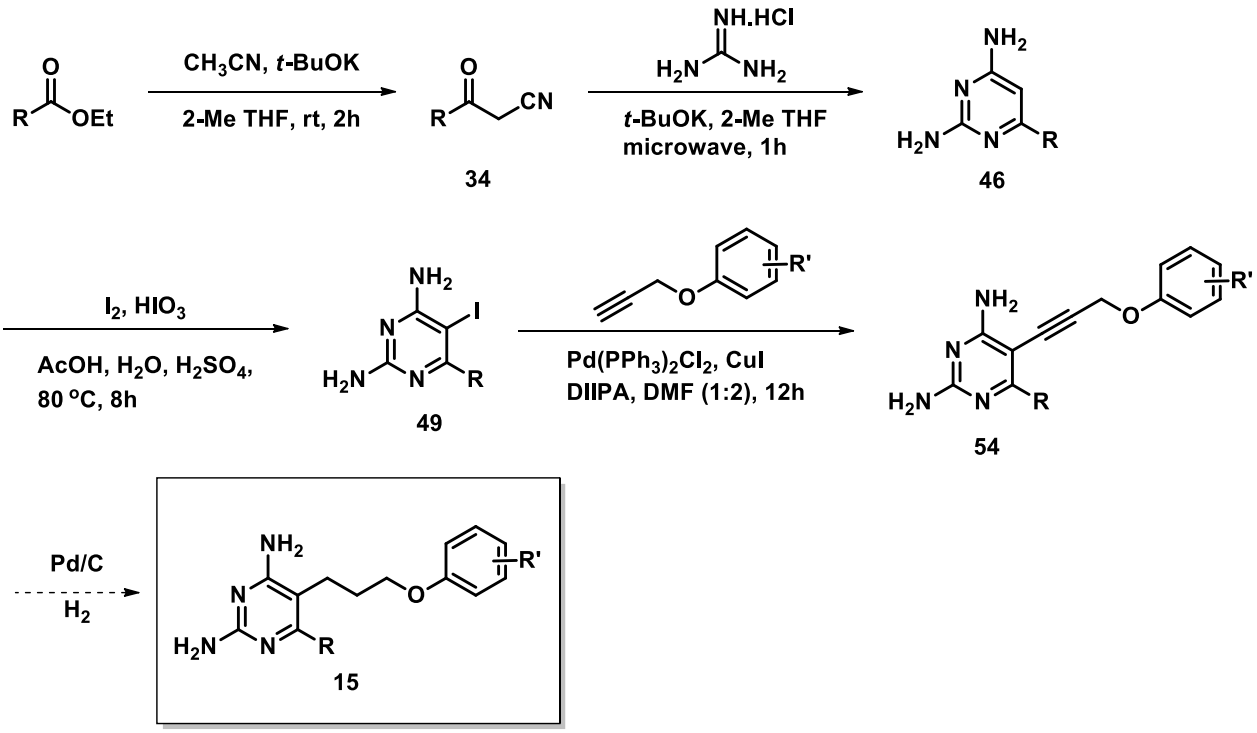

Scheme 31. *Newly developed synthetic procedure towards synthesis of second generation pyrimidines.*

In **Chapter 1**, we made mention of a molecular modelling campaign conducted in search of structural derivatives of the 1st generation 2,4-diaminopyrimidines with optimal affinity for the *Pf*DHFR active site. From the modelling studies, 2,4-

diaminopyrimidine derivatives **15** containing a phenoxy ring attached to the alkyl chain were more active than those bearing on all-C flexible linker between the phenyl and pyrimidine rings. Ideally, we would have prefered to synthesise these analogues. However, as the Sonogashira reaction was proven fruitless when the pre-functionalised acetylene formed from commercially available 4-fluorophenol was used, we opted to employ the proposed synthetic route outlined in **Scheme 6**, **Chapter 1**. However, the newly developed synthetic route offers an opportunity to make the desired 2,4-diaminopyrimidine derivatives with an O-atom in the flexible linker starting from commercially available esters (**Scheme 31**). The Sonogashira reaction is the key step that marries the iodinated pyrimidine ring **49** with a suitable acetylene to form the alkyne intermediate **54**. The acetylene functions as the key reagent that introduces the flexible linker between the heterocyclic ring system and the terminal phenoxy ring. Reduction of the triple bond in **53**, by a hydrogenation reaction will lead to a library of the desired 2nd generation 2,4-diaminopyrimidine analogues **15**. Should this prove successful, we will develop an improved synthetic route towards oxygen-containing analogues, **15**.

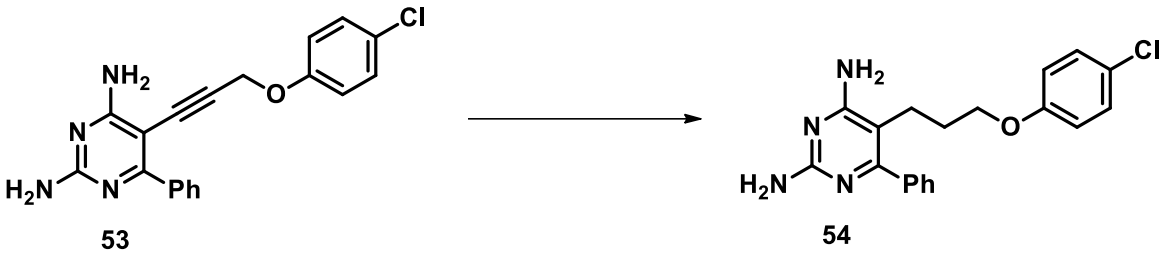

Scheme 32. *Reagents and conditions; H_2, Pd/C, EtOH, 16 h.*

To complete the synthetic route, we tested the Pd-catalysed hydrogenation reaction on compound **53**. The starting material **53** was dissolved in ethanol followed by addition of Pd/C in the presence of H_2 gas under atmospheric pressure for 16 hours. The product was isolated in 68% yield. After this time, the Pd-catalyst was removed by filtration through celite and the product was purified using silica gel column chromatography. Success of the reduction reaction was confirmed by NMR spectroscopy. The three aliphatic CH_2 signals resulting from reduction of the alkyne triple bond to a fully saturated hydrocarbon chain were observed at δ 3.81 (q, H3'), 2.53 (t, H1')

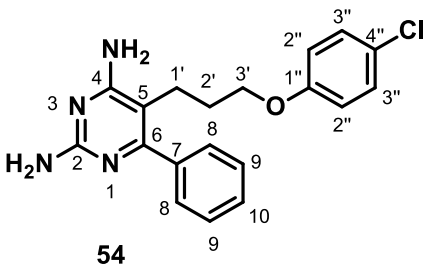

54

and 1.86 ppm (p, H2') in the ^{1}H NMR spectrum. These proton signals corresponded to C-peaks appearing in the ^{13}C NMR spectrum at 68.2, 23.0 and 29.1 ppm respectively. The distinctive disappearance of the acetylene C-peaks observed at δ 92.3 and 82.3 ppm affirmed that reduction of the alkyne functional group had taken place. Additionally, the HRMS indicated an ion peak of 355.1331 amu, which was in agreement with the calculated mass of 355.1320 amu for $(M+H)^{+}$ $C_{19}H_{19}ClN_4O$.

Success of the hydrogenation reaction marks the successful development of the synthetic route towards flexible 2,4-diaminopyrimidine derivatives. We were now ready to apply this synthetic route to pyrimidines substituted with an aliphatic group at position 6 of the pyrimidine ring.

3 CHAPTER 3: Results and discussion

3.1 Synthesis of 2,4-diaminopyrimidine analogues

As described in the previous chapter, we have successfully developed a synthetic route towards flexible 2,4-diaminopyrimidine derivatives, which entails the synthesis of these target compounds in five steps starting from commercially available esters. The key step is the Sonogashira reaction, which facilitates coupling of 2,4-diaminopyrimidine ring systems to pre-functionalised acetylenes forming new C-C bonds. The acetylenes are important because they introduce components of the flexible four-linker chain. Since the acetylenes are made from commercially available phenols, utilisation of substituted phenols will bring variation to the synthesised acetylenes, consequently building up a library of variable analogues. To synthesise 2,4-diaminopyrimidine analogues we started off by preparing acetylenes from commercially available analogues.

3.1.1 Preparation of the acetylenes

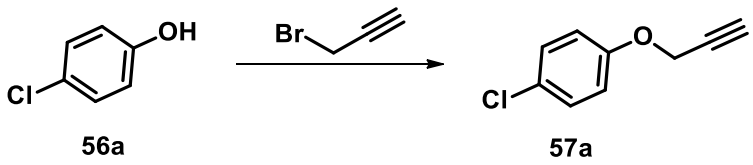

56a **57a**

Scheme 33. *Reagents and conditions; K_2CO_3, acetone, 56 °C reflux, 8 hr.*

Commercially available 4-chlorophenol **56a** was treated with 4.0 mol eq. of K_2CO_3 and propargyl bromide in acetone. The reaction mixture was stirred overnight at 56 °C.

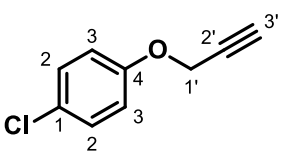

Under the described reaction conditions, the base deprotonates the phenol giving rise to the nucleophilic phenolate ion, which partakes in a nucleophilic substitution reaction with the alkylating agent, propargyl bromide. After this time, TLC confirmed complete consumption of the starting material and the product was isolated as a yellow oil in quantitative yields. Alkylation of the phenol was confirmed using NMR spectroscopy. Analysis of the ^{1}H NMR spectrum showed the presence of four signals that can attest to the successful alkylation of the commercially available phenol. In the aromatic

region there are two signals appearing at δ 7.31 – 7.15 and 6.98 – 6.77 ppm assigned to H2 and H3 of the phenolic ring respectively. The other two signals present appear in the aliphatic region, where the CH_2 signal is observed as a doublet integrating for two protons at δ 4.63 ppm. Notably, this signal appears in a rather deshielded region of the spectrum owing to the covalent bond between the CH_2 and the electronegative oxygen atom. In addition, the CH_2 group couples to the acetylene CH and splits the signal into a triplet found at δ 2.51 ppm with J = 2.4 Hz. The appearance of seven signals in the ^{13}C NMR spectrum further supports the success of the alkylation reaction. The alkyne carbons are distinctively observed at δ 78.3 and 76.0 ppm, which are assigned to C2' and C3' respectively, while the CH_2 signal corresponds to a peak at δ 56.1 ppm on the ^{13}C NMR spectrum, as determined by analysis of the HMBC spectrum. Several other acetylene analogues were synthesised using the described synthetic approach and products **57b-i** were isolated in exceptionally high yields ranging from 83% to quantitative (**Table 11**).

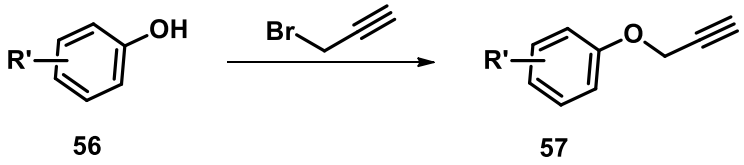

56 **57**

Scheme 34. *Reagents and conditions; K_2CO_3, acetone, 56 °C reflux, 8 hr.*

Key signals in the 1H NMR spectra are listed in **Table 11**. The choice of substituents R' was driven by modelling , and included both electron donating (OMe) and electron withdrawing (F, Cl) groups at positions *ortho*, *meta* and *para* to the phenolic oxygen. In the ^{13}C NMR characteristic C-F coupling was observed for **57b**, **57e** and **57h** (**Table 12**). All other signals were as expected for the products formed.

Table 11. *Key signals in the ^1H NMR spectra that prove alkylation of phenols to afford* ***57b-i***.

Prod #	R' =	Yield (%)	Phenolic protons (ppm)	CH_2 (ppm)	CH (ppm)
57b	4-F	83	7.11 – 6.85 (m, H2 & H3)	4.66 (d, *J* = 2.5 Hz)	2.53 (t, *J* = 2.4 Hz)
57c	4-OMe	95	6.98 – 6.81 (m, H2 & H3) 3.77 (s, OMe)	4.70 – 4.55 (m)	2.58 – 2.47 (m)
57d	3-Cl	98	7.22 – 7.14 (m, H5), 6.99 – 6.96 (m, H2), 6.96 – 6.93 (m, H6), 6.84 (ddd, H4)	4.64 (d, *J* = 2.5 Hz)	2.53 (t, *J* = 2.4 Hz)
57e	3-F	88	7.36 – 7.13 (m, H5), 6.86 – 6.62 (m, H2, H4 & 6)	4.68 (d, *J* = 2.4 Hz)	2.55 (t, *J* = 4.1, 2.0 Hz)
57f	3-OMe	100	7.26 – 7.06 (m, H5), 6.64 – 6.43 (m, H2, H4 & 6), 3.74 (s, 3H, OMe)	4.63 (t, *J* = 2.4 Hz)	2.50 (t, *J* = 2.4 Hz)
57g	2-Cl	100	7.36 (dd, *J* = 7.9, 1.7 Hz,H6), 7.21 (ddd, *J* = 8.2, 7.4, 1.7 z, H4), 7.06 (dd, *J* = 8.3, 1.5 Hz, H3), 6.93 (td, *J* = 7.7, 1.5 Hz, H5)	4.75 (d, *J* = 2.5 Hz)	2.55 (t, *J* = 2.4 Hz)
57h	2-F	92	7.19 – 7.04 (m, H3, H4 & H6), 7.02 – 6.84 (m, H5)	4.76 (d, *J* = 2.5 Hz)	2.55 (t, *J* = 2.4 Hz)
57i	2-OMe	100	7.03 (dt, *J* = 7.8, 1.7 Hz, H6), 6.97 (dt, *J* = 7.8, 1.5 Hz, H5), 6.95 – 6.85 (m, H3 & H4), 3.85 (s, OMe)	4.74 (t, *J* = 2.2 Hz)	2.50 (t, *J* = 2.4 Hz)

Table 12. *Key signals in the ^{13}C NMR spectra that prove alkylation of commercially available phenols to afford* ***57b-i***.

Prod. #	R'=	Phenolic C-peaks (ppm)	OMe (ppm)	C1' (ppm)	C2' (ppm)	C3' (ppm)
57b	4-F	157.8 (d, J_{C-F} = 239.0 Hz, C1), 153.7 (d, J_{C-F} = 2.2 Hz, C4), 116.3 (d, J_{C-F} = 8.0 Hz, C3), 116.0 (d, J_{C-F} = 23.1 Hz, C2),		56.5	78.6	75.7
57c	4-OMe	154.5 (C1), 151.7 (C4), 116.1 (C3), 114.6 (C2)	55.6	56.6	79.0	75.4
57d	3-Cl	158.3 (C3), 134.9 (C1), 130.3 (C5), 121.8 (C6), 115.5 (C2), 113.4 (C4)		56.0	78.1	76.1
57e	3-F	163.7 (d, J_{C-F} = 245.4 Hz, C1), 159.0 (d, J_{C-F} = 10.9 Hz, C3), 130.4 (d, J_{C-F} = 10.0 Hz, C5), 110.8 (d, J_{C-F} = 2.5 Hz, C4), 108.6 (d, J_{C-F} = 21.3 Hz, C6), 103.0 (d, J_{C-F} = 25.1 Hz, C2)		56.2	78.3	76.1
57f	3-OMe	160. 158.8 (C3), 129.9 (C5), 107.2 (C4), 106.9 (C6), 101.5 (C2)	55.3	55.8	78.6	75.6
57g	2-Cl	153.1 (C2), 130.4 (C6), 127.6 (C4), 123.2 (C1), 122.4 (C5), 114.3 (C3)		56.7	78.0	76.2
57h	2-F	153.0 (d, J_{C-F} = 246.0 Hz, C1), 145.5 (d, J_{C-F} = 10.5 Hz, C2), 124.3 (d, J_{C-F} = 3.9 Hz, C4), 122.4 (d, J_{C-F} = 6.9 Hz, C5), 116.4 (d, J_{C-F} = 18.3 Hz, C6), 116.2 (d, J_{C-F} = 1.6 Hz, C3),		57.2	78.2	76.2
57i	2-OMe	149.7 (C1), 146.7 (C2), 122.2 (C5), 120.6 (C4), 114.5 (C6), 111.8 (C3)	55.7	56.7	78.6	75.7

3.1.2 Coupling of the tert-butyl-pyrimidine ring with commercially available phenols

As described in chapter 2, we have successfully synthesised compound **53**, a 2,4-diaminopyrimidine containing a phenyl group at position 6 of the pyrimidine ring (**Scheme 30**). However, we are yet to test the synthetic route on 2,4-diaminopyrimidine scaffolds with an aliphatic group at C-6, which is the focus of this research project. With the success of the Sonogashira reaction, we were now ready to explore the reaction conditions on a pyrimidine ring with an aliphatic group at position 6.

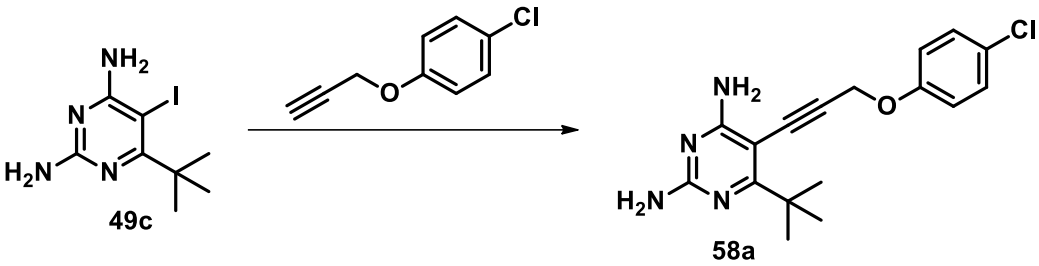

Scheme 35. *Reagents and conditions; alkyne, $Pd(PPh_3)_2Cl_2$, CuI, DIIPA/DMF (1;2), 12h, rt.*

Using the same reaction conditions described for compound **53**, we coupled 6-(*tert*-butyl)-5-iodopyrimidine-2,4-diamine **49c** together with a pre-functionalised acetylene **57a** in the presence of 10 mol% $Pd(PPh_3)_2Cl_2$, 20 mol% CuI and a 2:1 mixture of DMF and DIIPA as an amine base overnight (**Scheme 5**). The product **58a'** was isolated as a dark brown solid in 23% yield, which was disappointingly very low. This inspired the drive to optimize the reaction conditions. When the temperature of the reaction medium was raised to 80 °C, the yield increased slightly to 26% (**Table 13**, entry 4). Since no significant difference was observed when heat was applied to the system, we sought to focus on a systematic change of reagents starting with the Pd-catalyst.

The Sonogashira reaction is usually conducted under homogeneous conditions using a palladium-phosphate ligand complex as a catalyst. Commonly used complexes include $Pd(PPh_3)_4$, and $Pd(PPh_3)_2Cl_2$. The latter is commonly used because it is more stable.[161] Catalytic activities of three Pd catalysts were tested to couple the pyrimidine

ring with suitable acetylenes under Sonogashira reaction conditions. When varying the Pd-catalysts, $Pd(PPh_3)_2Cl_2$ displayed better catalytic properties than $Pd(PPh_3)_4$ and $Pd_2(dba)_3$, which gave no results for the Sonogashira reaction (**Table 13**, entry 1-6). Interestingly, when $Pd_2(dba)_3$ was employed, the iodinated starting material **49c** was isolated along with a decomposed residue of the acetylene. It seems as though the acetylene fragmented back to its phenol equivalent. Weakly ligated Pd sources such as $Pd_2(dba)_3$ have been employed with bulky phosphines to generate the catalyst *in situ*.[161,164] In our case, we employed $Pd_2(dba)_3$ with 30 mol% tri-*o*-tolyl phosphate to couple the iodinated pyrimidine **49c** with acetylene **57a** to produce compound **58a** (**Table 13**, entry 7). Although traces of the product were observed using NMR spectroscopy, the starting material **49c** was the major substance isolated from the reaction. Unfortunately, we could not separate the starting material from the product owing to the similarities in R*f* values of the two compounds. Similarly to $Pd_2(dba)_3$, $Pd(PPh_3)_2Cl_2$ was used in combination with 5.0 eq PPh_3 and only 21% of the product was isolated. Addition of the ligand did not seem to have a significant impact on improving the yield for the coupling reaction.

Table 13. *Summary of reaction conditions applied to optimise the Sonogashira reaction of **49** with **57a**. Variation in catalyst.*

Entry	R	R'	Cat.	Temp. (°C)	solvent	ligand	Yield %
1.	Ph	Cl	$Pd(PPh_3)_2Cl_2$	rt	DMF	-	54
2.	Ph	Cl	$Pd(PPh_3)_4$	rt	DMF	-	-
3.	*tert*-butyl	Cl	$Pd(PPh_3)_2Cl_2$	rt	DMF	-	24
4.	*tert*-butyl	Cl	$Pd(PPh_3)_2Cl_2$	80	DMF	-	26
5.	*tert*-butyl	Cl	$Pd_2(dba)_3$	80	DMF	-	-
6.	*tert*-butyl	Cl	$Pd(PPh_3)_2Cl_2$	80	DMF	5.0 eq PPh_3	21
7	*tert*-butyl	Cl	$Pd_2(dba)_3$	80	DMF	30 mol% $P(O\text{-}tol)_3$	-

As $Pd(PPh_3)_2Cl_2$ proved to be a superior catalyst when coupling halogenated 2,4-diaminopyrimidine ring systems with acetylenes via the Sonogashira cross-coupling

reaction, it was therefore utilised as a catalyst of choice. Despite the positive results obtained when using $Pd(PPh_3)_2Cl_2$ as a catalyst, the yields for the Sonogashira alkyne product **58a** were low. To optimise the coupling reaction further, we investigated the use of different amines in the reaction.

Amines are not only employed to deprotonate acetylenic protons of terminal alkynes, but also to prevent homocoupling,[165] a transition-metal catalysed heterogeneous reaction where terminal alkynes couple to themselves in the presence of air forming diynes. The presence of copper provides suitable reaction conditions for homocoupling to take effect, which is a competing reaction to the Pd-catalyzed Sonogashira reaction. To prevent homocoupling of the terminal alkynes, the amine base coordinates to copper species in the reaction mixture. Formation of stable copper-amine complexes reduces the concentration of free copper species in the reaction mixture, thereby limiting progression of the homocoupling reaction.[165] Due to the excess concentration of the amine base, the equilibrium favours formation of stable copper-amine complexes. As a result, it is not surprising that the Sonogashira reactions require excess amine. Initially, 4 times the amount of base by volume was utilised in relation to the solvent, DMF, and 26% of the product was isolated (**Table 14**, entry 1). In a quest to find suitable reaction conditions for the optimum productivity of the Sonogashira coupling reaction, we began to change the *v/v* ratio of the base in relation to the solvent. Addition of 2:1 mixture of DIIPA to DMF increased the reaction yield from 26% to 33% (entry 2). Interestingly, a reaction conducted in equal parts of the base and solvent had the opposite effect to prior applied reaction conditions (entry 3). Changing from DIIPA to a more bulky base DIPEA resulted in increased reaction yields (38% and 59% for entry 4 and 5 respectively). No reaction was observed when the less bulky amine, trimethylamine, was in use; in fact, the iodinated starting material was isolated from the reaction mixture. (entry 6).

Table 14. *Summary of reaction conditions applied to optimise the Sonogashira reaction: variation in base.*

Entry	R	R'	Base	solvent	Ratio B:S	Yield %
1.	*tert*-butyl	Cl	DIIPA	DMF	(4:1)	26
2.	*tert*-butyl	Cl	DIIPA	DMF	(2:1)	33
3.	*tert*-butyl	Cl	DIIPA	DMF	(1:1)	21
4.	*tert*-butyl	Cl	DIPEA	DMF	(4:1)	38
5.	*tert*-butyl	Cl	DIPEA	DMF	(2:1)	59
6.	*tert*-butyl	Cl	TEA	DMF	(2:1)	-
7.	*tert*-butyl	F	DIPEA	DMF	(2:1)	30
8.	*tert*-butyl	F	DIIPA	DMF	(2:1)	63

Having successfully devised reaction conditions that resulted in moderate yields for the Sonogashira alkyne **58a**, we choose to test the applied reaction conditions using a different acetylene. The starting material **49c** was treated with **57b**, previously synthesised from 4-fluorophenol. The coupling reaction was conducted in the presence of a 2:1 mixture of DIPEA: DMF. The Pd-catalysed coupling reaction afforded the product **58b** in 30% yield (**Table 14**, entry 7). When DIPEA was employed as the base, the purification process by silica gel column chromatography was rather challenging and the product was isolated in combination with triphenylphosphine oxide. We therefore assessed the reaction using DIIPA as a base instead. Although traces of the phosphine impurity were observed in some fractions of the product, the yield significantly improved to 63% (entry 8).

Purification of these intermediates was achieved by conventional silica gel column chromatography. This was a tedious and time consuming, exercise, mostly met with disappointing results as the product isolated was contaminated with phosphine impurities. As a measure to avert the use of long columns for purification, we resorted to separate the Sonogashira products **58** from phosphine impurities via an acid-base extraction. Pyrimidine ring systems have basic properties, and therefore accept

protons in acidic media. Taking advantage of their basic nature, the reaction mixture was dissolved in a 12 M aqueous HCl solution. At low pHs the alkynes **58** were readily soluble in aqueous medium, which allowed the separation of the products from the phosphine impurity. The isolated aqueous layer was then basified to pHs above 9, where the alkyne products formed a separate layer above the aqueous medium. The product was then extracted using an organic solvent, such as ethyl acetate. The extraction method was less time consuming, however the majority of the product was lost during the process and low yields were generally reported when the method was used. Therefore, the residue of the reaction is first run through a short silica gel plug column to ensure the removal of inorganic species and the amine base. A second plug column, loaded with basic aluminium oxide, then allows for the removal of the phosphine impurity with a suitable mobile phase, consequently affording pure coupled product.

The Sonogashira reaction relies heavily on the use of aprotic solvents such as DMF. However, due to health concerns related to the use of DMF, efforts have been made to find alternative sustainable solvents where possible. Inspired by the progress we had made from previous steps by formulating mild and environmentally friendly reaction conditions, we explored the possibility of replacing DMF with 2-Me THF. As mentioned above, 2-Me THF is a recommended green solvent beneficial to the environment because it is derived from biofuel. 2-Me THF has been explored as a solvent replacement for THF, which is one of the solvents widely utilised in the Sonogashira reaction. With the success of the Sonogashira reaction using iodinated pyrimidines and pre-functionalized acetylenes, we were confident to test the feasibility of the coupling reaction using THF. Coupling of the iodinated pyrimidine with acetylene **57a** was attempted in the presence of THF (**Table 15**). Unfortunately the reaction did not work. Several efforts made towards making the reaction work were sadly fruitless. Despite the failure of the Sonogashira reaction using THF, we were determined to test the reaction conditions using 2-Me THF as a solvent. Unfortunately, the reaction was also unsuccessful.

Table 15. *Summary of reaction conditions applied to optimise the Sonogashira reaction of **49c** with **57a**. Variation in Solvent.*

Entry	R	R'	Cat.	solvent	Base	Yield %
1.	*tert*-butyl	Cl	$Pd(PPh_3)_2Cl_2$	DMF	DIPEA	59
2.	*tert*-butyl	Cl	$Pd(PPh_3)_2Cl_2$	THF	DIPEA	-
3.	*tert*-butyl	Cl	$Pd(PPh_3)_2Cl_2$	2-Me THF	DIPEA	-

The Pd-catalysed cross-coupling of the iodinated 2,4-diaminopyrimidine **49c** to a pre-functionalised acetylene **57a** to yield compound **58a** carried out in DMF was confirmed by NMR spectroscopy. The three new signals in the ^{1}H NMR spectrum unambiguously confirmed the presence of the substituted acetylene functionality coupled to the pyridimidine ring forming a new C-C bond, two of which appear in the aromatic region at δ 7.33 and 7.08 ppm and the other is observed in the aliphatic region at 5.10 ppm.

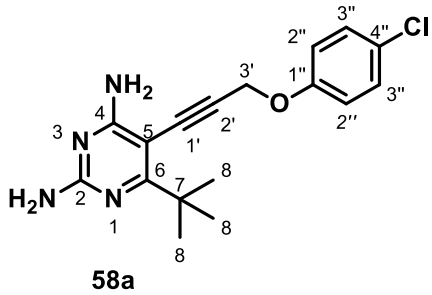

58a

The three signals are characteristic of the acetylene coupling partner and are assigned to H3'', H2'' and H3' respectively. In the ^{13}C NMR spectrum, the methylene carbon appears as a signal at 57.0 ppm, whereas the four phenoxy-ring peaks are distinctly observed in the aromatic region between 156.3 – 116.9 ppm. Two peaks due to the acetylene C≡C appear at δ 95.5 and 83.0 ppm. In addition to the ^{13}C NMR spectrum, the presence of the alkyne functionality was confirmed by the appearance of the C≡C stretch at 2214 cm^{-1} in the FTIR spectrum. Furthermore, the HRMS displayed a molecular ion peak at 331.1269 amu that correlates with the calculated mass for $C_{17}H_{19}ClN_4O$ of 331.1320 amu.

In light of all the information we had gained about the coupling of 2,4-diaminopyrimidine ring systems with pre-functionalized acetylenes via Pd catalysis, other analogues were synthesised using this methodology (**Scheme 36**). Pyrimidine **49c** was coupled with acetylenes **58b-i** (**Table 16**). Yields were not optimised in each case, and in particular the 2-Cl (**57g**) and 2-OMe (**57i**) substituted phenoxy acetylenes gave low yields of the products **58g** and **58i** respectively.

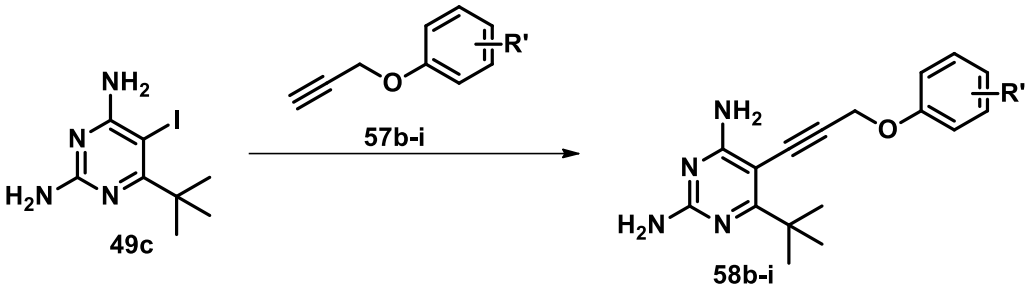

Scheme 36. *Reagents and conditions; alkyne, $Pd(PPh_3)_2Cl_2$, CuI, DIIPA, DMF (2:1), 80 °C, 12 h.*

Table 16. *Results of the Sonogashira coupling of **49c** with **57b-i**.*

Entry	Prod. #	R'	Yield (%)	m.p °C	HRMS calc.	HRMS found
1	**58b**	4-F	63	137	315.1616	315.1641
2	**58c**	4-OMe	27	107	327.1816	327.1781
3	**58d**	3-Cl	79	n/a	331.1320	331.1282
4	**58e**	3-F	73	n/a	315.1616	315.1576
5	**58f**	3-OMe	68	158	327.1816	327.1776
6	**58g**	2-Cl	10	97	331.1320	331.1266
7	**58h**	2-F	57	n/a	315.1616	315.1583
8	**58i**	2-OMe	14	n/a	327.1816	327.1768

In each case, the product was characterised by ^{1}H and ^{13}C NMR spectroscopy and HRMS. HRMS was in agreement with what was expected in each case (**Table 16**). Key signals in the ^{1}H NMR spectra can be found in **Tables 17**, where distinct peaks characteristic of the pyrimidines are observed. Signals for the two amino groups bonded to C-2 and C-4 of the pyrimidine ring were observed as singlets appearing at ~ 5.48 - 5.18 ppm and 5.29 - 4.90 ppm respectively. The signal for the *tert*-butyl group bonded to position 6 of the pyrimidine ring is distinctively observed at ~ 1.33 ppm as a singlet integrating for 9 protons in the ^{1}H NMR. In each case, four protons were observed in the aromatic region characteristic of the acetylene coupling precursor, and

H3' was observed at ~ 5.00 ppm as a singlets. Success of the coupling reaction was further confirmed by ^{13}C NMR spectra by observation of additional signals characteristic of the acetylene precursor (**Table 18**). Key signals characteristic of the phenoxy ring of the acetylene coupling precursor appear in the aromatic region, and the methylene carbon appears as a signal at ~ 57 ppm. Furthermore, two peaks due to the acetylene C≡C appear at ~ 95 and 83 ppm. In the ^{13}C NMR spectra, characteristic C-F coupling was observed for **58b**, **58e**, and **58h**, thus analogues with fluorine substituents on the phenoxy ring. ^{13}C NMR spectra for analogues **58c**, **58f** and **58i** have a signal observed at ~ 55 ppm due to the methoxy substituent on the phenoxy ring. These are all characteristic of the acetylene coupling precursor. The four signals due to the pyrimidine ring scaffolds were observed at 179, 165, 160 and 87 ppm for C6, C4, C2 and C5 respectively..

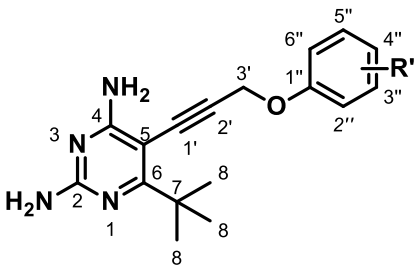

58b-i

Table 17. *Key signals in the ^{1}H NMR spectra that proves success of the Sonogashira coupling of **49c** with **57b-i**.*

Prod. #	R'	Phenolic protons (ppm)	NH_2	H3'	*Tert*-Butyl (H8)
58b	4-F	7.04 – 6.88 (m, H2'' & H3'')	5.30 (s) 5.08 (s)	4.96 (s)	1.33 (s)
58c	4-OMe	6.94 (d, *J* = 7.3 Hz, H2''/H3''), 6.83 (d, *J* = 9.1 Hz, H2''/H3'') 3.73 (s, OMe)	5.48 (s) 5.29 (s)	4.93 (s)	1.33 (s)
58d	3-Cl	7.19 (t, *J* = 8.2 Hz, H5''), 7.01 (s, H2''), 6.95 (d, *J* = 8.1 Hz, H4''), 6.88 (d, *J* = 8.4 Hz, H6''),	5.42 (s) 5.21 (s)	4.97 (s)	1.34 (s)
58e	3-F	7.21 (dd, *J* = 7.8, 7.1 Hz, H5''), 6.82 – 6.59 (m, H2'', H4'' & H6'')	5.46 (s) 5.24 (s)	4.97 (s)	1.34 (s)
58f	3-OMe	7.20 (dd, *J* = 8.4, 8.0 Hz, H5''), 6.67 – 6.47 (m, H2'', H4'' & H6'')	5.18 (s) 4.90 (s)	4.99 (s)	1.35 (s)
58g	2-Cl	7.37 (dd, *J* = 7.9, 1.6 Hz, H3''), 7.21 (ddd, *J* = 8.8, 7.4, 1.6 Hz, H5''), 7.10 (dd, *J* = 8.2, 1.5 Hz, H6''), 6.92 (ddd, *J* = 7.6, 7.6, 1.5 Hz, H4'')	5.38 (s) 5.13 (s)	5.09 (s)	1.32 (s)
58h	2-F	7.19 – 6.99 (m, H3'', H5'' & H6''), 6.96 – 6.86 (m, H4'')	5.45 (s) 5.27 (s)	5.09 (s)	1.31 (s)
58i	2-OMe	7.13 – 7.03 (m, H6''), 7.01 – 6.93 (m, H4''), 6.94 – 6.84 (m, H3'' & H5''), 3.87 (s, OMe)	5.22 (s) 4.99 (s)	5.09 (s)	1.33 (s)

Table 18. *Key signals in the ^{13}C NMR spectra that proves success of the Sonogashira coupling of **49c** with **57b-i**.*

Prod. #	R'	Pyrimidine C-peaks (ppm)	Phenolic C-peaks (ppm)	Alkyne C-peaks (ppm)	C3' (ppm)	*Tert*-Butyl C-peaks (ppm)
58b	4-F	179.0 (C6), 165.9 (C4), 160.5 (C2), 87.5 (C5),	157.8 (d, J_{C-F} = 239.4 Hz, C4''), 153.7 (d, J_{C-F} = 2.3 Hz, C1''), 116.5 (d, J_{C-F} = 8.0 Hz, C2''), 116.0 (d, J_{C-F} = 23.1 Hz, C3''),	95.6 83.0	57.6	38.8 (C7) 28.6 (C8)
58c	4-OMe	178.7 (C6), 165.8 (C4), 160.4 (C2), 87.4 (C5)	154.4 (C4''), 151.6 (C1''), 116.4 (C2''), 114.7 (C3''), 55.7 (OMe)	96.0 82.6	57.6	38.7 (C7) 28.6 (C8)
58d	3-Cl	179.1 (C6), 165.8 (C4), 160.4 (C2), 87.5 (C5)	158.3 (C1''), 135.0 (C3''), 130.4 (C5''), 121.8 (C4''), 115.5 (C2''), 113.8 (C6''),	95.2 83.3	57.0	38.8 (C7) 28.6 (C8)
58e	3-F	179.1 (C6), 165.9 (C4), 160.5 (C2), 87.3 (C5)	163.6 (d, J_{C-F} = 245.7 Hz, C3''), 158.9 (d, J_{C-F} = 10.6 Hz, C1''), 130.4 (d, J_{C-F} = 10.3 Hz, C5''), 110.9 (d, J_{C-F} = 2.9 Hz, C6''), 108.4 (d, J_{C-F} = 21.4 Hz, C2''), 103.1 (d, J_{C-F} = 25.1 Hz, C4''),	95.2 83.3	57.1	38.8 (C7) 28.6 (C8)
58f	3-OMe	178.9 (C6), 165.9 (C4), 160.4 (C2), 87.7 (C5)	161.0 (C3''), 158.9 (C1''), 130.1 (C5''), 107.3 (C6''), 107.2 (C4''), 101.9 (C2''),	95.8 82.9	55.4	38.8 (C7) 28.7 (C8)
58g	2-Cl	179.0 (C6), 165.9 (C4), 160.4 (C2), 87.4 (C5)	153.2 (C1''), 130.7 (C3''), 127.7 (C5''), 123.5 (C2''), 122.5 (C4''), 114.6 (C6''),	95.2 83.4	57.9	38.8 (C7) 28.6 (C8)
58h	2-F	178.9 (C6), 165.9 (C4), 160.5 (C2), 87.2 (C5)	153.2 (d, J_{C-F} = 245.8 Hz, C2''), 145.4 (d, J_{C-F} = 10.6 Hz, C1''), 124.3 (d, J_{C-F} = 3.9 Hz, C5''), 122.3 (d, J_{C-F} = 6.8 Hz, C4''), 116.6 (d, J_{C-F} = 18.4 Hz, C3''), 116.6 (d, J_{C-F} = 1.6 Hz, C6''),	95.3 83.4	58.3	38.7 (C7) 28.6 (C8)

Prod. #	R'	Pyrimidine C-peaks (ppm)	Phenolic C-peaks (ppm)	Alkyne C-peaks (ppm)	C3' (ppm)	*Tert*-Butyl C-peaks (ppm)
58i	2-OMe	178.8 (C6), 165.9 (C4), 160.4 (C2), 87.7 (C5)	150.0 (C2''), 146.8 (C1''), 122.4 (C4''), 120.8 (C5''), 114.8 (C6''), 112.1 (C3''), 55.9 (OMe)	95.9 83.0	57.9	38.8 (C7) 28.6 (C8)

FTIR analysis of products **58b-i** further confirmed the formation of the desired products. **58b-i**, with the characteristic C≡C stretch visible at ~2200 cm^{-1} (**Table 19**).

Table 19. *Key signal of the C≡C stretch in the FTIR spectrum for **58b-i**.*

Prod. #	R'	C≡C (cm^{-1})	Prod. #	R'	C≡C (cm^{-1})
58b	4-F	2217	**58f**	3-OMe	2223
58c	4-OMe	2215	**58g**	2-Cl	2203
58d	3-Cl	2202	**58h**	2-F	2203
58e	3-F	2204	**58i**	2-OMe	2203

3.1.3 Coupling of 5-iodo-6-isopropylpyrimidine-2,4-diamine (49d) with substituted acetylenes (57a-i).

To expand the library of 2,4-diaminopyrimidines, we synthesised the second series of analogues with an isopropyl group at position 6 of the pyrimidine ring. This was achieved by coupling the iodinated pyrimidine **49d** to acetylenes **57a'-i'** under the described Sonogashira reaction conditions (**Scheme 37**). Results of these reactions are summarised in **Table 20** below.

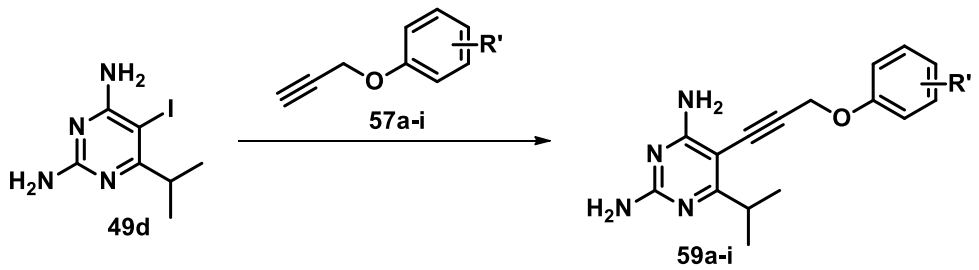

Scheme 37. *Reagents and conditions; alkyne, $Pd(PPh_3)_2Cl_2$, CuI, DIIPA, DMF (2:1), 80 °C, 12 h.*

Table 20. *Results of the Sonogashira coupling of 49d with* ***57b-i****.*

Entry	Prod. #	R'	Yield (%)	m.p °C	HRMS calc.	HRMS found
1	**59a**	4-Cl	46	78	317.1164	317.1186
2	**59b**	4-F	59	158	301.1459	301.1484
3	**59c**	4-OMe	63	n/a	313.1659	313.1681
4	**59d**	3-Cl	14	117	317.1164	317.1183
5	**59e**	3-F	41	n/a	301.1459	301.1482
6	**59f**	3-OMe	56	128	313.1659	313.1682
7	**59g**	2-Cl	10	78	317.1164	317.1184
8	**59h**	2-F	32	88	301.1459	301.1481
9	**59i**	2-OMe	23	205	313.1659	313.1683

We have successfully synthesised the second series of alkyne intermediates of the desired 2,4-diaminopyrimidines using the Sonogashira coupling reaction. It is worth highlighting that the yields for this reaction vary depending on the substituent and the position of the substituent on the phenoxy ring of the acetylene precursor. The yields for the *tert*-butyl alkyne analogues **58a-i** range from 10 – 79%, whereas those for the isopropyl alkyne analogues **59a-i** range from 10 – 63%. In general, the *tert*-butyl alkyne analogues were isolated in higher yields than the isopropyl analogues. This is true particularly looking at the statistical mean of the percentage yields, where the percentage yield mean for *tert*-butyl and isopropyl analogues is 47% and 38% respectively. By comparison of percentage yields in accordance to the type and position of individual substituent on the phenoxy ring of the acetylene precursor (**Figure 28**, *tert*-butyl analogues were generally higher yielding than the isopropyl analogues; with the exception of analogues containing 4-Cl, 4-OMe and 2-OMe groups on the phenoxy ring. In the case of compound **58a** (4-Cl), we utilised the percentage yield of 33% instead of the highest yield of 59% reported for the product obtained using DIPEA as a base. A yield of 33% was obtained when the Sonogashira reaction was carried out in the presence of DIIPA as a base (**Table 14**, entry 2). The reason we used this result is because all of the other analogues were synthesised in the presence

of DIIPA as a base. Each individual reaction was not optimised, and so it is not known whether this holds true for the reactions under optimised conditions.

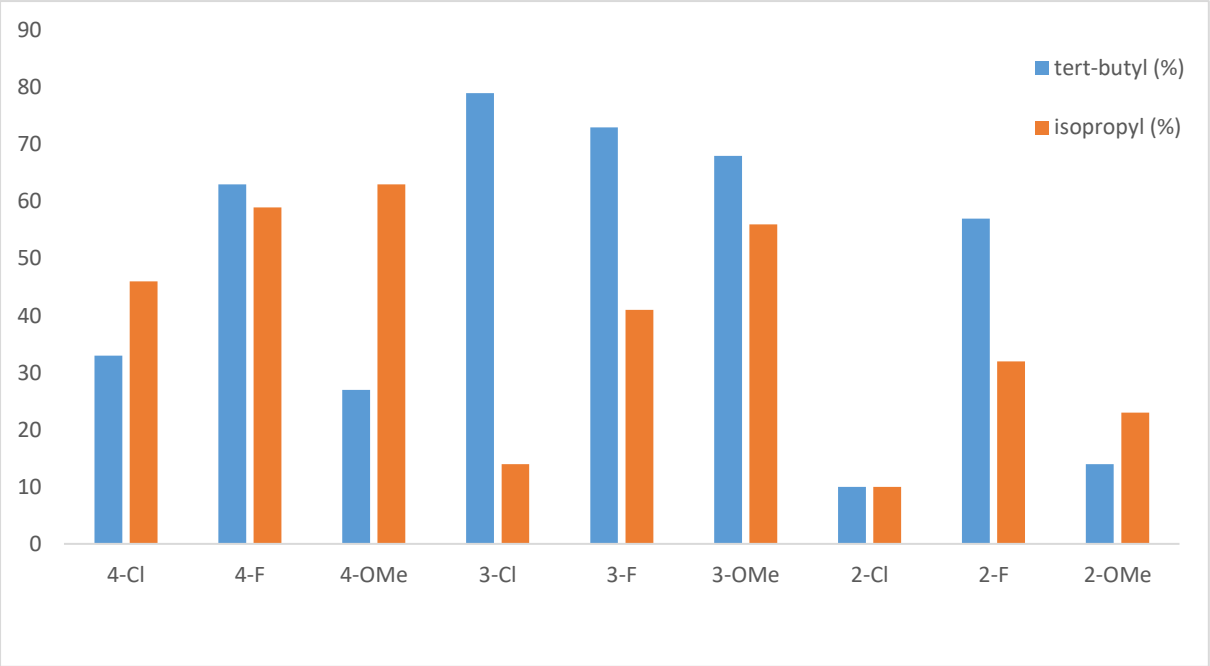

Figure 28. *Percentage yields of the Sonogashira alkyne products for both analogues with the tert-butyl group and the isopropyl group at C-6.*

Notably, compounds containing the 2-Cl substituent are the lowest yielding, with a reported yield of 10% for both *tert*-butyl and isopropyl analogues. Generally, the low yields could be attributed to the multiple columns performed to purify and isolate the products from the phosphine oxide impurity, or the competing side reactions such as homocoupling of the acetylenes could be responsible. In the presence of copper salt and amine base, the Sonogashira reaction conditions provide a suitable environment for homocoupling to take place.[166,167] However, no diynes were isolated from the Sonogashira cross-coupling reactions to provide evidence for homocoupling. We are more inclined to consider that the poor reactivity at C-5 is liable for the low yields. Pyrimidines are π deficient heteroaromatic compounds, and therefore facile to nucleophilic substitution. The electronegative N-atom makes pyrimidines more reactive at C-2 and C4 because the intermediate anion is stabilised by the N-atom and delocalization of π-electrons about the ring (**Figure 29**, a). However, the resulting

anion from nucleophilic substitution at C-5 is not stabilised by the N-atom, as illustrated in **Figure 29** (b), although it can be delocalised around the ring.[168]

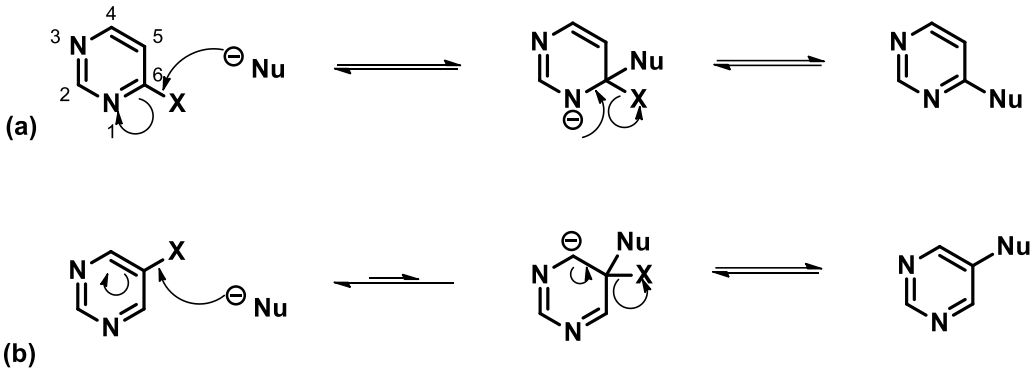

***Figure 29**. Stabilisation of the anion intermediate resulting from nucleophilic substitution of pyrimidine ring systems.*

Successful coupling of the pyrimidine **49d** to acetylenes **57a-i** was unquestionably confirmed by NMR spectroscopy (**Tables 21** and **22**). The two amino-groups characteristic of the pyrimidine ring of the Sonogashira products **59** appear between δ 5.57 – 5.08 ppm as two singlets adjacent to each other in the ^{1}H NMR spectra, and both integrating for two protons, with the exception of compounds **59e** and **59g**, where the NH_2 signals are overlapping and therefore observed as one singlet integrating for four protons. Furthermore, signals of the isopropyl-group attached to C-6 of the pyrimidine were distinctively observed in the aliphatic region. The signals appearing at approximately δ 3.22 ppm integrating for one proton was assigned to H7 of the isopropyl-groups, whereas the doublets at approximately δ1.13 ppm were assigned to H8. The newly added signals from the acetylenes **57a-i**, further confirmed the success of the Pd-catalysed reaction. New signals integrating for a total of four protons were observed in the aromatic region across the entire series **59a-i** on the analysed ^{1}H NMR spectra, indicative of the phenoxy-protons. The CH_2 denoted as H3' was observed at ~ 5.00 ppm, corresponding to the peak appearing at approximately 57 ppm in the ^{13}C NMR spectra. This peak was undeniably confirmed by DEPT as a CH_2 peak in each case.

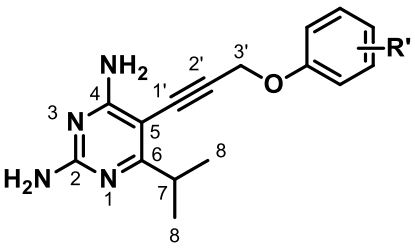

59

The four peaks in the ^{13}C NMR spectra observed at approximately 177, 164, 161 and 88 ppm belong to C-atoms on the pyrimidine ring assigned as C6, C4, C2 and C5 respectively. Upon comparison of the ^{13}C NMR spectrum of the starting material and those of the products, a significant shift of the C-5 peak was noted. The C-5 peak observed at δ 66.1 ppm of the starting material **49d**, shifted significantly to 88 ppm for the products **59**. The shift indicates the chemical transformation that occurred when the acetylenes **57a-i** were coupled to the pyrimidine ring forming new C-C bonds. Additionally, the acetylene C≡C peaks were distinctively observed at approximately δ 93.0 and 81.0 ppm in the ^{13}C NMR spectra, which further supports the identity of the product. The presence of the alkyne functional group in the products was further confirmed by FTIR. A sharp peak due to the C≡C stretch was observed at ~2200 cm^{-1} in each case (**Table 23**).

Table 21. *Key signals in the ^{1}H NMR spectra that prove success of the Sonogashira coupling of **49d** with **57b-i**.*

Prod. #	R'	Phenolic protons including p-substituents (ppm)	NH_2	H3'	H7 & H8
59a	4-Cl	7.25 (d, *J* = 9.0 Hz, H3''), 6.93 (d, *J* = 9.0 Hz, H2''),	5.54 (s) 5.49 (s)	4.94 (s)	3.19 (h, H7), 1.13 (d, H8)
59b	4-F	7.12 – 6.87 (m, H2'' & H3'')	5.17 (s) 5.08 (s)	4.94 (s)	3.20 (h, H7), 1.13 (d, H8)
59c	4-OMe	6.96 (d, *J* = 9.1 Hz, H2''/H3''), 6.84 (d, *J* = 9.1 Hz, H2''/H3''), 3.73 (s, OMe)	5.20 (s) 5.13 (s)	4.92 (s)	3.21 (h, H7), 1.14 (d, H8)
59d	3-Cl	7.22 (t, *J* = 8.1 Hz, H5''), 7.03 (t, *J* = 2.2 Hz, H2''), 6.98 (ddd, *J* = 7.9, 1.9, 0.9 Hz,H4''), 6.90 (ddd, *J* = 8.3, 2.5, 0.9 Hz, H6'')	5.19 (s) 5.08 (s)	4.97 (s)	3.22 (h, H7), 1.14 (d, H8)
59e	3-F	7.24 (q, *J* = 8.1 Hz, H5''), 6.86 – 6.60 (m, H2'', H4'' & H6'')	5.45 (s)	4.96 (s)	3.22 (h, H7), 1.14 (d, H8)
59f	3-OMe	7.17 (t, *J* = 8.2 Hz, H5''), 6.63 – 6.45 (m, H2'', H4'' & H6'')	5.57 (s) 5.55 (s)	4.93 (s)	3.23 (h,H7), 1.13 (d, H8)
59g	2-Cl	7.38 (dd, *J* = 7.9, 1.6 Hz, H3''), 7.21 (ddd, *J* = 8.3, 7.4, 1.7 Hz, H5'') 7.11 (dd, *J* = 8.2, 1.5 Hz, H6''), 6.93 (td, *J* = 7.7, 1.4 Hz, H4'')	5.44 (s)	5.06 (s)	3.19 (h,H7), 1.12 (d, H8)
59h	2-F	7.18 – 7.04 (m, H3'', H5'' & H6''), 7.03 – 6.89 (m, H4'')	5.20 (s) 5.15 (s)	5.06 (s)	3.19 (h,H7) 1.14 (d, H8)
59i	2-OMe	7.09 (dd, *J* = 8.1, 1.7 Hz, 1H, H6''), 7.01 – 6.95 (m, 1H, H4''), 6.94 – 6.88 (m, 2H, H3'' & H5'') 3.88 (s, OMe)	5.16 (s) 5.09 (s)	5.06 (s)	3.20 (h, H7) 1.13 (d, H8)

Table 22. *Key signals in the ^{13}C NMR spectra that prove success of the Sonogashira coupling of **49d** with **57b-i**.*

Prod. #	R'	Pyrimidine C-peaks (ppm)	Phenolic C-peaks (ppm)	Alkyne C-peaks (ppm)	C3' (ppm)	isopropyl C-peaks (ppm)
59a	4-Cl	177.8 (C6), 164.5 (C4), 161.4 (C2), 88.3 (C5)	156.1 (C1''), 129.4 (C3''), 126.5 (C4''), 116.5 (C2''),	93.0 81.3	57.1	33.5 (C7) 20.7 (C8)
59b	4-F	178.0 (C6), 164.6 (C4), 161.5 (C2), 88.6 (C5)	157.9 (d, J_{C-F} = 239.5 Hz, C4''), 153.7 (d, J_{C-F} = 2.2 Hz, C1''), 116.5 (d, J_{C-F} = 8.1 Hz, C2''), 116.0 (d, J_{C-F} = 23.1 Hz, C3''),	93.3 81.3	57.6	33.6 (C7) 20.8 (C8)
59c	4-OMe	177.7 (C6), 164.6 (C4), 161.4 (C2), 88.7 (C5)	154.6 (C4''), 151.6 (C1''), 116.6 (C2''), 114.7 (C3''), 55.8 (OMe)	93.8 80.9	57.7	33.5 (C7) 20.9 (C8)
59d	3-Cl	178.1 (C6), 164.6 (C4), 161.5 (C2), 88.5 (C5)	158.3 (C1''), 135.0 (C3''), 130.4 (C5''), 121.8 (C4''), 115.5 (C2''), 114.0 (C6'')	92.9 81.7	57.1	33.6 (C7) 20.8 (C8)
59e	3-F	178.0 (C6), 164.7 (C4), 161.5 (C2) 88.4 (C5)	163.6 (d, J_{C-F} = 245.4 Hz, C3''), 158.9 (d, J_{C-F} = 11.0 Hz, C1''), 130.4 (d, J_{C-F} = 9.9 Hz, C5''), 111.0 (d, J_{C-F} = 2.9 Hz, C6''), 108.4 (d, J_{C-F} = 21.3 Hz, C2''), 103.1 (d, J_{C-F} = 24.9 Hz, C4'')	93.0 81.5	57.1	33.6 (C7) 20.8 (C8)
59f	3-OMe	177.7 (C6), 164.5 (C4), 161.2 (C2), 88.5 (C5)	160.9 (C3''), 158.7 (C1''), 130.0 (C5''), 107.2 (C6''), 107.1 (C4''), 101.8 (C2''), 55.3 (OMe)	93.5 80.9	56.8	33.5 (C7) 20.7 (C8)
59g	2-Cl	177.8 (C6), 164.4 (C4), 161.2 (C2), 88.3 (C5)	153.0 (C1''), 130.6 (C3''), 127.5 (C5''), 123.6 (C2''), 122.4 (C4''), 114.7 (C6''),	92.9 81.5	57.9	33.5 20.7

Prod. #	R'	Pyrimidine C-peaks (ppm)	Phenolic C-peaks (ppm)	Alkyne C-peaks (ppm)	C3' (ppm)	isopropyl C-peaks (ppm)
59h	2-F	177.3 (C6), 164.6 (C4), 161.1 (C2), 88.7 (C5)	153.4 (d, J_{C-F} = 245.8 Hz, C2''), 145.4 (d, J_{C-F} = 10.6 Hz, C1''), 124.3 (d, J_{C-F} = 3.7 Hz, C5''), 122.6 (d, J_{C-F} = 7.0 Hz, C4''), 116.8 (d, J_{C-F} = 1.8 Hz, C6''), 116.7 (d, J_{C-F} = 18.7 Hz, C3''),	93.2 81.4	58.5	33.5 20.8
59i	2-OMe	177.5 (C6), 164.6 (C4), 161.2 (C2), 88.9 (C5)	150.1 (C2''), 146.7 (C1''), 122.4 (C4''), 120.7 (C5''), 114.9 (C6''), 112.0 (C3''), 56.0 (OMe)	93.7 81.1	57.9	33.5 20.8

***Table 23**. Key signal of the C≡C stretch in the FTIR spectrum for **59a-i**.*

Prod. #	R'	C≡C (cm^{-1})	Prod. #	R'	C≡C (cm^{-1})
59a	4-Cl	2217	**59f**	3-OMe	2198
59b	4-F	2220	**59g**	2-Cl	2217
59c	4-OMe	2215	**59h**	2-F	2215
59d	3-Cl	2214	**59i**	2-OMe	2208
59e	3-F	2216			

3.1.4 Reduction of the Sonogashira Intermediates

Having successfully synthesised the alkyne intermediates, we were now ready to test the final step of the synthesis: the reduction of the C≡C to give a saturated C-C bond. Reduction of the alkyne functional group is the direct addition of H-atoms to the C≡C bond catalysed by a transition metal. This reaction can also be referred to as catalytic hydrogenation of alkynes. The reaction cannot take place without the catalyst due to the high activation energy. The catalysts lowers the activation energy of the reaction by breaking H-H σ bonds. Palladium and platinum catalysts are transition-metal catalysts commonly used to facilitate this heterogeneous reaction.

The reduction of alkynes is a stereoselective syn-addition reaction. If the reaction was to be interrupted by poisoning the catalyst, then hydrogenation of the alkyne will selectively generate an equivalent *cis* alkene. The stereoselective nature of the reaction can be explained from the reaction mechanism. In the first step, (**Figure 30**), H_2 gas molecules chemically adsorb onto the surface of the metal catalyst, as a result H-H σ bonds are broken.[168] Then the alkyne complexes to the metal by overlapping its π orbitals with vacant orbitals of the metal.[169] The catalytic hydrogenation occurs on the surface of the metal, with both H-atoms transferred from the metal to the alkyne on the same side of the C≡C giving rise to the *cis* alkene intermediate. In the absence of catalyst poisoning, the *cis* alkene is further reduced to the alkane.

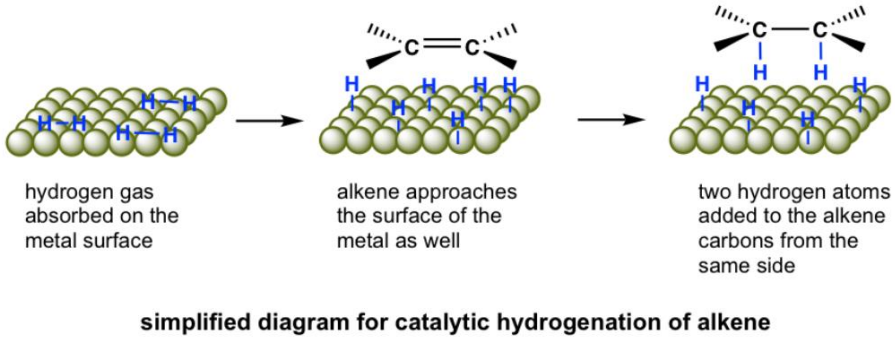

Figure 30. *Schematic diagram of the mechanism of a hydrogenation reaction.*[169]

3.1.4.1 Preparation of 6-*tert*-butyl-2,4-diaminopyrimidine analogues by catalytic hydrogenation

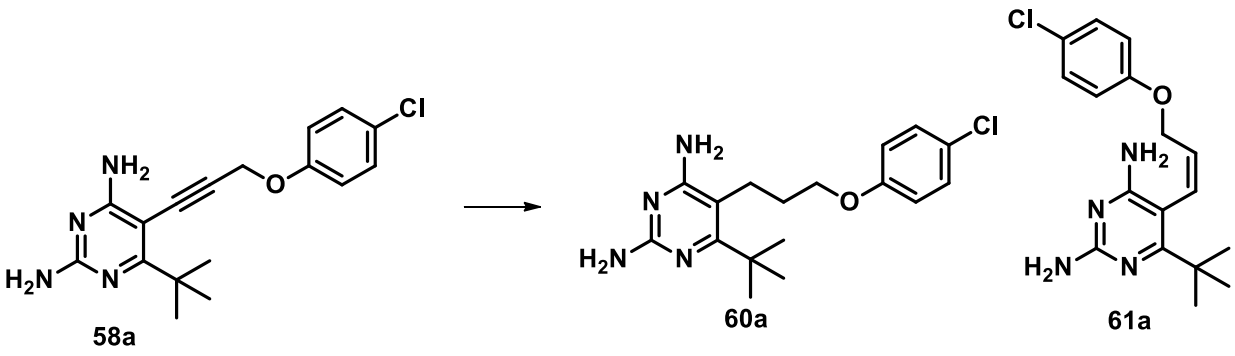

Scheme 38. *Reagents and conditions; H_2, Pd/C, EtOH, 16 h, 2 bars.*

Utilising the reaction conditions described in Chapter 2, where compound **53** was reduced to **54**, we now set about reducing alkynes **58** from the same conditions (see

Chapter 2, **Scheme 32**). We attempted a hydrogenation reaction on the alkyne substrate **58a** in ethanol using catalytic amounts of Pd/C in the presence of an atmosphere of H_2 (gas) (**Scheme 38**). Unfortunately, no reaction occurred and the alkyne starting material **58a** was recovered. As the reaction did not work under these conditions, we repeated the reaction at a higher pressure in a reactor (2 bar H_2). To our delight, the very first 2nd generation 2,4-diaminopyrimidine product **60a** was isolated in 21% yield. Surprisingly though, the (*Z*)-alkene equivalent **61a** was isolated as the major product, in a yield of 56% (**Scheme 38**).

Key signals in the NMR spectra of the product confirm the success for hydrogenation of the C≡C bond to the fully saturated 2,4-diaminopyrimidine analogue **60a**. In the ^{1}H NMR spectrum, two new signals are found in the aliphatic region due to the 2 newly formed CH_2 groups denoted as H1' and H2', resulting from the reduction of the C≡C bond. H1' is responsible for the multiplet observed at δ 2.85 – 2.67, whereas H2' is observed at 1.99 (dq, *J* = 11.1, 5.6 Hz). The third CH_2 group observed in the ^{1}H NMR spectrum appears at 4.02 ppm and it is assigned to H3'. Previously, the signal for H3' was a singlet. The change in multiplicity of H3' from a singlet in substrate **58a** to a triplet observed in the product **60a** affirms success of the hydrogenation reaction. The triplet arises as a result of the H3' protons coupling to H2' protons splitting them into a triplet (*J* = 5.5 Hz). 2D NMR spectroscopic analysis indicate correlation of the observed CH_2 groups (H3', H2' and H1') to three peaks appearing at δ 68.1, 28.4 and 23.5 ppm in the ^{13}C NMR spectrum respectively. The ^{13}C NMR spectrum also confirmed the disappearance of the distinct acetylene peaks between 93 – 81 ppm from the starting material **58a**. Furthermore, a molecular ion of 335.1573 amu was reported in the HRMS, which is in agreement with the calculated mass for $C_{17}H_{23}ClN_4O$ of 335.1633 amu.

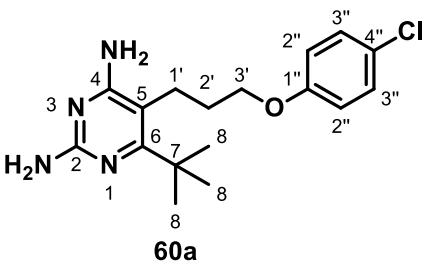

60a

The NMR spectra of the alkene intermediate **61a** differs slightly from the alkyne starting material **58a** in that distinct alkene peaks are observed. Signals for alkene protons appear at 6.62 δ (dt, *J* = 10.9, 1.4 Hz) and 6.08 ppm (dt, *J* = 11.0, 6.3 Hz) assigned to H1' and H2'' respectively. The reported *J*-coupling constant of ~11 Hz for the alkene protons confirms that the geometric isomer isolated from the hydrogenation reaction is the "*Z*" isomer. This confirms that the alkyne substrate undergoes a syn-addition of H-atoms facilitated by the Pd-catalyst giving a stereoselective *cis* product.[170] The ^{13}C NMR spectrum further confirms formation of the alkene, with C=C peaks observed at δ 130.2 and 128.6 ppm. Analysis of HRMS showed a molecular ion of 333.1437 amu, which is in good agreement with the calculated of mass 333.1477 amu for $C_{17}H_{21}ClN_4O$.

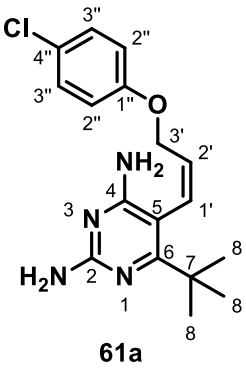

61a

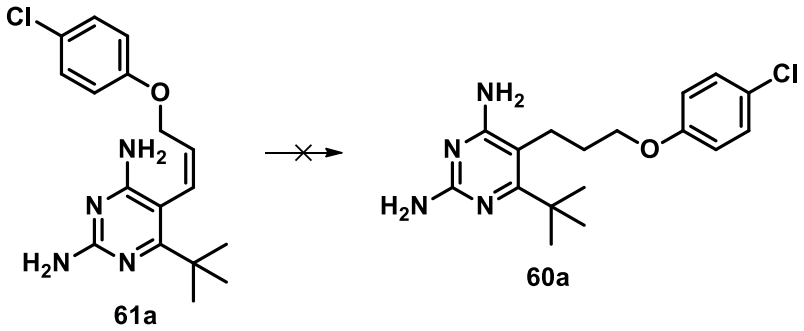

Scheme 39. *Reagents and conditions; H_2, Pd/C, EtOH, 16 h, 2 bars.*

Formation of the alkene "by product" was an unexpected surprise, since the set reaction conditions were suitable to hydrogenate the alkene intermediate further to the alkane product. The reaction was ran under pressure and no catalyst poison was added to interrupt the reaction, therefore it was not clear why the reaction stopped at the alkene intermediate. In an attempt to further reduce the alkene to the desired 2,4-diaminopyrimine **60a**, we subjected compound **61a** to a Pd-catalysed hydrogenation reaction in a hydrogen reactor set at 2 bar overnight (**Scheme 39**). After this time the reaction mixture was filtered through celite to remove Pd/C and the residue was purified using silica gel column chromatography, unfortunately, the alkene starting material **61a** was isolated.

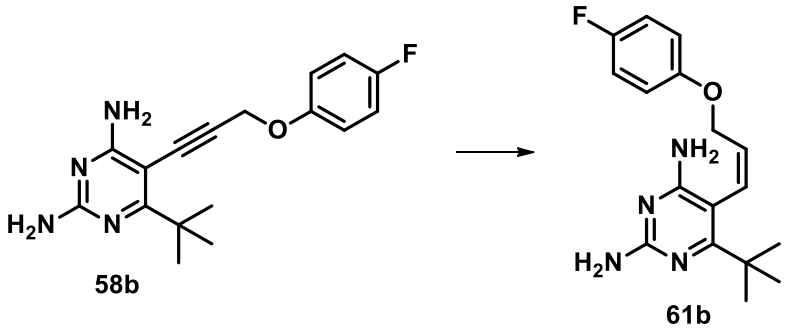

***Scheme 40**. Reagents and conditions; H_2, Pd/C, EtOH, 16 h, 2 bars.*

Failing to understand why the hydrogenation did not work, we attempted the reaction on a different substrate. The Sonogashira product **58b**, was subjected to the same reaction conditions (**Scheme 40**). Unfortunately, this time around, the alkene intermediate **61b** was the only product isolated from the reaction. Changing the catalyst to Pt (IV) oxide did not yield different results. From this, we can conclude that catalyst poisoning is not responsible for the formation of the *cis*-alkene product

To get a better understanding of why the hydrogenation reaction does not go to completion, we explored the 3D structure of the alkene product. To determine what could be obstructing the hydrogenation reaction from taking place. Ideally, a crystal structure of the substrate would have been helpful, but unfortunately, we could not grow crystals from the alkene products isolated. We therefore utilised a simulated 3D model structure of the alkene substrate generated from CHEM Bio-ultra application. Although it is not the actual 3D geometric structure of the alkene, the model does give a somewhat realistic visualisation of the 3D structure.

From literature, we understand that the *cis* isomer is thermodynamically unstable because the bulky-substituents about the C=C bond are in close proximity The *tert*-butyl group bonded to C-6 of the pyrimidine ring is bulky and therefore exerts steric hindrance to groups close to it. The 3D model shows that the *tert*-butyl group is relatively close to the alkene double bond and could therefore interfere with reactions occurring at this position.

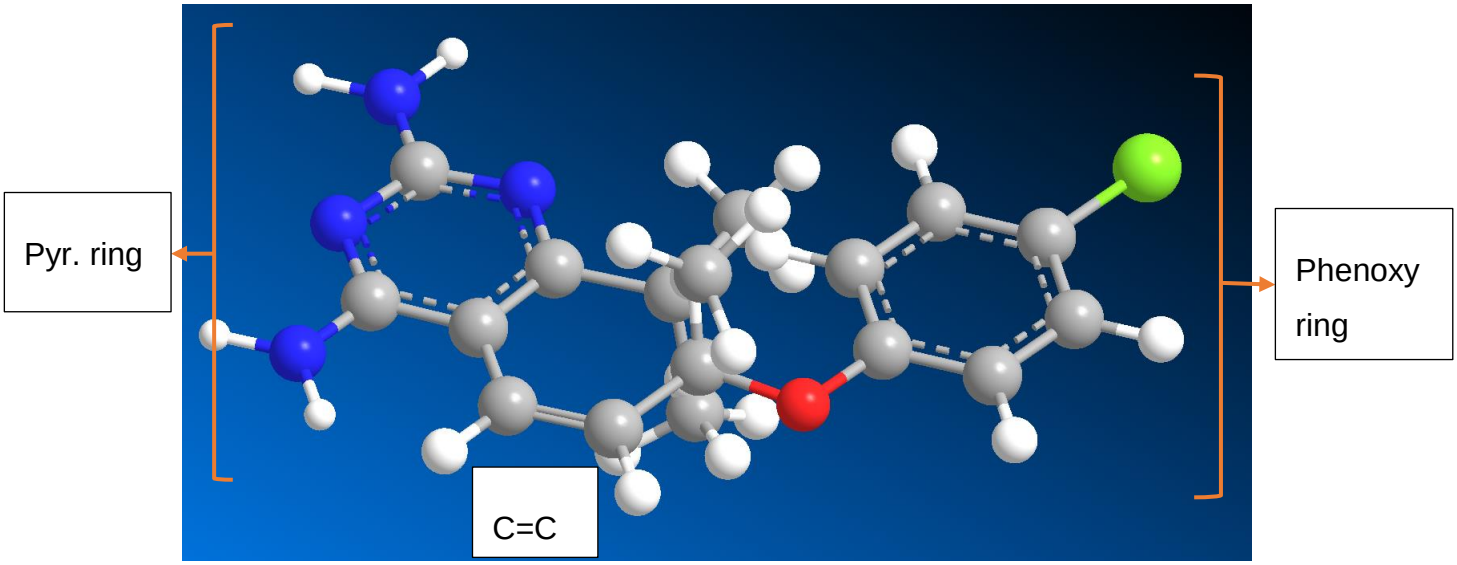

Figure 31. *Simulated model of the 3-D geometric structure of compound **60a**.*

Considering the reaction mechanism, in order for a hydrogenation reaction to take effect the alkene has to interact with the Pd-catalyst by overlapping its π orbitals with vacant orbitals of the Pd metal. Looking at the 3D model, the methyl groups of the *tert*-butyl substituent are on either side of the alkene C=C bond. We hypothesise that the bulky methyl groups of the *tert*-butyl obstruct the alkene C=C bond from coordinating to the metal catalyst. To test this theory, the hydrogenation was attempted on an alkyne with an isopropyl group at position 6 of the 2,4-diaminopyrimidine system. Compound **59a** was therefore subjected to the hydrogenation reaction conditions and only the product **62a** was isolated in 48 % yield (**Scheme 41**). No evidence for the formation of the *cis*-alkene was observed. The exclusive isolation of compound **62a** supports our hypothesis that the *tert*-butyl group is preventing hydrogenation of the alkene.

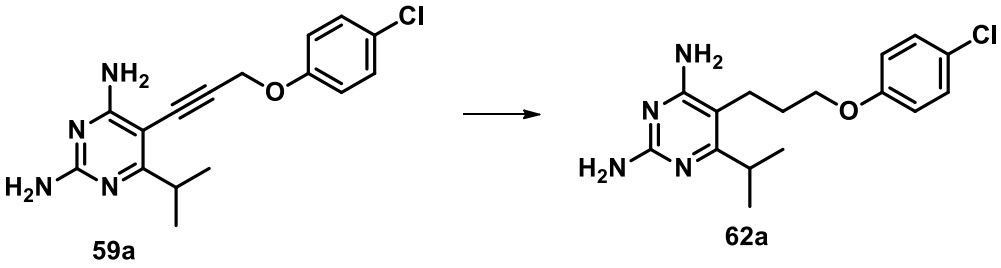

Scheme 41. *Reagents and conditions; H_2, Pd/C, EtOH, 16 h, 2 bars.*

The remaining *tert*-butyl alkynes were reduced to their equivalent alkenes and/or alkanes using the described reaction conditions (**Scheme 42**). Hydrogenation

reactions were conducted in a reactor set at 2 bars over 16 hours as described above. It was apparent that for some reactions traces of the fully reduced products **60** were detected using TLC. Notably, the desired products were detected as a faint spot by TLCand the alkene intermediate showed more prominence. Hydrogenation of the alkynes in the reactor set at higher pressure (3-6 bars) and shorter periods resulted in the exclusive isolation of the alkene intermediates. This indicates that the desired fully reduced 6-*tert*-butyl-2,4-diaminopyrimidine products required extended periods in order to form. From the *tert*-butyl series, we only managed to isolate three fully reduced products; Compounds **60a**, **60c** and **60d** where R' = 4-Cl, 4-OMe and 3-Cl respectively. Hydrogenation of the other analogues yielded the alkene intermediates exclusively. As observed in **Table 24**, the fully reduced analogues were isolated in low yields, and similar to the 4-Cl analogue **60a**, their alkene equivalents were the major products.

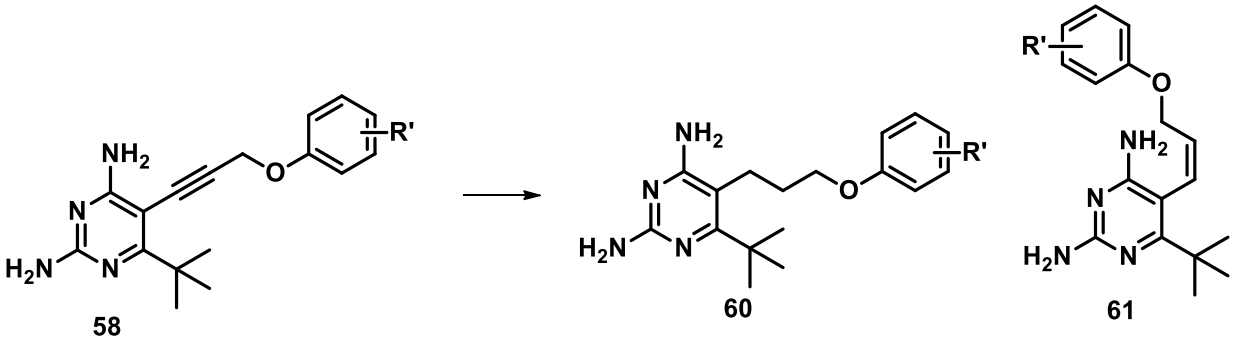

Scheme 42. *Reagents and conditions; H_2, Pd/C, EtOH, 16 h, 2 bars.*

NMR spectroscopy certainly proved formation of the reduced products **60c** and **60d** (**Tables 25** and **26**). From the studied ^{1}H NMR spectra, conservation of the pyrimidine ring was observed by the 2 singlets signalling for the amino groups observed at δ 5.00 and 4.50 ppm respectively. In addition, the distinct singlet in the aliphatic region (δ 1.35 ppm) due to the *tert*-buty group further confirmed the integrity of the pyrimidine ring during the chemical conversion. The newly observed CH_2 signals confirmed reduction of the C≡C bond. H1' is observed as a signal at δ 2.85 – 2.67 ppm, H2' gives rise to a signal at 2.00 ppm as a dq (*J* = 10.8, 5.7 Hz) and because of the electronegative O-atom attached to H3', it gives rise to a signal observed at 4.00 ppm as a triplet (*J* = 5.5 Hz).

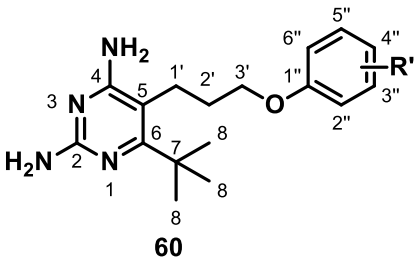

The similarities in the *J* values between H2' and H3' indicates that they do in fact couple to each other. The CH_2 signals, confirmed by HSQC, correlate with carbon peaks observed at approximately δ 68.0, 28.0, and 23.4 on the ^{13}C NMR spectra respectively. Furthermore, the presence of the CH_2 groups was distinctively confirmed by DEPT. Notably, there is a significant difference in the chemical shift observed for C-5 of the pyrimidine ring. The carbon-13 signal was observed at approximately δ 88.0 ppm in the ^{13}C NMR spectra of the alkyne starting materials **58c** and **58d**, and currently the C-5 signal is observed further up field at 105.0 ppm in the ^{13}C NMR spectra of the products **60c** and **60d**. The significant shift in carbon signals observed indicates that C-5 of the products is in a different chemical environment in comparison to that of the alkyne starting materials. Previously, it was covalently bonded to an *sp* hybridised C-atom, whereas currently it is bonded to an sp^3 hybridised C-atom. Therefore, although C-5 was previously bonded to a C-atom, hybridisation of the C-atom it is covalently attached to has a significant effect on the chemical shift of C-5. HRMS data also confirmed formation of the products **60c** and **60d** as ionic molecular mass obtained for products agreed with the expected mass (see **Table 24**).

Table 24*. Summary of yields and HRMS data for the fully saturated 6-tert-butyl-2,4-diaminopyrimidines* ***60c*** *and* ***60d****.*

Entry	Prod. #	R'	Yield (%)	m.p °C	HRMS calc.	HRMS found
1	**60c**	4-OMe	14	106	331.2129	331.2083
2	**60d**	3-Cl	13	n/a	335.1633	335.1579

Table 25. Key ^1H NMR signals indicating formation of the desired 6-tert-butyl-2,4-diaminopyrimidines **60c** and **60d**.

Entry	Prod. #	2(NH_2) ppm	H3' (ppm)	H2' (ppm)	H1' (ppm)
1	**60c**	5.01 (s), 4.54 (s),	4.00 (t, *J* = 5.4 Hz)	1.97 (tt, *J* = 11.1, 5.5 Hz)	2.85 – 2.67 (m)
2	**60d**	4.95 (s), 4.59 (s)	4.04 (t, *J* = 5.5 Hz)	2.02 (dt, *J* = 10.8, 5.7 Hz)	2.86 – 2.67 (m)

Table 26. *Key ^{13}C NMR signals indicating formation of the desired 6-tert-butyl-2,4-diaminopyrimidines **60c** and **60d**.*

Entry	Prod. #	Pyr. C peaks (ppm)	C3' (ppm)	C2' (ppm)	C1' (ppm)
1	**60c**	173.0 (C6), 164.0 (C4), 160.0 (C2), 105.0 (C5),	68.4	28.7	23.4
2	**60d**	173.3 (C6), 163.8 (C4), 159.8 (C2), 104.7 (C5)	68.0	28.3	23.5

For the remaining substrates **58b-i**, alkene products are products **61b-i** were recovered from the hydrogenation reaction (**Table 27**).

Table 27. *Summary of yields and HRMS data for the alkene intermediates of the 6-tert-butyl-2,4-diaminopyrimidine series **61b-i**.*

Entry	Prod. #	R'	Yield (%)	m.p °C	HRMS calc.	HRMS found
1	**61b**	4-F	13	84	317.1772	317.1734
2	**61c**	4-OMe	24	n/a	329.1972	329.1924
3	**61d**	3-Cl	22	86	333.1477	333.1404
4	**61e**	3-F	18	101	317.1772	317.1731
5	**61f**	3-OMe	76	77	329.1972	329.1932
6	**61g**	2-Cl	69	74	333.1477	333.1424
7	**61h**	2-F	58	87	317.1772	317.1732
8	**61i**	2-OMe	71	n/a	329.1972	329.1928

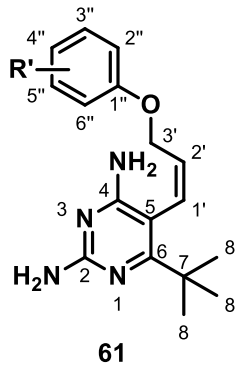

61

Hydrogenation of the alkyne substrates **58b-i** to their alkene equivalents **61b-i** resulted in the addition of two H-atoms on each C-atom of the C≡C bond. Therefore, success of the hydrogenation reaction was confirmed by two alkene CH signals observed at δ 6.68 – 6.58 and 6.17 – 6.07 ppm in the ^{1}H NMR spectra of the products, each integrating for one proton (**Table 28**). The observed *J* values resulting from coupling of the alkene protons is

~ 11 Hz, correlating with *J* values observed for vicinal *cis* isomers. This indicates that we have successfully synthesised the cis alkenes **61b-i** . Furthermore, the presence of the alkene C=C bond is confirmed by the two alkene C-peaks observed in the ^{13}C NMR spectra at δ 131.0 -130.0 ppm for C2' and 129.1 – 128.1 ppm for C1' respectively (**Table 29**). Despite the undisputed evidence provided by NMR spectroscopy, HRMS data further supports successful formation of the alkene intermediates **61b-i**. The reported ionic molecular mass are in good agreement with the calculated masses for products **61b-i** (**Table 27**).

Table 28. *Key ^{1}H NMR signals indicating formation of the alkene intermediates of the 6-tert-butyl-2,4-diaminopyrimidine series* ***61b-i****.*

Entry	Prod. #	2(NH_2) ppm	H1' (ppm)	H2' (ppm)	H3' (ppm)
1	**61b**	4.80 (s), 4.69 (s)	6.61 (d, *J* = 11.0 Hz)	6.09 (dt, *J* = 11.5, 6.3 Hz)	4.36 (d, *J* = 5.6 Hz)
2	**61c**	4.80 (d), 4.67 (d)	6.59 (d, *J* = 10.9 Hz)	6.09 (dt, *J* = 11.3, 6.3 Hz)	4.36 (d, *J* = 6.0 Hz,),
3	**61d**	4.95 (s), 4.86 (s)	6.62 (d, *J* = 10.9 Hz)	6.07 (dt, *J* = 12.3, 6.3 Hz)	4.46 – 4.28 (m)
4	**61e**	4.80 (s), 4.70 (s)	6.55 (dt, *J* = 10.9, 2.3 Hz, H1'')	6.08 (dt, *J* = 11.0, 6.3 Hz)	4.38 (d, *J* = 5.2 Hz)
5	**61f**	4.88 (s), 4.76 (s)	6.60 (dt, *J* = 10.9, 1.4 Hz)	6.09 (dt, *J* = 11.0, 6.3 Hz)	4.39 (d, *J* = 5.9 Hz)
6	**61g**	4.99 (s), 4.86 (s)	6.64 (d, *J* = 11.0 Hz)	6.15 (dt, *J* = 11.0, 6.5 Hz)	4.45 (d, *J* = 6.4 Hz)
7	**61h**	4.92 (s), 4.80 (s)	6.63 (d, *J* = 11.0 Hz)	6.14 (dt, *J* = 11.0, 6.4 Hz)	4.46 (d, *J* = 5.9 Hz)
8	**61i**	4.97 (s) 4.85 (s)	6.58 (d, *J* = 11.0 Hz)	6.17 (dt, *J* = 11.1, 6.3 Hz),	4.45 (d, *J* = 6.0 Hz)

Table 29. *Key ^{13}C NMR signals indicating formation of the alkene intermediates of the 6-tert-butyl-2,4-diaminopyrimidine series* ***61b-i***.

Entry	Prod. #	Pyr. C peaks (ppm)	C1' (ppm)	C2' (ppm)	C3' (ppm)
1	**61b**	173.8 (C6), 162.0 (C4), 160.9 (C2), 101.1 (C5)	128.4	130.5	66.1
2	**61c**	173.9 (C6), 162.0 (C4), 161.1 (C2), 101.2 (C5)	128.3	130.8	66.3
3	**61d**	173.9 (C6), 161.8 (C4), 160.9 (C2), 100.9 (C5)	128.7	130.0	65.5
4	**61e**	173.9 (C6), 161.9 (C4), 161.1 (C2), 101.0 (C5)	128.8	130.0	65.6
5	**61f**	173.8 (C6), 161.9 (C4), 161.0 (C2), 101.1 (C5)	128.4	130.5	65.4
6	**61g**	173.9 (C6), 161.9 (C4), 161.0 (C2), 100.8 (C5)	129.1	130.4	66.3
7	**61h**	173.9 (C6), 161.9 (C4), 161.1 (C2), 100.9 (C5)	128.9	130.1	66.8
8	**61i**	173.5 (C6), 161.9 (C4), 160.8 (C2), 101.1 (C5)	128.1	131.0	66.6

3.1.4.2 Preparation of 5-(3-(4-chlorophenoxy)propyl)-6-isopropylpyrimidine-2,4-diamine 62a by catalytic hydrogenation

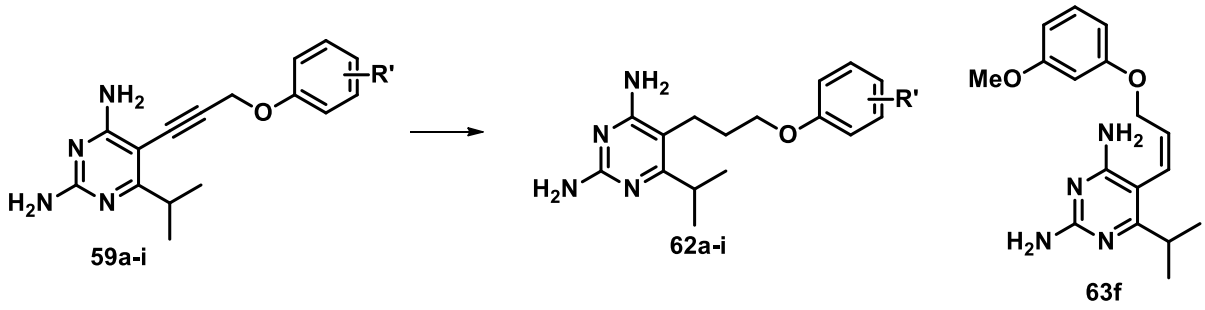

Scheme 43. *Reagents and conditions; H_2, Pd/C, EtOH, 16 h, 2 bars.*

The hydrogenation reaction conditions described for the *tert*-butyl series were applied to the isopropyl series. Alkyne substrates **59a-i'** resulting from the Sonogashira reaction were subjected to Pd-catalysed hydrogenation reaction in a reactor set at 2 bar pressure (**Scheme 43**). The desired target products were successfully synthesised and isolated in moderate to exceptional yields, ranging between 23 and 96% (**Table 30**). Due to the presence of a less bulky group at position 6 of the pyrimidine ring, the isopropyl substituent, fully reduced products were exclusively isolated, with the exception of the 3-OMe analogue, where compound **62f** was isolated with the alkene intermediate **63f** (**Scheme 43**). In this case the product **62f** was isolated as the minor product in 23% yield, whilst the alkene intermediate **63f** was isolated in 55% yield. However, in contrast to the *tert*-butyl analogues further hydrogenation of the alkene intermediate resulted in the production of the desired reduced product compound **62f**. Upon observation of the melting points, it was apparent the products are low melting solids, with the lowest reported melting point of 61 °C. In contrast, the ortho-substituted analogues had higher melting points, with reported m.p of 148 °C determined for the 2-Cl analogue and 220 °C observed for the 2- OMe analogue. Compound **62h** was not isolated in pure enough form and will be repeated (**Table 30**, entry 7).

Table 30*. Summary of yields and HRMS data for the desired of the 6-isopropyl-2,4-diaminopyrimidine series* ***62a-i****.*

Entry	Prod. #	R'	Yield (%)	m.p °C	HRMS calc.	HRMS found
1	**62a**	4-Cl	48	114	321.1477	321.1499
2	**62b**	4-F	96	72	305.1772	305.1789
3	**62c**	4-OMe	81	61	317.1972	317.1988
4	**62d**	3-Cl	90	119	321.1477	321.1494
5	**62e**	3-F	75	68	305.1772	305.1789
6	**62f**	3-OMe	23	100	317.1972	317.1988
7	**62g**	2-Cl	54	148	321.1477	321.1498
8	**62h**	2-F	-	-	-	-
9	**62i**	2-OMe	65	220	317.1972	317.1990

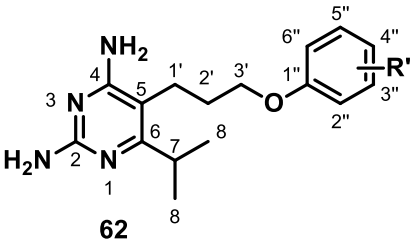

62

Successful synthesis of the target isopropyl analogues **62** was undoubtedly confirmed by NMR spectroscopy (**Tables 31 and 32**). The newly observed CH_2 groups in the aliphatic region of the ^1H NMR spectra confirms success of the hydrogenation reaction. H3' and H1' give rise to the triplets observed at 4.09 – 3.88 ppm and 2.70 -2.51 ppm respectively, while H2' is responsible for the pentet observed at 1.98 – 1.91 ppm in each case (**Table 31**). Similar to the alkyne starting materials **59a-i**, two amino groups bonded to C2 and C4 of the pyrimidine ring were distinctively observed as singlets between δ 6.08 – 4.63 ppm each integrating for 2 protons, which indicate the presence of the heteroaromatic ring. Signals for the branched aliphatic isopropyl group bonded to C6 of the pyrimidine ring were assigned as H7 and H8. H7 appeared as a signal at ~ 3.00 ppm in the aliphatic region as a heptet or pentet integrating for one proton, whilst H8 gives rise to a doublet observed at ~ 1.15 ppm integrating for six protons. This confirms successful hydrogenation of the alkyne triple bond, while keeping the flexible linker chain covalently bonded to the pyrimidine.

Conservation of the marriage between the pyrimidine rings and the acetylenes is further confirmed by the four pyrimidine type signals at approximately 172 (C6), 163 (C4), 161 (C2), and 103 ppm (C5) as observed in the ^{13}C NMR spectrum of each product (**Table 32**). These peaks are characteristic of the pyrimidine ring. Similar to the *tert*-butyl analogues, the signal for C5 shifts significantly from 88 ppm for the starting material to 103 ppm for the product in each case, indicating the change in the hybridisation of the C-atom bonded to C5. Furthermore, the newly formed CH_2 groups, confirmed by DEPT, were observed at approximately 29 and 21 ppm. The CH_2 (C3') bonded to an O-atom is observed further up field at δ ~ 66 ppm. The distinct disappearance of the alkyne signals is a clear indication of the successful hydrogenation of the Sonogashira products giving rise to the desired flexible 6-isopropyl-2,4-diaminopyrimidines **62**.

***Table 31**. Key ^1H NMR signals indicating formation of the desired 6-isopropyl-2,4-diaminopyrimidine series **62a-i**.*

Entry	Prod. # (*p*)	2(NH_2) ppm	H3' (ppm)	H2' (ppm)	H1' (ppm)
1	**62a**	4.91 (s) 4.78 (s)	3.93 (t, *J* = 5.6 Hz)	1.93 (p, *J* = 6.5 Hz)	2.58 (t, *J* = 7.3 Hz)
2	**62b**	5.07 (d), 4.99 (d)	3.92 (t, *J* = 5.5 Hz)	1.92 (p, *J* = 7.1 Hz)	2.58 (t, *J* = 7.3 Hz)
3	**62c**	4.94 (s), 4.69 (s)	3.91 (t, *J* = 5.5 Hz)	1.91 (p, *J* = 7.1 Hz),	2.59 (t, *J* = 7.3 Hz)
4	**62d**	6.08 – 5.58 (m), 5.43 (s)	3.97 (t, *J* = 5.5 Hz)	1.93 (p, *J* = 6.5 Hz)	2.58 (t, *J* = 7.4 Hz)
5	**62e**	4.88 (s), 4.74 (s)	3.88 (t, *J* = 5.6 Hz)	1.87 (p, *J* = 6.4 Hz)	2.51 (t, *J* = 7.4 Hz)
6	**62f**	5.91 (s), 5.63 (s)	3.96 (t, *J* = 5.3 Hz)	1.98 – 1.83 (m)	2.59 (t, *J* = 7.2 Hz)
7	**62g**	Signal under H_2O peak	4.09 (t, *J* = 5.5 Hz)	1.98 (p, *J* = 6.2 Hz),	2.70 (t, *J* = 7.6 Hz)
8	**62i**	5.29 (s), 4.63 (s)	4.02 (t, *J* = 5.4 Hz)	1.96 (p, *J* = 6.5 Hz)	2.63 (t, *J* = 7.2 Hz)

***Table 32**. Key ^{13}C NMR signals indicating formation of the desired 6-isopropyl-2,4-diaminopyrimidine series.*

Entry	Prod. # (*p*)	Pyr. C peaks (ppm)	C3' (ppm)	C2' (ppm)	C1' (ppm)
1	**62a**	172.4 (C6), 163.1 (C4), 161.1 (C2), 103.0 (C5)	66.8	29.0	21.2
2	**62b**	172.0 (C6), 163.1 (C4), 160.9 (C2), 103.1 (C5)	67.1	29.0	21.2
3	**62c**	172.4 (C6), 163.2 (C4), 161.3 (C2), 103.2 (C5)	67.0	29.2	21.2
4	**62d**	171.0 (C6), 162.8 (C4), 159.7 (C2), 103.0 (C5)	66.7	28.8	21.1
5	**62e**	172.4 (C6), 163.1 (C4), 161.3 (C2), 103.0 (C5)	66.8	28.9	21.2
6	**62f**	169.8 (C6), 163.2 (C4), 159.4 (C2), 103.2 (C5	66.3	28.9	21.1
7	**62g**	172.2 (C6), 165.7 (C4), 159.9 (C2), 104.9 (C5)	68.4	29.4	21.8
8	**62i'**	171.3 (C6), 163.5 (C4), 160.9 (C2), 103.5 (C5)	67.1	29.1	20.9

3.1.4.3 Preparation of 6-cyclopropyl-5-(3-(4-fluorophenoxy)propyl)pyrimidine-2,4-diamine

We have successfully synthesised 2,4-diaminopyrimidine analogues **60** and **62** with branched aliphatic groups at C-6 of the pyrimidine ring. However, as mentioned in Chapter 1, analogues containing an isopropyl or cyclopropyl group at position 6 scored

higher in the molecular docking studies, which can translate to high potency against both the wild-type and quadruple malaria mutant enzyme models. In the final aspects of this work, we hoped to apply the developed total synthesis to a pyrimidine ring system substituted with an aliphatic ring at C-6.

To this end, the synthesis of a 2,4-diaminopyrimidine analogue with an aliphatic ring at position 6 was initiated by subjecting the iodinated pyrimidine **49a** to a Sonogashira cross-coupling reaction. This particular pyrimidine system was selectively chosen because it bares the cyclopropyl ring at C-6. The molecular modelling studies did inform the potential potency of 2,4-diaminopyrimidine derivaties bearing this aliphatic ring on both the wild and mutant enzymes. Therefore, successful synthesis of these derivatives will allow for an actual evaluation of the compounds against both wild type and mutant *P*fDHFR *in vitro*. Ideally we would like to obtain a comparative study on the potency of isopropyl analogues vs cyclopropyl analogues in the biochemistry enzyme essay. However, due to time constrains we were limited to only demonstrating the feasibility of this synthetic approach by preparing one analogue from the cyclopropyl series.

The iodinated pyrimidine **49a** was utilised as the electrophile meant in a Pd-catalysed cross-coupling reaction with acetylene **57a**. The reaction was conducted in the presence of $Pd(PPh_3)_2Cl_2$, CuI and DIIPA as a base, under N_2 atmosphere at 100 °C over 12 hours. The reaction mixture generated the product **64** in 42% yield (**Scheme 44**).

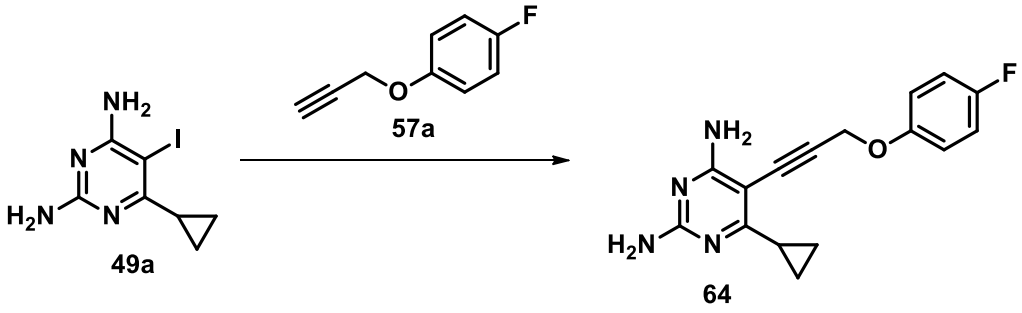

Scheme 44. *Reagents and conditions; alkyne, $Pd(PPh_3)_2Cl_2$, CuI, DIIPA/DMF (2:1), 12 h, rt.*

The duccess of the coupling reaction was confirmed by signals characteristic of both the pyrimidine ring and the acetylene substrate observed on the ^{1}H NMR spectrum. The pyrimidine was distinctively characterised by two singlets appearing at δ 5.20 and 4.97 ppm due to the amino groups, and signals appearing in the aliphatic region due to the cyclopropyl ring bonded to C6. H7 was observed at 2.22 ppm as a triplet of triplets, whilst the two CH_2 groups denoted as H8 were observed at 1.03 (dt, *J* = 6.2, 3.3 Hz) and 0.88 (dq, *J* = 7.2, 3.6 Hz). The two signals observed for H8 and the similarity in the coupling constant (*J* = 3.3Hz) shows that the axial protons of the CH_2 groups in the cyclopropyl ring couple to the equatorial protons. This in fact comes as no surprise because the cyclopropyl ring is very rigid, thus free rotation about the single bonds is expected to be restricted. Features of the coupling partner, the acetylene, were characterised by the multiplet observed in the aromatic region integrating for 4 protons. Lastly, H3' was responsible for the singlet observed at δ 4.95 ppm integrating for 2 protons. Notably, the acetylenic proton that appeared at 2.53 ppm in the ^{1}H NMR spectrum of the acetylene substrate, has disappeared, supporting the success of the coupling reaction.

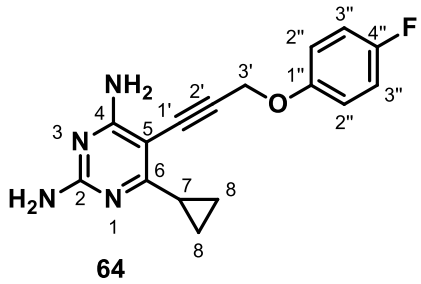

64

The 13 peaks observed in the ^{13}C NMR spectrum further confirmed formation of the product. Since the acetylene substrate has a fluoro-substituent at the *para* position, the four newly added peaks in the aromatic region due to the phenolic carbons were easily identified and characterized as a result of carbon-fluorine coupling. Furthermore, distinct C≡C peaks were observed at δ 92.8 and 81.6 ppm respectively. The significant difference in the chemical shift of C-5 from 64.3 ppm for the iodinated starting material to 89.5 ppm for the product shows the success of the coupling reaction at C-5, giving rise to formation of a new C-C bond. HRMS data further supports formation of the product, with the observed ionic molecular mass of 299.1319 amu matching the one calculated for $C_{16}H_{15}FN_4O$ of 299.1303 amu.

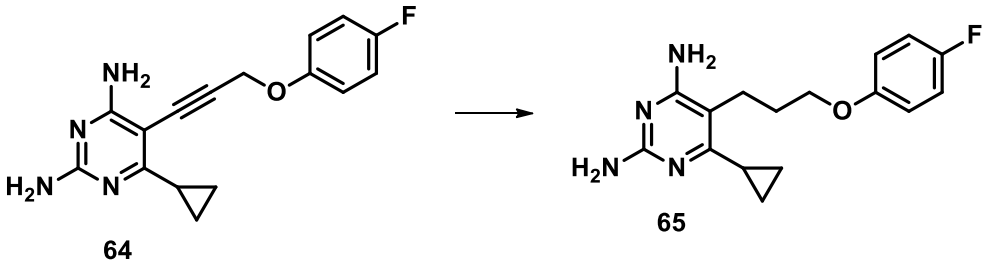

Scheme 45. *Reagents and conditions; H_2, Pd/C, EtOH, 16 h, 2 bars.*

Satisfied with the alkyne product **64**, we were now ready to hydrogenate the multiple bond to yield the desired 6-cyclopropyl-2,4-diaminopyrimidine derivative **65**. In a reactor at 2 bar pressure, a solution of the alkyne starting material **64** in ethanol was treated with Pd/C in the presence of H_2 gas to produce compound **65** as a brown solid in 77% yield. The ^{1}H NMR spectra undoubtedly proved that the hydrogenation reaction was a success. The two newly formed CH_2-groups were observed at δ 2.72 (t, *J* = 7.0 Hz) and 2.00 ppm (dt, *J* = 12.6, 6.0 Hz). The latter, H2', couples to H3' found at 3.92 ppm as a triplet integrating for two protons. The three CH_2 groups correlate to the three carbon peaks in the ^{13}C NMR spectrum observed at 21.1, 28.6 and 66.9 ppm respectively. Another notable feature that confirms the success of the hydrogenation reaction is the unmistakable disappearance of the C≡C peaks in the ^{13}C NMR spectrum.

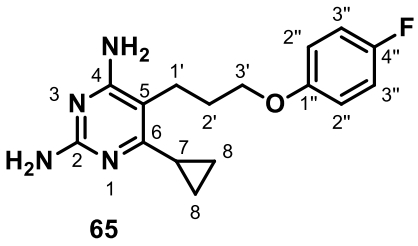

In conclusion, we have successfully synthesised two series of 2,4-diaminopyrimidine analogues, i.e. the *tert*-butyl analogues **60a-c** and the isopropyl analogues **62a-i**. Unfortunately we could not fully reduce all the *tert*-butyl alkynes to the desired 2,4-diaminopyrimidines with a saturated flexible 4-linker chain, due to the bulky *tert*-butyl group, however, alkenes **61a-i** were isolated and characterised, and will be tested for activity against both wild type and mutant *Pf*DHFR. We have also successfully applied the developed synthetic plan towards the synthesis of an aliphatic analogue with a cyclopropyl at position 6 of the pyrimidine ring. Success of the Sonogashira reaction on this particular compound suggests that the methodology can be used to further expand the library of analogues.

3.2 Synthesis of analogues containing other heteroatoms

Thus far, the Sonogashira reaction has proven to be reproducible when applied to halogenated heteroaromatic pyrimidine rings in the presence of nucleophilic alkynes derived from phenols. To investigate the robustness of this reaction on other systems, Sonogashira reaction conditions were employed using alkynes derived from aniline as nucleophiles. This interest led us to attempt the synthesis of 2,4- diaminopyrimidines with a different hetero-atom other than oxygen in the flexible linker, such as compound **68**, using the developed synthetic route (**Scheme 46**).

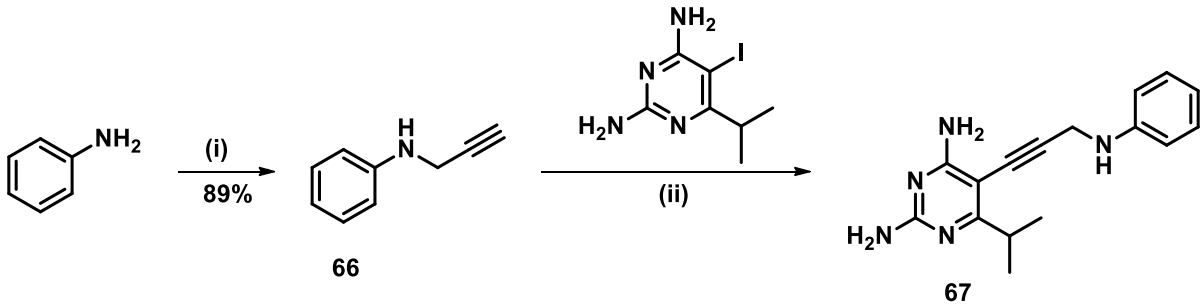

Scheme 46. *Reagents and conditions; (i) propargyl bromide, K_2CO_3, DMF, r.t, 8 h; (ii) $Pd(PPh_3)_2Cl_2$, CuI, DIIPA, DMF (2:1), 80 °C, 12 h.*

We attempted the Sonogashira reaction on an alkyne substrate prepared from aniline. To our delight, the alkyne was coupled with compound **49d** via a Pd-catalysed Sonogashira cross-coupling reaction to give the product **67** in 60% yield (**Scheme 46**). Formation of the product was confirmed by key signals characteristic of the pyrimidine ring system and the alkyne observed on the ^{1}H NMR spectrum. The two amino groups

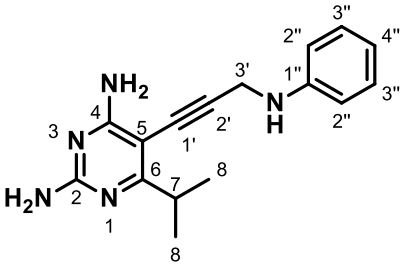

were observed as singlets appearing at δ 5.04 and 4.98 ppm, while signals for the isopropyl group were observed in the aliphatic region. H7 appeared at 3.19 ppm and H8 at 1.12 ppm as a doublet integrating for 6 protons. All this addresses the integrity of the 2,4-diaminopyrimidine ring system. Signals observed in the aromatic region integrated for a total of five protons, due to the phenyl ring originating from aniline. With the help of a CH correlation experiment, we were able to correlate the phenyl protons to the phenyl carbon peaks appearing between δ 129.4– 114.2 ppm in the ^{13}C NMR

spectrum. The quaternary carbon (C1'') of the phenyl ring was observed at δ 147.1 ppm. The alkyne peaks distinctively appeared at 96.1 ppm and 77.4 ppm, further point to the success of the coupling reaction. Furthermore, upon analysis of the HMBC 2D NMR spectrum, it was evident that the isopropyl peaks couple with C5 and C6 of the pyrimidine appearing at 89.3 and 177.1 ppm respectively. In addition, a molecular ion peak observed on the HRMS with a mass of 282.1731 amu confirmed formation of compound **67.**

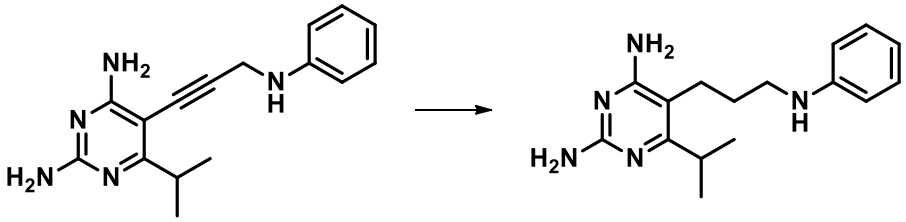

Scheme 47. *Reagents and conditions; H_2, Pd/C, EtOH, 16 h, 2 bars.*

The success of the Sonogashira reaction, a key reaction for the synthesis of these 2,4- diaminolpyrimidines, afforded us the opportunity to test the hydrogenation reaction. Using reaction conditions previously described, we subjected compound **67** to a reduction reaction catalysed by Pd/C in the presence of H_2 gas under pressure (**Scheme 47**). This reaction was conducted in a hydrogen reactor utilised as a reaction vessel set at a pressure of 2 bar. Progress of the reaction was monitored by TLC, of which indicated complete conversion of the starting material to the product after 16 hours. The catalyst was filtered off, and the remaining filtrate was concentrated on the rotary evaporator. The product was purified further using basic aluminium oxide column chromatography and isolated as a white solid in 58%.

Formation of the product was indisputably confirmed by NMR spectroscopy. The two observed signals at 2.54 (t, J = 7.8 Hz) and 1.76 (p, J = 6.8 Hz) in the ^{1}H NMR spectrum were due to the newly formed CH_2 groups resulting from reduction of the C≡C bond. H2' coupled to H3' and split it into a triplet observed at 3.15 (t, J = 6.5 Hz) ppm. This further confirmed success of the hydrogenation reaction, as H3' was observed as a singlet in the ^{1}H NMR spectrum of the starting material. Proton signals of the CH_2 groups corresponded to the three distinct carbons appearing in the aliphatic region on

the ^{13}C NMR spectrum. Furthermore, the unmistakable disappearance of the alkyne C-peaks supports formation of the product **68**.

We have successfully applied the Sonogashira reaction using an alkyne containing a heteroatom other than oxygen. This proves the robustness of the Sonogashira reaction to accommodate a vast spectrum of alkyne reagents that can be utilised as nucleophiles. Having successfully utilised the newly developed synthetic route on this derivative of 2,4-diaminopyrimidine **68**, we can further expand the library of compounds by introducing substituents on the phenyl ring.

4 CHAPTER 4: Results and discussion

4.1 Biological data

It is more urgent than ever to discover novel antimalarial agents as the pressure to combat resistance against currently used antifolates keeps mounting. Malaria causing parasites are constantly gaining resistance against current drugs such as pyrimethamine (**Figure 32**), an antifolate that inhibits *Pf*DHFR. Therefore, the development of new antifolates is imperative to effectively target the folate pathway in this pathogenic species. Resistance towards pyrimethamine is attributed towards the rigid bi-aryl structure of pyrimethamine. The antifolate has a heteroaromatic ring covalently connected to an aryl ring by a rigid σ-bond as illustrated in **Figure 32**. It has been shown that resistance to pyrimethamine is due to the rigidity of the structure which clashes with mutant amino acids in the *Pf*DHFR active site. To bypass resistance brought about these point mutations in the active site of the enzyme, drug candidates with flexible structures have been developed.

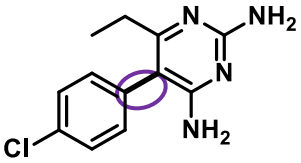

Figure 32. *Chemical structure of pyrimethamine.*

A molecular modelling campaign conducted by a colleague in our laboratory, Matthew Maree, led to the design of 2nd generation 2,4-diaminopyrimidine derivatives **15** with aliphatic groups at position 6 of the pyrimidine core (**Figure 33**). These compounds contain an aromatic heterocyclic ring connected to a terminal aryl ring by a flexible 4-atom linker. Their structure was inspired by the folate co-factor DHF, which is made up of a pterin ring moiety connected to *p*-aminobenzoate and glutamate (**Figure 33**). These derivatives mimic the structure of DHF and could potentially inhibit the catalytic function of *Pf*DHFR, thereby inhiting parasitic replication.

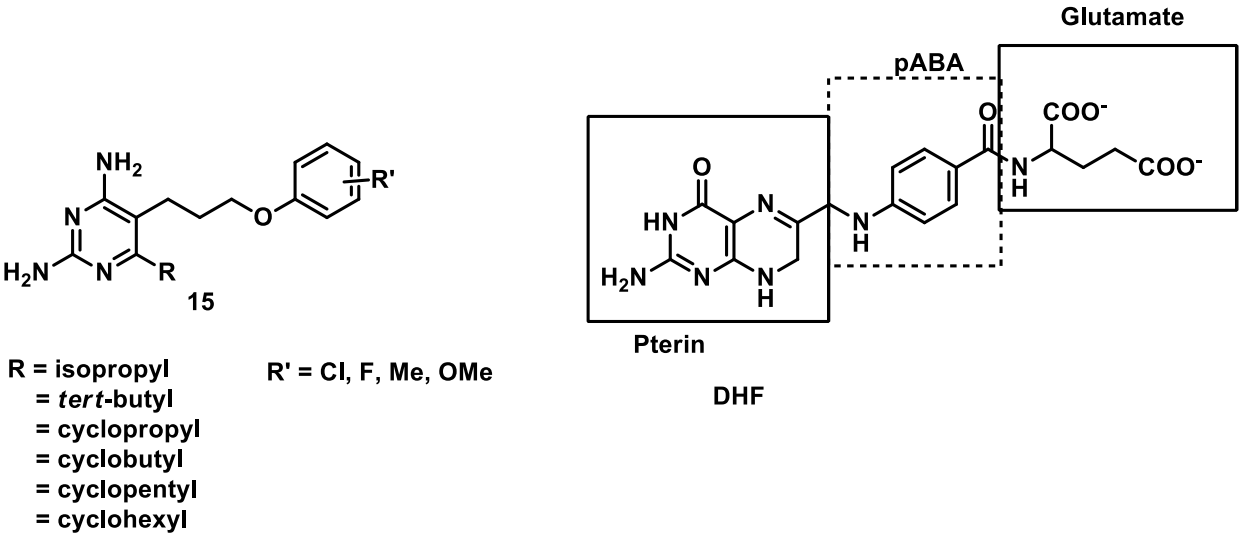

Figure 33. *Chemical structure of the designed analogues **15** and DHF.*

4.1.1 Enzymatic assays

The modelling studies interrogated virtual interactions between the designed pyrimidine structures **15** with different forms of the *Pf*DHFR enzyme, i.e. both the wild type and the quadruple mutant. From the studies, we learnt that compounds with an aliphatic group at position 6 of the pyrimidine ring displayed a high binding affinity to the active site of *Pf*DHFR. Thus, the designed pyrimidine structures **15** showed the potential to inhibit *Pf*DHFR. We therefore developed a synthetic route towards these compounds. In a five step synthetic procedure, a series of both the *tert*-butyl analogues and the isopropyl analogues were successfully synthesised, using the Sonogashira reaction as the key step towards formation of these systems. Of the synthesised analogues, 15 compounds were sent for preliminary tests to assess their inhibitory activity against both wild type and mutant *Pf*DHFR enzymes in a series of *in vitro* biochemical enzyme assays. These compounds were also tested for inhibitory activity against human DHFR to evaluate selectivity and toxicity. Compounds from the *tert*-butyl series that were sent for biological testing included the reduced products **60**, and the alkenes **61**. Furthermore, we saw it necessary to include the Sonogashira alkyne scaffolds **58**, after a report by Beierlein et al. in 2008.[159] They described a novel series of *Bacillus anthracis* DHFR inhibitors. These antifolates **66** are structural derivatives of trimethoprim with a propargyl linker between the aromatic heteroatom ring and the substituted aryl ring (**Figure 34**). They displayed inhibitory activity against

*Ba*DHFR and the lead compound was found to be 82-fold more potent than trimethoprim against *B. anthracis*, a virulent Gram-positive bacteria that causes anthrax.[159] Similar to the Sonogashira alkyne products **58**, the reported *Ba*DHFR inhibitors contain a C≡C in the linker (**Figure 34**). As a result, we were interested to find out whether our alkyne intermediates **58** would display any inhibitory activity against *Pf*DHFR.

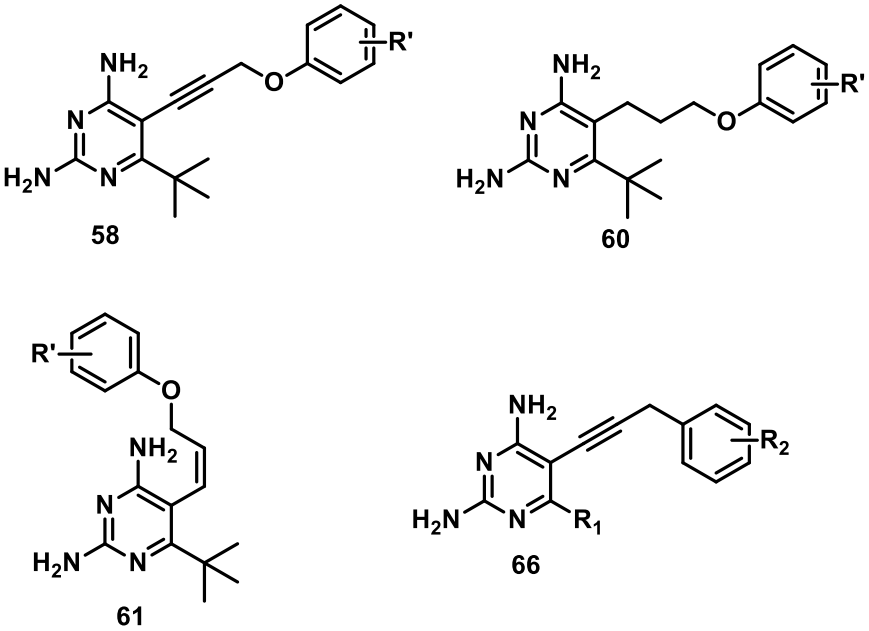

***Figure 34**. Chemical structures of compounds **58**, **60** and **61**, and that of BaDHFR inhibitors.*[159]

Prof Yongyuth Yuthavong and colleagues at BIOTEC, Thailand, conducted the assays, which showed very promising results. From the Ki values reported (**Table 33**) we can deduce that all tested compounds had a lower binding affinity for human DHFR, when compared with *Pf*DHFR. This suggest that compounds show selectivity for *Pf*DHFR over human DHFR.

Table 33. *Evaluation of inhibition of human DHFR and PfDHFR wild type and mutant type.*

Entry	R'	*Pf*DHFR-WT (nM)[a]		*Pf*DHFR-QM (nM)[b]		*Hs*DHFR (nM)[c]	
		Ki	SD	Ki	SD	Ki	SD
58a	4-Cl	0.49	0.06	1.95	0.04	54.58	3.6
58b	4-F	0.29	0.02	1.28	0.06	27.26	0.41
58c	4-OMe	0.26	0.02	0.85	0.04	30.49	1.63
58d	3-Cl	0.34	0.04	0.88	0.03	45.06	3.47
58e	3-F	0.38	0.01	1.21	0.05	36.67	1.61
58f	3-OMe	0.30	0.01	0.78	0.02	25.02	1.02
58g	2-Cl	0.71	0.05	1.65	0.07	45.35	1.46
58h	2-F	0.34	0.02	1.32	0.05	28.49	0.98
60a	4-Cl	0.99	0.06	4.81	0.18	289.93	5.64
60c	4-OMe	0.36	0.05	1.3	0.06	57.84	0.9
61b	4-F	1.90	0.13	3.46	0.12	>250000	
61c	4-OMe	1.56	0.1	2.11	0.07	222.68	10.12
61d	3-Cl	1.88	0.07	2.37	0.1	396.48	11
61f	3-OMe	0.80	0.05	0.8	0.04	>500000	
61h	2-F	1.57	0.02	4.64	0.2	690.2	33.8
PYR		0.34	0.02	29.34	1.47	40.96	1.33
TMP		0.59	0.02	49.07	0.68	>1000000	

[a] WT= wild type; [b] QM= quadruple mutant; [c] HS= Homosapies; PYR= pyrimethamine; TMP= trimethoprim

Most importantly, all the tested compounds inhibited both the wild type and quadruple mutant *Pf*DHFR in the low nanomolar range, with high inhibitory activity observed for the wild type enzyme with K_i values ranging between 0.26 – 1.9 nM (**Table 33**). To our

surprise, the alkyne products **58** were the most potent against both forms of the parasitic enzyme. This is illustrated on the graph below (**Figure 35**), where the x-axis is plotted from the most active inhibitor on the left hand side to the least potent inhibitor on the right. The most active inhibitor, compound **58'** with a 3-OMe substituent on the phenoxy ring, exhibits a K_i value of 0.78 nM against the *Pf*DHFR quadruple mutant type. Whereas, compound **60a**, which contains a 4-Cl substituent on the phenoxy ring, showed the least inhibitory activity with a K_i value of 4.81 nM against the quadruple mutant. Although compound **60a** displayed a lower binding affinity relative to the other tested compounds, it still inhibited the mutant type enzyme in the low nanomolar range and to a far greater extent than pyrimethamine (PYR) (utilised as a known standard) with K_i = 29.34 nM, or trimethoprim (TMP) (K_i = 49.07 nM) which is significantly the weakest inhibitory activity against the *Pf*DHFR quadruple mutant observed in this series.

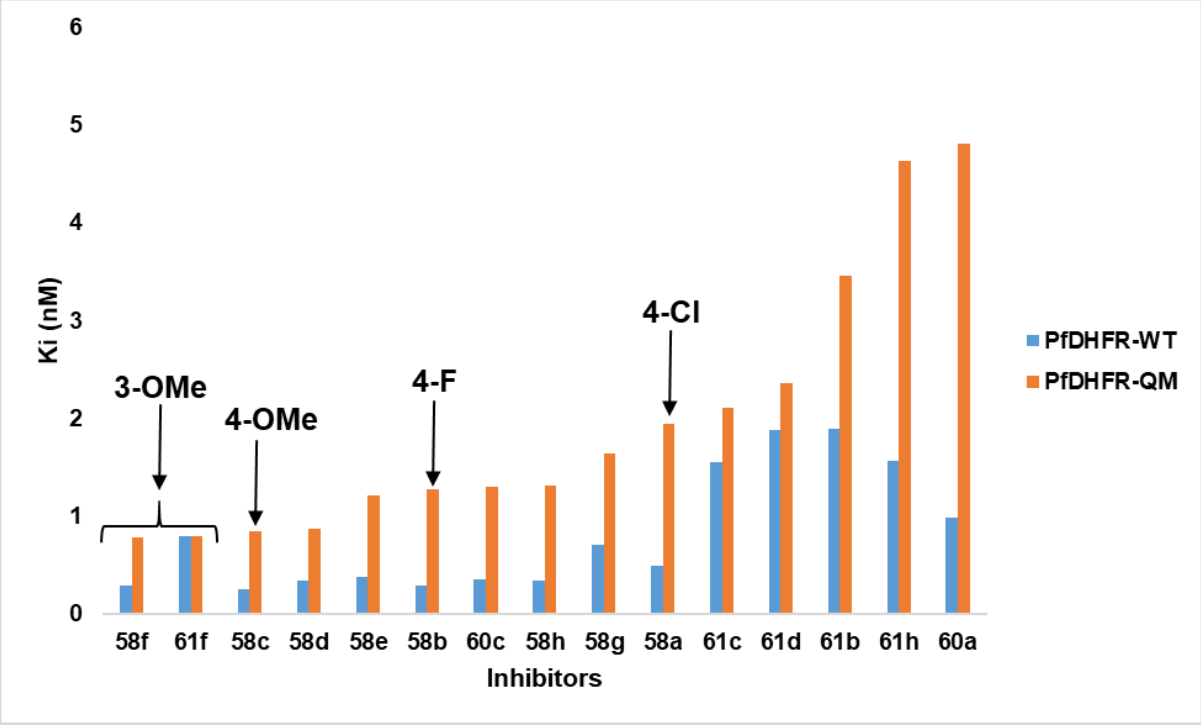

Figure 35. *Inhibitory activity of both the PfDHFR wild type and quadruple mutant type ranging from the most active to the least active.*

In general, we noticed that the methoxy containing analogues were better inhibitors compared to those containing chloro- and fluoro-substituents bonded at the same position on the phenoxy ring. Compound **58c** with a 4-OMe substituent was the most

active alkyne containing a substituent at the para-position, with a K_i value of 0.85 nM against the quadruple mutant. By comparison, the 4-Cl containing compound **58a** and the 4-F compound **58b** exhibited K_i values of 1.95 and 1.28 nM respectively. Similarly, compound **61f** with a 3-OMe substituent was the most active "alkene" inhibitor with a K_i value of 0.80 nM against the quadruple mutant, while compound **61d**, with a 3-Cl substituent exhibited enzymatic inhibition against mutant *Pf*DHFR at 2.37 nM. From this appears that the methoxy containing analogues seem to be better inhibitors of quadruple mutant *Pf*DHFR.

4.1.2 Whole cell *P. falciparum* assays

The *tert*-butyl compounds **58**, **60** and **61** were exceptionally potent inhibitors in the enzymatic assays as all the tested compounds inhibited both the wild type and mutant *Pf*DHFR in the low nanomolar range. With such optimistic results, we then set out to further assess antiplasmodial activity of these compounds *in vitro* in a whole cell *P. falciparum* assay against the drug sensitive TM4/8.2 strain carrying WT *Pf*DHFR and the multidrug resistant strain V1S carrying the QM *Pf*DHFR enzyme of the parasite. Antiplasmodial activity was measured using ^{3}H hypoxanthine incorporation assay.[171] All the experiments were carried out in triplicates and their results are summarised in **Table 34**.

***Table 34**. Evaluation of antiplasmodial activity against drug sensitive and multi-drug resistant P. falciparum strains, and cytotoxicity against normal.*

entry	R'	IC_{50} (μM) *Pf*TM4/8.2	IC_{50} (μM) *Pf*V1S	[a]RI	IC_{50} (μM) VERO	[b]SI_1	[c]SI_2
58a	4-Cl	5.06 ± 0.64	64.0± 13.8	12.65	26.6 ± 17.4	5.26	0.42
58b	4-F	2.94 ± 0.16	37.7± 7.02	12.82	11.8 ± 4.00	4.01	0.31
58c	4-OMe	0.77 ± 0.06	50.6 ± 7.74	65.71	8.63 ±3.80	11.21	0.17
58d	3-Cl	4.12 ± 0.28	50.4±9.33	12.23	12.2 ± 6.01	2.96	0.24
58e	3-F	1.11 ± 0.30	41.4± 7.56	37.30	11.8 ± 3.68	10.63	0.29
58f	3-OMe	0.28 ± 0.02	21.9± 2.82	78.21	0.72 ± 0.17	2.57	0.03
58g	2-Cl	7.06 ± 0.73	23.0 ± 1.01	3.26	31.5 ± 3.93	4.46	1.37
58h	2-F	4.42 ± 0.34	44.0 ± 9.11	9.95	16.1 ± 1.01	3.64	0.37
60a	4-Cl	11.8 ± 1.60	22.8 ± 1.51	1.93	>50	3.64	0.37
60c	4-OMe	3.79± 0.28	18.5 ± 1.17	4.88	28.7 ± 3.45	7.57	1.55
61b	4-F	17.4± 1.09	17.6 ± 1.88	1.01	63.2 ± 4.32	3.63	3.59
61c	4-OMe	9.41± 0.23	18.6 ± 1.11	1.98	63.4 ±9.08	6.74	3.41
61d	3-Cl	11.7± 1.58	23.6 ± 098	2.02	>50	4.27	2.12
61f	3-OMe	19.9 ± 0.65	21.0 ± 0.57	1.06	76.1 ± 4.08	3.82	3.62
61h	2-F	23.4 ± 1.06	22.4 ± 0.86	0.96	82.6 ± 7.84	3.53	3.69
TRP		6.37± 0.63	>100	15.70	>100	15.70	1.00
ELPTC-OLD		ND	ND		3.51 ± 0.95		
Cyc		0.034 ± 0.005	92.4 ± 6.11	2717.65	>100	2941.18	1.08
Pyr		0.053 ± 0.007	>100	1886.79	26.9 ± 2.07	507.55	0.27

ELPTC-OLD = ellipticine, TRP = trimethoprim, Cyc = cycloguanil, Pyr = pyrimethamine, ND = Never determined

[a]RI, resistance index: the ratio of the IC_{50} (*Pf*V1S)/ IC_{50} (*Pf*TM4/8.2). Selectivity index, [b]SI_1 = IC_{50} VERO/ IC_{50} (*Pf*TM4/8.2), [c]SI_2 = IC_{50} VERO/ IC_{50} (*Pf*V1S).

The tested compounds displayed moderate antiplasmodial activity in the low micromolar range with IC_{50} values of 0.28 -23.4 µM against the drug sensitive strain and 17.6 – 64.0 µM against the multidrug resistant strain (**Table 34**). Compounds harbouring the alkyne bond were the most active against the drug sensitive strain (IC_{50} = 0.28 – 7.06 µM) as seen in **Figure 36**(a). Similar to the *Pf*DHFR inhibition studies, compound **58f** containing a methoxy substituent at the *meta* position was the most active against the drug sensitive strain. Eight of the tested alkyne products (**58a**-**58f** & **58h**) are comparable with trimethoprim with an IC_{50} value of 6.37 µM against the drug sensitive strain. However, their antiplasmodial activity is significantly lower in comparison to cycloguanil and pyrimethamine with IC_{50} values of 0.034 and 0.083 µM respectively. The least active compound against the drug sensitive strain is the alkene product **61h**, which contains a 2-F substituent (IC_{50} = 23.4 µM). As observed for the biochemical enzyme assays, methoxy containing compounds displayed the highest inhibitory activity against the drug sensitive strain. For instance, the alkyne product **58f** is the most active compound as mentioned above, whilst the most potent alkene is compound **61c** bearing a 4-OMe substituent on the phenoxy ring. Additionally, compound **60c** displayed better antiplasmodial activity than **60a** against the drug sensitive strain.

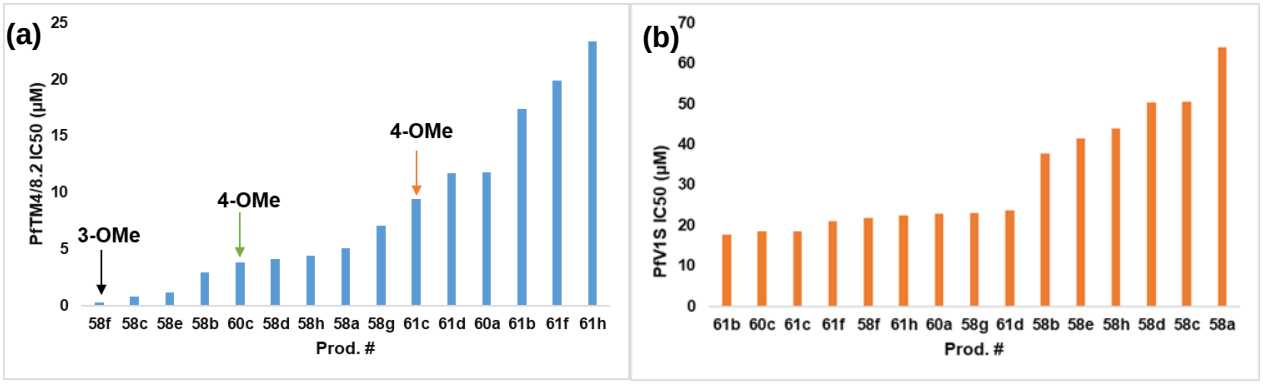

Figure 36. *Antimalarial activity of the tert-butyl compounds against (a) the drug sensitive TM4/8 strain and (b) the multi-drug resistant V1S strain ranging from the most active to the least active compound.*

The tested compounds displayed varying antiplasmodial activity ranging between 17.6 – 64 µM against the multi-drug resistant strain. By virtue of malaria drug discovery, the acceptable IC_{50} value for compounds considered as hits should be less than 1 µM.[172]

Since the tested compounds displayed extremely low antiplasmodial activity with IC_{50} values > 17 µM against the multi-drug resistant strain, none of the compounds qualify for further development as antimalarial agents. The highest antiplasmodial activity against the multi-drug resistant strain is observed for the alkenes **61** with IC_{50} values ranging from 17.6 – 23.6 µM (**Figure 36** (b)). The most potent compound, **61b** with an IC_{50} value of 17.6 µM, contained a 4-F substituent. However, compounds bearing a methoxy substituent (such as **58f**, **60c**, **61c** and **61f**) were amongst the most active compounds. Similar to the enzymatic assay, potency of compounds containing the methoxy substituent was evident.

The novel triazines synthesised at CSIR on which these compounds were based displayed antiplasmodial activity in the low nM range against the drug resistant strain in a whole cell assay,[96] whilst our compounds display moderate antiplasmodial activity in the low µM range. The apparent loss in activity between the enzymatic and whole cell assays could be attributed to the pharmacokinetic properties of these compounds. Considering that the compounds can effectively inhibit both wild type and quadruple mutant *Pf*DHFR in the low nM range in the biochemical enzyme assay but not to the same extend in the whole cell assay, suggests that pharmacokinetic properties such as liphophilicity of the compounds or solubility at physiological conditions could be affecting their antiplasmodial activity *in vitro*. To better understand these results, further assessments will be considered for future work. Most significantly, we await the results of the remaining compounds prepared in this project in both the enzymatic and whole cell assays.

4.1.3 Cytotoxicity assay and selectivity index

Safety and efficacy are essential attributes that a drug must possess in drug discovery of new antimalarials. As such, cytotoxicity studies assess effects on the viability of normal mammalian cells in the presence of new compounds and this identifies whether compounds are toxic or non-toxic to normal mammalian cell lines. Additionally, data from such assays allows compounds to be classified in accordance to their respective toxicity ranging between IC_{50} values > 100 µM for compounds considered non-toxic to < 10 µM for compounds considered highly toxic. The toxicity ranges are reported as follows in literature:

- Non-lowly toxic with IC_{50} values > 100 µM,[173]
- Weakly toxic with IC_{50} values > 50 and < 100 µM,[174]
- Mild-moderately toxic with IC_{50} values > 10 and < 50 µM[175]
- and significant- highly toxic with IC_{50} values < 10 µM.[174]

Furthermore, if compounds are found active and non-toxic, we can rule out basal toxicity as a contributor to observed antiplasmodial activity. Compounds that posses low toxicity or considered non-toxic to healthy mammalian cells are deemed favourable for further exploration as antimalarial agents, their activity indicates interaction between the compound and plasmodial parasite.

Mammalian (VERO) cells were treated with synthesised compounds to test for cytotoxicity using the sulforhodamine B. (SRB) assay. Cytotoxicity IC_{50} values determined for the tested compounds **58, 60** and **61** against the VERO cells range between 0.71 – 82.6 µM. According to the literature cytotoxicity ranges, these compounds are considered toxic to mammalian cells. Compounds **61b**-**d**, **61f** and **61h** were the least toxic in the series. These alkene products are mild to moderately toxic to VERO cells with IC_{50} values > 50 to 82.6 µM (**Table 34**). The highest toxicity observed is for **58c** and **58f**, alkyne compounds harbouring a *tert*-butyl group and a methoxy group on the phenol ring, with IC_{50} values of 8.63 and 0.72 µM against VERO cells respectively. Unfortunately, the tested compounds display mild to high toxicity towards VERO cells. Therefore, the observed antiplasmodial activity with IC_{50} values of 0.28 – 23.4 µM against the drug sensitive strain and 17.6 – 64.0 µM against the multidrug resistant strain could potentially be due to basal toxicity as a major contributor (**Table 34**).

Compounds may be cytotoxic to normal mammalian cells, and yet be selective of pathogenic cells when exposed to them in the presence of healthy mammalian ones. Therefore, the selectivity index (SI) of the compound is an important parameter to measure selectivity of the compounds for parasitized cells. SI was obtained through the relationship between cytotoxicity and antiplasmodial activity of each compound. In our case, SI is calculated with respect to the drug sensitive strain (SI_1) and the drug resistant strain (SI_2). The higher the SI, the more non-cytotoxic or safer the compound is. Ideally, compounds should possess IC_{50} values of < 1 µM and a minimum SI value of 10 to be considered as a hit in the development of antimalarial drugs.[176,177]

Compounds **58c** and **58f** are the only two compounds out of 15 with SI_1 values above 10 (**Table 34**). Although both compounds may seem selective for parasitic cells in relation to the drug sensitive strain, they are non-selective for the parasitic cells of the drug resistant strain. By observation, the SI_2 values of all tested compounds are less than 10, ranging between 3 and 0 (**Table 34**). The compounds will have the same effect on normal mammalian cell as plasmodial cells.

4.1.4 Resistance index

Another important parameter to consider during drug discovery of antimalarial agents is resistance index (RI). We define RI as the ratio of the biological activity (IC_{50} value) of the compounds against the drug resistant strain to the IC_{50} values observed against the drug sensitive strain.[172] It indicates the potency of a drug candidate as a result of resistance. This is of particular importance as we set out to synthesise 2,4-diaminopyrimidines with a flexible linker to overcome resistance imposed by *P. falciparum* against pyrimethamine. As mentioned in **Chapter 1**, pyrimethamine is a 2,4-diaminopyrimidine derivative with a rigid single bond in between the bi-aryl rings. It is believed that due to torsional constraints, the antifolate fails to overcome resistance imposed by the *Plasmodium* parasite as a result of point mutations occurring in the active site of the drug target enzyme, DHFR. Therefore, the lower the RI the least activity lost through resistance and hence the better the compound. The RI values for the tested compounds (**58a-h**, **60a**, **60c**, **61a-d**, **61f** & **61h**) vary between 1 – 78 (**Table 34**). The calculated RI values are by far better than the RI value observed for the controls, pyrimethamine and cycloguanil, with RI values of 2717 and 1886 respectively, indicating high-levels of resistance. [172] RI value of < 10 may indicate an intermediate resistance level.[172] Most of the tested alkynes **58a-f**, with a *tert*-butyl group at position 6 of the diamino heteroaromatic ring, indicated a significant loss in activity against the *Pf*V1S strain with RI values > 10. Of the tested alkynes, **58g** and **58h** are the only two with suggestive intermediate resistance, with 3- and 10-fold loss in activity against the *Pf*V1S respectively. RI values calculated for Compound **60a** and **60c** are among the low calculated RI values, 2 and 5 respectively. It is worth noting that compound **60a** and **60c** contain just σ bonds connecting the flexible 4-atom linker. Therefore, the low RI values suggest that torsional freedom is essential for the compound to retain activity against drug resistant strains. Compound **61b**, **61f** and

61h display equipotency against both the drug sensitive (*Pf*TM4/8.2) and drug resistant (*Pf*V1S) strain with RI values = 1. They display equal efficacy against both strains.

5 CHAPTER 5: Conclusions and Future work

In this project, we set out to synthesise novel second generation 2,4-diaminopyrimidines as potential antimalarial agents. The target compounds were meant to maintain many of the structural features of the active dihydrotriazine **7**, but eliminate the stereogenic centre. The synthetic dihyrotriazines contained a heteroatom ring system bonded to a 4-atom linker at, which separated the heteroatomic ring system from a substituted phenyl ring. [96] In contrast, the 2,4-diaminopyrimidines proposed in this work eliminate the challenges associated with isolation of enantiomers as potential pharmaceuticals. We also intended to synthesise these pyrimidines with an aliphatic group at position 6 of the pyrimidine ring, as a loss in activity was observed for the 1st generation 2,4-diaminopyrimidines that contained a phenyl ring at C-6 of the pyrimidine scaffold.

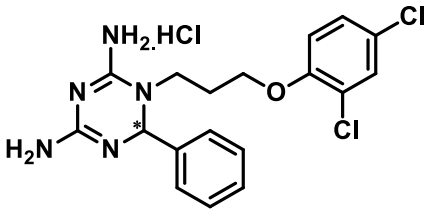

7

Figure 37*. Chemical structure of the dihydrotriazine 7 synthesised previously.*

We have successfully developed a 5-step synthetic route towards the desired 2nd generation 2,4-diaminopyrimidines **15** and have synthesised a series of 2,4- diaminopyrimidines with aliphatic groups at position 6 of the pyrimidine scaffold (**Scheme 31**). Synthesised compounds were substituted with *tert*-butyl, isopropyl or cyclopropyl at C-6, since designed compounds containing these groups were amongst the highest scoring during molecular modelling, indicating their potential to inhibit *Pf*DHFR.

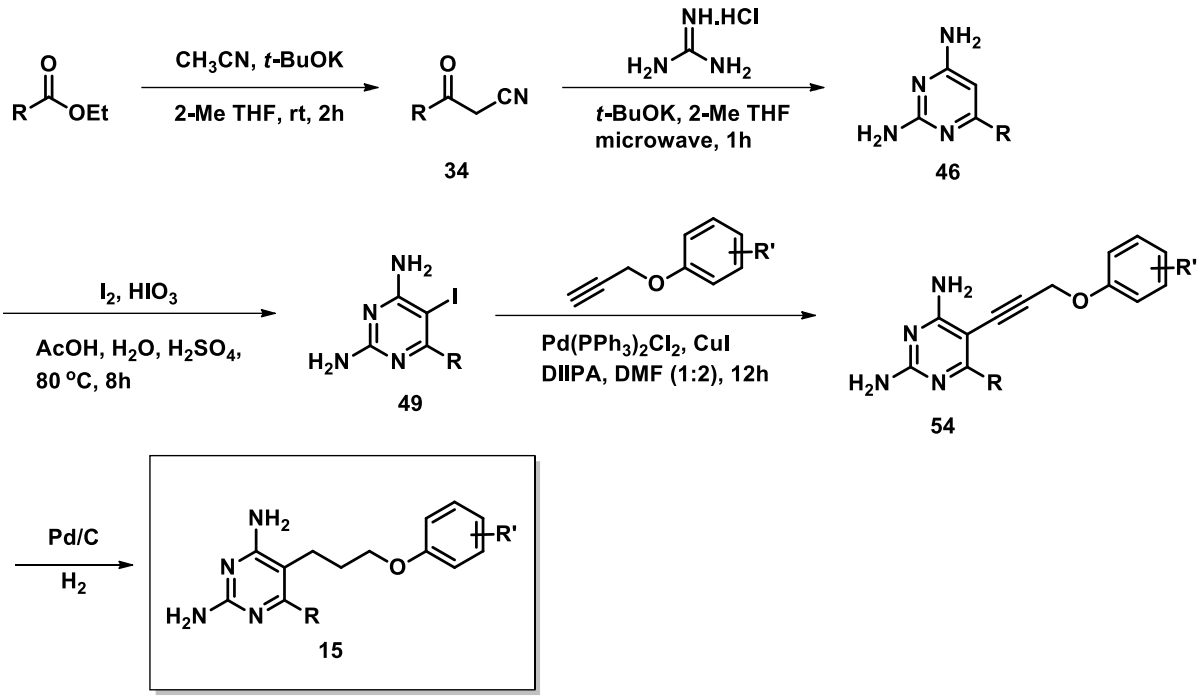

Scheme 48. *Newly developed synthetic procedure towards synthesis of second generation pyrimidines.*

The newly developed synthetic route was initiated by synthesis of β-ketonitriles. The β- ketonitriles were successfully synthesised using an environmentally friendly and green synthetic procedure developed in our laboratory (**Scheme 31**, step 1). This entailed preparation of β- ketonitriles by acylation of acetonitrile using 2 mole equivalents of *t*-BuOK and 1 mole equivalent of the appropriate substituted ester. The reaction was conducted under mild conditions in the presence 2-Me THF as a solvent, a green solvent produced by direct reduction of furfural, a furan aldehyde derived from lignocellulose biomass of corncobs. The method was applied to several aliphatic and aromatic esters, which are susceptible to nucleophilic attack. We can therefore conclude that the reaction conditions can accommodate a vast spectrum of substrate esters that can be converted to β-ketonitriles using the approach, as reported in 2019.[126]

The next step was the synthesis of 2,4-diaminopyrimidine ring scaffolds from the prepared β-ketonitriles (**Scheme 31**, step 2). Formation of the heteroaromatic ring was successfully mediated by microwave irradiation. The reaction was conducted in the presence of an inexpensive and environmentally friendly base *t*-BuOK, and 2-Me THF

as the solvent. Development of the synthetic procedure using microwave irradiation was inspired by Goswami *et al*.[149] They synthesised a series of functionalised pyrimidines under microwave irradiation from various nucleophilic N-C-N synthons and C-C-C electrophilic sources such as β-dicarbonyl compounds, ethyl cyanoacetate and malonitrile. Following the same green chemistry theme, we developed a synthetic procedure where 2,4-diaminopyrimidine ring systems were synthesised from β-ketonitriles as the C-C-C electrophiles. A variety of C-C-C synthons have been utilised in this classic condensation reaction to form pyrimidine ring systems, however, very little has been reported about the synthesis of such scaffolds using β-ketonitriles. In contrast, many reports are available on the synthesis of pyrimidines by condensation of guanidine with enol ethers. These enol ethers are prepared from β-ketonitriles by reaction with diazomethane, a reagent with well-known risks. Preparation of pyrimidine ring sytems from β-ketonitriles offers a new and much safer synthetic procedure over the diazomethane procedure. Furthermore, this procedure is robust enough to accommodate β-ketonitriles derived from both aliphatic and aromatic esters.

Since the reaction conditions were closely similar to the reaction conditions applied previously during formation of the β-ketonitriles, we attempted a “one-pot-two-step” reaction. Formation of the pyrimidine scaffold from commercially available esters was successful. However, the yields were disappointingly low at this scale, more so than the overall yield taken from the two individual steps to get the desired products.

With the successful formation of the pyrimidine scaffold, we were now ready to functionalise the pyrimidine ring system at C-5 via the Sonogashira cross-coupling reaction.This Pd-catalysed homogeneous reaction was utilised to introduce the pre-functionalised alkyne groups, prepared from commercially available phenols, at C-5. It was in fact the success of the Sonogashira cross-coupling reaction using pre-functionalised acetylenes, that led to the reduction in synthetic steps in the planned approach towards the desired 2,4-diaminopyrimidines. The initial proposed synthetic plan was 7-steps in length and required the use of the Sonogashira reaction to introduce acetylene TMS to the iodinated pyrimidine, followed by deprotection and a copper catalysed alkyne-alkyne coupling reaction to form diynes. Introduction of the pre-functionalised acetylenes via the Sonogashira reaction skips the two latter steps,

thus giving rise to a synthetic route with only 5-steps towards our desired pyrimidines with a flexible linker.

The final step was the hydrogenation reaction (**Scheme 31**, step 5), which entailed reduction of the C≡C bond by H_2 (gas) in the presence of a Pd catalyst. As expected, hydrogenation of the isopropyl and cyclopropyl analogues gave their equivalent fully reduced products. These results were supported by the mechanism of the hydrogenation reaction, which occurs on the surface of the metal and gives rise to a *cis* alkene intermediate. In the absence of catalyst poisoning, the *cis* alkene is further reduced to the "alkane" equivalent. Unfortunately, the stereoselective *cis*-alkene equivalents were isolated for the *tert*-butyl analogues. This was unexpected since we did not apply catalyst poison. We have since concluded that the presence of the bulky *tert*-butyl group, hinders reduction of the "alkene products" to their fully reduced equivalents.

In summary, we have successfully developed a synthetic procedure that applies basic concepts of green chemistry where possible, such as the use of environmentally friendly reagents and green solvents. We have also utilised catalysis and microwave irradiation to promote feasibility of reactions that were otherwise rather unsuccessful under normal conventional settings.

The synthesised pyrimidine analogues were intended to target *P. falciparum* DHFR. Of the synthesised analogues, 15 compounds were sent for preliminary tests to assess their inhibitory activity against both wild type and mutant type *Pf*DHFR enzymes. They inhibited both the *Pf*DHFR wild type and quadruple mutant at low nanomolar concentrations, with high inhibitory activity observed for the wild type enzyme with K_i values ranging between 0.26 – 1.9 nM. Additionally, these compounds were also tested against the human DHFR to evaluate their selectivity. All tested compounds were selective for *Pf*DHFR over human DHFR.

With such optimistic inhibitory results, we then set out to further assess the antiplasmodial activity of these compounds *in vitro* in a whole cell *P. falciparum* assay against the drug sensitive TM4/8.2 strain carrying WT *Pf*DHFR and the multidrug resistant strain V1S carrying the QM *Pf*DHFR enzyme of the parasite. The tested compounds displayed moderate antiplasmodial activity in the micromolar range with

IC_{50} values of 0.28 - 23.4 µM against the drug sensitive strain and 17.`6 – 64.0 µM against the multidrug resistant strain. Unfortunately, the newly prepared antimalarials were found to be significantly less potent than the dihydrotriazines synthesised previously, which displayed antiplasmodial activity in the nanomolar range. The loss in antimalarial activity could be attributed to pharmacokinetic properties of these compounds, considering that the prepared compounds can effectively inhibit wild type and mutant *Pf*DHFR enzymes at nM concentrations.

The tested compounds dissappointingly displayed mild to high cytotoxicity towards VERO cells. Therefore, basal toxicity may contribute toward the antiplasmodial activity observed. Further interrogation of the selectivity index indicated that the tested compounds did not display any selectivity for the plasmodial parasite over VERO cells. This implies that inhibition of the *Plasmodium* strains in the whole cell *in vitro* assay is not only due to compounds interacting with the parasite but also the effects of the compounds on the viability of erythrocytes.

5.1 Future Work

We set out to synthesise 2,4-diaminopyrimidines with a flexible 4-atom linker bonded by σ-bonds between the bi-aryl rings. To complete the *tert*-butyl series, it would be beneficial to explore other alternative reducing strategies such as the use of reducing agents.

We plan to utilise the developed synthetic route to introduce variation to the synthesised 2,4-diaminopyrimidine derivatives in order to further understand the pharmacokinetic properties that led to the loss in antimalarial activity. This will include addressing aspects of solubility and membrane permeability and will include incorporation of polar functional groups and variation of the heteroatom in the flexible linker.

The synthesised analogues contained small substituents (F, Cl & OMe) on the phenoxy ring, which predominantly explored electronic affects. To further expand on the structure activity relationships (SAR) of these compounds, we could incorporate bulkier groups as substituents. This will allow us to explore steric effects around the phenoxy ring.

The research project could be extended further by design of derivatives for compound **68**. Thus the 2,4-diaminopyrimidine prepared from aniline instead of phenol. Analogues from this series could be essential in the assessment of SAR for non-phenoxy aryl substituents.

All the remaining compounds prepared have been sent for assessment in both wild type and mutant *Pf*DHFR enzymatic assays and for antiplasmodial activity *in vitro* in a whole cell *P. falciparum* assay. The data from these studies will inform the design of future analogues.

.

6 CHAPTER 6: Experimental procedure

6.1 General Procedure

6.1.1 Reagents and solvents

Solvents used for chromatographic techniques (methanol, dichloromethane, ethyl acetate and hexane) were purified by conventional distillation to remove none volatiles. All solvents employed for chemical reactions were of analytical grade. 2-Methyl tetrahydrofuran purchased from Sigma-Aldrich was utilised as is, whereas, dimethylformamide was it was dried over barium oxide overnight, then distilled and stored under N_2 atmosphere. Absolute ethanol and acetone were obtained from commercial sources without further purification. Reagents utilised for reactions were purchased from Sigma-Aldrich and used as received.

6.1.2 Chromatographic techniques

Column chromatography was conducted with silica gel 60 (Machery-Nagel, particle size 0.063 – 0.200 mm) and aluminium oxide, activated basic (Brockmann I, 58 Å pore size). Thin layer chromatography was carried out on Merck aluminium foil F_{254} plates coated with silica gel 60, and visualised under UV-light (254 nm).

6.1.3 Spectroscopic data

^{1}H and ^{13}C nuclear magnetic resonance spectra were recorded either on the Bruker Avance 300 MHz, Avance III 400 MHz or the Avance III 500 MHz spectrometer. For spectra recorded in deuterated chloroform ($CDCl_3$), chemical shifts were referenced against the internal standard trimethylsilane (TMS) given an assignment at chemical shift (δ) zero parts per million for ^{1}H NMR, and δ 77.0 ppm for ^{13}C NMR, while spetra recorded in deuterated DMSO were referenced to the central peak of the solvent. Chemical shifts are recorded in ppm, and coupling constant (*J*-values) are in Hertz.

The infra-red spectra were acquired from a Bruker Tensor-27 Fourier Transform spectrometer. IR measurements were made by direct loading of the sample on a diamond cell. The measurements are reported on the wavenumber scale (ν, cm^{-1}).

High resolution mass spec data were obtained from a Bruker Compact Q-TOF mass spectrometer. Samples were diluted to a concentration of approxiamately 10 ppm in HPLC grade methanol and introduced by injection into a dionex Ultimate 3000 UHPC system. The ionization mode was electrospray positive with a capillary voltage of 4500 V and a desolvation temperature of 220 ^{o}C using N_2 gas at 9 L min^{-1}.

6.1.4 Physical data

All melting points were uncorrected and they were determined using a Stuart SMP10 melting point apparatus.

Microwave reactions were carried out in a CEM Discover microwave.

6.2 Synthesis of aliphatic β-ketonitriles using NaH [122]

6.2.1 Synthesis of 3-cyclopropyl-3-oxopropanenitrile 34a

A solution of ethyl cyclopropane carboxylate (5.00 ml, 42.1 mmol) and anhydrous acetonitrile (2.60 ml ml, 50.5 mmol) dissolved in 5 ml THF was added dropwise to a suspension of NaH (1.16 g, 48.4 mmol) in 15 ml THF at 70 °C. The resulting heterogeneous mixture was stirred for 16 hours at 70 °C under reflux. Within 2 hours of the reaction a gelatinous white precipitate was observed. After the 16-hour period, the reaction was cooled to room temperature (rt.) and diluted with 100 ml of ethyl acetate and 100 ml of 1 M aq. HCl solution. The organic layer was extracted and washed with 100 ml of brine and dried over $MgSO_4$. The solvent was removed under reduced pressure. Unfortunately, the product was not isolated pure, therefore, it was further purified using silica gel column chromatography (20 % EtOAc/Hex) to afford 3-cyclopropyl-3-oxopropanenitrile **34a** as a light yellow oil (1.11 g, 24 %).

6.3 General procedure for the synthesis of aliphatic β-ketonitriles using the green approach[126]

6.3.1 Synthesis of 3-cyclopropyl-3-oxopropanenitrile 34a

To a solution of ethyl cyclopropane carboxylate (2.00 ml, 16.8 mmol) in 10 ml 2-Me THF was added isopropanol (0.26 ml, 3.40 mmol), acetonitrile (1.75 ml, 33.6 mmol) and *t*-BuOK (3.77 g, 33.6 mmol). The reaction mixture was stirred at room temperature for an hour under N_2 atmosphere, then dosed-up with an additional 1.0 mol eq. of acetonitrile and *t*-BuOK respectively. The reaction was further stirred for an hour, quenched with 200 ml of saturated aq. NH_4Cl solution and the organic layer was extracted with 200 ml DCM. DCM was dried over Na_2SO_4 and solvent removed by rotary evaporation. The resulting residue was purified by silica gel column chromatography (20% EtOAc/Hex) to afford 3-cyclopropyl-3-oxopropanenitrile **34a** as a light yellow oil (0.90 g, 48%).

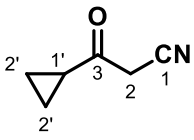

R*f* = 0.56 (1:1 EtOAc/Hex); **^{1}H NMR** (300 MHz, $CDCl_3$) δ 3.65 (s, 2H, H2), 2.14 – 1.90 (m, 1H, H1'), 1.22 – 0.85 (m, 4H, H2'); **^{13}C NMR** (75 MHz, $CDCl_3$) δ 198.4 (C3), 114.5 (C1), 33.0 (C2), 20.6 (C1'), 13.0 (C2'); **HRMS** (ES^+) calculated for C_6H_7NO $[M + Na]^+$: 132.0420, found: 132.0420.

6.3.2 Synthesis of 3-oxo-3-phenylpropanenitrile 34b

A solution of methyl benzoate (4.00 ml, 31.7 mmol), acetonitrile (3.40 ml, 63.4 mmol), *t*-BuOK (7.11 g, 63.4 mmol) and isopropanol (0.48 ml, 6.30 mmol) in 2-Me THF resulted in 3-oxo-3-phenylpropanenitrile **34b** as a light yellow solid (2.18 g, 47%).

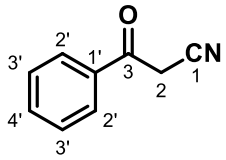

R*f* = 0.68 (1:1 EtOAc/Hex); **mp**: 75 °C (lit. mp. 70-72 °C);[178] **^{1}H NMR** (300 MHz, $CDCl_3$) δ 7.98 – 7.87 (m, 2H, H2'), 7.73 – 7.62 (m, 1H, H4'), 7.59 – 7.47 (m, 2H, H3'), 4.10 (s, 2H, H2); **^{13}C NMR** (75 MHz, $CDCl_3$) δ 187.3 (C3), 134.9 (C4'), 134.4 (C1'), 129.3, 128.6, 113.9 (C1), 29.5 (C2); **HRMS** (ES^+) calculated for C_9H_7NO $[M + Na]^+$: 168.0420, found: 168.0403.

6.3.3 Synthesis of 4,4-dimethyl-3-oxopentanenitrile 34c

Methyl pivalate (2.00 ml, 15.0 mmol), acetonitrile (1.57 ml, 30.0 mmol), *t*-BuOK (3.37 g, 30.0 mmol) and isopropanol (0.23 ml, 3.00 mmol) were combined as described in the general procedure to afford 4,4-dimethyl-3-oxopentanenitrile **34c** (0.89 g, 47%) as a light yellow solid.

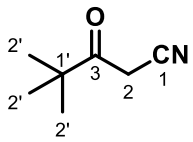

R*f* = 0.78 (1:1 EtOAc/Hex); **mp**: 68 °C (lit mp: 67-68 °C);[179] **^{1}H NMR** (300 MHz, $CDCl_3$) δ 3.63 (s, 2H, H2), 1.19 (s, 9H, H2'); **^{13}C NMR** (75 MHz, $CDCl_3$) δ 202.8 (C3), 114.2 (C1), 44.7 (C1'), 27.5 (C2), 26.2 (C2'); **HRMS** (ES^+) calculated for $C_7H_{11}NO$ $[M + Na]^+$: 148.0733, found: 148.0724.

6.3.4 Synthesis of 4-methyl-3-oxopentanenitrile 34d

The general procedure was followed using commercially available methyl isobutyrate (2.00 ml, 17.4 mmol), 20 ml of 2-Me THF, isopropanol (0.27 ml, 3.48 mmol), acetonitrile (1.80 ml, 34.8 mmol) and *t*-BuOK (3.92 g, 34.8 mmol) to afford a yellow oil **34d** (1.46 g, 76%).

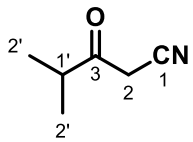

R*f* = 0.68 (1:1 EtOAc/Hex); **^{1}H NMR** (300 MHz, $CDCl_3$) δ 3.56 (s, 2H, H2), 2.71 (hept, *J* = 6.9 Hz, 1H, H1'), 1.09 (d, *J* = 7.0 Hz, 6H, H2'); **^{13}C NMR** (75 MHz, $CDCl_3$) δ 201.7 (C3), 114.2 (C1), 40.5 (C1'), 30.1 (C2), 17.7 (C2'); **HRMS** (ES^+) calculated for C_6H_9NO $[M + Na]^+$: 134.0577, found: 134.0568.

6.3.5 Synthesis of 3-cyclopentyl-3-oxopropanenitrile 34e

3-Cyclopentyl-3-oxopropanenitrile **34e** was synthesized from methyl cyclopentanecarboxylate (2.42 g, 15.6 mmol), acetonitrile (1.63 ml, 31.2 mmol), *t*- BuOK (3.80 g, 31.2 mmol) and isopropanol (0.24 ml, 3.10 mmol) as described in the general procedure. The product was isolated as a yellow oil **34e** (0.92 g, 43%).

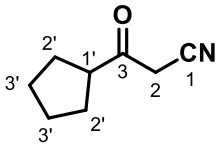

R*f* = 0.94 (1:1 EtOAc/Hex); **^{1}H NMR** (300 MHz, $CDCl_3$) δ 3.53 (s, 2H, H2), 3.05 – 2.95 (m, 1H, H1'), 1.98 – 1.47 (m, 8H, H2' & 3'); **^{13}C NMR** (75 MHz, $CDCl_3$) δ 200.2 (C3), 114.2 (C1), 50.8 (C1'), 31.2 (C2), 28.8 (C2'), 25.9 (C3'); **HRMS** (ES^+) calculated for $C_8H_{11}NO$ $[M + Na]^+$: 160.0733, found: 160.0710.

6.3.6 Synthesis of 3-(cyclopent-3-en-1-yl)-3-oxopropanenitrile 34f

The general procedure was followed to synthesize 3-(cyclopent-3-en-1-yl)-3-oxopropane nitrile. A mixture of commercially available methyl 3-cyclopentenecarboxylate (0.80 ml, 6.50 mmol), acetonitrile (0.68 ml, 13.0 mmol), *t*-BuOK (1.46 g, 13.0 mmol) and isopropanol (0.10 ml, 1.30 mmol) afforded desired compound **34f** as a brown oil (0.39 g, 29%).

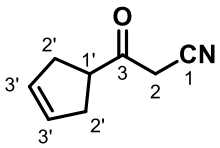

R*f* = 0.61 (1:1 EtOAc/Hex); **^{1}H NMR** (300 MHz, $CDCl_3$) δ 5.59 (s, 2H, H3'), 3.57 (s, 2H, H2), 3.35 (ddd, *J* = 15.9, 8.9, 7.0 Hz, 1H, H1'), 2.70 – 2.47 (m, 4H, H2'); **^{13}C NMR** (75 MHz, $CDCl_3$) δ 199.1 (C3), 128.5 (C3'), 114.1 (C1), 48.4 (C1'), 34.9 (C2'), 30.7 (C2); **HRMS** (ES^+) calculated for C_8H_9NO $[M + H]^+$: 136.0757, found: 136.0746.

6.3.7 Synthesis of 3-cyclohexyl-3-oxopropanenitrile 34g

Commercially available methyl cyclohexanecarboxylate (2.00 ml, 14.0 mmol), acetonitrile (1.46 ml, 28.0 mmol), *t*-BuOK (3.14 g, 28.0 mmol) and isopropanol (0.21 ml, 2.80 mmol) were reacted as described in the general procedure above to afford 3-cyclohexyl-3-oxopropanenitrile **34g** as a yellow oil (1.43 g, 68%).

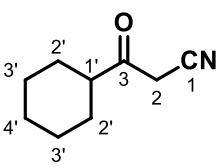

R*f* = 0.93 (1:1 EtOAc/Hex);**^{1}H NMR** (300 MHz, $CDCl_3$) δ 3.53 (s, 2H, H2), 2.52 – 2.43 (m, 1H, H1'), 2.04 – 1.00 (m, 10H, H2', H3' & H4'); **^{13}C NMR** (75 MHz, $CDCl_3$) δ 200.7 (C3), 114.2 (C1), 50.0 (C1'), 30.4

(C2), 28.1 (C2'), 25.5 (C4'), 25.2 (C3'); **HRMS** (ES^+) calculated for $C_9H_{13}NO$ $[M + Na]^+$: 174.0890, found 174.0866.

6.4 Test Reaction for the microwave approach

6.4.1 Synthesis of 4,6-dimethylpyrimidin-2-amine 48[149]

A mixture of acetylacetone (1.00 ml, 9.80 mmol), guanidine hydrochloride (0.93 g, 9.80 mmol) and K_2CO_3 (1.35 g, 9.80 mmol) in a conical flask was subjected to irradiation at 300 W, 80 °C for 10 min. After this time, saturated aq. NH_4Cl was added to the conical flask and the organic layer was extracted with EtOAc. The organic solvent was dried over $MgSO_4$, after filtration it was evaporated on the rotary evaporator. The resulting residue was purified by recrystallization and 0.50 g of a light brown solid was isolated in 42% yield.

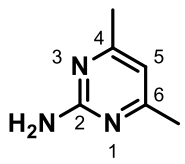

R*f* = 0.41 (1:9 MeOH/DCM); **mp**: 153 °C (lit mp: 153 °C);[180] **^{1}H NMR** (300 MHz, $CDCl_3$) δ 6.29 (s, 1H, H5), 5.70 (s, 2H, NH_2), 2.22 (s, 6H, 2(CH_3)); **^{13}C NMR** (75 MHz, $CDCl_3$) δ 167.7 (C4 & C6), 163.2 (C2), 110.3 (C5), 23.7 (2(CH_3)).

6.5 General Procedure for the synthesis of the 2,4-diamiopyrimidine ring

6.5.1 Synthesis of 6-cyclopropylpyrimidine-2,4-diamine 46a

Guanidine HCl (0.88 g, 9.20 mmol), 3-cyclopropyl-3-oxopropanenitrile (0.50 g, 4.60 mmol), and *t*-BuOK (1.03 g, 9.20 mmol) were combined in a microwave tube. The dry reagents were mixed together before addition of ~2 ml 2-MeTHF to make a paste like heterogeneous mixture. The mixture was subjected to microwave radiation set at 100 W, 150 °C for an hour. The residue was dissolved in EtOAc and quenched with saturated aq. NH_4Cl to pH 7,5. The organic layer was extracted with EtOAc and dried over $MgSO_4$. After filtering the $MgSO_4$ off, the solvent was evaporated using a rotary evaporator and the residue was further purified by silica gel column chromatography (60% EtOAc/Hex) to afford a cream white solidof **46a** (0.20 g, 29%)

R*f* = 0.18 (1:9 MeOH/DCM) ; **mp**: 148 °C; **IR** (v/cm^{-1}): 3352 (NH str), 3172 (NH str), 2923 (CH), 1627 (NH bend) ; **^{1}H NMR** (300 MHz, DMSO) δ 6.04 (s, 2H, NH_2), 5.66 (s, 2H, NH_2), 5.61 (s, 1H, H5), 1.61 (tt, *J* = 8.0, 4.8 Hz, 1H, H1'), 0.93 – 0.64 (m, 4H, H2'); **^{13}C NMR** (75 MHz, DMSO) δ 169.0 (C6), 164.1 (C4), 163.4 (C2), 91.8 (C5), 16.2 (C1'), 7.9 (C2'); **HRMS** (ES$^+$) calculated for $C_7H_{10}N_4$ $[M + H]^+$: 151.0978, found: 151.0996.

6.5.2 Synthesis of 6-phenylpyrimidine-2,4-diamine 46b

3-Oxo-3-phenylpropanenitrile (0.50 g, 3.40 mmol), guanidine HCl (0.66 g, 6.90 mmol) and *t*-BuOK (0.77 g, 6.90 mmol) were dissolved in 2 ml 2-Me THF to afford a cream white solid of **46b** (0.37 g, 57%).

R*f* = 0.39 (1:9 MeOH/DCM); **mp**:153 °C ; **IR** (v/cm^{-1}): 3308 (NH str), (3181 NH str), 3054 (=C-H), 1608 (NH bend); **^{1}H NMR** (300 MHz, DMSO) δ 7.89 (dd, *J* = 7.5, 2.1 Hz, 2H, H2'), 7.53 – 7.35 (m, 3H, H3' and H4'), 6.37 (s, 2H, NH_2), 6.22 (s, 1H, H5), 6.00 (s, 2H, NH_2); **^{13}C NMR** (75 MHz, DMSO) δ 165.2 (C4), 163.7 (C2), 162.3 (C6), 138.3 (C1'), 129.4 (C4'), 128.4 (C3'), 126.2 (C2'), 90.6 (C5); **HRMS** (ES$^+$) calculated for $C_{10}H_{10}N_4$ $[M +H]^+$: 187.0978, found: 187.0967.

6.5.3 Synthesis of 6-(*tert*-butyl)pyrimidine-2,4-diamine 46c

A mixture of 4,4-dimethyl-3-oxopentanenitrile (1.00 g, 8.00 mmol), guanidine HCl (1.53 g, 16.0 mmol) and *t*BuOk (1.79 g, 16.0 mmol) in 2-Me THF afforded 6-(*tert*-butyl)pyrimidine-2,4-diamine **46c** as a cream white solid (0.81 g, 61%)

R*f* = 0.32 (1:9 MeOH/DCM); **mp**: 130 °C; **IR** (v/cm^{-1}): 3353 (NH str), 3205 (NH str), 2955 (CH), 1609 (NH bend);**^{1}H NMR** (300 MHz, DMSO) δ 6.17 (s, 2H, NH_2), 5.80 (s, 2H, NH_2), 5.71 (s, 1H, H5), 1.14 (s, 9H, H2'); **^{13}C NMR** (75 MHz, DMSO)) δ 175.6 (C6), 164.9 (C4), 163.0 (C2), 89.5 (C5), 36.2 (C1'), 29.2 (C2'); **HRMS** (ES$^+$) calculated for $C_8H_{14}N_4$ $[M +H]^+$: 167.1291, found: 167.1290.

6.5.4 Synthesis of 6-isopropylpyrimidine-2,4-diamine 46d

A heterogeneous mixture of 4-methyl-3-oxopentanenitrile (1.00 g, 9.00 mmol), guanidine HCl (1.27 g, 18.0 mmol), and *t*-BuOK (2.02 g, 18.0 mmol), dissolved in 2 ml

2-Me THF were subjected to microwave irradiation to afford the product as a yellow solid **46d** (1.32 g) in 97% yield.

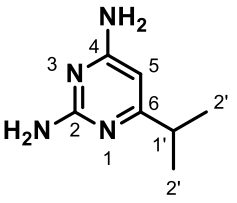

R*f* = 0.10 (1:9 MeOH/DCM); **mp**: 130 °C; **IR** (v/cm^{-1}): 3314 (NH str), 3189 (NH str), 2964 (CH), 1617 (NH bend); ^{1}H NMR (400 MHz, $CDCl_3$) δ 5.69 (s, 1H, H5), 5.20 (s, 2H, NH_2), 5.00 (s, 2H, NH_2), 2.61 (hept, *J* = 7.0 Hz, 1H, H1'), 1.15 (d, *J* = 7.0 Hz, 6H, H2'); **^{13}C NMR** (101 MHz, $CDCl_3$) δ 176.0 (C6), 164.6 (C4), 163.0 (C2), 92.0 (C5), 35.6 (C1'), 21.7 (C2'); **HRMS** (ES$^+$) calculated for $C_7H_{12}N_4$ [M +H]$^+$: 153.1135, found: 153.1132.

6.6 General procedure for Iodination of the 2,4-diaminopyrimidine ring systems

6.6.1 Synthesis of 6-cyclopropyl-5-iodopyrimidine-2,4-diamine 49a[6]

In a solution of 4.00 ml gl. acetic acid, 0.12 ml sulfuric acid and 0.80 ml of water, 6- cyclopropylpyrimidine-2,4-diamine (0.20 g, 1.20 mmol), followed by addition of iodic acid (55.0 mg, 0.31 mmol) and iodine (92.3 mg, 0.60 mmol). The reaction mixture was heated to 80 °C overnight. The indigo coloured heterogeneous mixture was neutralized by addition of 12M aq. NaOH. The organic layer was extracted with DCM, washed with a saturated solution of sodium thiosulfate and brine. The organic layer was dried over Na_2SO_4 and solvent removed on the rotary evaporator to afford the product as a yellow solid **49a** (0.21 g, 57%) without any further purification.

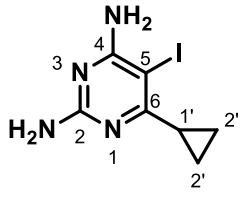

R*f* = 0.67 (1:9 MeOH/DCM); **mp**: 133 °C; **IR** (v/cm^{-1}): 33030 (NH str), 3174 (NH str), 1621 (NH bend), 523 (C-I); **^{1}H NMR** (300 MHz, DMSO) δ 6.34 (s, 2H, NH_2), 5.91 (s, 2H, NH_2), 2.19 (tt, *J* = 7.6, 4.9 Hz, 1H, H1'), 1.01 – 0.64 (m, 4H, 2').; **^{13}C NMR** (75 MHz, DMSO) δ 169.2 (C6), 162.5 (C4), 162.5 (C2), 64.3 (C5), 19.5 (C1'), 9.3 (C2'); **HRMS** (ES$^+$) calculated for $C_7H_9IN_4$ [M + H]$^+$: 276.9945, found: 276.9930.

6.6.2 Synthesis of 6-cyclopropyl-5-iodopyrimidine-2,4-diamine 49b

A mixture of H_2SO_4 (0.12 ml), AcOH (4.00 ml), H_2O (0.80 ml), HIO_3 (0.10 g, 0.60 mmol mmol), I_2 (0.22 g, 0.86 mmol) and starting material **36b** (0.41 g, 2.20 mmol) gave the product **49b** as a yellow soild (0.47 g, 69%).

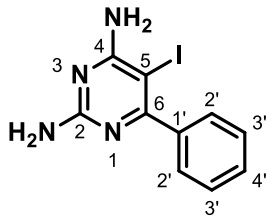

R*f* = 0.67 (1:9 MeOH/DCM); **mp**: 190 °C; **IR** (v/cm^{-1}); 3293 (NH str), 3169 (NH str), 3053 (=C-H), 1626 (NH bend), 578 (C-I); **^{1}H NMR** (300 MHz, DMSO) δ 7.39 (s, 5H, Ph), 6.51 (s, 2H, NH_2), 6.17 (s, 2H, NH_2).; **^{13}C NMR** (75 MHz, DMSO) δ 168.4 (C6), 163.7 (C4), 162.5 (C2), 142.1 (C1'), 128.5 (C3'), 128.3 (C4'), 127.6 (C2'), 62.6 (C5); **HRMS** (ES^+) calculated for $C_{10}H_9IN_4$ $[M + H]^+$: 312.9945, found: 312.9931.

6.6.3 Synthesis of 6-(*tert*-butyl)-5-iodopyrimidine-2,4-diamine 49c

A mixture of 6-(*tert*-butyl)pyrimidine-2,4-diamine (2.00 g, 12.0 mmol), HIO_3 (0.55 g, 3.10 mmol), I_2 (1.53 g, 6.00 mmol), in a solution of 16.0 ml AcOH, 3.20 ml H_2O and 0.48 ml H_2SO_4 afforded 6-(*tert*-butyl)-5-iodopyrimidine-2,4-diamine **49c** as a bright yellow solid in 77% yield (2.71 g).

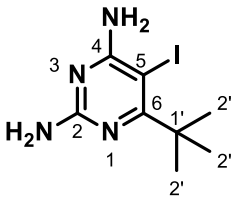

R*f* = 0.56 (1:9 MeOH/DCM); **mp**: 117 °C; **IR** (v/cm^{-1}): 3367 (NH str), 3139 (NH str), 2992 (CH), 1618 (NH bend), 552 (C-I); **^{1}H NMR** (400 MHz, $CDCl_3$) δ 5.77 (s, 2H, NH_2), 5.15 (s, 2H, NH_2), 1.68 (s, 9H, 2').; **^{13}C NMR** (101 MHz, $CDCl_3$) δ 175.6 (C6), 163.7 (C4), 161.4 (C2), 62.2 (C5), 39.8 (C1'), 28.9 (C2'); **HRMS** (ES^+) calculated for $C_8H_{13}IN_4$ $[M + H]^+$: 293.0258, found: 293.0250.

6.6.4 Synthesis of 5-iodo-6-isopropylpyrimidine-2,4-diamine 49d

6-Isopropylpyrimidine-2,4-diamine (8.00 g, 52.6 mmol) was dissolved into a solution of AcOH (32.0 ml), H_2O (6.40 ml) and H_2SO_4 (0.96 ml), followed by addition of HIO_3 (2.40 g, 13.7 mmol), I_2 (6.67 g, 26.3 mmol) to afford the product **49d** as a yellow solid (8.80 g, 60%).

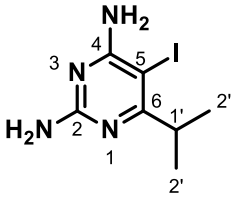

R*f* = 0.48 (1:9 MeOH/DCM); **mp**: 115 °C; **IR** (v/cm^{-1}): 3306 (NH str), 3146 (NH str), 2964 (C-H), 1620 (NH bend), 582 (C-I); **^{1}H NMR** (400 MHz, $CDCl_3$) δ 5.33 (s, 2H, NH_2), 4.95 (s, 2H, NH_2), 3.24 (p, *J* = 6.7 Hz, 1H, H1'), 1.15 (d, *J* = 6.8 Hz, 6H, H2'); **^{13}C NMR** (101 MHz, $CDCl_3$) δ 175.6 (C6), 162.9 (C4), 162.7 (C2), 66.1 (C5), 37.7 (C1'), 20.9 (C2'); **HRMS** (ES^+) calculated for $C_7H_{11}IN_4$ $[M + H]^+$: 279.0101, found: 279.0079.

6.7 Sonogashira cross-coupling reactions

6.7.1 Synthesis of 6-cyclopropyl-5-[(trimethylsilyl)ethynyl]pyrimidine-2,4-diamine 50.[162]

A two-necked round bottom flask equipped with a stirrer bar was dried under *vacuo* and purged with N_2 gas for 15 minutes. After this time the Pd-catalyst, $Pd(PPh_3)_2Cl_2$ (35.6 mg, 50.7 µmol), was added to the flask along with the CuI (9.66 mg, 50.7 µmol) co-catalyst. The reaction vessel was further purged with N_2 gas before addition of the starting material **49a** (0.20 g, 0.70 mmol),10 ml diisopropylamine and dry THF (10 ml). The acetylene TMS (0.40 ml, 2.90 mmol) was added slowly via a syringe, and the reaction mixture was stirred for 18 hours under N_2 atmosphere at reflux. The solvent was concentrated on the rotary evaporator and the resulting residue was partitioned between 100 ml of saturated aq. NH_4Cl solution and 100 ml DCM. The organic layer was isolated, dried over $MgSO_4$ and the solvent was removed. The product was further purified using silica gel column chromatography resulting in a brownish viscous oil (68.00 mg, 38%).

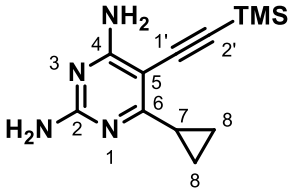

R*f* = 0.67 (1:9 MeOH/DCM); **^{1}H NMR** (300 MHz, DMSO) δ 6.17 (s, 4H, 2(NH_2), 2.23 (tt, *J* = 7.8, 3.9 Hz, 1H, H7), 0.99 – 0.78 (m, 4H, H8), 0.21 (s, 9H, 3(CH_3)); **^{13}C NMR** (75 MHz, DMSO) δ 171.7 (C6), 164.0 (C4), 161.4 (C2), 101.9 (C2'), 100.4 (C1'), 88.0 (C5), 14.4 (C7), 9.1 (C8), 0.3 (3(CH_3)).

6.7.2 Synthesis of 5-[3-(4-chlorophenoxy)prop-1-yn-1-yl]-6-phenylpyrimidine-2,4-diamine 53

DMF (12 ml) was added to a dry 2 neck flask, flushed with N_2. The solvent was subjected to reduced pressure under high vacuum and purged with N_2 gas to remove oxygen. 6- Cyclopropyl-5-iodopyrimidine-2,4-diamine **49b** (0.40 g, 1.30 mmol), $Pd(PPh_3)_2Cl_2$ (90.0 mg, 0.10 mmol) and the co-catalyst Cu(I)I (48.8 mg, 0.30 mmol) were added to the reaction flask, followed by addition of 6 ml DIIPA. The acetylene, 1-chloro-4-(prop-2-yn-1-yloxy)benzene (0.43 g, 2.60 mmol), was added to the reaction mixture which was left stirring overnight at r.t under N_2 atmosphere. The dark black heterogeneous mixture was diluted with H_2O and the organic layer was extracted with

EtOAc. The organic layer was further washed 4 times with brine, then dried over $MgSO_4$. The drying agent was filtered through celite and the filtrate was concentrated on the rotary evaporator. The residue was purified using silica gel column chromatography. Due to the presence of triphenyl phosphine oxide impurities, the product was further purified by recrystallization to afford the product **53** as a dark brown solid (0.24 g, 54%).

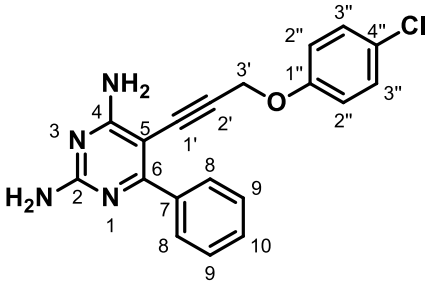

R*f* = 0.56 (1:9 MeOH/DCM); **mp**: 193°C; **^{1}H NMR** (400 MHz, $CDCl_3$) δ 7.80 (d, *J* = 7.2 Hz, 2H, H8), 7.50 – 7.41 (m, 1H, H10), 7.38 (t, *J* = 7.3 Hz, 2H, H9), 7.20 (d, *J* = 8.8 Hz, 2H, H3''), 6.84 (d, *J* = 8.8 Hz, 2H, H2''), 5.28 (s, 2H, NH_2), 5.06 (s, 2H, NH_2), 4.85 (s, 2H, H3'); **^{13}C NMR** (101 MHz, $CDCl_3$) δ 168.0 (C6), 165.4 (C4), 161.2 (C2), 156.2 (C1''), 138.1 (C7), 129.8 (C10), 129.5 (C3''), 128.8 (C8), 128.1 (C9), 126.6 (C4''), 116.5 (C2''), 92.3 (C2'), 88.7 (C5), 82.3 (C1'), 57.1 (C3'); **HRMS** (ES^+) calculated for $C_{19}H_{15}ClN_4O$ $[M + H]^+$: 351.1007, found: 351.0961.

6.8 Hydrogenation reaction

6.8.1 Synthesis of 5-[3-(4-chlorophenoxy)propyl]-6-phenylpyrimidine-2,4-diamine 54

The starting material (16.0 mg, 45.6 µmol), 5-[3-(4-chlorophenoxy)prop-1-yn-1-yl]-6-phenylpyrimidine-2,4-diamine, was dissolved in 2 ml EtOH, followed by addition of Pd/C (1.46 mg, 13.7 µmol). The reaction was carried under H_2 atmosphere for 16 hours. The black heterogeneous mixture was filtered through celite and solvent was removed on the rotary evaporator. The residue was purified by silica gel column chromatography and the product **54** was isolated as a cream white solid (11.0 mg, 68% yield).

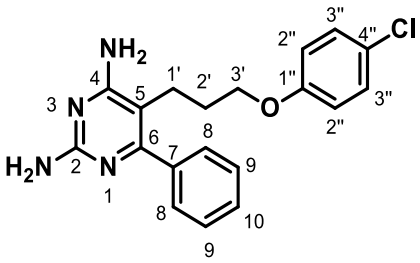

R*f* = 0.31 (1:9 MeOH/DCM); **^{1}H NMR** (500 MHz, MeOD) δ 7.44 – 7.37 (m, 3H, Ph), 7.37 – 7.30 (m, 2H, Ph), 7.19 (d, *J* = 8.9 Hz, 2H, H3''), 6.71 (d, *J* = 8.9 Hz, 2H, H2''), 5.49 (s, 2H, NH_2), 3.81 (t, *J* = 5.8 Hz, 2H, H3'), 2.53 (t, *J* = 7.6 Hz, 2H, H1'), 1.86 (p, *J* = 6.2 Hz, 3H, H2'); **^{13}C NMR** (126 MHz, MeOD) δ 165.5 (C6), 163.6 (C4), 161.0 (C2), 158.9 (C4''), 139.4 (C7), 130.2 (C3''), 129.8 (C10), 129.4 (C8), 129.3 (C9), 126.4 (C4''), 116.9 (C2''), 106.1(C5), 68.2 (C3'), 29.1 (C2'), 23.0 (C1'); **HRMS** (ES^+) calculated for $C_{19}H_{19}ClN_4O$ $[M + H]^+$: 355.1320, found: 355.1331.

6.9 General Procedure for the synthesis of the alkynes[181]

6.9.1 Synthesis of 1-chloro-4-(prop-2-yn-1-yloxy)benzene 57a.[182]

4-Chlorophenol (5.00 g, 38.9 mmol) was treated with K_2CO_3 (21.5 g, 0.16 mol) in 100 ml of acetone. Then propargyl bromide (4.77 ml, 42.8 mmol.) was added in the heterogeneous mixture. The temperature was raised to 54 ˚C and the reaction was left stirring overnight under reflux. The reaction was cooled to r.t. and the residue was concentrated on a rotary evaporator. The residue was transferred to a separating funnel where 125 ml of saturated aq. NH_4Cl solution was added to neutralize the base, followed by 125 ml of DCM to extract the organic layer. The organic layer was collected, dried over $MgSO_4$ and the drying agent was filtered off. The extract was concentrated on the rotary evaporator. The product **57a** was isolated after purification via silica gel column chromatography (20% EtOAc/Hex) as light yellow oil (6.47 g, 100%)

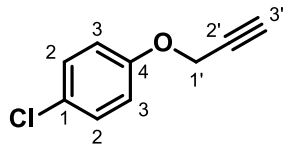

R*f* = 0.74 (3:7 EtOAc/Hex); **^{1}H NMR** (300 MHz, $CDCl_3$) δ 7.31 – 7.15 (m, 2H, H2), 6.98 – 6.77 (m, 2H, H3), 4.63 (d, *J* = 2.5 Hz, 2H, H1'), 2.51 (t, *J* = 2.4 Hz, 1H, H3'); **^{13}C NMR** (75 MHz, $CDCl_3$) δ 156.2 (C4), 129.4 (C2), 126.6 (C3), 116.3 (C1), 78.3 (C2'), 76.0 (C3'), 56.1 (C1').

6.9.2 Synthesis of 1-fluoro-4-(prop-2-yn-1-yloxy)benzene 57b[182]

1-Fluoro-4-(prop-2-yn-1-yloxy)benzene was synthesized by means of an alkylation reaction between commercially available 4-fluorophenol (5.00 g, 44.6 mmol) and

propargyl bromide (5.46 ml, 4.90 mmol) in the presence of K_2CO_3 (24.6 g, 0.20 mol) as a base and acetone (100 ml) as the solvent. The product **57b** was isolated as a yellow oil (5.53 g, 83%).

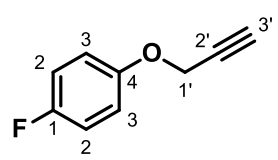

R*f* = 0.81 (3:7 EtOAc/Hex); **^{1}H NMR** (300 MHz, $CDCl_3$) δ 7.11 – 6.85 (m, 4H, H2 & H3), 4.66 (d, *J* = 2.5 Hz, 2H, H1'), 2.53 (t, *J* = 2.4 Hz, 1H, H3'); **^{13}C NMR** (75 MHz, $CDCl_3$) δ 157.8 (d, $J_{C\text{-}F}$ = 239.0 Hz, C1), 153.7 (d, $J_{C\text{-}F}$ = 2.2 Hz, C4), 116.3 (d, $J_{C\text{-}F}$ = 8.0 Hz, C3), 116.0 (d, $J_{C\text{-}F}$ = 23.1 Hz, C2), 78.6 (C2'), 75.7 (C3'), 56.5 (C1').

6.9.3 Synthesis of 1-methoxy-4-(prop-2-yn-1-yloxy)benzene 57c[183]

Commercially available 4-methoxyphenol (5.00 g, 40.3 mmol) was subjected to an alkylation reaction with propargyl bromide (4.93 ml, 44.3 mmol) in the presence of K_2CO_3 (22.2 g, 0.20 mol) and 100 ml of acetone as a solvent. A yellow oil of the product **57c** (6.21 g, 95%) was recovered.

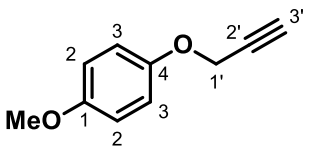

R*f* = 0.79 (3:7 EtOAc/Hex); **^{1}H NMR** (300 MHz, $CDCl_3$) δ 6.98 – 6.90 (m, 2H, H3), 6.89 – 6.81 (m, 1H, H2), 4.70 – 4.55 (m, 2H, H1'), 3.77 (s, 3H, OMe), 2.58 – 2.47 (m, 1H, H3'); **^{13}C NMR** (75 MHz, $CDCl_3$) δ 154.5 (C1), 151.7 (C4), 116.1 (C3), 114.6 (C2), 79.0 (C2'), 75.4 (C3'), 56.6 (C1'), 55.6 (OMe).

6.9.4 Synthesis of 1-chloro-3-(prop-2-yn-1-yloxy)benzene 57d[184]

A mixture of commercially available 3-chlorophenol (5.00 g, 38.9 mmol) and propargyl bromide (4.76 ml, 42.8 mmol) in the presence of K_2CO_3 (21.5 g, 0.20 mol) and 100 ml acetone produced 1-chloro-3-(prop-2-yn-1-yloxy)benzene **57d**, as an amber brown oil in 98% yield (6.35 g).

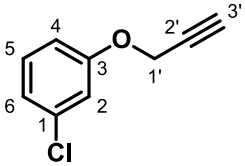

R*f* = 0.79 (3:7 EtOAc/Hex); **^{1}H NMR** (300 MHz, CDCl3) δ 7.22 – 7.14 (m, 1H, H5), 6.99 – 6.96 (m, 1H, H2), 6.96 – 6.93 (m, 1H, H6), 6.84 (ddd, *J* = 8.3, 2.3, 1.1 Hz, 1H, H4), 4.64 (d, *J* = 2.5 Hz, 2H, H1'), 2.53 (t, *J* = 2.4 Hz, 1H, H3'); **^{13}C NMR** (75 MHz, $CDCl_3$) δ 158.3 (C3), 134.9 (C1), 130.3 (C5), 121.8 (C6), 115.5 (C2), 113.4 (C4), 78.1 (C2'), 76.1 (C3'), 56.0 (C1').

6.9.5 Synthesis of 1-fluoro-3-(prop-2-yn-1-yloxy)benzene 57e[183]

1-Fluoro-3-(prop-2-yn-1-yloxy)benzene was synthesized as described in the general procedure. 3-Fluorophenol (5.00 ml, 55.2 mmol) was reacted with propargyl bromide (6.76 ml, 60.7 mmol) and K_2CO_3 (30.5 g, 0.20 mol) in 100 ml acetone to produce the product **57e**, a yellow oil (7.30 g, 88%).

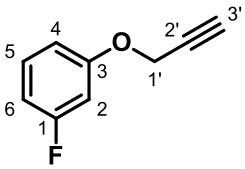

R*f* = 0.81 (3:7 EtOAc/Hex); **^{1}H NMR** (300 MHz, $CDCl_3$) δ 7.36 – 7.13 (m, 1H, H5), 6.86 – 6.62 (m, 3H, H2, H4 & H6), 4.68 (d, *J* = 2.4 Hz, 2H, H1'), 2.55 (t, *J* =3.7 Hz, 1H, H3'); **^{13}C NMR** (75 MHz, $CDCl_3$) δ 163.7 (d, $J_{C\text{-}F}$ = 245.4 Hz, C1), 159.0 (d, $J_{C\text{-}F}$ = 10.9 Hz, C3), 130.4 (d, $J_{C\text{-}F}$ = 10.0 Hz, C5), 110.8 (d, $J_{C\text{-}F}$ = 2.5 Hz, C4), 108.6 (d, $J_{C\text{-}F}$ = 21.3 Hz, C6), 103.0 (d, $J_{C\text{-}F}$ = 25.1 Hz, C2), 78.3 (C2'), 76.1 (C3'), 56.2 (C1').

6.9.6 Synthesis of 1-methoxy-3-(prop-2-yn-1-yloxy)benzene 57f[183]

A heterogeneous mixture of 3-methoxyphenol (5.00 ml, 45.6 mmol), propargyl bromide (5.58 ml, 50.1 mmol) and K_2CO_3 (25.2 g, 0.18 mmol) in acetone (100 ml) afforded 1-methoxy-3-(prop-2-yn-1-yloxy)benzene **57f** as a yellow oil (7.39 g, 100%).

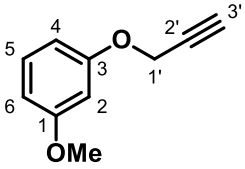

R*f* = 0.81 (3:7 EtOAc/Hex); **^{1}H NMR** (300 MHz, $CDCl_3$) δ 7.26 – 7.06 (m, 1H, H5), 6.64 – 6.43 (m, 3H, H2, H4 & H6), 4.63 (t, *J* = 2.4 Hz, 2H, H1'), 3.74 (s, 3H, OMe), 2.50 (t, *J* = 2.4 Hz, 1H, H3'); **^{13}C NMR** (75 MHz, $CDCl_3$) δ 160.8 (C1), 158.8 (C3), 129.9 (C5), 107.2 (C4), 106.9 (C6), 101.5 (C2), 78.6 (C2'), 75.6 (C3'), 55.8 (C1'), 55.3 (OMe).

6.9.7 Synthesis of 1-chloro-2-(prop-2-yn-1-yloxy)benzene 57g[185]

A solution of 2-chlorophenol (5.00 ml, 48.3 mmol), in 100 ml acetone was treated with propargyl bromide (5.91 ml, 53.1 mmol) and K_2CO_3 (26.7 g, 0.20 mol) to afford 1- chloro-2-(prop-2-yn-1-yloxy)benzene as described in the general procedure. 8.04 g of the product **57g** was afforded as a yellow oil in 100% yield.

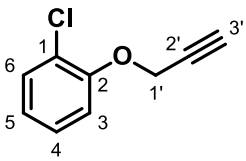

R*f* = 0.75 (3:7 EtOAc/Hex); **^{1}H NMR** (300 MHz, $CDCl_3$) δ 7.36 (dd, *J* = 7.9, 1.7 Hz, 1H, H6), 7.21 (ddd, *J* = 8.2, 7.4, 1.7 Hz, 1H, H4), 7.06 (dd, *J* = 8.3, 1.5 Hz, 1H, H3), 6.93 (td, *J* = 7.7, 1.5 Hz, 1H, H5), 4.75 (d, *J* = 2.5 Hz, 2H, H1'), 2.55 (t, *J* = 2.4 Hz, 1H, H3');**^{13}C NMR** (75 MHz,

$CDCl_3$) δ 153.1 (C2), 130.4 (C6), 127.6 (C4), 123.2 (C1), 122.4 (C5), 114.3 (C3), 78.0 (C2'), 76.2 (C3'), 56.7 (C1').

6.9.8 Synthesis of 1-fluoro-2-(prop-2-yn-1-yloxy)benzene 57h[186]

As described in the general procedure, 1-fluoro-2-(prop-2-yn-1-yloxy)benzene was synthesized by alkylation of 2-fluorophenol (5.00 ml, 56.0 mmol) in the presence of propargyl bromide (6.86 ml, 61.6 mmol), K_2CO_3 (31.0 g, 0.20 mol) as a base and 100 ml acetone. The product **57h** was isolated as a yellow oil in 92% yield (7.77 g).

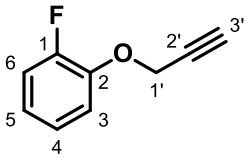

R*f* = 0.78 (3:7 EtOAc/Hex); **^{1}H NMR** (300 MHz, $CDCl_3$) δ 7.19 – 7.04 (m, 3H, H3, H4 & H6), 7.02 – 6.84 (m, 1H, H5), 4.76 (d, *J* = 2.5 Hz, 2H, H1'), 2.55 (t, *J* = 2.4 Hz, 1H, H3'); **^{13}C NMR** (75 MHz, $CDCl_3$) δ 153.0 (d, $J_{C\text{-}F}$ = 246.0 Hz, C1), 145.5 (d, $J_{C\text{-}F}$ = 10.5 Hz, C2), 124.3 (d, $J_{C\text{-}F}$ = 3.9 Hz, C4), 122.4 (d, $J_{C\text{-}F}$ = 6.9 Hz, C5), 116.4 (d, $J_{C\text{-}F}$ = 18.3 Hz, C6), 116.2 (d, $J_{C\text{-}F}$ = 1.6 Hz, C3), 78.2 (C2'), 76.2 (C3'), 57.2 (C1').

6.9.9 Synthesis of 1-methoxy-2-(prop-2-yn-1-yloxy)benzene 57i[183]

The general procedure was followed to synthesize 1-methoxy-2-(prop-2-yn-1-yloxy)benzene from commercially available guaiacol (5.00 ml, 45.5 mmol), propargyl bromide (5.57 ml, 50.0 mmol) and K_2CO_3 (25.1 g, 0.20 mol) in 100 ml acetone. The product **57i** was isolated as a light yellow oil (7.38 g) in 100% yield.

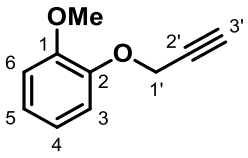

R*f* = 0.69 (3:7 EtOAc/Hex); **^{1}H NMR** (400 MHz, CDCl) δ 7.03 (dt, *J* = 7.8, 1.7 Hz, 1H, H6), 6.97 (dt, *J* = 7.8, 1.5 Hz, 1H, H5), 6.95 – 6.85 (m, 2H, H3 & H4), 4.74 (t, *J* = 2.2 Hz, 2H, H1'), 3.85 (s, 3H, OMe), 2.50 (t, *J* = 2.4 Hz, 1H, H3'); **^{13}C NMR** (101 MHz, $CDCl_3$) δ 149.7 (C1), 146.7 (C2), 122.2 (C5), 120.6 (C4), 114.5 (C6), 111.8 (C3), 78.6 (C2'), 75.7 (C3'), 56.7 (C1'), 55.7 (OMe).

6.10 General Procedure for the Sonogashira reaction

6.10.1 Synthesis of the 6-(*tert*-butyl)-2,4-diaminopyrimidine analogues

6.10.1.1 Synthesis of 6-(*tert*-butyl)-5-[3-(4-chlorophenoxy)prop-1-yn-1-yl]pyrimidine-2,4-diamine 58a.

In a dry 2 neck flask, flushed with N_2, was added 6-(*tert*-butyl)-5-iodopyrimidine-2,4-diamine (0.20 g, 0.70 mmol), $Pd(PPh_3)_2Cl_2$ (48.0 mg, 6.80 µmol) and the co-catalyst Cu(I)I (26.0 mg, 0.14 mmol). DMF (6 ml), was subjected to high vac. and purged with N_2 before addition to the dry reagents. Followed by addition of the base (12.0 ml, 85.6 mmol) DIIPA and the reaction was stirred for a further 10 min. before 1-chloro-4-(prop-2-yn-1-yloxy)benzene (0.23 g, 1.40 mmol) was introduced dropwise to the mixture. The reaction temperature was raised to 100 ^oC and refluxed for 16 hours under N_2 atmosphere. The dark black heterogeneous mixture was transferred to a separating funnel and the organic layer was partitioned between saturated aq. NH_4Cl and EtOAc to remove copper. The organic layer was washed 5 times with brine, then dried over $MgSO_4$. The drying agent was filtered through celite and the filtrate concentrated on a rotary evaporator. The residue was first purified by silica gel column chromatography (60 % EtOAC/Hex). Then the residue was adsorbed onto aluminium oxide and further purified by means of aluminium oxide column chromatography (30%- 60% EtOAc/Hex), followed by (5% - 10% MeOH/DCM). The product **58a** was recovered as a dark brown solid (0.13 g, 59%).

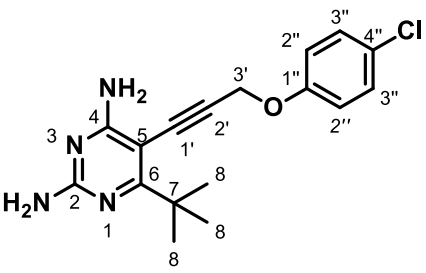

R*f* = 0.61 (1:9 MeOH/DCM); **mp**: 139 °C; **IR** (v/cm^{-1}): 3360 (NH str), 3215 (NH str), 2960 (CH), 2214 (C≡C), 1624 (NH bend), 1260 (C-O); **^{1}H NMR** (300 MHz, DMSO) δ 7.33 (d, *J* = 9.0 Hz, 2H, H3''), 7.08 (d, *J* = 9.0 Hz, 2H, H2''), 6.43 (s, 2H, NH_2), 6.22 (s, 2H, NH_2), 5.10 (s, 2H, H3'), 1.24 (s, 9H, H8); **^{13}C NMR** (75 MHz, DMSO) δ 177.0 (C6), 166.0 (C4), 160.7 (C2), 156.3 (C1''), 129.1 (C3''), 124.7 (C4''), 116.9 (C2''), 95.5 (C2'), 84.8 (C5), 83.0 (C1'), 57.0 (C3'), 38.2 (C7), 28.5 (C8); **HRMS** (ES^+) calculated for $C_{17}H_{19}ClN_4O$ $[M + H]^+$: 331.1320, found: 331.1269.

6.10.1.2 Synthesis of 6-(*tert*-butyl)-5-[3-(4-fluorophenoxy)prop-1-yn-1-yl]pyrimidine-2,4-diamine 58b.

6-(*tert*-Butyl)-5-iodopyrimidine-2,4-diamine (1.00 g, 3.40 mmol) in the presence of the catalyst $Pd(PPh_3)_2Cl_2$ (0.24 g, 0.30 mmol), Cu(I)I (0.13 g, 0.70 mmol), 1-fluoro-4-(prop-2-yn-1-yloxy)benzene (1.01 g, 6.90 mmol) and DIIPA (24.0 ml, 0.20 mol) was dissolved in 12 ml dry DMF to afford the product **58b** (0.68 g, 63%) as a cream white solid.

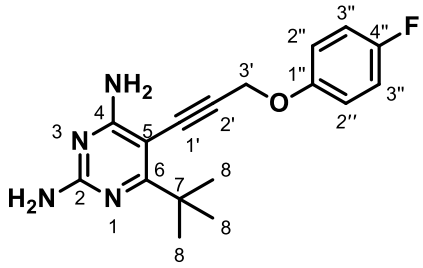

R*f* = 0.54 (1:9 MeOH/DCM); **mp**: 137 °C; **IR** (v/cm^{-1}):, 3307 (NH str), 3146 (NH str), 2960 (CH), 2217 (C≡C), 1642 (NH bend), 1231 (C-O); **^{1}H NMR** (400 MHz, $CDCl_3$) δ 7.04 – 6.88 (m, 4H, H2'' & H3''), 5.30 (s, 2H, NH_2), 5.08 (s, 2H, NH_2), 4.96 (s, 2H, H3'), 1.33 (s, 9H, H8); **^{13}C NMR** (101 MHz, $CDCl_3$) δ 179.0 (C6), 165.9 (C4), 160.5 (C2), 157.8 (d, $J_{C\text{-}F}$ = 239.4 Hz, C4''), 153.7 (d, $J_{C\text{-}F}$ = 2.3 Hz, C1''), 116.5 (d, $J_{C\text{-}F}$ = 8.0 Hz, C2''), 116.0 (d, $J_{C\text{-}F}$ = 23.1 Hz, C3''), 95.6 (C2'), 87.5 (C5), 83.0 (C1'), 57.6 (C3'), 38.8 (C7), 28.6 (C8); **HRMS** (ES^+) calculated for $C_{17}H_{19}FN_4O$ $[M + H]^+$: 315.1616, found: 315.1641.

6.10.1.3 Synthesis of 6-(*tert*-butyl)-5-[3-(4-methoxyphenoxy)prop-1-yn-1-yl]pyrimidine-2,4-diamine 58c.

6-(*tert*-Butyl)-5-iodopyrimidine-2,4-diamine (1.00 g, 3.40 mmol) was subjected to Sonogashira reaction conditions in the presence of $Pd(PPh_3)_2Cl_2$ (0.24 g, 0.30 mmol), Cu(I)I (0.13 g, 0.70 mmol), 1-methoxy-4-(prop-2-yn-1-yloxy)benzene (1.11 g, 6.90 mmol), DIIPA (24.0 ml, 0.20 mol) and 12 ml DMF to afford the product **58c** (0.30 g, 27%) as a light brown solid.

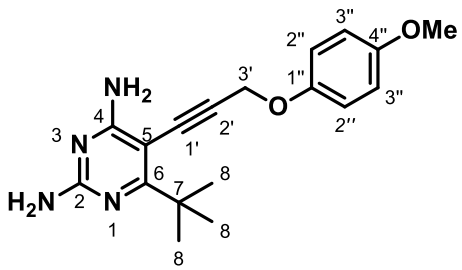

R*f* = 0.50 (1:9 MeOH/DCM); **mp**: 107 °C; **IR** (v/cm^{-1}): 3314 (NH str), (3157 NH str), 2215 (C≡C), 1645 (NH bend), 1263 (C-O); **^{1}H NMR** (400 MHz, $CDCl_3$) δ 6.94 (d, *J* = 7.3 Hz, 2H, H2''/H3''), 6.83 (d, *J* = 9.1 Hz, 2H, H2''/H3''), 5.48 (s, 2H, NH_2), 5.29 (s, 2H, NH_2), 4.93 (s, 2H, H3'), 3.73 (s, 3H, OMe), 1.33 (s, 9H, H8); **^{13}C NMR** (101 MHz, $CDCl_3$) δ 178.7 (C6), 165.8 (C4), 160.4 (C2), 154.4 (C4''), 151.6 (C1''), 116.4 (C2''/3''), 114.7 (C2''/3''), 96.0 (C2'), 87.4 (C5), 82.6 (C1'), 57.6 (C3'), 55.7 (OMe), 38.7

(C7), 28.6 (C8); **HRMS** (ES^+) calculated for $C_{18}H_{22}N_4O_2$ $[M + H]^+$: 327.1816 , found: 327.1781.

6.10.1.4 Synthesis of 6-(*tert*-butyl)-5-[3-(3-chlorophenoxy)prop-1-yn-1-yl]pyrimidine-2,4-diamine 58d

The general procedure was followed to synthesise 6-(*tert*-butyl)-5-[3-(3-chlorophenoxy)prop-1-yn-1-yl]pyrimidine-2,4-diamine. 6-(*tert*-Butyl)-5-iodopyrimidine -2,4-diamine (1.00 g, 3.40 mmol) was dissolved in 12 ml dry DMF in the presence of the acetylene substrate (1.14 g, 6.90 mmol), 1-chloro-3-(prop-2-yn-1-yloxy)benzene, $Pd(PPh_3)_2Cl_2$ (0.24 g, 0.30 mmol), Cu(I)I (0.13 g, 0.70 mmol) and DIIPA (24.0 ml, 0.20 mol) to afford the product **58d** as a golden brown viscous oil (0.89 g, 79%).

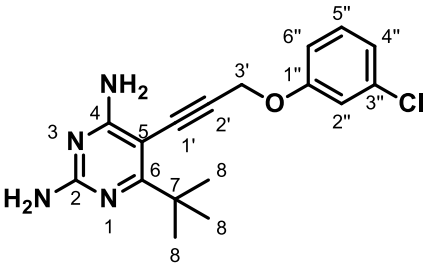

R*f* = 0.46 (1:9 MeOH/DCM); **IR** (v/cm^{-1}): 3325 (NH str), 3197 (NH str), 2958 (CH), 2202 (C≡C), 1277 (C-O); **^{1}H NMR** (400 MHz, $CDCl_3$) δ 7.19 (t, *J* = 8.2 Hz, 1H, H5''), 7.01 (s, 1H, H2''), 6.95 (d, *J* = 8.1 Hz, 1H, H4''), 6.88 (d, *J* = 8.4 Hz, 1H, H6''), 5.42 (s, 2H, NH_2), 5.21 (s, 2H, NH_2), 4.97 (s, 2H, H3'), 1.34 (s, 9H, H8); **^{13}C NMR** (101 MHz, $CDCl_3$) δ 179.1 (C6), 165.8 (C4), 160.4 (C2), 158.3 (C1''), 135.0 (C3''), 130.4 (C5''), 121.8 (C4''), 115.5 (C2''), 113.8 (C6''), 95.2 (C2'), 87.3 (C5), 83.3 (C1'), 57.0 (C3'), 38.8 (C7), 28.6 (C8); **HRMS** (ES^+) calculated for $C_{17}H_{19}ClN_4O$ $[M + H]^+$: 331.1320, found: 331.1282.

6.10.1.5 Synthesis of 6-(*tert*-butyl)-5-[3-(3-fluorophenoxy)prop-1-yn-1-yl]pyrimidine-2,4-diamine 58e

A mixture of 6-(*tert*-butyl)-5-iodopyrimidine-2,4-diamine (1.00 g, 3.40 mmol), $Pd(PPh_3)_2Cl_2$ (0.24 g, 0.30 mmol) and Cu(I)I (0.13 g, 0.70 mmol) was dissolved in 12 ml of dry DMF, followed by addition of DIIPA (24.0 ml, 0.20 mol) and 1-fluoro-3-(prop-2-yn-1-yloxy)benzene (1.01 g, 6.90 mmol) to afford the product **58e** (0.78 g, 73%) as a dark brown viscous oil.

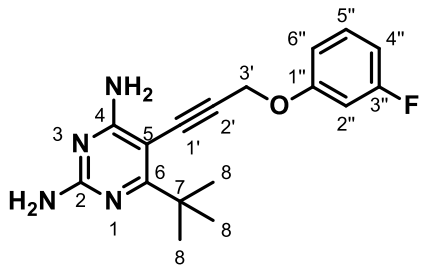

R*f* = 0.50 (1:9 MeOH/DCM); **IR** (v/cm^{-1}): 3316 (NH str), 3193 (NH str), 2957 (CH), 2204 (C≡C), 1261 (C-O); **^{1}H NMR** (400 MHz, $CDCl_3$) δ 7.21 (dd, *J* = 7.8, 7.1 Hz, Hz, 1H, H5''), 6.82 – 6.59 (m, 3H, H2'', H4'' & H6''), 5.46 (s, 2H, NH_2), 5.24 (s, 2H, NH_2), 4.97 (s,

2H, H3'), 1.34 (s, 9H, H8); **^{13}C NMR** (101 MHz, $CDCl_3$) δ 179.1 (C6), 165.9 (C4), 163.6 (d, J_{C-F} = 245.7 Hz, C3''), 160.5 (C2), 158.9 (d, J_{C-F} = 10.6 Hz, C1''), 130.4 (d, J_{C-F} = 10.3 Hz, C5''), 110.9 (d, J_{C-F} = 2.9 Hz, C6''), 108.4 (d, J_{C-F} = 21.4 Hz, C2''), 103.1 (d, J_{C-F} = 25.1 Hz, C4''), 95.2(C2'), 87.3 (C5), 83.3 (C1'), 57.1 (C3'), 38.8 (C7), 28.6 (C8); **HRMS** (ES^+) calculated for $C_{17}H_{19}FN_4O$ $[M + H]^+$: 315.1616, found: 315.1576.

6.10.1.6 Synthesis of 6-(*tert*-butyl)-5-[3-(3-methoxyphenoxy)prop-1-yn-1-yl]pyrimidine-2,4-diamine 58f

The general procedure was followed to synthesise 6-(*tert*-butyl)-5-[3-(3-methoxyphenoxy)prop-1-yn-1-yl]pyrimidine-2,4-diamine. The starting material, 6-(*tert*-butyl)-5-iodopyrimidine-2,4-diamine (1.00 g, 3.40 mmol), was dissolved in 12 ml DMF in the presence of $Pd(PPh_3)_2Cl_2$ (0.24 g, 0.30 mmol) and Cu(I)I (0.13 g, 0.70 mmol), followed by addition of DIIPA (24.0 ml, 0.20 mol) and 1-methoxy-3-(prop-2-yn-1-yloxy)benzene 1.11 g, 6.90 mmol) to afford the product **58f** (0.76 g, 68%) as a cream white solid.

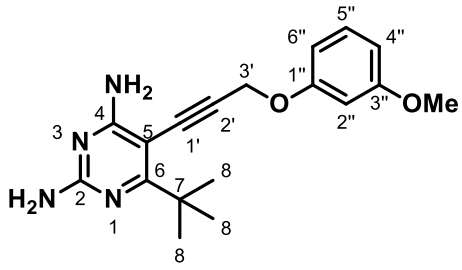

R*f* = 0.53 (1:9 MeOH/DCM); **mp**: 158 °C; **I.R** (v/cm^{-1}): 3314 (NH str), 3160 (NH str), 2971 (CH), 2223 (C≡C), 1257 (C-O); **^{1}H NMR** (300 MHz, $CDCl_3$) δ 7.20 (dd, *J* = 8.4, 8.0 Hz, 1H, H5''), 6.67 – 6.47 (m, 3H, H2'', H4'' & H6''), 5.18 (s, 2H, NH_2), 4.99 (s, 2H, H3'), 4.90 (s, 2H, NH_2), 3.78 (s, 2H, OMe), 1.35 (s, 9H, H8); **^{13}C NMR** (75 MHz, $CDCl_3$) δ 178.9 (C6), 165.9 (C4), 161.0 (C3''), 160.4 (C2), 158.9 (C1''), 130.1 (C5''), 107.3 (C6''), 107.2 (C4''), 101.9 (C2''), 95.8 (C2'), 87.7 (C5), 82.9 (C1'), 57.0 (C3'), 55.4 (OMe), 38.8 (C7), 28.7 (C8); **HRMS** (ES^+) calculated for $C_{18}H_{22}N_4O_2$ $[M + H]^+$: 327.1816, found: 327.1776.

6.10.1.7 Synthesis of 6-(*tert*-butyl)-5-[3-(2-chlorophenoxy)prop-1-yn-1-yl]pyrimidine-2,4-diamine 58g

A mixture of 12 ml DMF and 6-(*tert*-butyl)-5-iodopyrimidine-2,4-diamine (1.00 g, 3.40 mmol), was subjected to Sonogashira reaction conditions in the presence of $Pd(PPh_3)_2Cl_2$ (0.24 g, 0.30 mmol), Cu(I)I (0.13 g, 0.70 mmol), DIIPA (24.0 ml, 0.20 mol) and 1-chloro-2-(prop-2-yn-1-yloxy)benzene **58g** (1.14 g, 6.90 mmol) to afford the product (0.12 g, 10%) as a dark brown solid.

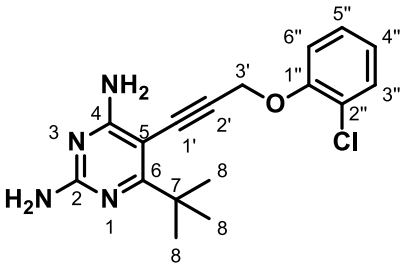

R*f* =0.53 (1:9 MeOH/DCM); **mp**: 97 °C; **IR** (v/cm^{-1}): 3321(NH str), 3187 (NH str), 2957 (CH), 2203 (C≡C), 1225 (C-O); **^{1}H NMR** (300 MHz, $CDCl_3$) δ 7.37 (dd, *J* = 7.9, 1.6 Hz, 1H, H3''), 7.21 (ddd, *J* = 8.8, 7.4, 1.6 Hz, 1H, H5''), 7.10 (dd, *J* = 8.2, 1.5 Hz, 1H, H6''), 6.92 (ddd, *J* = 7.6, 7.6, 1.5 Hz, 1H, H4''), 5.38 (s, 2H, NH_2), 5.13 (s, 2H, NH_2), 5.09 (s, 2H, H3'), 1.32 (s, 9H, H8); **^{13}C NMR** (75 MHz, $CDCl_3$) δ 179.0 (C6), 165.9 (C4), 160.4 (C2), 153.2 (C1''), 130.7 (C3''), 127.7 (C5''), 123.5 (C2''), 122.5 (C4''), 114.6 (C6''), 95.2 (C2'), 87.4 (C5), 83.4 (C1'), 57.9 (C3'), 38.8 (C7), 28.6 (C8); **HRMS** (ES^+) calculated for $C_{17}H_{19}ClN_4O$ $[M + H]^+$: 331.1320, found: 331.1266.

6.10.1.8 Synthesis of 6-(*tert*-butyl)-5-[3-(2-fluorophenoxy)prop-1-yn-1-yl] pyrimidine-2,4-diamine 58h

6-(*tert*-Butyl)-5-iodopyrimidine-2,4-diamine (1.00 g, 3.40 mmol), $Pd(PPh_3)_2Cl_2$ (0.24 g, 0.30 mmol), Cu(I)I (0.13 g, 0.70 mmol), DIIPA (24.0 ml, 0.20 mol) and 1-chloro-2-(prop-2-yn-1-yloxy)benzene (1.14 g, 6.90 mmol) were dissolved in 12 ml DMF to produce the product **58h**, a dark brown viscous oil (0.61 g, 57%).

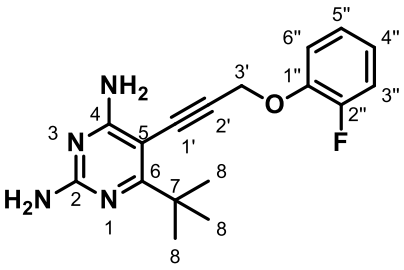

R*f* = 0.56 (1:9 MeOH/DCM); **IR** (v/cm^{-1}): 3323 (NH str), 3195 (NH str), 2958 (CH), 2203 (C≡C), 1255 (C-O); **^{1}H NMR** (300 MHz, $CDCl_3$) δ 7.19 – 6.99 (m, 3H, H3'', H5'' & H6''), 6.96 – 6.86 (m, H4''), 5.45 (s, 2H, NH_2), 5.27 (s, 2H, NH_2), 5.07 (s, 2H, H3'), 1.31 (s, 9H, H8); **^{13}C NMR** (75 MHz, $CDCl_3$) δ 178.9 (C6), 165.9 (C4), 160.5 (C2), 153.2 (d, $J_{C\text{-}F}$ = 245.8 Hz, C2''), 145.4 (d, $J_{C\text{-}F}$ = 10.6 Hz, C1''), 124.3 (d, $J_{C\text{-}F}$ = 3.9 Hz, C5''), 122.3 (d, $J_{C\text{-}F}$ = 6.8 Hz, C4''), 116.6 (d, $J_{C\text{-}F}$ = 18.4 Hz, C3''), 116.6 (d, $J_{C\text{-}F}$ = 1.6 Hz, C6''), 95.3 (C2'), 87.2 (C5), 83.4 (C1'), 58.3 (C3'), 38.7 (C7), 28.6 (C8); **HRMS** (ES^+) calculated for $C_{17}H_{19}FN_4O$ $[M + H]^+$: 315.1616, found: 315.1583.

6.10.1.9 Synthesis of 6-(*tert*-butyl)-5-[3-(2-methoxyphenoxy)prop-1-yn-1-yl]pyrimidine-2,4-diamine 58i

The general procedure was followed to synthesise 6-(*tert*-butyl)-5-[3-(2-methoxyphenoxy)prop-1-yn-1-yl]pyrimidine-2,4-diamine by means of subjecting 6- (*tert*-butyl)-5-iodopyrimidine-2,4-diamine (1.00 g, 3.40 mmol) to Sonogashira

reaction conditions in the presence of 1-methoxy-2-(prop-2-yn-1-yloxy)benzene (1.11g, 6.90 mmol), $Pd(PPh_3)_2Cl_2$ (0.24 g, 0.30 mmol), Cu(I)I (0.13 g, 0.70 mmol) and DIIPA (24.0 ml, 0.20 mol) as a base. The reagents were dissolved in 12 ml DMF. 0.16 g of the product **58i** was isolated as a dark brown viscous oil (14%).

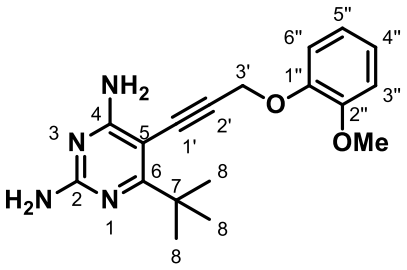

R*f* = 0.47 (1:9 MeOH/DCM); **IR** (v/cm^{-1}): 3329 (NH str), 3197 (NH str), 3068 (=C-H), 2956 (CH), 2203 (C≡C), 1247 (C-O); **^{1}H NMR** (400 MHz, $CDCl_3$) δ 7.13 – 7.03 (m, 1H, H6''), 7.01 – 6.93 (m, 1H, H4''), 6.94 – 6.84 (m, 2H, H3'' & H5''), 5.22 (s, 2H, NH_2), 5.09 (s, 2H, CH_2), 4.99 (s, 2H, NH_2), 3.87 (s, 3H, OMe), 1.33 (s, 9H, H8), **^{13}C NMR** (101 MHz, $CDCl_3$) δ 178.8 (C6), 165.9 (C4), 160.4 (C2), 150.0 (C2''), 146.8 (C1''), 122.4 (C4''), 120.8 (C5''), 114.8 (C6''), 112.1 (C3''), 95.9 (C2'), 87.7 (C5), 83.0 (C1'), 57.9 (C3'), 55.9 (OMe), 38.8 (C7), 28.6 (C8), **HRMS** (ES^+) calculated for $C_{18}H_{22}N_4O_2$ $[M + H]^+$: 327.1816, found: 327.1768.

6.10.2 Synthesis of the 6-isopropylpyrimidine-2,4-diamine analogues.

6.10.2.1 Synthesis of 5-[3-(4-chlorophenoxy)prop-1-yn-1-yl]-6-isopropyl pyrimidine-2,4-diamine 59a

A heterogeneous mixture of 5-iodo-6-isopropylpyrimidine-2,4-diamine (0.50 g, 1.80 mmol), $Pd(PPh_3)_2Cl_2$ (0.13 g, 0.20 mmol) and Cu(I)I (68.5 mg, 0.40 mmol) was dissolved in 6 ml DMF, followed by addition of the base, DIIPA (12.0 ml, 89.9 mmol), and 1-chloro-4-(prop-2-yn-1-yloxy)benzene (0.60 g, 3.60 mmol) to produce 0.26 g (46%) of 5-[3-(4-chlorophenoxy)prop-1-yn-1-yl]-6-isopropylpyrimidine-2,4-diamine **59a** as a cream white solid.

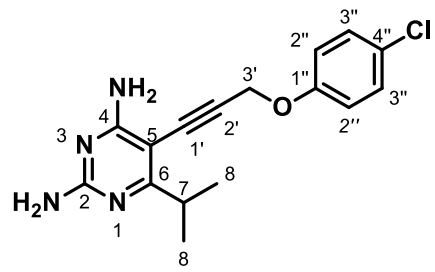

R*f* = 0.47 (1:9 MeOH/DCM); **mp**: 78 °C; **IR** (v/cm^{-1}): 3360 (NH str), 3123 (NH str), 2976 (CH), 2217 (C≡C), 1246 (C-O); **^{1}H NMR** (300 MHz, $CDCl_3$) δ 7.25 (d, *J* = 9.0 Hz, 2H, H3''), 6.93 (d, *J* = 9.0 Hz, 2H, H2''), 5.54 (s, 2H, NH_2), 5.49 (s, 2H, NH_2), 4.94 (s, 2H, H3'), 3.19 (h, *J* = 6.8 Hz, 1H, H7), 1.13 (d, *J* = 6.9 Hz, 6H, H8); **^{13}C NMR** (75 MHz, $CDCl_3$) δ 177.8 (C6), 164.5 (C4), 161.4 (C2), 156.1 (C1''), 129.4 (C3''), 126.5 (C4''),

116.5 (C2''), 93.0 (C2'), 88.3 (C5), 81.3 (C1'), 57.1 (C3'), 33.5 (C7), 20.7 (C8); **HRMS** (ES^+) calculated for $C_{16}H_{17}ClN_4O$ $[M + H]^+$: 317.1164, found: 317.1186.

6.10.2.2 Synthesis of 5-[3-(4-fluorophenoxy)prop-1-yn-1-yl]-6-isopropyl pyrimidine-2,4-diamine 59b

5-Iodo-6-isopropylpyrimidine-2,4-diamine (0.50 g, 1.80 mmol) in the presence of the catalyst $Pd(PPh_3)_2Cl_2$ (0.13 g, 0.20 mmol), Cu(I)I (68.5 mg, 0.40 mmol), 1-fluoro-4-(prop-2-yn-1-yloxy)benzene (0.53 g, 3.60 mmol) and DIIPA (12.0 ml, 89.9 mmol) was dissolved in 6 ml dry DMF to afford the product **59b** (0.32 g, 59%) as a light yellow solid.

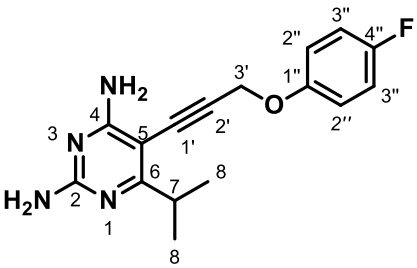

R*f* = 0.34 (1:9 MeOH/DCM); **mp**: 158 °C; **IR** (v/cm^{-1}): 3319 (NH str), 3173 (NH str), 2962 (CH), 2220 (C≡C), 1240 (C-O); **^{1}H NMR (**400 MHz, $CDCl_3$) δ 7.12 – 6.87 (m, 4H, H2'' & H3''), 5.17 (s, 2H, NH_2), 5.08 (s, 2H, NH_2), 4.94 (s, 2H, H3'), 3.20 (h, *J* = 6.8 Hz, 1H, H7), 1.13 (d, *J* = 6.8 Hz, 6H, H8); **^{13}C NMR** (101 MHz, $CDCl_3$) δ 178.0 (C6), 164.6 (C4), 161.5 (C2), 157.9 (d, $J_{C\text{-}F}$ = 239.5 Hz, C4''), 153.7 (d, $J_{C\text{-}F}$ = 2.2 Hz, C1''), 116.5 (d, $J_{C\text{-}F}$ = 8.1 Hz, C2''), 116.0 (d, $J_{C\text{-}F}$ = 23.1 Hz, C3''), 93.3 (C2'), 88.6 (C5), 81.3 (C1'), 57.6 (C3'), 33.6 (C7), 20.8 (C8); **HRMS** (ES^+) calculated for $C_{16}H_{17}FN_4O$ $[M + H]^+$: 301.1459, found: 301.1484.

6.10.2.3 Synthesis of 6-isopropyl-5-[3-(4-methoxyphenoxy)prop-1-yn-1-yl] pyrimidine-2,4-diamine 59c

5-Iodo-6-isopropylpyrimidine-2,4-diamine (0.50 g, 1.80 mmol) was subjected to Sonogashira reaction conditions in the presence of $Pd(PPh_3)_2Cl_2$ (0.13 g, 0.20 mmol), Cu(I)I (68.5 mg, 0.40 mmol), 1-methoxy-4-(prop-2-yn-1-yloxy)benzene (0.58 g, 3.60 mmol), DIIPA (12.0 ml, 89.9 mmol) and 6 ml DMF to afford the product **59c** (0.36 g, 63%) as an amber brown viscous oil.

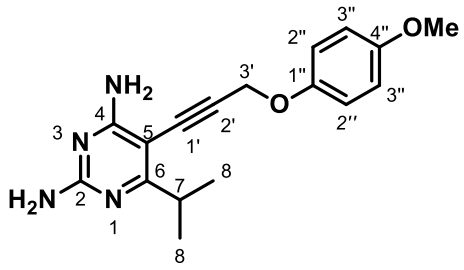

R*f* = 0.28 (1:9 MeOH/DCM); **IR** (v/cm^{-1}): 3320 (NH str), 3180 (NH str), 2965 (CH), 2215 (C≡C), 1240 (C-O); **^{1}H NMR** (300 MHz, $CDCl_3$) δ 6.96 (d, *J* = 9.1 Hz, 2H, H2''/H3''), 6.84 (d, *J* = 9.1 Hz, 2H, H2''/H3''), 5.20 (s, 2H, NH_2), 5.13 (s, 2H, NH_2), 4.92 (s, 2H, H3'), 3.76 (s, 3H, OMe), 3.21 (h, *J* = 6.8 Hz, 1H, H7), 1.14 (d, *J* = 6.8 Hz, 6H, H8); **^{13}C NMR** (75 MHz, $CDCl_3$) δ 177.7 (C6), 164.6 (C4), 161.4 (C2), 154.6 (C4''), 151.6 (C1''), 116.6 (C2''), 114.7 (C3''), 93.8 (C2'), 88.7 (C5), 80.9 (C1'), 57.7 (C3'), 55.8 (OMe), 33.5 (C7), 20.9 (C8); **HRMS** (ES^+) calculated for $C_{17}H_{20}N_4O_2$ $[M + H]^+$: 313.1659, found: 313.1681.

6.10.2.4 Synthesis of 5-[3-(3-chlorophenoxy)prop-1-yn-1-yl]-6-isopropyl pyrimidine-2,4-diamine 59d

The general procedure was followed to synthesise 5-[3-(3-chlorophenoxy)prop-1-yn-1-yl]-6-isopropylpyrimidine-2,4-diamine. 5-Iodo-6-isopropylpyrimidine-2,4-diamine (0.50 g, 1.80 mmol) was dissolved in 6 ml dry DMF in the presence of the acetylene substrate (0.60 g, 3.60 mmol), 1-chloro-3-(prop-2-yn-1-yloxy)benzene, $Pd(PPh_3)_2Cl_2$ (0.13 g, 0.20 mmol), Cu(I)I (68.5 mg, 0.40 mmol) and DIIPA (12 ml, 89.9 mmol) to afford the pyrimidine **59d** as a cream white solid (78.0 mg, 14%).

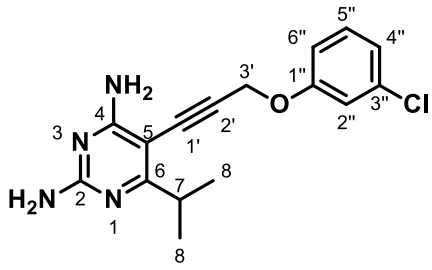

R*f* = 0.51 (1:9 MeOH/DCM); **mp**: 117 °C; **IR** (v/cm^{-1}): 3311 (NH str), 3147 (NH str), 2958 (CH); 2214 (C≡C), 1275 (C-O); **^{1}H NMR** (400 MHz, $CDCl_3$) δ 7.22 (t, *J* = 8.1 Hz, 1H, H5''), 7.03 (t, *J* = 2.2 Hz, 1H, H2''), 6.98 (ddd, *J* = 7.9, 1.9, 0.9 Hz, 1H, H4''), 6.90 (ddd, *J* = 8.3, 2.5, 0.9 Hz, 1H, H6''), 5.19 (s, 2H, NH_2), 5.08 (s, 2H, NH_2), 4.97 (s, 2H, H3'), 3.22 (h, *J* = 6.8 Hz, 1H, H7), 1.14 (d, *J* = 6.9 Hz, 6H, H8); **^{13}C NMR** (101 MHz, $CDCl_3$) δ 178.1 (C6), 164.6 (C4), 161.5 (C2), 158.3 (C1''), 135.0 (C3''), 130.4 (C5''), 121.8 (C4''), 115.5 (C2''), 114.0 (C6''), 92.9 (C2'), 88.5 (C5), 81.7 (C1'), 57.1 (C3'), 33.6 (C7), 20.8 (C8); **HRMS** (ES^+) calculated for $C_{16}H_{17}ClN_4O$ $[M + H]^+$: 317.1164, found: 317.1183.

6.10.2.5 Synthesis of 5-[3-(3-fluorophenoxy)prop-1-yn-1-yl]-6-isopropyl pyrimidine-2,4-diamine 59e

A mixture of 5-iodo-6-isopropylpyrimidine-2,4-diamine (0.50 g, 1.80 mmol), $Pd(PPh_3)_2Cl_2$ (0.13 g, 0.20 mmol) and Cu(I)I (68.5 mg, 0.40 mmol) was dissolved in 6 ml of dry DMF, followed by addition of DIIPA (12.0 ml, 89.9 mmol) and 1-fluoro-3-(prop-2-yn-1-yloxy)benzene (0.53 g, 3.6 mmol) to afford the product **59e** (0.22 g, 41%) as a brown viscous oil.

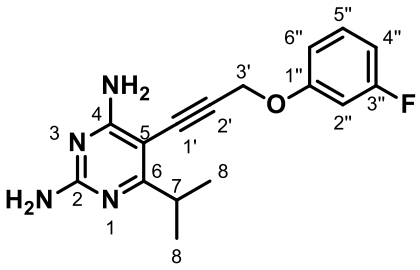

R*f* = 0.43 (1:9 MeOH/DCM); **IR**(v/cm^{-1}): 3319 (NH str), 3183 (NH str), 2966 (CH); 2216 (C≡C), 1260 (C-O); **^{1}H NMR** (400 MHz, $CDCl_3$) δ 7.24 (q, *J* = 8.1 Hz, 1H, H5''), 6.86 – 6.60 (m, 3H, H2'', H4'' & H6''), 5.45 (s, 4H, 2(NH_2)), 4.96 (s, 2H, H3'), 3.22 (h, *J* = 6.8 Hz, 1H, H7), 1.14 (d, *J* = 6.8 Hz, 6H, H8); **^{13}C NMR** (101 MHz, $CDCl_3$) δ 178.0 (C6), 164.7 (C4), 163.6 (d, $J_{C\text{-}F}$ = 245.4 Hz, C3''), 161.5 (C2), 158.9 (d, $J_{C\text{-}F}$ = 11.0 Hz, C1''), 130.4 (d, $J_{C\text{-}F}$ = 9.9 Hz, C5''), 111.0 (d, $J_{C\text{-}F}$ = 2.9 Hz, C6''), 108.4 (d, $J_{C\text{-}F}$ = 21.3 Hz, C2''), 103.1 (d, $J_{C\text{-}F}$ = 24.9 Hz, C4''), 93.0 (C2'), 88.4 (C5), 81.5 (C1'), 57.1 (C3'), 33.6 (C7), 20.8 (C8); **HRMS** (ES^+) calculated for $C_{16}H_{17}FN_4O$ $[M + H]^+$: 301.1459, found: 301.1482.

6.10.2.6 Synthesis of 6-isopropyl-5-[3-(3-methoxyphenoxy)prop-1-yn-1-yl] pyrimidine-2,4-diamine 59f

The general procedure was followed to synthesise 6-isopropyl-5-[3-(3-methoxyphenoxy)prop-1-yn-1-yl]pyrimidine-2,4-diamine. The starting material, 5-iodo-6-isopropylpyrimidine-2,4-diamine (1.00 g, 3.60 mmol), was dissolved in 12 ml DMF in the presence of $Pd(PPh_3)_2Cl_2$ (0.25 g, 0.40 mmol) and Cu(I)I (0.14 g, 0.70 mmol), followed by addition of DIIPA (24.0 ml, 0.20 mol) and 1-methoxy-3-(prop-2-yn-1-yloxy)benzene 1.17 g, 7.20 mmol) to afford the product **59f** (0.63 g, 56%) as a light brown solid.

R*f* = 0.42 (1:9 MeOH/DCM); **mp**: 128 °C; **I.R** (v/cm^{-1}): 3315 (NH str), 3162 (NH str), 2960 (CH); 2198 (C≡C), 1644 (NH bend),1286 (C-O); **^{1}H NMR** (400 MHz, $CDCl_3$) δ 7.17 (t, *J* = 8.2 Hz, 1H, H5''), 6.63 – 6.45 (m, 3H, H2'', H4'' & H6''), 5.57 (s, 2H, NH_2), 5.55 (s, 2H, NH_2), 4.93 (s, 2H, H3'), 3.76 (s, 3H, OMe), 3.23 (h, *J* = 6.9 Hz, 1H, H7), 1.13 (d, *J* = 6.9 Hz, 6H, H8); **^{13}C NMR** (101 MHz, $CDCl_3$) δ 177.7 (C6), 164.5 (C4), 161.2 (C2), 160.9 (C3''), 158.7 (C1''), 130.0 (C5''), 107.2 (C6''), 107.1 (C4''), 101.8 (C2''), 93.5 (C2'), 88.5 (C5), 80.9 (C1'), 56.8 (C3'), 55.3 (OMe), 33.5 (C7), 20.7 (C8); **HRMS** (ES$^+$) calculated for $C_{17}H_{20}N_4O_2$ [M + H]$^+$: 313.1659, found: 313.1682.

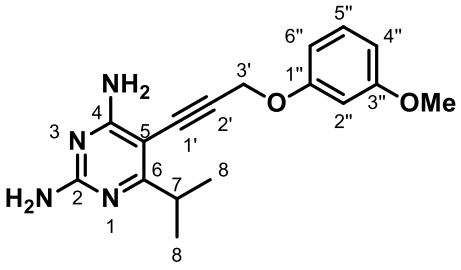

6.10.2.7 Synthesis of 5-(3-[2-chlorophenoxy)prop-1-yn-1-yl]-6-isopropyl pyrimidine-2,4-diamine 59g

A mixture of 12 ml DMF and 5-iodo-6-isopropylpyrimidine-2,4-diamine (1.00 g, 3.60 mmol), was subjected to Sonogashira reaction conditions in the presence of $Pd(PPh_3)_2Cl_2$ (0.25 g, 0.40 mmol), Cu(I)I (0.14 g, 0.70 mmol), DIIPA (24.0 ml, 0.20 mol) and 1-chloro-2-(prop-2-yn-1-yloxy)benzene (1.20 g, 7.20 mmol) to afford the product **59g** (0.11 g, 10%) as a dark brown solid.

R*f* = 0.39 (1:9 MeOH/DCM); **mp**: 78 °C; **IR** (v/cm^{-1}): 3340 (NH str), 3108 (NH str), 2976 (CH); 2217 (C≡C), 1619 (NH bend), 1246 (C-O); **^{1}H NMR** (400 MHz, $CDCl_3$) δ 7.38 (dd, *J* = 7.9, 1.6 Hz, 1H, H3''), 7.21 (ddd, *J* = 8.3, 7.4, 1.7 Hz, 1H, H5''), 7.11 (dd, *J* = 8.2, 1.5 Hz, 1H, H6''), 6.93 (td, *J* = 7.7, 1.4 Hz, 1H, H4''), 5.44 (s, 4H, 2(NH_2)), 5.06 (s, 2H, H3'), 3.19 (h, *J* = 6.8 Hz, 1H, H7), 1.12 (d, *J* = 6.9 Hz, 6H, H8). **^{13}C NMR** (101 MHz, $CDCl_3$) δ 177.8 (C6), 164.4 (C4), 161.2 (C2), 153.0 (C1''), 130.6 (C3''), 127.5 (C5''), 123.6 (C2''), 122.4 (C4''), 114.7 (C6''), 92.9 (C2'), 88.3 (C5), 81.5 (C1'), 57.9 (C2'), 33.5 (C7), 20.7 (C8); **HRMS** (ES$^+$) calculated for $C_{16}H_{17}ClN_4O$ [M + H]$^+$: 317.1164, found: 317.1184.

6.10.2.8 Synthesis of 5-[3-(2-fluorophenoxy)prop-1-yn-1-yl]-6-isopropyl pyrimidine-2,4-diamine 59h

5-Iodo-6-isopropylpyrimidine-2,4-diamine (1.00 g, 3.60 mmol), $Pd(PPh_3)_2Cl_2$ (0.25 g, 0.40 mmol), Cu(I)I (0.14 g, 0.70 mmol), DIIPA (24.0 ml, 0.20 mol) and 1-chloro-2-

(prop-2-yn-1-yloxy)benzene (1.08 g, 7.20 mmol) were dissolved in 12 ml DMF to produce the product **59h** as a dark brown solid (0.34 g, 32%).

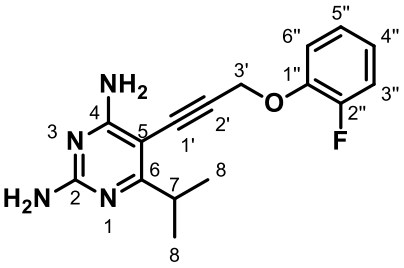

R*f* = 0.42 (1:9 MeOH/DCM); **mp**: 88 °C; **IR** (v/cm^{-1}): 3321 (NH str), 3180 (NH str), 2964 (CH); 2215 (C≡C), 1254 (C-O); **^{1}H NMR** (400 MHz, $CDCl_3$) δ 7.18 – 7.04 (m, 3H, H3'', H5'' & H6''), 7.03 – 6.89 (m, H4''), 5.20 (s, 2H, NH_2), 5.15 (s, 2H, NH_2), 5.06 (s, 2H, H3'), 3.19 (h, *J* = 6.8 Hz, 1H, H7), 1.14 (d, *J* = 6.8 Hz, 6H, H8); **^{13}C NMR** (101 MHz, $CDCl_3$) δ 177.3 (C6), 164.6 (C4), 161.1 (C2), 153.4 (d, $J_{C\text{-}F}$ = 245.8 Hz, C2''), 145.4 (d, $J_{C\text{-}F}$ = 10.6 Hz, C1''), 124.3 (d, $J_{C\text{-}F}$ = 3.7 Hz, C5''), 122.6 (d, $J_{C\text{-}F}$ = 7.0 Hz, C4''), 116.8 (d, $J_{C\text{-}F}$ = 1.8 Hz, C6''), 116.7 (d, $J_{C\text{-}F}$ = 18.7 Hz, C3''), 93.2 (C2'), 88.7 (C5), 81.4 (C1'), 58.5 (C3'), 33.5 (C7), 20.8 (C8); **HRMS** (ES$^+$) calculated for $C_{16}H_{17}FN_4O$ [M + H]$^+$: 301.1459, found: 301.1481.

6.10.2.9 Synthesis of 6-isopropyl-5-[3-(2-methoxyphenoxy)prop-1-yn-1-yl] pyrimidine-2,4-diamine 59i

The general procedure was followed to synthesise 6-isopropyl-5-[3-(2-methoxyphenoxy]prop-1-yn-1-yl)pyrimidine-2,4-diamine by subjecting 5-iodo-6-isopropylpyrimidine-2,4-diamine (1.00 g, 3.60 mmol) to Sonogashira reaction conditions in the presence of 1-methoxy-2-(prop-2-yn-1-yloxy)benzene (1.17g, 7.20 mmol), $Pd(PPh_3)_2Cl_2$ (0.25 g, 0.40 mmol), Cu(I)I (0.14 g, 0.70 mmol) and DIIPA (24.0 ml, 0.17 mol) as a base. The reagents were dissolved in 12 ml DMF. 0.26 g of the product **59i** was isolated as a light brown solid (23%).

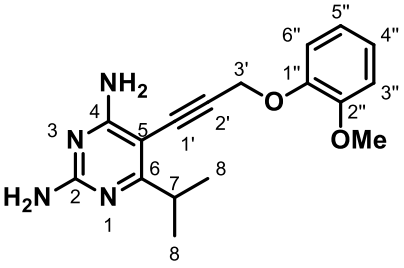

R*f* = 0.53 (1:9 MeOH/DCM); **mp**: 205 °C; **IR** (v/cm^{-1}): 3327 (NH str), 3145 (NH str), 2960 (CH); 2208 (C≡C), 1627 (NH bend), 1244 (C-O); **^{1}H NMR** (400 MHz, $CDCl_3$) δ 7.09 (dd, *J* = 8.1, 1.7 Hz, 1H, H6''), 7.01 – 6.95 (m, 1H, H4''), 6.94 – 6.88 (m, 2H, H3'' & H5''), 5.16 (s, 2H, NH_2), 5.09 (s, 2H, NH_2), 5.06 (s, 2H, H3'), 3.88 (s, 3H, OMe), 3.20 (h, *J* = 6.8 Hz, 1H, H7), 1.13 (d, *J* = 6.8 Hz, 6H, H8); **^{13}C NMR** (101 MHz, $CDCl_3$) δ 177.5 (C6), 164.6 (C4), 161.2 (C2), 150.1 (C2''), 146.7 (C1''), 122.4 (C4''), 120.7 (C5''), 114.9 (C6''), 112.0 (C3''), 93.7 (C2'), 88.9 (C5), 81.1(C1'), 57.9

(C3'), 56.0 (OMe), 33.5 (C7), 20.8 (C8); **HRMS** (ES^+) calculated for $C_{17}H_{20}N_4O_2$ $[M + H]^+$: 313.1659, found: 313.1683.

6.11 General Procedure for the hydrogenation reaction

6.11.1 Reduction of the 6-(*tert*-butyl)pyrimidine-2,4-diamine analogues

6.11.1.1 Synthesis of 6-(*tert*-butyl)-5-[3-(4-chlorophenoxy)propyl] pyrimidine-2,4-diamine 60a and (*Z*)-6-(*tert*-butyl)-5-[3-(4-chlorophenoxy)prop-1-en-1-yl]pyrimidine-2,4-diamine 61a

Hydrogenation reaction of 6-(*tert*-butyl)-5-[3-(4-chlorophenoxy)prop-1-yn-1-yl]pyrimidine-2,4-diamine **58a** (0.24 g, 0.70 mmol) was carried out at under set pressure in a hydrogenator apparatus. The starting material was dissolved in 4 ml Abs. EtOH followed by addition of Pd/C (23.6 mg, 0.20 mmol). The heterogeneous mixture was stirred under H_2 gas at 2 Bars degassed overnight. The reaction mixture was filtered through celite to remove the catalyst and the solvent was evaporated on the rotary evaporator. The resulting residue was further purified by silica gel column chromatography (5% MeOH/DCM) to produce (*Z*)-6-(*tert*-butyl)-5-[3-(4-chlorophenoxy)prop-1-en-1-yl]pyrimidine-2,4-diamine **61a** (0.13 g, 56 %) as a light brown viscous oil and 6-(*tert*-butyl)-5-[3-(4-chlorophenoxy)propyl]pyrimidine-2,4-diamine **60a** (50.0 mg, 21%) as a brown solid, respectively.

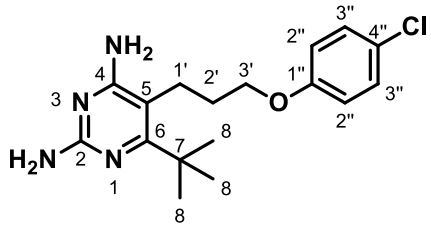

R*f* = 0.40 (1:9 MeOH/DCM); **mp**: 118 °C **IR** (v/cm^{-1}): 3323 (NH str), 3185 (NH str), 2954 (CH), 1601 (NH bend), 1240 (C-O); **^{1}H NMR** (400 MHz, $CDCl_3$) δ 7.26 – 7.21 (m, 2H, H3''), 6.85 – 6.80 (m, 2H, H2''), 4.98 (s, 2H, NH_2), 4.61 (s, 2H, NH_2), 4.02 (t, *J* = 5.5 Hz, 2H, H3'), 2.85 – 2.67 (m, 2H, H1'), 1.99 (tt, *J* = 11.1, 5.6 Hz, 2H, H2'), 1.34 (s, 9H, H8); **^{13}C NMR** (101 MHz, $CDCl_3$) δ 173.2 (C6), 163.9 (C4), 160.0 (C2), 157.4 (C1''), 129.6 (C3''), 126.1 (C4''), 115.8 (C2''), 104.7 (C5), 68.1 (C3'), 38.6 (C7), 30.5 (C8), 28.4 (C2'), 23.5 (C1'); **HRMS** (ES^+) calculated for $C_{17}H_{23}ClN_4O$ $[M + H]^+$: 335.1633, found: 335.1573.

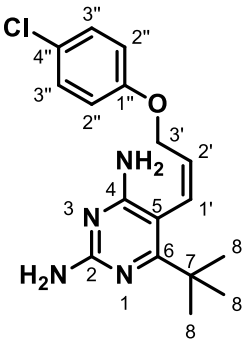

R*f* = 0.54 (1:9 MeOH/DCM); **IR** (v/cm^{-1}): 3356 (NH str), 3199 (NH str), 3023 (=CH), 2958 (CH), 1541 (C=C); **^{1}H NMR** (300 MHz, $CDCl_3$) δ 7.23 – 7.16 (m, 2H, H3''), 6.80 – 6.71 (m, 2H, H2''), 6.62 (dt, *J* = 10.9, 1.4 Hz, 1H, H1'), 6.08 (dt, *J* = 11.0, 6.3 Hz, 1H, H2'), 4.81 (s, 2H, NH_2), 4.73 (s, 2H, NH_2), 4.37 (d, *J* = 6.1 Hz, 2H, H3'), 1.27 (s, 9H, H8); **^{13}C NMR** (75 MHz, $CDCl_3$) δ 174.0 (C6), 161.8 (C4), 161.0 (C2), 157.2 (C1''), 130.2 (C2'), 129.5 (C3''), 128.6 (C1'), 126.0 (C4''), 116.0 (C2''), 101.0 (C5), 65.7 (C3'), 38.9 (C7), 29.3 (C8); **HRMS** (ES^+) calculated for $C_{17}H_{21}ClN_4O$ $[M + H]^+$: 333.1477, found: 333.1437.

6.11.1.2 Synthesis of (*Z*)-6-(*tert*-butyl)-5-[3-(4-fluorophenoxy)prop-1-en-1-yl]pyrimidine-2,4-diamine 61b

The starting material, 5-[3-(4-fluorophenoxy)prop-1-yn-1-yl]-6-isopropylpyrimidine-2,4-diamine (0.19 g, 0.60 mmol), was dissolved in 4 ml Abs. EtOH in the presence of Pd/C (19.0 mg, 0.20 mmol). The reaction was conducted under pressure in H_2 atmosphere to produce *(Z)*-6-(*tert*-butyl)-5-[3-(4-fluorophenoxy)prop-1-en-1-yl]pyrimidine-2,4-diamine **61b** (25.0 mg, 13%) as a cream white solid.

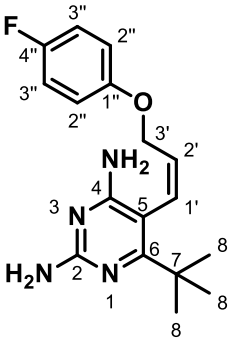

R*f* = 0.47 (1:9 MeOH/DCM); **mp**: 84 °C; **IR** (v/cm^{-1}): 3302 (NH str), 3190 (NH str), 2958 (CH), 1611 (NH bend), 1541 (C=C); **^{1}H NMR** (500 MHz, $CDCl_3$) δ 6.93 (t, *J* = 8.6 Hz, 2H, H3''), 6.78 (dd, *J* = 8.9, 4.2 Hz, 2H, H2''), 6.61 (d, *J* = 11.0 Hz, 1H, H1'), 6.09 (dt, *J* = 11.5, 6.3 Hz, 1H, H2'), 4.80 (s, 2H, NH_2), 4.69 (s, 2H, NH_2), 4.36 (d, *J* = 5.6 Hz, 2H, H3'), 1.28 (s, 9H, H8); **^{13}C NMR** (126 MHz, $CDCl_3$) δ 173.8 (C6), 162.0 (C4), 160.9 (C2), 157.6 (d, $J_{C\text{-}F}$ = 238.4 Hz, C4''), 154.8 (d, $J_{C\text{-}F}$ = 2.3 Hz, C1''), 130.5 (C2'), 128.4 (C1'), 116.0 (d, $J_{C\text{-}F}$ = 23.1 Hz, C3''), 115.9 (d, $J_{C\text{-}F}$ = 8.1 Hz, C2''), 101.1 (C5), 66.1 (C3'), 38.9 (C7), 29.4 (C8); **HRMS** (ES^+) calculated for $C_{17}H_{21}FN_4O$ $[M + H]^+$: 317.1772, found: 317.1734.

6.11.1.3 Synthesis of 6-(*tert*-butyl)-5-[3-(4-methoxyphenoxy)propyl] pyrimidine-2,4-diamine 60c and (*Z*)-6-(*tert*-butyl)-5-[3-(4-methoxyphenoxy)prop-1-en-1-yl] pyrimidine-2,4-diamine 61c

The general procedure described above was followed by subjecting 6-(*tert*-butyl)-5-[3-(4-methoxyphenoxy)prop-1-yn-1-yl] pyrimidine-2,4-diamine (0.17 g, 0.50 mmol) to a

reduction reaction in the presence of Pt(IV)O_2 (16.9 mg, 74.4 µmol) as a catalyst in 8 ml Abs. EtOH. *(Z)*-6-(*Tert*-butyl)-5-[3-(4-methoxyphenoxy)prop-1-en-1-yl]pyrimidine-2,4-diamine **61c** (41.0 mg, 24%) and 6-(*tert*-butyl)-5-[3-(4-methoxyphenoxy) propyl] pyrimidine-2,4-diamine **60c** (24.0 mg, 14%) were isolated as a light brown viscous oil and a cream white solid respectively.

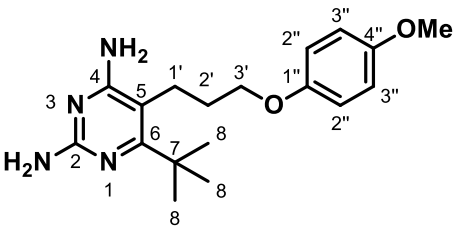

R*f* = 0.23 (1:9 MeOH/DCM); **mp**: 106 °C; **IR** (v/cm^{-1}): 3330 (NH str), 3165 (NH str), 2956 (CH), 1655 (NH bend);**^{1}H NMR** (300 MHz, $CDCl_3$) δ 6.85 (s, 4H, H2'' & H3''), 5.01 (s, 2H, NH_2), 4.54 (s, 2H, NH_2), 4.00 (t, *J* = 5.4 Hz, 2H, H3'), 3.77 (s, 3H, OMe), 2.85 – 2.67 (m, 2H, H1'), 1.97 (tt, *J* = 11.1, 5.5 Hz, 2H, H2'), 1.35 (s, 9H, H8); **^{13}C NMR** (75 MHz, $CDCl_3$) δ 173.0 (C6), 164.0 (C4), 160.0 (C2), 154.2 (C4''), 152.9 (C1''), 115.6 (C2''/C3''), 114.9 (C2''/C3''), 105.0 (C5), 68.4 (C3'), 55.9 (OMe), 38.6 (C7), 30.5 (C8), 28.7 (C2'), 23.4 (C1'); **HRMS** (ES$^+$) calculated for $C_{18}H_{26}N_4O_2$ [M + H]$^+$: 331.2129, found: 331.2083.

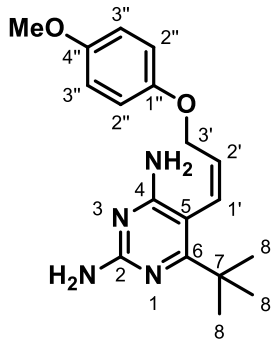

R*f* = 0.42 (1:9 MeOH/DCM); **IR** (v/cm^{-1}): 3310 (NH str), 3189 (NH str), 2999 (=CH), 2955 (CH), 1609 (NH bend), 1539 (C=C); **^{1}H NMR** (400 MHz, $CDCl_3$) δ 6.79 (s, 4H, H2'' & H3''), 6.59 (d, *J* = 10.9 Hz, 1H, H1'), 6.09 (dt, *J* = 11.3, 6.3 Hz, 1H, H2'), 4.80 (d, *J* = 10.7 Hz, 2H, NH_2), 4.67 (d, *J* = 13.5 Hz, 2H, NH_2), 4.36 (d, *J* = 6.0 Hz, 2H, H3'), 3.75 (s, 3H, OMe), 1.27 (s, 9H, H8); **^{13}C NMR** (101 MHz, $CDCl_3$) δ 173.9 (C6), 162.0 (C4), 161.1 (C2), 154.3 (C4''), 152.8 (C1''), 130.8 (C2'), 128.3 (C1'), 116.0 (C2''), 114.8 (C3''), 101.2 (C5), 66.3 (C3'), 55.9 (OMe), 38.9 (C7), 29.4 (C8); **HRMS** (ES$^+$) calculated for $C_{18}H_{24}N_4O_2$ [M + H]$^+$: 329.1972, found: 329.1924.

6.11.1.4 Synthesis of 6-(*tert*-butyl)-5-[3-(3-chlorophenoxy)propyl] pyrimidine-2,4-diamine 60d and (Z)-6-(*tert*-butyl)-5-[3-(3-chlorophenoxy) prop-1-en-1-yl] pyrimidine-2,4-diamine 61d

A heterogeneous mixture of 6-(*tert*-butyl)-5-[3-(3-chlorophenoxy)prop-1-yn-1-yl] pyrimidine-2,4-diamine (0.23 g, 0.70 mmol) and Pd/C (23.1 mg, 0.20 mmol) in 4 ml Abs. EtOH produced (*Z*)-6-(*tert*-butyl)-5-[3-(3-chlorophenoxy)prop-1-en-1-

yl]pyrimidine-2,4-diamine **61d** (50.0 mg, 22%) and 6-(*tert*-butyl)-5-[3-(3-chlorophenoxy)propyl]pyrimidine-2,4-diamine **60d** (31.0 mg, 13%) as a brown solid and yellow viscous oil respectively.

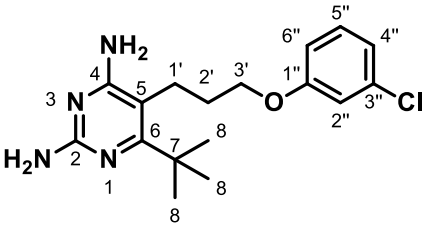

R*f* = 0.25 (1:9 MeOH/DCM); **IR** (v/cm^{-1}): 3342 (NH str), 2942 (CH), 1609 (NH bend), 1247 (C-O); **^{1}H NMR** (300 MHz, $CDCl_3$) δ 7.22 (t, *J* = 8.1 Hz, 1H, H5''), 6.96 (ddd, *J* = 8.1, 2.0, 0.9 Hz, 1H, H4''), 6.92 (t, *J* = 2.1 Hz, 1H, H2''), 6.80 (ddd, *J* = 8.4, 2.6, 1.7 Hz, 1H, H6''), 4.95 (s, 2H, NH_2), 4.59 (s, 2H, NH_2), 4.04 (t, *J* = 5.5 Hz, 2H, H3'), 2.86 – 2.67 (m, 2H, H1'), 2.02 (dt, *J* = 10.8, 5.7 Hz, 2H, H2'), 1.35 (s, 9H. H8); **^{13}C NMR** (75 MHz, $CDCl_3$) δ 173.3 (C6), 163.8 (C4), 159.8 (C2), 159.5 (C1''), 135.1 (C3''), 130.5 (C5''), 121.4 (C4''), 115.0 (C2''), 113.1 (C6''), 104.7 (C5), 68.0 (C3'), 38.7 (C7), 30.5 (C8), 28.3 (C2'), 23.5 (C1'); **HRMS** (ES^+) calculated for $C_{17}H_{23}ClN_4O$ $[M + H]^+$: 335.1633, found: 335.1579.

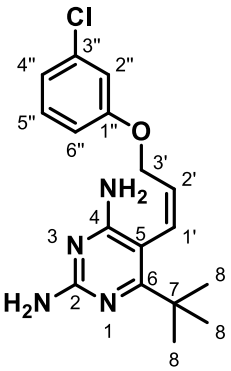

R*f* = 0.54 (1:9 MeOH/DCM); **mp**: 86 °C; **IR** (v/cm^{-1}): 3304 (NH str), 3190 (NH str), 3030 (=CH), 2957 (CH), 1611 (NH bend), 1538 (C=C); **^{1}H NMR** (400 MHz, $CDCl_3$) δ 7.15 (t, *J* = 8.1 Hz, 1H, H5''), 6.91 (d, *J* = 7.5 Hz, 1H, H4''), 6.83 (s, 1H, H2''), 6.72 (dd, *J* = 8.3, 2.0 Hz, 1H, H6''), 6.62 (d, *J* = 10.9 Hz, 1H, H1'), 6.07 (dt, *J* = 12.3, 6.3 Hz, 1H, H2'), 4.95 (s, 2H, NH_2), 4.86 (s, 2H, NH_2), 4.46 – 4.28 (m, 2H, H3'), 1.27 (s, 9H, H8); **^{13}C NMR** (101 MHz, $CDCl_3$) δ 173.9 (C6), 161.8 (C4), 160.9 (C2), 159.3 (C1''), 135.0 (C3''), 130.3 (C5''), 130.0 (C2'), 128.7 (C1'), 121.3 (C4''), 115.1 (C2''), 113.2 (C6''), 100.9 (C5), 65.5 (C3'), 38.9 (C7), 29.3 (C8); **HRMS** (ES^+) calculated for $C_{17}H_{21}ClN_4O$ $[M + H]^+$: 333.1477, found: 333.1404.

6.11.1.5 Synthesis of (Z)-6-(*tert*-butyl)-5-[3-(3-fluorophenoxy)prop-1-en-1-yl] pyrimidine-2,4-diamine 61e

To a solution of 6-(*tert*-butyl)-5-[3-(3-fluorophenoxy)prop-1-yn-1-yl]pyrimidine-2,4-diamine (0.10 g, 0.30 mmol) in 4 ml Abs. EtOH, Pd/C (10.0 mg, 94.0 µmol) was added. The reaction mixture was stirred under H_2 gas to afford (*Z*)-6-(*tert*-butyl)-5-[3-(3-

fluorophenoxy)prop-1-en-1-yl]pyrimidine-2,4-diamine **61e** as a white solid (19.0 mg, 18%).

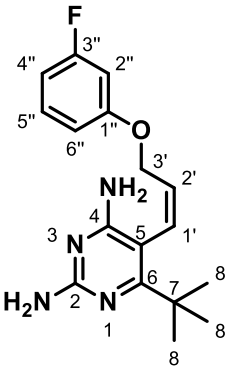

R*f* =0.48 (1:9 MeOH/DCM); **mp**: 101 °C; **IR** (v/cm^{-1}): 3301 (NH str), 3189 (NH str), 3046 (=CH), 2956 (CH), 1610 (NH bend), 1536 (C=C); **^{1}H NMR** (400 MHz, $CDCl_3$) δ 7.18 (dd, *J* = 8.2, 8.2 Hz, 1H, H5''), 6.68 – 6.59 (m, 3H, H2'', H4'' & 6''), 6.55 (dt, *J* = 10.9, 2.3 Hz, 1H, H1''), 6.08 (dt, *J* = 11.0, 6.3 Hz, 1H, H2'), 4.80 (s, 2H, NH_2), 4.70 (s, 2H, NH_2), 4.38 (d, *J* = 5.2 Hz, 2H, H3'), 1.27 (s, 9H, H8); **^{13}C NMR** (101 MHz, $CDCl_3$) δ 173.9 (C6), 163.7 (d, $J_{C\text{-}F}$ = 245.4 Hz, C3''), 161.9 (C4), 161.1 (C2), 160.0 (d, $J_{C\text{-}F}$ = 10.8 Hz, C1''), 130.4 (d, $J_{C\text{-}F}$ = 10.0 Hz, C5''), 130.0 (C2'), 128.8 (C1'), 110.4 (d, $J_{C\text{-}F}$ = 2.9 Hz, C6''), 108.0 (d, $J_{C\text{-}F}$ = 21.3 Hz, C2''), 102.6 (d, $J_{C\text{-}F}$ = 24.8 Hz, C4''), 101.0 (C5), 65.6 (C3'), 38.9 (C7), 29.3 (C8); **HRMS** (ES^+) calculated for $C_{17}H_{21}FN_4O$ $[M + H]^+$: 317.1772, found: 317.1731.

6.11.1.6 Synthesis of (Z)-6-(*tert*-butyl)-5-[3-(3-methoxyphenoxy)prop-1-en-1-yl]pyrimidine-2,4-diamine 61f

A solution of 6-(*tert*-butyl)-5-[3-(3-methoxyphenoxy)prop-1-yn-1-yl]pyrimidine-2,4-diamine (0.12 g, 0.40 mmol) in 4 ml Abs. EtOH, was subjected to a hydrogenation reaction in the presence of Pd/C (6.50 mg, 61.1 µmol) as a catalyst. The product, (*Z*)-6-(*tert*-butyl)-5-[3-(3-methoxyphenoxy)prop-1-en-1-yl]pyrimidine-2,4-diamine **61f**, was isolated as a light brown solid (94.0 mg) in 76% yield.

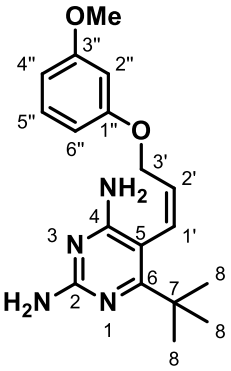

R*f* = 0.53 (1:9 MeOH/DCM); **mp**: 77 °C; **IR** (v/cm^{-1}): 3300 (NH str), 3193 (NH str), 2958 (CH), 1608 (NH bend), 1537 (C=C); **^{1}H NMR** (400 MHz, $CDCl_3$) δ 7.14 (t, *J* = 8.2 Hz, 1H, H5''), 6.60 (dt, *J* = 10.9, 1.4 Hz, 1H, H1'), 6.50 (dd, *J* = 8.2, 1.8 Hz, 1H, H6''), 6.44 (dd, *J* = 8.1, 1.9 Hz, 1H, H4''), 6.41 (t, *J* = 2.3 Hz, 1H, H2''), 6.09 (dt, *J* = 11.0, 6.3 Hz, 1H, H2'), 4.88 (s, 2H, NH_2), 4.76 (s, 2H, NH_2), 4.39 (d, *J* = 5.9 Hz, 2H, H3'), 3.76 (s, 3H, OMe), 1.28 (s, 9H, H8); **^{13}C NMR** (101 MHz, $CDCl_3$) δ 173.8 (C6), 161.9 (C4), 161.0 (C2), 160.9 (C3''), 159.9 (C1''), 130.5 (C2'), 130.0 (C5''), 128.4 (C1'), 106.9 (C4''), 106.6 (C6''), 101.3 (C2''), 101.1

(C5), 65.4 (C3'), 55.4 (OMe), 38.9 (C7), 29.3 (C8); **HRMS** (ES^+) calculated for $C_{18}H_{24}N_4O_2$ $[M + H]^+$: 329.1972, found: 329.1932.

6.11.1.7 Synthesis of (Z)-6-(*tert*-butyl)-5-[3-(2-chlorophenoxy)prop-1-en-1-yl]pyrimidine-2,4-diamine 61g

(*Z*)-6-(*tert*-Butyl)-5-[3-(2-chlorophenoxy)prop-1-en-1-yl]pyrimidine-2,4-diamine was produced by means of reducing 6-(*tert*-butyl)-5-[3-(2-chlorophenoxy)prop-1-yn-1-yl] pyrimidine-2,4-diamine. The starting material (0.10 g, 0.30 mmol) was subjected to a reduction reaction in the presence of Pd/C (10.0 mg, 94.0 µmol). The reaction mixture was dissolved in 4 ml Abs. EtOH to afford the product **61g** as an amber brown solid (70.0 mg, 69%)

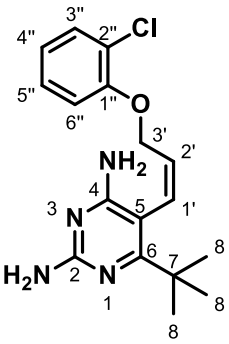

R*f* =0.65 (1:9 MeOH/DCM); **mp**: 74 °C; **IR** (v/cm^{-1}): 3307 (NH str), 3188 (NH str),3015 (=CH), 2958 (CH), 1610 (NH bend), 1536 (C=C); **^{1}H NMR** (300 MHz, $CDCl_3$) δ 7.32 (dd, *J* = 7.8, 1.4 Hz, 1H, H3''), 7.21 – 7.08 (m, 1H, H5''), 6.92 – 6.79 (m, 2H, H4'' & H6''), 6.64 (d, *J* = 11.0 Hz, 1H, H1'), 6.15 (dt, *J* = 11.0, 6.5 Hz, 1H, H2'), 4.99 (s, 2H, NH_2), 4.86 (s, 2H, NH_2), 4.45 (d, *J* = 6.4 Hz, 2H, H3'), 1.27 (s, 9H, H8); **^{13}C NMR** (75 MHz, $CDCl_3$) δ 173.9 (C6), 161.9 (C4), 161.0 (C2), 154.1 (C1''), 130.4 (C3''), 129.8 (C2'), 129.1 (C1'), 127.8 (C5''), 123.0 (C2''), 121.9 (C4''), 114.0 (C6''), 100.8 (C5), 66.3 (C3'), 38.9 (C7), 29.3 (C8); **HRMS** (ES^+) calculated for $C_{17}H_{21}ClN_4O$ $[M + H]^+$: 333.1477, found: 333.1424.

6.11.1.8 Synthesis of (Z)-6-(*tert*-butyl)-5-[3-(2-fluorophenoxy)prop-1-en-1-yl]pyrimidine-2,4-diamine 61h

6-(*tert*-Butyl)-5-[3-(2-fluorophenoxy)prop-1-yn-1-yl]pyrimidine-2,4-diamine (0.10 g, 0.30 mmol) was subjected to a reduction reaction in the presence of Pd/C (10.0 mg, 94.0 µmol) and 4 ml Abs. EtOH as a solvent to afford (*Z*)-6-(*tert*-butyl)-5-[3-(2-fluorophenoxy)prop-1-en-1-yl]pyrimidine-2,4-diamine **61h** (58.0 mg) as a light brown solid in 58% yield.

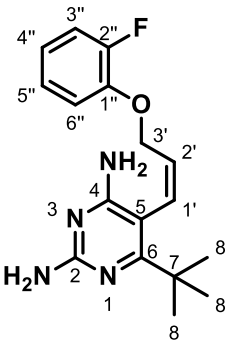

R*f* =0.50 (1:9 MeOH/DCM); **mp**: 87 °C; **IR** (v/cm^{-1}): 3301 (NH str), 3191 (NH str), 3031 (=CH), 2957 (CH), 1611 (NH bend), 1536 (C=C); **^{1}H NMR** (400 MHz, $CDCl_3$) δ 7.09 – 6.95 (m, 2H, H3'' & H5''), 6.92 – 6.83 (m, 2H, H4'' & H6''), 6.63 (d, *J* = 11.0 Hz, 1H, H1'), 6.14 (dt, *J* = 11.0, 6.4 Hz, 1H, H2'), 4.92 (s, 2H, NH_2), 4.80 (s, 2H, NH_2), 4.46 (d, *J* = 5.9 Hz, 2H, H3'), 1.26 (s, 9H, H8); **^{13}C NMR** (101 MHz, $CDCl_3$) δ 173.9 (C6), 161.9 (C4), 161.1 (C2), 152.9 (d, $J_{C\text{-}F}$ = 245.4 Hz, C2''), 146.7 (d, $J_{C\text{-}F}$ = 10.6 Hz, C1''), 130.1 (C2'), 128.9 (C1'), 124.4 (d, $J_{C\text{-}F}$ = 4.0 Hz, C5''), 121.7 (d, $J_{C\text{-}F}$ = 7.0 Hz, C4''), 116.3 (d, $J_{C\text{-}F}$ = 18.0 Hz, C3''), 115.6 (d, $J_{C\text{-}F}$ = 1.8 Hz, C6''), 100.9 (C5), 66.8 (C3'), 38.9 (C7), 29.3 (C8); **HRMS** (ES^+) calculated for $C_{17}H_{21}FN_4O$ $[M + H]^+$: 317.1772, found: 317.1732.

6.11.1.9 Synthesis of (Z)-6-(*tert*-butyl)-5-[3-(2-methoxyphenoxy)prop-1-en-1-yl]pyrimidine-2,4-diamine 61i

Pd/C (10.0 mg, 94.0 µmol) was added to a solution of 6-(*tert*-butyl)-5-[3-(2-methoxyphenoxy)prop-1-yn-1-yl]pyrimidine-2,4-diamine (0.10 g, 0.30 mmol) in 4 ml Abs. EtOH to produce (*Z*)-6-(*tert*-butyl)-5-[3-(2-methoxyphenoxy)prop-1-en-1-yl] pyrimidine-2,4-diamine **61i** (72.0 mg) as a light brown viscous oil in 71% yield.

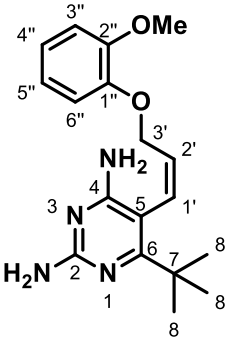

R*f* =0.16 (1:9 MeOH/DCM); **IR** (v/cm^{-1}): 3371 (NH str), 3188 (NH str), 3077 (=CH), 2956(CH), 1540 (C=C); **^{1}H NMR** (300 MHz, $CDCl_3$) δ 6.97 – 6.77 (m, 4H, H3'', H4'', H5'' & H6''), 6.58 (d, *J* = 11.0 Hz, 1H, H1'), 6.17 (dt, *J* = 11.1, 6.3 Hz, 1H, H2'), 4.97 (s, 2H, NH_2), 4.85 (s, 2H, NH_2), 4.45 (d, *J* = 6.0 Hz, 2H. H3'), 3.83 (s, 3H, OMe), 1.27 (s, 9H, H8); **^{13}C NMR** (75 MHz, $CDCl_3$) δ 173.5 (C6), 161.9 (C4), 160.8 (C2), 149.7 (C2''), 148.0 (C1''), 131.0 (C2'), 128.1 (C1'), 121.8 (C4''), 120.9 (C5''), 114.3 (C6''), 111.9 (C3''), 101.1 (C5), 66.6 (C3'), 55.9 (OMe), 38.8 (C7), 29.3 (C8); **HRMS** (ES^+) calculated for $C_{18}H_{24}N_4O_2$ $[M + H]^+$: 329.1972, found: 329.1928.

6.11.2 Reduction of the 6-(isopropyl)pyrimidine-2,4-diamine analogues

6.11.2.1 Synthesis of 5-[3-(4-chlorophenoxy)propyl]-6-isopropylpyrimidine-2,4-diamine 62a

The starting material, 5-[3-(4-chlorophenoxy)prop-1-yn-1-yl]-6-isopropylpyrimidine-2,4-diamine (62.0 mg, 0.20 mmol), was dissolved in 4 ml Abs. EtOH in the presence of Pd/C (6.20 mg, 58.3 µmol). The reaction was conducted under pressure in H_2 atmosphere to produce 5-[3-(4-chlorophenoxy)propyl]-6-isopropylpyrimidine-2,4-diamine **62a** (30.0 mg, 48%) as a cream white solid.

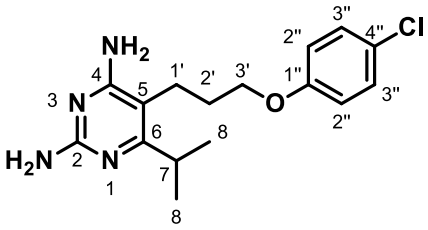

R*f* = 0.31 (1:9 MeOH/DCM); **mp**: 114 °C; **IR** (v/cm^{-1}): 3368 (NH str), 3179 (NH str) 2955 (CH), 1616 (NH bend), 1255 (C-O);**^{1}H NMR** (300 MHz, $CDCl_3$) δ 7.25 – 7.19 (m, 2H, H3''), 6.88 – 6.70 (m, 2H, H2''), 4.91 (s, 2H, NH_2), 4.78 (s, 2H, NH_2), 3.93 (t, *J* = 5.6 Hz, 2H, H3'), 3.06 (h, *J* = 6.7 Hz, 1H, H7), 2.58 (t, *J* = 7.3 Hz, 2H, H1'), 1.93 (p, *J* = 6.5 Hz, 2H, H2'), 1.15 (d, *J* = 6.7 Hz, 6H, H8); **^{13}C NMR** (75 MHz, $CDCl_3$) δ 172.4 (C6), 163.1 (C4), 161.1 (C2), 157.2 (C1''), 129.6 (C3''), 126.1 (C4''), 115.9 (C2''), 103.0 (C5), 66.8 (C3'), 30.3 (C7), 29.0 (C2'), 21.7 (C8), 21.2 (C1'); **HRMS** (ES^+) calculated for $C_{16}H_{21}ClN_4O$ $[M + H]^+$: 321.1477, found: 321.1499.

6.11.2.2 Synthesis of 5-[3-(4-fluorophenoxy)propyl]-6-isopropylpyrimidine-2,4-diamine 62b

The general procedure described above was followed by subjecting 5-[3-(4-fluorophenoxy)prop-1-yn-1-yl]-6-isopropylpyrimidine-2,4-diamine (55.7 mg, 0.20 mmol) to a reduction reaction in the presence of Pd/C (5.60 mg, 52,6 µmol) as a catalyst in 4 ml Abs. EtOH. 5-[3-(4-Fluorophenoxy)propyl]-6-isopropylpyrimidine-2,4-diamine **62b** (54.0 mg, 96%) was isolated as a yellow solid.

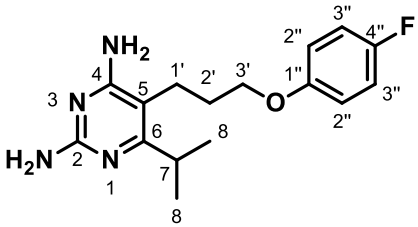

R*f* =0.39 (1:9 MeOH/DCM); **mp**: 72 °C; **IR** (v/cm^{-1}): 3333 (NH str), 3192 (NH str) 2966 (CH), 1617 (NH bend), 1248 (C-O);**^{1}H NMR** (400 MHz, $CDCl_3$) δ 7.04 – 6.92 (m, 2H, C3''), 6.88 – 6.79 (m, 2H, C2''), 5.07 (s,

2H, NH_2), 4.99 (s, 2H, NH_2), 3.92 (t, *J* = 5.5 Hz, 2H, H3'), 3.06 (h, *J* = 6.7 Hz, 1H, H7), 2.58 (t, *J* = 7.3 Hz, 2H, H1'), 1.92 (p, *J* = 7.1 Hz, 2H, H2'), 1.15 (d, *J* = 6.8 Hz, 6H, H8); **^{13}C NMR** (101 MHz, $CDCl_3$) δ 172.0 (C6), 163.1 (C4), 160.9 (C2), 157.5 (d, J_{C-F} = 238.4 Hz, C4''), 154.7 (d, J_{C-F} = 2.2 Hz,C1''), 116.1 (d, J_{C-F} = 23.1 Hz, C3''), 115.6 (d, J_{C-F} = 8.1 Hz, C2''), 103.1 (C5), 67.1 (C3'), 30.3 (C7), 29.0 (C2'), 21.6 (C9), 21.2 (C1'); **HRMS** (ES^+) calculated for $C_{16}H_{21}FN_4O$ $[M + H]^+$: 305.1772, found: 305.1789.

6.11.2.3 Synthesis of 6-isopropyl-5-[3-(4-methoxyphenoxy)propyl] pyrimidine-2,4-diamine 62c

A heterogeneous mixture of 6-isopropyl-5-[3-(4-methoxyphenoxy)prop-1-yn-1-yl] pyrimidine-2,4-diamine (50.0 mg, 0.20 mmol) and Pd/C (5.00 mg, 47.0 µmol) in 4 ml Abs. EtOH produced 6-isopropyl-5-[3-(4-methoxyphenoxy)propyl]pyrimidine-2,4-diamine **62c** (41.0 mg, 81%) as an off-white solid.

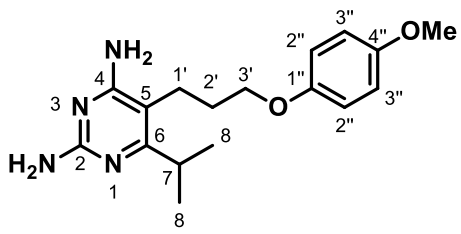

R*f* = 0.22 (1:9 MeOH/DCM); **mp**: 61 °C; **IR** (v/cm^{-1}): 3335 (NH str), 3234 (NH str) 2959 (CH), 1615 (NH bend), 1264 (C-O);**^{1}H NMR** (400 MHz, $CDCl_3$) δ 6.83 (s, 4H, H2'' & H3''), 4.94 (s, 2H, NH_2), 4.69 (s, 2H, NH_2), 3.91 (t, *J* = 5.5 Hz, 2H, H3'), 3.76 (s, 3H, OMe), 3.06 (p, *J* = 6.7 Hz, 1H, H7), 2.59 (t, *J* = 7.3 Hz, 2H, H1'), 1.91 (h, *J* = 7.1 Hz, 2H, H2'), 1.15 (d, *J* = 6.7 Hz, 6H, H8); **^{13}C NMR** (101 MHz, $CDCl_3$) δ 172.4 (C6), 163.2 (C4), 161.3 (C2), 154.2 (C4''), 152.7 (C1''), 115.6 (C2''), 114.9 (C3''), 103.2 (C5), 67.0 (C3'), 55.8 (OMe), 30.3 (C7), 29.2 (C2'), 21.7 (C8), 21.2 (C1'); **HRMS** (ES^+) calculated for $C_{17}H_{24}N_4O_2$ $[M + H]^+$: 317.1972, found: 317.1988.

6.11.2.4 Synthesis of 5-[3-(3-chlorophenoxy)propyl]-6-isopropylpyrimidine-2,4-diamine 62d

To a solution of 5-[3-(3-chlorophenoxy)prop-1-yn-1-yl]-6-isopropylpyrimidine-2,4-diamine (11.0 mg g, 34.7 µmol) in 4 ml Abs. EtOH, Pd/C (1.10 mg, 10.3 µmol) was added. The reaction mixture was stirred under H_2 gas to afford 5-[3-(3-chlorophenoxy)propyl]-6-isopropylpyrimidine-2,4-diamine **62d** as a cream white solid (10.0 mg, 90%).

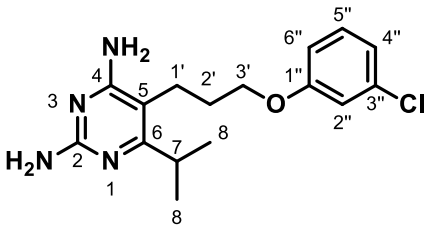

R*f* = 0.30 (1:9 MeOH/DCM); **mp**: 119 °C; **IR** (v/cm^{-1}): 3329 (NH str), 3157 (NH str) 2962 (CH), 1624 (NH bend), 1229(C-O);**^{1}H NMR** (400 MHz, $CDCl_3$) δ 7.21 (t, *J* = 8.1 Hz, 1H, H5''), 6.96 (ddd, *J* = 8.0, 1.9, 0.9 Hz, 1H, H4''), 6.90 (t, *J* = 2.2 Hz, 1H, H2''), 6.79 (ddd, *J* = 8.3, 2.5, 0.8 Hz, 1H, H6''), 6.08 – 5.58 (m, 2H, NH_2), 5.43 (s, 2H, NH_2), 3.97 (t, *J* = 5.5 Hz, 2H, H3'), 3.08 (h, *J* = 6.8 Hz, 1H, H7), 2.58 (t, *J* = 7.4 Hz, 2H, H1'), 1.93 (p, *J* = 6.5 Hz, 2H, H2'), 1.19 (d, *J* = 6.8 Hz, 6H, H8); **^{13}C NMR** (101 MHz, $CDCl_3$) δ 171.0 (C6), 162.8 (C4), 159.7 (C2), 159.3 (C1''), 135.2 (C3''), 130.5 (C5''), 121.6 (C4''), 115.1 (C2''), 113.1 (C6''), 103.0 (C5), 66.7 (C3'), 30.3 (C7), 28.8 (C2'), 21.3 (C8), 21.1 (C1'); **HRMS** (ES^+) calculated for $C_{16}H_{21}ClN_4O$ $[M + H]^+$: 321.1477, found: 321.1494.

6.11.2.5 Synthesis of 5-[3-(3-fluorophenoxy)propyl]-6-isopropylpyrimidine-2,4-diamine 62e

A solution of 5-[3-(3-fluorophenoxy)prop-1-yn-1-yl]-6-isopropylpyrimidine-2,4-diamine (67.0 mg, 0.20 mmol) in 4 ml Abs. EtOH, was subjected to a hydrogenation reaction in the presence of Pd/C (6.70 mg, 63.0 µmol) as a catalyst. The product, 5-[3-(3-fluorophenoxy)propyl]-6-isopropylpyrimidine-2,4-diamine **62e**, was isolated as a light yellow solid (51.0 mg) in 75% yield.

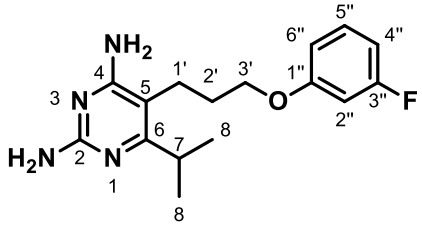

R*f* = 0.50 (1:9 MeOH/DCM); **m.p**: 68°C; **IR** (v/cm^{-1}): 3336 (NH str), 3238 (NH str) 2966 (CH), 1610 (NH bend), 1262 (C-O);**^{1}H NMR** (300 MHz, $CDCl_3$) δ 7.23 – 7.07 (m, 1H, H5''), 6.67 – 6.45 (m, 3H, H2'', H4'' & H6''), 4.88 (s, 2H, NH_2), 4.74 (s, 2H, NH_2), 3.88 (t, *J* = 5.6 Hz, 2H, H3'), 3.00 (h, *J* = 6.8 Hz, 1H, H7), 2.51 (t, *J* = 7.4 Hz, 2H, H1'), 1.87 (p, *J* = 6.4 Hz, 2H, H2'), 1.08 (d, *J* = 6.8 Hz, 6H, H8); **^{13}C NMR** (75 MHz, $CDCl_3$) δ 172.4 (C6), 163.7 (d, $J_{C\text{-}F}$ = 245.4 Hz, C3''), 163.1 (C4), 161.3 (C2), 160.0 (d, $J_{C\text{-}F}$ = 10.8 Hz. C1''), 130.5 (d, $J_{C\text{-}F}$ = 10.1 Hz, C5''), 110.4 (d, $J_{C\text{-}F}$ = 2.9 Hz, C6''), 108.0 (d, $J_{C\text{-}F}$ = 21.3 Hz, C4''), 103.0 (C5), 102.3 (d, $J_{C\text{-}F}$ = 24.8 Hz, C2'') , 66.8 (C3'), 30.3 (C7), 28.9 (C2'), 21.7 (C8), 21.2 (C1'); **HRMS** (ES^+) calculated for $C_{16}H_{21}FN_4O$ $[M + H]^+$: 305.1772, found: 305.1789.

6.11.2.6 Synthesis of 6-isopropyl-5-[3-(3-methoxyphenoxy)propyl] pyrimidine-2,4-diamine 62f and (Z)-6-isopropyl-5-[3-(3-methoxyphenoxy) prop-1-en-1-yl]pyrimidine -2,4-diamine 63f

The starting material, 6-isopropyl-5-[3-(3-methoxyphenoxy)prop-1-yn-1-yl]pyrimidine-2,4-diamine **59f** (70.0 mg, 0.20 mmol), was subjected to a reduction reaction in the presence of Pd/C (7.00 mg, 65.8 µmol). The reaction mixture was dissolved in ~10 ml Abs. EtOH to afford (Z)-6-isopropyl-5-[3-(3-methoxyphenoxy)prop-1-en-1-yl] pyrimidine-2,4-diamine **63f** and 6-isopropyl-5-[3-(3-methoxyphenoxy)propyl] pyrimidine-2,4-diamine **62f** as a brown solid (39.0 mg, 55%) and a light brown solid (16.0 mg, 23%) respectively.

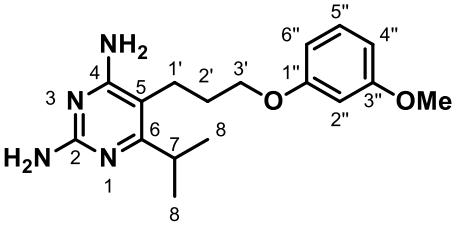

R*f* = 0.33 (1:9 MeOH/DCM); **mp**: 100 °C; **IR** (v/cm^{-1}): 3366 (NH str), 3171 (NH str) 2961 (CH), 1651 (NH bend), 1269 (C-O); **^{1}H NMR** (400 MHz, $CDCl_3$) δ 7.18 (t, *J* = 8.2 Hz, 1H, H5''), 6.57 – 6.40 (m, 3H, H2'', H4'' & H6''), 5.91 (s, 2H, NH_2), 5.63 (s, 2H, NH_2), 3.96 (t, *J* = 5.3 Hz, 2H, H3'), 3.79 (s, 3H, OMe), 3.10 (h, *J* = 6.7 Hz, 1H, H7), 2.59 (t, *J* = 7.2 Hz, 2H, H1'), 1.98 – 1.83 (m, 2H, H2'), 1.21 (d, *J* = 6.7 Hz, 6H, H8); **^{13}C NMR** (101 MHz, $CDCl_3$) δ 169.8 (C6), 163.2 (C4), 161.0 (C3''), 159.7 (C1''), 159.4 (C2), 130.2 (C5''), 106.9 (C6''), 106.7 (C4''), 103.2 (C5), 101.2 (C2''), 66.3 (C3'), 55.5 (OMe), 30.2 (C7), 28.9 (C2'), 21.3 (C8), 21.1 (C1'); **HRMS** (ES^+) calculated for $C_{17}H_{24}N_4O_2$ $[M + H]^+$: 317.1972, found: 317.1988.

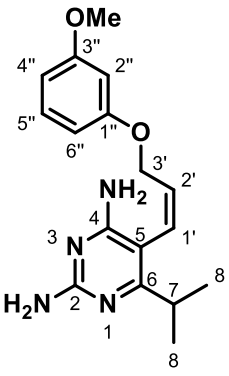

R*f* = 0.43 (1:9 MeOH/DCM); **mp**: 120 °C; **IR** (v/cm^{-1}): 3325 (NH str), 3177 (NH str), 3031 (=CH), 2966 (CH), 1610 (NH bend), 1569 (C=C) 1263 (C-O);**^{1}H NMR** (400 MHz, $CDCl_3$) δ 7.14 (t, *J* = 8.1 Hz, 1H, H5''), 6.49 (dd, *J* = 7.9, 2.2 Hz, 1H, H4''), 6.44 – 6.34 (m, 3H, H1', H2'' & H6''), 6.11 (dt, *J* = 11.1, 6.5 Hz, 1H, H2'), 5.01 (s, 2H, NH_2), 4.94 (s, 2H, NH_2), 4.41 (d, *J* = 6.4 Hz, 2H, H2'), 3.76 (s, 3H, OMe), 2.92 (h, *J* = 6.8 Hz, 1H, H7), 1.13 (d, *J* = 6.8 Hz, 6H, H8); **^{13}C NMR** (101 MHz, $CDCl_3$) δ 172.4 (C6), 162.1 (C4), 161.2 (C2), 160.9 (C3''), 159.7 (C1''), 131.4 (C2'), 130.0 (C5''), 125.9 (C1'), 106.8 (C6''), 106.7 (C4''), 101.3 (C2''),

100.7 (C5), 65.1 (C2'), 55.4 (0Me), 32.0 (C7), 21.0 (C8); **HRMS** (ES^+) calculated for $C_{17}H_{22}N_4O_2$ $[M + H]^+$: 315.1816, found: 315.1839.

6.11.2.7 Synthesis of 5-[3-(2-chlorophenoxy)propyl]-6-isopropylpyrimidine-2,4-diamine 62g

5-[3-(2-Chlorophenoxy)prop-1-yn-1-yl]-6-isopropylpyrimidine-2,4-diamine (27.8 mg, 87.8 µmol) was subjected to a reduction reaction in the presence of Pd/C (2.78 mg, 26.1 µmol) and 4 ml Abs. EtOH as a solvent to afford 5-[3-(2-chlorophenoxy)propyl]-6-isopropylpyrimidine-2,4-diamine **62g** as a cream white solid (15.0 mg, 54%).

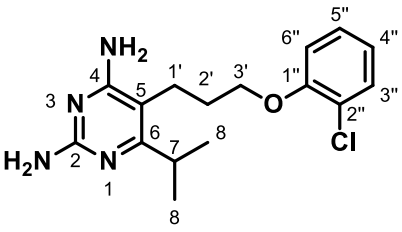

R*f* =0.34 (1:9 MeOH/DCM); **mp**: 148 °C; **I.R** (v/cm^{-1}): 3327 (NH str), 3203 (NH str), 2956 (CH), 1560 (C=C); **^{1}H NMR** (500 MHz, MeOD) δ 7.37 (dd, *J* = 7.9, 1.7 Hz, 1H, H3''), 7.25 (t, *J* = 7.3 Hz, 1H, H5''), 7.05 (d, *J* = 8.1 Hz, 1H, H6''), 6.92 (t, *J* = 7.3 Hz, 1H, H4''), 4.09 (t, *J* = 5.5 Hz, 2H, H3'), 3.24 – 3.16 (m, 1H, H7), 2.70 (t, *J* = 7.6 Hz, 2H, H1'), 1.98 (p, *J* = 6.2 Hz, 2H, H2'), 1.14 (d, *J* = 6.9 Hz, 6H, H8); **^{13}C NMR** (126 MHz, MeOD) δ 172.2 (C6), 165.7 (C4), 159.9 (C2), 155.5 (C1''), 131.2 (3''), 129.2 (C5''), 123.6 (C2''), 122.5 (C4''), 114.5 (C6''), 104.9 (C5), 68.4 (C3'), 30.3 (C7), 29.4 (C2'), 21.8 (C1'), 21.2 (C8); **HRMS** (ES^+) calculated for $C_{16}H_{21}ClN_4O$ $[M + H]^+$: 321.1477, found: 321.1495.

6.11.2.8 Synthesis of 6-isopropyl-5-[3-(2-methoxyphenoxy)propyl] pyrimidine-2,4-diamine 62h

Reduction of 6-isopropyl-5-[3-(2-methoxyphenoxy)prop-1-yn-1-yl]pyrimidine-2,4-diamine **59h** to 6-isopropyl-5-[3-(2-methoxyphenoxy)propyl]pyrimidine-2,4-diamine **62h** was achieved by subjecting the starting material (43.0 mg, 0.10 mmol) to a hydrogenation reaction in the presence of Pd/C (4.30 mg, 40.4 µmol) and H_2(g) atmosphere, dissolved in 4 ml Abs. EtOH. 28.0 mg of the product **62h** was isolated as an off-white solid (65% yield).

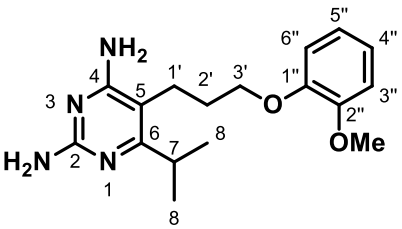

R*f* = 0.23 (1:9 MeOH/DCM); **mp**: 220 °C; **IR** (v/cm^{-1}): 3346 (NH str), 3195 (NH str) 2986 (CH), 1620 (NH bend), 1247 (C-O); **^{1}H NMR** (500 MHz, $CDCl_3$) δ 7.04 – 6.74 (m, 4H, H3'', H4'', H5'' & H6''), 5.29 (s, 2H, NH_2), 4.63 (s, 2H, NH_2), 4.02 (t, *J* = 5.4 Hz, 2H, H3'), 3.85 (s,

3H, OMe), 3.08 (h, *J* = 5.9 Hz, 1H, H7), 2.63 (t, *J* = 7.2 Hz, 2H, H1'), 1.96 (p, *J* = 6.5 Hz, 2H, H2'), 1.19 (d, *J* = 6.7 Hz, 6H, H8); **^{13}C NMR** (126 MHz, $CDCl_3$) δ 171.3 (C6), 163.5 (C4), 160.9 (C2), 149.4 (C2''), 148.0 (C1'), 121.5 (C4''), 121.1 (C5''), 113.1 (C6''), 111.7 (C3''), 103.5 (C5), 67.1 (C3'), 55.8 (OMe), 30.3 (C7), 29.1 (C2'), 21.7 (C8), 20.9 (C1'); **HRMS** (ES^+) calculated for $C_{17}H_{24}N_4O_2$ $[M + H]^+$: 317.1972, found: 317.1990.

6.11.3 Synthesis of the 6-cyclopropyl-2,4-diaminopyrimidine analogue.

6.11.3.1 Synthesis of 6-cyclopropyl-5-[3-(4-fluorophenoxy)prop-1-yn-1-yl] pyrimidine-2,4-diamine 64

Using the general procedure descried for a Sonogashira reaction, compound **62** was synthesised. To a heterogeneous mixture of 6-cyclopropyl-5-iodopyrimidine-2,4-diamine (0.30 g, 1.10 mmol),), $Pd(PPh_3)_2Cl_2$ (76.3 mg, 0.10 mmol) and Cu(I)I (41.4 mg, 0.20 mmol) in 6 ml DMF, (12.0 ml, 89.9 mmol) DIIPA was added, followed by addition of 1-fluoro-4-(prop-2-yn-1-yloxy)benzene (0.33 g, 2.20 mmol) to give 0.14 g product **64** in 42% yield as a cream white solid.

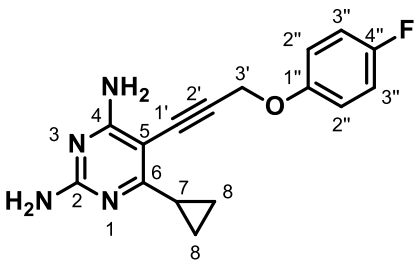

R*f* = 0.46 (1:9 MeOH/DCM); **mp**: 137 °C; **IR** (v/cm^{-1}): 3314 (NH str), 3176 (NH str), 3007 (=C-H), 2210 (C≡C), 1243 (C-O); **^{1}H NMR** (400 MHz, $CDCl_3$) δ 7.09 – 6.90 (m, 4H, H2'' & H3''), 5.20 (s, 2H, NH_2), 4.97 (s, 2H, NH_2), 4.95 (s, 2H, H3'), 2.22 (tt, *J* = 8.4, 4.7 Hz, 1H. H7), 1.03 (dt, *J* = 6.2, 3.3 Hz, 2H, H8), 0.88 (dq, *J* = 7.2, 3.6 Hz, 2H, H8); **^{13}C NMR** (101 MHz, $CDCl_3$) δ 173.8 (C6), 164.0 (C4), 161.3 (C2), 157.9 (d, $J_{C\text{-}F}$ = 239.2 Hz, C4''), 153.7 (C1''), 116.6 (d, $J_{C\text{-}F}$ = 8.1 Hz, C2''), 116.0 (d, $J_{C\text{-}F}$ = 23.1 Hz, C3''), 92.8 (C2'), 89.5 (C5), 81.6 (C1'), 57.7 (C3'), 15.0 (C7), 10.0 (C8); **HRMS** (ES^+) calculated for $C_{16}H_{15}FN_4O$ $[M + H]^+$: 299.1303, found: 299.1319.

6.11.3.2 Synthesis of 6-cyclopropyl-5-[3-(4-fluorophenoxy)propyl] pyrimidine-2,4-diamine 65

Compound **65** was synthesized using the general methodology described for hydrogenation. The starting material, 6-cyclopropyl-5-[3-(4-fluorophenoxy)prop-1-yn-1-yl]pyrimidine-2,4-diamine (50.0 mg, 0.20 mmol), was dissolved in 4 ml Abs. EtOH in the presence of Pd/C (5.00 mg, 47.0 µmol). The reaction was conducted under pressure in H_2 atmosphere to produce 6-cyclopropyl-5-[3-(4-fluorophenoxy)propyl] pyrimidine-2,4-diamine **65** (39.0 mg, 77%) as a light brown solid.

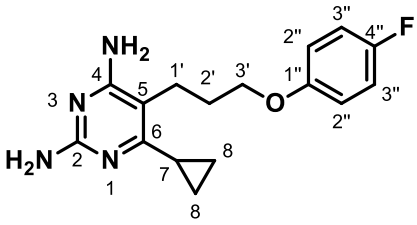

R*f* = 0.42 (1:9 MeOH/DCM); **mp**: 107 °C; **IR** (v/cm^{-1}): 3320 (NH str), 3181 (NH str), 2922 (CH), 1608 (NH bend), 1249 (C-O);**^{1}H NMR** (400 MHz, $CDCl_3$) δ 7.04 – 6.90 (m, 2H, H3''), 6.89 – 6.74 (m, 2H, H2''), 4.99 (s, 2H, NH_2), 4.72 (s, 2H, NH_2), 3.92 (t, *J* = 5.5 Hz, 2H, H3'), 2.72 (t, *J* = 7.0 Hz, 2H, H1'), 2.00 (dt, *J* = 12.6, 6.0 Hz, 2H, H2'), 1.93 (tt, *J* = 8.2, 4.8 Hz, 1H, H7), 1.01 (dt, *J* = 6.2, 3.1 Hz, 2H, H8), 0.79 (dt, *J* = 8.0, 3.1 Hz, 2H, H8); **^{13}C NMR** (101 MHz, $CDCl_3$) δ 167.9 (C6), 162.4 (C4), 160.8 (C2), 157.5 (d, $J_{C\text{-}F}$ = 238.5 Hz, C4''), 154.8 (d, $J_{C\text{-}F}$ = 2.1 Hz, C1''), 116.0 (d, $J_{C\text{-}F}$ = 23.1 Hz, C3''), 115.6 (d, $J_{C\text{-}F}$ = 7.9 Hz, C2''), 104.1(C5), 66.9 (C3'), 28.6 (C2,), 21.1 (C1'), 12.7 (C7), 9.0 (C8); **HRMS** (ES$^+$) calculated for $C_{16}H_{19}FN_4O$ $[M + H]^+$: 303.1616, found: 303.1635.

6.11.4 Synthesis of the phenyl-amino derivative from aniline.

6.11.4.1 Synthesis of N-(prop-2-yn-1-yl)aniline 66[187]

The heterogeneous mixture of aniline (6.14 ml, 67.3 mmol) and K_2CO_3 (4.65 g, 33.6 mmol) in 20 ml DMF was stirred for 5 minutes before propargyl bromide (1.87 ml, 16.8 mmol) was added dropwise. The reaction mixture was stirred overnight at r.t. under N_2 atmosphere. The organic layer was extracted with 200 ml EtOAc and washed with 200 ml of brine. The wash was repeated 4 times with the same volume of brine. After collection of the organic layer, it was dried over $MgSO_4$, and the drying agent was filtered off. After removal of the solvent on the rotary evaporator, the residue was purified by silica gel column chromatography (20 % EtOAc/Hex) to give *N*-(prop-2-yn-1-yl)aniline **66** (1.95 g, 89%) as a yellow oil.

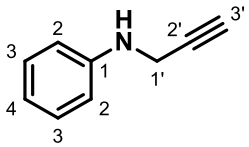

R*f* = 0.73 (3:7 EtOAc/Hex); **^{1}H NMR** (400 MHz, $CDCl_3$) δ 7.17 (dd, *J* = 8.6, 8.0 Hz, 2H, H3), 6.81 – 6.70 (m, 1H, H4), 6.68 – 6.53 (m, 2H, H2), 3.84 (s, 2H, H1'), 2.16 (br s, 1H, H3'); **^{13}C NMR** (101 MHz, $CDCl_3$) δ 146.8 (C1), 129.2 (C3), 118.6 (C4), 113.5 (C2), 81.2 (C2'), 71.3 (C3'), 33.6 (C1').

6.11.4.2 Synthesis of 6-isopropyl-5-[3-(phenylamino)prop-1-yn-1-yl]pyrimidine-2,4-diamine 67

Compound **67** was synthesised following the general procedure outlined for Sonogashira reaction. The heterogeneous mixture of 5-iodo-6-iso-propylpyrimidine-2,4-diamine (0.50 g, 1.80 mmol), $Pd(PPh_3)_2Cl_2$ (0.13 g, 0.20 mmol) and Cu(I)I (68.5 mg, 0.40 mmol) was dissolved in 6 ml of dry DMF, followed by addition of DIIPA (12.0 ml, 89.9 mmol) as a base and the acetylene, N-(*prop*-2-yn-1-yl)aniline (0.47 g, 3.6 mmol) to afford 6-isopropyl-5-[3-(phenylamino)prop-1-yn-1-yl]pyrimidine-2,4-diamine **67** as a light brown solid (0.30 g, 60%).

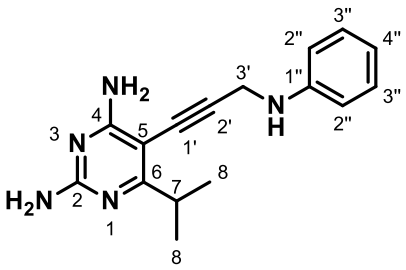

R*f* = 0.47 (1:9 MeOH/DCM); **mp**: 84 °C; **IR** (v/cm^{-1}): 3298 (NH str), 3173 (NH str), 2964 (CH), 2178 (C≡C); **^{1}H NMR** (400 MHz, $CDCl_3$) δ 7.23 (t, *J* = 7.8 Hz, 2H, H3''), 6.81 (t, *J* = 7.3 Hz, 1H, H4''), 6.76 (d, *J* = 7.9 Hz, 2H, H2''), 5.04 (s, 2H, NH_2), 4.98 (s, 2H, NH_2), 4.22 (s, 2H, H3'), 3.19 (h, *J* = 6.8 Hz, 1H, H7), 1.12 (d, *J* = 6.8 Hz, 6H, H8); **^{13}C NMR** (101 MHz, $CDCl_3$) δ 177.1 (C6), 164.5 (C4), 161.0 (C2), 147.1 (C1''), 129.4 (C3''), 119.0 (C4''), 114.2 (C2''), 96.1 (C2'), 89.3 (C5), 77.4 (C1'), 35.1 (C3'), 33.5 (C7), 20.8 (C8); **HRMS** (ES^+) calculated for $C_{16}H_{19}N_5$ $[M + H]^+$: 282.1713, found: 282.1731.

6.11.4.3 Synthesis of 6-isopropyl-5-[3-(phenylamino)propyl]pyrimidine-2,4-diamine 68

Compound **68** was synthesised following the general procedure for the hydrogenation reaction. The general procedure described above was followed by subjecting 6-isopropyl-5-[3-(phenylamino)prop-1-yn-1-yl]pyrimidine-2,4-diamine (56.0 mg, 0.20 mmol) to a reduction reaction in the presence of Pd/C (5.00 mg, 47.0 µmol) as a catalyst in 4 ml Abs. EtOH. 6-isopropyl-5-[3-(phenylamino)propyl]pyrimidine-2,4-diamine **68** (33.0 mg, 58%) was isolated as a white solid.

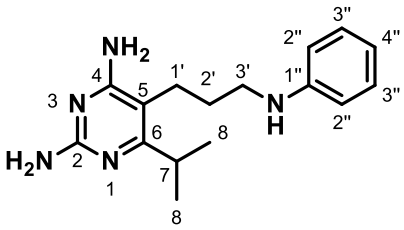

R*f* =0.15 (1:9 MeOH/DCM); **mp**: 242 °C; **I.R**: (v/cm^{-1}): 3326 (NH str), 3187 (NH str), 2958 (CH); **^{1}H NMR** (500 MHz, MeOD) δ 7.11 (t, *J* = 7.9 Hz, 2H, H3''), 6.67 (d, *J* = 7.8 Hz, 2H, H2''), 6.63 (t, *J* = 7.3 Hz, 1H, H4''), 3.34 – 3.26 (m, *J* = 3.2, 1.7 Hz, 1H, H7), 3.15 (t, *J* = 6.5 Hz, 2H,H3'), 2.54 (t, *J* = 7.8 Hz, 2H, H1'), 1.76 (p, *J* = 6.8 Hz, 2H, H2'), 1.14 (d, *J* = 6.8 Hz, 6H, H8); **^{13}C NMR** (126 MHz, MeOD) δ 178.0 (C6), 165.8 (C4), 159.8 (C2), 150.1 (C1''), 130.1 (3''), 118.3 (C4''), 114.4 (C2''), 105.5 (C5), 44.0 (C3'), 30.3 (C7), 29.6 (C2'), 22.9 (C1'), 21.2 (C8); **HRMS** (ES^{+}) calculated for $C_{16}H_{23}N_5$ $[M + H]^+$: 286.2026, found: 286.2044.

6.12 Biology

6.12.1 Enzyme preparation and inhibition assays

*Pf*DHFRs and *Hs*DHFR enzymes were expressed under T7 promotor of pET17b plasmids in *E. Coli* BL21(DE3) by cultivation in Lysogeny broth (LB) agar.[188] Enzyme inhibition assays were determined spectrophotometrically and Kinetic parameters were calculated as described by a nonlinear least-square fit of data to the Michaelis-Menten equation.[189,190]

6.12.2 Parasite culture, antimalarial and cytotoxicity testing *in vitro*.

Each compound was tested for antiplasmodial activity against two *P. falciparum* strains, TM4/8.2 (wild type *Pf*DHFR) and V1/S (QM *Pf*DHFR). Parasitic strains were cultured in human erythrocytes at 37°C under 3% CO_2 in RPMI 1640 culture media containing 25mM HEPES, 0.2% $NaHCO_3$, 40 µg/mL gentamicin and 8% human serum. *In vitro* antimalarial activity was determined by ^{3}H-hypoxanthine incorporation method.[191]

Cytotoxicity properties of the compounds were determined against Vero African green monkey kidney epithelial cells. by quantitative staining of cellular proteins using sulforhodamine B stain. [191,192] Cultures for the assays were carried out as described by Vichai and Kirtikara (2006) in triplicates.[192] Ellipticine in 10% (vol/vol) DMSO was used as a positive control, while wells containing cells in 10 µl of the solvent were used

as negative controls. For the purpose of calculating selectivity index (SI), IC_{50} values greater than 50 or 100 were taken as being 50 or 100, respectively.

7 References

(1) Tjong, E.; Dimri, M.; Mohiuddin, S. S. Biochemistry, Tetrahydrofolate. In *StatPearls*; StatPearls Publishing, 2022.

(2) Nzila, A. The Past, Present and Future of Antifolates in the Treatment of Plasmodium Falciparum Infection. *J Antimicrob Chemother* **2006**, *57*, 1043–1054.

(3) Nixon, M. R.; Saionz, K. W.; Koo, M. S.; Szymonifka, M. J.; Jung, H.; Roberts, J. P.; Nandakumar, M.; Kumar, A.; Liao, R.; Rustad, T.; Sacchettini, J. C.; Rhee, K. Y.; Freundlich, J. S.; Sherman, D. R. Folate Pathway Disruption Leads to Critical Disruption of Methionine Derivatives in Mycobacterium Tuberculosis. *Chem Biol* **2014**, *21* (7), 819–830.

(4) Nzila, A.; Ward, S. A.; Marsh, K.; Sims, P. F. G.; Hyde, J. E. Comparative Folate Metabolism in Humans and Malaria Parasites (Part I): Pointers for Malaria Treatment from Cancer Chemotherapy. *Trends Parasitol* **2005**, *21* (6), 292–298.

(5) Hyde, J. E. Exploring the Folate Pathway in Plasmodium Falciparum. *Acta Trop* **2005**, *94*, 191–206.

(6) Nzila, A.; Ward, S. A.; Marsh, K.; Sims, P. F. G.; Hyde, J. E. Comparative Folate Metabolism in Humans and Malaria Parasites (Part II): Activities as yet Untargeted or Specific to Plasmodium. *Trends Parasitol* **2005**, *21* (7), 334–339.

(7) Olliaro, P. L.; Yuthavong, Y. An Overview of Chemotherapeutic Targets for Antimalarial Drug Discovery. *Pharmacol Ther* **1999**, *81* (2), 91–110.

(8) Kompis, I. M.; Islam, K.; Then, R. L. DNA and RNA Synthesis: Antifolates. *Chem Rev* **2005**, *105* (2), 593–620.

(9) Müller, I. B.; Hyde, J. E. Folate Metabolism in Human Malaria Parasites-75 Years On. *Mol Biochem Parasitol* **2013**, *188*, 63–77.

(10) Hajian, B.; Scocchera, E.; Keshipeddy, S.; G-Dayanandan, N.; Shoen, C.; Krucinska, J.; Reeve, S.; Cynamon, M.; Anderson, A. C.; Wright, D. L. Propargyl-Linked Antifolates Are Potent Inhibitors of Drug-Sensitive and Drug-Resistant Mycobacterium Tuberculosis. *PLoS One* **2016**, 1–13.

(11) Dias, M. V. B.; Tyrakis, P.; Domingues, R. R.; Leme, A. F. P.; Blundell, T. L. Mycobacterium Tuberculosis Dihydrofolate Reductase Reveals Two Conformational States and a Possible Low Affinity Mechanism to Antifolate Drugs. *Structure* **2014**, *22* (1), 94–103.

(12) Oefner, C.; D'Arcy, A.; Winkler, F. K. Crystal Structure of Human Dihydrofolate Reductase Complexed with Folate. *Eur J Biochem* **1988**, *174* (2), 377–385.

(13) Champness, J.; Achari, A.; Ballantine, S.; Bryant, P.; Delves, C.; Stammers, D. The Structure of Pneumocystis Carinii Dihydrofolate Reductase to 1.9 å Resolution. *Structure* **1994**, *2* (10), 915–924.

(14) Yun, M. K.; Wu, Y.; Li, Z.; Zhao, Y.; Waddell, M. B.; Ferreira, A. M.; Lee, R. E.; Bashford, D.; White, S. W. Catalysis and Sulfa Drug Resistance in Dihydropteroate Synthase: Crystal Structures Reveal the Catalytic Mechanism of DHPS and the Structural Basis of Sulfa Drug Action and Resistance. *Science* **2012**, *335* (6072), 1110–1114.

(15) Gardner, M. J.; Hall, N.; Fung, E.; White, O.; Berriman, M.; Hyman, R. W.; Carlton, J. M.; Pain, A.; Nelson, K. E.; Bowman, S.; Paulsen, I. T.; James, K.; Eisen, J. A.; Rutherford, K.; Salzberg, S. L.; Craig, A.; Kyes, S.; Chan, M.-S.; Nene, V.; Shallom, S. J.; Suh, B.; Peterson, J.; Angiuoli, S.; Pertea, M.; Allen, J.; Selengut, J.; Haft, D.; Mather, M. W.; Vaidya, A. B.; Martin, D. M. A.; Fairlamb, A. H.; Fraunholz, M. J.; Roos, D. S.; Ralph, S. A.; Mcfadden, G. I.; Cummings, L. M.; Subramanian, G. M.; Mungall, C.; Venter, J. C.; Carucci, D. J.; Hoffman, S. L.; Newbold, C.; Davis, R. W.; Fraser, C. M.; Barrell, B. Genome Sequence of the Human Malaria Parasite Plasmodium Falciparum. *Nature* **2002**, *419*, 498–511.

(16) *World malaria report 2021*. https://www.who.int/teams/global-malaria-programme/reports/world-malaria-report-2021 (accessed 2022-05-17).

(17) Yuki, K.; Fujiogi, M.; Koutsogiannaki, S. COVID-19 Pathophysiology: A Review. *Clinical Immunology* **2020**, *215* (108427), 1–7.

(18) Ezenduka, C. C.; Daniel, •; Falleiros, R.; Godman, B. B. Evaluating the Treatment Costs for Uncomplicated Malaria at a Public Healthcare Facility in Nigeria and the Implications. *Pharmacoecon Open* **2017**, *1*, 184–194.

(19) *From 30 million cases to zero: China is certified malaria-free by WHO*. https://www.who.int/news/item/30-06-2021-from-30-million-cases-to-zero-china-is-certified-malaria-free-by-who (accessed 2022-05-18).

(20) Rudzinska, M. A. The Fine Structure of Malaria Parasites. *Int Rev Cytol* **1969**, *25* (C), 161–199.

(21) Bray, R. S. The Life-Cycle of Primate Malaria Parasistes. *Br Med Bull* **1982**, *38* (2), 117–122.

(22) Nureye, D.; Assefa, S. Prevention, and Treatment of Malaria Including Perspectives in Ethiopia. *Sci World J* **2020**, *2020*, 1–17.

(23) Tuteja, R. Malaria - An Overview. *FEBS Journal* **2007**, *274* (18), 4670–4679.

(24) Krettli, A. U.; Miller, L. H. Malaria: A Sporozoite Runs through It. *Curr Biol* **2001**, *11* (10), 409–412.

(25) Aikawa, M.; Miller, L. H.; Johnson, J.; Rabbege, J. Erythrocyte Entry by Malaria Parasites. A Moving Junction between Erythrocyte and Parasite. *J Cell Biol* **1978**, *77* (1), 72–82.

(26) Joy, D. A.; Feng, X.; Mu, J.; Furuya, T.; Chotivanich, K.; Krettli, A. U.; Ho, M.; Wang, A.; White, N. J.; Suh, E.; Beerli, P.; Su, X. zhuan. Early Origin and Recent Expansion of Plasmodium Falciparum. *Science (1979)* **2003**, *300* (5617), 318–321.

(27) Menkin-Smith, L.; Winders, W. T. Plasmodium Vivax Malaria. In *StatPearls*; StatPearls Publishing, 2021.

(28) McCarthy James S.; Price Richard N. *Methods and Techniques for Assessing Exposure to Antimalarial Drugs in Clinical Field Studies : Informal Consultation Organized by the World Health Organization with the Technical Support of the Worldwide Antimalarial Resistance Network, 22-24 February 2010, Bangkok, Thailand.*; World Health Organization, 2011.

(29) Aly, A. S. I.; Vaughan, A. M.; Kappe, S. H. I.; Org, T. K. Malaria Parasite Development in the Mosquito and Infection of the Mammalian Host. *Annu Rev Microbiol* **2009**, *63*, 195–221.

(30) Bogitsh, B. J.; Carter, C. E.; Oeltmann, T. N. Blood and Tissue Protistans II: Human Malaria. *Human Parasitology* **2019**, 111–133.

(31) Picot, S.; Bienvenu, A.-L. Plasmodium. In *Encyclopedia of Infection and Immunity*; Elsevier, 2022; pp 655–665.

(32) Mueller, I.; Zimmerman, P. A.; Reeder, J. C. Plasmodium Malariae and Plasmodium Ovale – the 'Bashful' Malaria Parasites. *Trends Parasitol* **2007**, *23* (6), 278–283.

(33) Fairhurst, R. M.; Wellems, T. E. Malaria (Plasmodium Species). *Principles and Practice of Infectious Diseases* **2014**, *2*, 3010-3090.el.

(34) Taylor, T.; Agbenyega, T. Malaria. In *Hunter's Tropical Medicine and Emerging Infectious Disease: Ninth Edition*; Elsevier Inc., 2012; pp 695–717.

(35) Hendrickse, R. G.; Adeniyi, A. Quartan Malarial Nephrotic Syndrome in Children. *Kidney Int* **1979**, *16* (1), 64–74.

(36) Howes, R. E.; Battle, K. E.; Mendis, K. N.; Smith, D. L.; Cibulskis, R. E.; Baird, J. K.; Hay, S. I. Global Epidemiology of Plasmodium Vivax. *Am J Trop Med Hyg* **2016**, *95* (6_Suppl), 15–34.

(37) Gething, P. W.; Elyazar, I. R. F.; Moyes, C. L.; Smith, D. L.; Battle, K. E.; Guerra, C. A.; Patil, A. P.; Tatem, A. J.; Howes, R. E.; Myers, M. F.; George, D. B.; Horby, P.; Wertheim, H. F. L.; Price, R. N.; Mü Eller 10, I.; Baird, J. K.; Hay, S. I. A Long Neglected World Malaria Map: Plasmodium Vivax Endemicity in 2010. *PLoS Negl Trop Dis* **2012**, *6* (9), 1814–1825.

(38) Singh, B.; Daneshvar, C. Human Infections and Detection of Plasmodium Knowlesi. *Clin Microbiol Rev* **2013**, *26* (2), 165–184.

(39) Amir, A.; Cheong, F. W.; de Silva, J. R.; Liew, J. W. K.; Lau, Y. L. Plasmodium Knowlesi Malaria: Current Research Perspectives. *Infect Drug Resist* **2018**, *11*, 1145–1155.

(40) Singh, B.; Sung, L. K.; Matusop, A.; Radhakrishnan, A.; Shamsul, S. S. G.; Cox-Singh, J.; Thomas, A.; Conway, D. J. A Large Focus of Naturally Acquired Plasmodium Knowlesi Infections in Human Beings. *Lancet* **2004**, *363* (9414), 1017–1024.

(41) Gupta, H.; Srivastava, S.; Chaudhari, S.; Vasudevan, T. G.; Hande, M. H.; D'souza, S. C.; Umakanth, S.; Satyamoorthy, K. New Molecular Detection Methods of Malaria Parasites with Multiple Genes from Genomes. *Acta Trop* **2016**, *160*, 15–22.

(42) Sallum, M.; Peyton, E.; Harrison, B.; Wilkerson Richard. Revision of the Leucophyrus Group of Anopheles (Cellia) (Diptera, Culicidae))). *Rev Bras Entomol* **2005**, *49* (1), 1–152.

(43) Sutherland, C. J.; Tanomsing, N.; Nolder, D.; Oguike, M.; Jennison, C.; Pukrittayakamee, S.; Dolecek, C.; Hien, T. T.; do Rosário, V. E.; Arez, A. P.; Pinto, J.; Michon, P.; Escalante, A. A.; Nosten, F.; Burke, M.; Lee, R.; Blaze, M.; Otto, T. D.; Barnwell, J. W.; Pain, A.; Williams, J.; White, N. J.; Day, N. P. J.; Snounou, G.; Lockhart, P. J.; Chiodini, P. L.; Imwong, M.; Polley, S. D. Two Nonrecombining Sympatric Forms of the Human Malaria Parasite Plasmodium Ovale Occur Globally. *J Infect Dis* **2010**, *201* (10), 1544–1550.

(44) Okafor, C. N.; Finnigan, N. A. Plasmodium Ovale Malaria. In *StatPearls*; StatPearls Publishing, 2018.

(45) Health Organization, W. *World Malaria Report 2017. Geneva: World Health Organization; 2017. Licence: CC BY-NC-SA 3.0 IGO.*; 2017.

(46) Rowe, J. A.; Claessens, A.; Corrigan, R. A. Adhesion of Plasmodium Falciparum-Infected Erythrocytes to Human Cells: Molecular Mechanisms and Therapeutic Implications. *Expert Rev Mol Med* **2009**, *11*, 1–29.

(47) Dondorp, A. M.; Pongponratn, E.; White, N. J. Reduced Microcirculatory Flow in Severe Falciparum Malaria: Pathophysiology and Electron-Microscopic Pathology. *Acta Trop* **2004**, *89* (3), 309–317.

(48) Gamboa, D.; Ho, M.-F.; Bendezu, J.; Torres, K.; Chiodini, P. L.; Barnwell, J. W.; Incardona, S.; Perkins, M.; Bell, D.; Mccarthy, J.; Cheng, Q. A Large Proportion of P. Falciparum Isolates in the Amazon Region of Peru Lack Pfhrp2 and Pfhrp3: Implications for Malaria Rapid Diagnostic Tests. *PLOS one* **2010**, *5* (1), 8091–8099.

(49) Raghavendra, K.; Barik, T. K.; Bhatt, R. M.; Srivastava, H. C.; Sreehari, U.; Dash, A. P. Evaluation of the Pyrrole Insecticide Chlorfenapyr for the Control of Culex Quinquefasciatus Say. *Acta Trop* **2011**, *118* (1), 50–55.

(50) Riar, N. K. Bifenthrin. In *Encyclopedia of Toxicology: Third Edition*; Academic Press, 2014; pp 449–451. https://doi.org/10.1016/B978-0-12-386454-3.01169-6.

(51) Katsuda, Y. Progress and Future of Pyrethroids. *Top Curr Chem* **2012**, *314*, 1–30.

(52) Ngufor, C.; Critchley, J.; Fagbohoun, J.; N'guessan, R.; Todjinou, D.; Rowland, M. Chlorfenapyr (A Pyrrole Insecticide) Applied Alone or as a Mixture with Alpha-Cypermethrin for Indoor Residual Spraying against Pyrethroid Resistant Anopheles Gambiae Sl: An Experimental Hut Study in Cove, Benin. *PLoS One* **2016**, *11* (9), 1–14.

(53) Kadenbach, B.; Ramzan, R.; Wen, L.; Vogt, S. New Extension of the Mitchell Theory for Oxidative Phosphorylation in Mitochondria of Living Organisms. *Biochim Biophys Acta Gen Subj* **2010**, *1800* (3), 205–212.

(54) Raghavendra, K.; Barik, T. K.; Sharma, P.; Bhatt, R. M.; Srivastava, H. C.; Sreehari, U.; Dash, A. P. Chlorfenapyr: A New Insecticide with Novel Mode of Action Can Control Pyrethroid Resistant Malaria Vectors. *Malar J* **2011**, *10* (16), 1–7.

(55) Terada, H. Uncouplers of Oxidative Phosphorylation. *Environ Health Perspect* **1990**, *87*, 213–218.

(56) The Lancet. Malaria Vaccine Approval: A Step Change for Global Health. *The Lancet* **2021**, *398* (10309), 1381–1381.

(57) Efficacy and Safety of RTS,S/AS01 Malaria Vaccine with or without a Booster Dose in Infants and Children in Africa: Final Results of a Phase 3, Individually Randomised, Controlled Trial. *The Lancet* **2015**, *386* (9988), 31–45.

(58) Chandramohan, D.; Zongo, I.; Sagara, I.; Cairns, M.; Yerbanga, R.-S.; Diarra, M.; Nikièma, F.; Tapily, A.; Sompougdou, F.; Issiaka, D.; Zoungrana, C.; Sanogo, K.; Haro, A.; Kaya, M.; Sienou, A.-A.; Traore, S.; Mahamar, A.; Thera, I.; Diarra, K.; Dolo, A.; Kuepfer, I.; Snell, P.; Milligan, P.; Ockenhouse, C.; Ofori-Anyinam, O.; Tinto, H.; Djimde, A.; Ouédraogo, J.-B.; Dicko, A.; Greenwood, B. Seasonal Malaria Vaccination with or without Seasonal Malaria Chemoprevention. *N Engl J Med* **2021**, *385* (11), 1005–1017.

(59) Achan, J.; Talisuna, A. O.; Erhart, A.; Yeka, A.; Tibenderana, J. K.; Baliraine, F. N.; Rosenthal, P. J.; Alessandro, U. D. ’. Quinine, an Old Anti-Malarial Drug in a Modern World: Role in the Treatment of Malaria Background and Historical Perspective. *Malar J* **2011**, *10* (144), 1–12.

(60) Petersen, I.; Eastman, R.; Lanzer, M. Drug-Resistant Malaria: Molecular Mechanisms and Implications for Public Health. *FEBS Lett* **2011**, *585* (11), 1551–1562.

(61) Goldberg, D. E. Complex Nature of Malaria Parasite Hemoglobin Degradation. *PNAS* **2013**, *110* (14), 5283–5284.

(62) Zhou, W.; Wang, H.; Yang, Y.; Chen, Z. S.; Zou, C.; Zhang, J. Chloroquine against Malaria, Cancers and Viral Diseases. *Drug Discov Today* **2020**, *25* (11), 2012–2022.

(63) *treatment_of_malaria [TUSOM | Pharmwiki]*. https://tmedweb.tulane.edu/pharmwiki/doku.php/treatment_of_malaria (accessed 2022-05-25).

(64) O'Neill, P. M.; Barton, V. E.; Ward, S. A. The Molecular Mechanism of Action of Artemisinin - The Debate Continues. *Molecules* **2010**, *15* (3), 1705–1721. ht

(65) Aweeka, F. T.; German, P. I. Clinical Pharmacology of Artemisinin-Based Combination Therapies. *Clin Pharmacokinet* **2008**, *47* (2), 91–102.

(66) Meshnick, S. R. Artemisinin: Mechanisms of Action, Resistance and Toxicity. *Int J Parasitol* **2002**, *32* (13), 1655–1660.

(67) Stocks, P. A.; Bray, P. G.; Barton, V. E.; Al-Helal, M.; Jones, M.; Araujo, N. C.; Gibbons, P.; Ward, S. A.; Hughes, R. H.; Biagini, G. A.; Davies, J.; Amewu, R.; Mercer, A. E.; Ellis, G.; O'Neill, P. M. Evidence for a Common Non-Heme Chelatable-Iron-Dependent Activation Mechanism for Semisynthetic and Synthetic Endoperoxide Antimalarial Drugs. *Angew Chem Int Ed* **2007**, *46* (33), 6278–6283.

(68) Kavishe, R. A.; Koenderink, J. B.; Alifrangis, M. Oxidative Stress in Malaria and Artemisinin Combination Therapy: Pros and Cons. *FEBS Journal* **2017**, *284* (16), 2579–2591.

(69) Jackman Ann; Forster Martin; Ng Matthew. *Cancer Drug Design and Discovery*, 1st ed.; Neidle Stephen, Ed.; Elsevier, 2008.

(70) Garg, D.; Henrich, S.; Salo-Ahen, O. M. H.; Myllykallio, H.; Costi, M. P.; Wade, R. C. Novel Approaches for Targeting Thymidylate Synthase To Overcome the

Resistance and Toxicity of Anticancer Drugs. *J Med Chem* **2010**, *53* (18), 6539–6549.

(71) Itoh, F.; Yukishige, K.; Wajima, M.; Ootsu, K.; Akimoto, H. Non-Glutamate Type Pyrrolo[2, 3-d]Pyrimidine Antifolates. I : Synthesis and Biological Properties of Pyrrolo[2, 3-d]Pyrimidine Antifolates Containing Tetrazole Congener of Glutamic Acid. *Chem Pharm Bull (Tokyo)* **1995**, *43* (2), 230–235.

(72) Miwa Testuo; Hitaka Takenori; Akimoto Hiroshi; Nomura Hiroaki. Novel Pyrrolo[2,3-d]Pyrimidine Antifolates: Synthesis and Antitumor Activities. *J Med Chem* **1991**, *34* (2), 555–560.

(73) Mcguire, J. J. Anticancer Antifolates: Current Status and Future Directions. *Curr Pharm Des* **2003**, *9* (31), 2593–2613.

(74) Jackson, R. C.; Fry, D. W.; Boritzki, T. J.; Besserer, J. A.; Leopold, W. R.; Sloan, B. J.; Elslager, E. F. Biochemical Pharmacology of the Lipophilic Antifolate, Trimetrexate. *Adv Enzyme Regul* **1984**, *22* (C), 187–206.

(75) Gangjee, A.; Jain, H. D.; Phan, J.; Lin, X.; Song, X.; Mcguire, J. J.; Kisliuk, R. L. Dual Inhibitors of Thymidylate Synthase and Dihydrofolate Reductase as Antitumor Agents: Design, Synthesis, and Biological Evaluation of Classical and Nonclassical Pyrrolo[2,3-d]Pyrimidine Antifolates 1. *J Med Chem* **2006**, *49* (3), 1055–1065.

(76) Walsh, C. Molecular Mechanisms That Confer Antibacterial Drug Resistance. *Nature* **2000**, *406* (6797), 775–781.

(77) Zhou, W.; Scocchera, E. W.; Wright, D. L.; Anderson, A. C. Antifolates as Effective Antimicrobial Agents: New Generations of Trimethoprim Analogs. *Medchemcomm* **2013**, *4* (6), 908–915.

(78) Minato, Y.; Thiede, J. M.; Kordus, S. L.; Mcklveen, E. J.; Turman, B. J.; Baughn, A. D. Mycobacterium Tuberculosis Folate Metabolism and the Mechanistic Basis for Para-Aminosalicylic Acid Susceptibility and Resistance. *Antimicrob Agents Chemother* **2015**, *59* (9), 5097–5106.

(79) Peppard, W. J.; Schuenke, C. D. Iclaprim, a Diaminopyrimidine Dihydrofolate Reductase Inhibitor for the Potential Treatment of Antibiotic-Resistant Staphylococcal Infections. *Curr Opin Investig Drugs* **2008**, *9* (2), 210–225.

(80) Michel, R. Comparative Study of the Association of Sulfalene and Pyrimethamine and of Sulfalene Alone in Mass Chemoprophylaxis of Malaria. *Medicine tropicale (Mars)* **1968**, *28* (4), 488–494.

(81) Laing, A. B. G. Treatment of Acute Falciparum Malaria with Sulphorthodimethoxine (Fanasil). *Br Med J* **1965**, *1* (5439), 905.

(82) Gregson, A.; Plowe, C. v. Mechanisms of Resistance of Malaria Parasites to Antifolates. *Pharmacol Rev* **2005**, *57* (1), 117–145.

(83) Olliaro, P. Mode of Action and Mechanisms of Resistance for Antimalarial Drugs. *Pharmacol Ther* **2001**, *89* (2), 207–219.

(84) Peterson, D. S.; Milhous, W. K.; Wellems, T. E. Molecular Basis of Differential Resistance to Cycloguanil and Pyrimethamine in Plasmodium Falciparum Malaria. *Proc Natl Acad Sci U S A* **1990**, *87* (8), 3018–3022.

(85) Kamchonwongpaisan, S.; Quarrell, R.; Charoensetakul, N.; Ponsinet, R.; Vilaivan, T.; Vanichtanankul, J.; Tarnchompoo, B.; Sirawaraporn, W.; Lowe, G.; Yuthavong, Y. Inhibitors of Multiple Mutants of Plasmodium Falciparum Dihydrofolate Reductase and Their Antimalarial Activities. *J Med Chem* **2004**, *47* (3), 673–680.

(86) Hurly, M. G. D. Potentiation of Pyrimethamine by Sulphadiazine in Human Malaria. *Trans R Soc Trop Med Hyg* **1959**, *53* (5), 412–413.

(87) Richards, W. H. G. Antimalarial Activity of Sulphonamides and a Sulphone, Singly and in Combination with Pyrimethamine, against Drug Resistant and Normal Strains of Laboratory Plasmodia. *Nature* **1966**, *212* (5069), 1494–1495.

(88) Gerum, A. B.; Ulmer, J. E.; Jacobus, D. P.; Jensen, N. P.; Sherman, D. R.; Sibley, C. H. Novel Saccharomyces Cerevisiae Screen Identifies WR99210

Analogues That Inhibit Mycobacterium Tuberculosis Dihydrofolate Reductase. *Antimicrob Agents Chemother* **2002**, *46* (11), 3362–3369.

(89) Bunnag, D.; Harinasuta, T.; Pinichpongse, S.; Suntharasamai, P. Effect of Primaquine on Gametocytes of Plasmodium Falciparum in Thailand. *The Lancet* **1980**, *316* (8185), 91–91.

(90) Spencer, H. C. Drug-Resistant Malaria-Changing Patterns Mean Difficult Decisions. *Trans R Soc Trop Med Hyg* **1985**, *79* (6), 748–758.

(91) Kinyanjui, S. M.; Mberu, E.; Winstanley, P.; Jacobus, D.; Watkins, W. The Antimalarial Triazine WR99210 and the Prodrug PS-15: Folate Reversal of in Vitro Activity against Plasmodium. *Am J Trop Med Hyg* **1999**, *60* (6), 943–947.

(92) Yuthavong, Y.; Tarnchompoo, B.; Vilaivan, T.; Chitnumsub, P.; Kamchonwongpaisan, S.; Charman, S. A.; McLennan, D. N.; White, K. L.; Vivas, L.; Bongard, E.; Thongphanchang, C.; Taweechai, S.; Vanichtanankul, J.; Rattanajak, R.; Arwon, U.; Fantauzzi, P.; Yuvaniyama, J.; Charman, W. N.; Matthews, D. Malarial Dihydrofolate Reductase as a Paradigm for Drug Development against a Resistance-Compromised Target. *Proc Natl Acad Sci U S A* **2012**, *109* (42), 16823–16828.

(93) Hekmat-Nejad, M.; Rathod, P. K. Plasmodium Falciparum: Kinetic Interactions of WR99210 with Pyrimethamine-Sensitive and Pyrimethamine-Resistant Dihydrofolate Reductase. *Exp Parasitol* **1997**, *87* (3), 222–228.

(94) Fidock, D. A.; Wellems, T. E. Transformation with Human Dihydrofolate Reductase Renders Malaria Parasites Insensitive to WR99210 but Does Not Affect the Intrinsic Activity of Proguanil. *Proc Natl Acad Sci U S A* **1997**, *94* (20), 10931–10936.

(95) Mital, A. Recent Advances in Antimalarial Compounds and Their Patents. *Curr Med Chem* **2007**, *14* (7), 759–773.

(96) U Lourens, A. C.; Gravestock, D.; van Zyl, R. L.; Hoppe, H. C.; Kolesnikova, N.; Taweechai, S.; Yuthavong, Y.; Kamchonwongpaisan, S.; Rousseau, A. L.

Design, Synthesis and Biological Evaluation of 6-Aryl-1,6-Dihydro-1,3,5-Triazine-2,4-Diamines as Antiplasmodial Antifolates. *Org Biomol Chem* **2016**, *14*, 7899–7911.

(97) Gravestock, D.; Rousseau, A. L.; Lourens, A. C. U.; Moleele, S. S.; van Zyl, R. L.; Steenkamp, P. A. Expeditious Synthesis and Biological Evaluation of Novel 2,N 6-Disubstituted 1,2-Dihydro-1,3,5-Triazine-4,6-Diamines as Potential Antimalarials. *Eur J Med Chem* **2011**, *46* (6), 2022–2030.

(98) Seanego, D. T. Synthesis of Antimalarial Antifolates, 2015.

(99) Maurya, R. A.; Park, C. P.; Lee, J. H.; Kim, D. P. Continuous in Situ Generation, Separation, and Reaction of Diazomethane in a Dual-Channel Microreactor. *Angew Chem Int Ed* **2011**, *50* (26), 5952–5955.

(100) Vanichtanankul, J.; Taweechai, S.; Yuvaniyama, J.; Vilaivan, T.; Chitnumsub, P.; Kamchonwongpaisan, S.; Yuthavong, Y. Trypanosomal Dihydrofolate Reductase Reveals Natural Antifolate Resistance. *ACS Chem Biol* **2011**, *6* (9), 905–911.

(101) Tarnchompoo, B.; Chitnumsub, P.; Jaruwat, A.; Shaw, P. J.; Vanichtanankul, J.; Poen, S.; Rattanajak, R.; Wongsombat, C.; Tonsomboon, A.; Decharuangsilp, S.; Anukunwithaya, T.; Arwon, U.; Kamchonwongpaisan, S.; Yuthavong, Y. Hybrid Inhibitors of Malarial Dihydrofolate Reductase with Dual Binding Modes That Can Forestall Resistance. *ACS Med Chem Lett* **2018**, *9* (12), 1235–1240.

(102) Yuvaniyama, J.; Chitnumsub, P.; Kamchonwongpaisan, S.; Vanichtanankul, J.; Sirawaraporn, W.; Taylor, P.; Walkinshaw, M. D.; Yuthavong, Y. Insights into Antifolate Resistance from Malarial DHFR-TS Structures. *Nat Struct Mol Biol* **2003**, *10* (5), 357–365.

(103) Nzila, A.; Rottmann, M.; Chitnumsub, P.; Kiara, S. M.; Kamchonwongpaisan, S.; Maneeruttanarungroj, C.; Taweechai, S.; Yeung, B. K. S.; Goh, A.; Lakshminarayana, S. B.; Zou, B.; Wong, J.; Ma, N. L.; Weaver, M.; Keller, T. H.; Dartois, V.; Wittlin, S.; Brun, R.; Yuthavong, Y.; Diagana, T. T. Preclinical Evaluation of the Antifolate QN254, 5-Chloro-N′6′- (2,5-Dimethoxy-Benzyl)-

Quinazoline-2,4,6-Triamine, as an Antimalarial Drug Candidate. *Antimicrob Agents Chemother* **2010**, *54* (6), 2603–2610.

(104) Molatsane, T.; Rousseau, A.; de Koning, C. Synthesis and Modification of Antiplasmodial Antifolates, 2019.

(105) Thorand, S.; Krause, N. Improved Procedures for the Palladium-Catalyzed Coupling of Terminal Alkynes with Aryl Bromides (Sonogashira Coupling). *J Org Chem* **1998**, *63* (23), 8551–8553.

(106) Sirichaiwat, C.; Intaraudom, C.; Kamchonwongpaisan, S.; Vanichtanankul, J.; Thebtaranonth, Y.; Yuthavong, Y. Target Guided Synthesis of 5-Benzyl-2,4-Diaminopyrimidines: Their Antimalarial Activities and Binding Affinities to Wild Type and Mutant Dihydrofolate Reductases from Plasmodium Falciparum. *J Med Chem* **2004**, *47* (2), 345–354.

(107) Velcicky, J.; Miltz, W.; Oberhauser, B.; Orain, D.; Vaupel, A.; Weigand, K.; Dawson King, J.; Littlewood-Evans, A.; Nash, M.; Feifel, R.; Loetscher, P. Development of Selective, Orally Active GPR4 Antagonists with Modulatory Effects on Nociception, Inflammation, and Angiogenesis. *J Med Chem* **2017**, *60* (9), 3672–3683.

(108) Klahn, P.; Kirsch, S. F. IBX-Mediated Dehydrogenation of Substituted β-Oxonitriles. *European J Org Chem* **2014**, *2014* (15), 3149–3155.

(109) Marković, R.; Baranac, M.; Džambaski, Z.; Stojanović, M.; Steel, P. J. High Regioselectivity in the Heterocyclization of β-Oxonitriles to 4-Oxothiazolidines: X-Ray Structure Proof. *Tetrahedron* **2003**, *59* (39), 7803–7810.

(110) Kiyokawa, K.; Nagata, T.; Minakata, S. Recent Advances in the Synthesis of β-Ketonitriles. *Synthesis (Stuttg)* **2017**, *50*, 485–495.

(111) Wallace, A. A.; Dauletyarov, Y.; Sanov, A. Diradical Interactions in Ring-Open Isoxazole. *J Phys Chem A* **2021**, *125* (1), 317–326.

(112) Na, J.; Houk, K. N.; Hilvert, D. Transition State of the Base-Promoted Ring-Opening of Isoxazoles. Theoretical Prediction of Catalytic Functionalities and Design of Haptens for Antibody Production. *J Am Chem Soc* **1996**, *118* (27), 6462–6471.

(113) Munnich, A.; Rustin, P. Cytochrome c Oxidase Deficiency. *Am. J. Med. Genet. C Semin. Med. Get.* **2001**, *106* (1), 46–52.

(114) Pardo, Tr. M. C.; Miller, R. D. *Basics of Anesthesia*, 7th Edition.; Elsevier, Inc.: Philadelphia, 2018.

(115) Donslund, A. S.; Neumann, K. T.; Corneliussen, N. P.; Grove, E. K.; Herbstritt, D.; Daasbjerg, K.; Skrydstrup, T. Access to β-Ketonitriles through Nickel-Catalyzed Carbonylative Coupling of α-Bromonitriles with Alkylzinc Reagents. *Chem Eur J* **2019**, *25* (42), 9856–9860.

(116) Schoenberg, A.; Heck, R. F. Palladium-Catalyzed Amidation Palladium-Catalyzed Amidation of Aryl, Heterocyclic, and Vinylic Halides. *J. Org. Chem* **1974**, *39* (23), 30.

(117) Park, A.; Lee, S. Synthesis of Benzoylacetonitriles from Pd-Catalyzed Carbonylation of Aryl Iodides and Trimethylsilylacetonitrile. *Org Lett* **2012**, *14* (4), 1118–1121.

(118) Dorsch John B.; McElvain S.M. The Preparation of Benzoylacetic Ester and Some of Its Homologs. *J Am Chem Soc* **1932**, *54*, 2960–2964.

(119) Eby, C. J.; Hauser, C. R. Acylations of Nitriles with Esters by Sodium Amide in Liquid Ammonia to Form β-Ketonitriles. Consideration of Amidine Formation. *J Am Chem Soc* **1957**, *79* (3), 723–725.

(120) Levine, R.; Hauser, C. R. The Acylation and Carbethoxylation of Nitriles in the Presence of Sodium Amide1. *J Am Chem Soc* **1946**, *68*, 760–761.

(121) Miyamoto, Y.; Banno, Y.; Yamashita, T.; Fujimoto, T.; Oi, S.; Moritoh, Y.; Asakawa, T.; Kataoka, O.; Yashiro, H.; Takeuchi, K.; Suzuki, N.; Ikedo, K.;

Kosaka, T.; Tsubotani, S.; Tani, A.; Sasaki, M.; Funami, M.; Amano, M.; Yamamoto, Y.; Aertgeerts, K.; Yano, J.; Maezaki, H. Discovery of a 3-Pyridylacetic Acid Derivative (TAK-100) as a Potent, Selective and Orally Active Dipeptidyl Peptidase IV (DPP-4) Inhibitor. *J Med Chem* **2011**, *54* (3), 831–850.

(122) Getlik, M.; Grütter, C.; Simard, J. R.; Nguyen, H. D.; Robubi, A.; Aust, B.; van Otterlo, W. A. L.; Rauh, D. Structure-Based Design, Synthesis and Biological Evaluation of N-Pyrazole, N′-Thiazole Urea Inhibitors of MAP Kinase P38α. *Eur J Med Chem* **2012**, *48*, 1–15.

(123) Havel, S.; Khirsariya, P.; Akavaram, N.; Paruch, K.; Carbain, B. Preparation of 3,4-Substituted-5-Aminopyrazoles and 4-Substituted-2-Aminothiazoles. *J Org Chem* **2018**, *83* (24), 15380–15405.

(124) Rowbottom, M. W.; Faraoni, R.; Chao, Q.; Campbell, B. T.; Lai, A. G.; Setti, E.; Ezawa, M.; Sprankle, K. G.; Abraham, S.; Tran, L.; Struss, B.; Gibney, M.; Armstrong, R. C.; Gunawardane, R. N.; Nepomuceno, R. R.; Valenta, I.; Hua, H.; Gardner, M. F.; Cramer, M. D.; Gitnick, D.; Insko, D. E.; Apuy, J. L.; Jones-Bolin, S.; Ghose, A. K.; Herbertz, T.; Ator, M. A.; Dorsey, B. D.; Ruggeri, B.; Williams, M.; Bhagwat, S.; James, J.; Holladay, M. W. Identification of 1-(3-(6,7-Dimethoxyquinazolin-4-Yloxy)Phenyl)-3-(5-(1,1, 1-Trifluoro-2-Methylpropan-2-Yl)Isoxazol-3-Yl)Urea Hydrochloride (CEP-32496), a Highly Potent and Orally Efficacious Inhibitor of V-RAF Murine Sarcoma Viral Oncogene Homologue B1 (BRAF) V600E. *J Med Chem* **2012**, *55* (3), 1082–1105.

(125) Brown, T. L.; LeMay, Jr. H. E.; Bursten, B. E.; Murphy, C. J.; Woodward, P. M.; Stoltzfus, M. W. *Chemistry : The Central Science*, 14th Edition.; Pearsons, 2018.

(126) Pienaar, D. P.; Butsi, K. R.; Rousseau, A. L.; Brady, D. A Green, Economical Synthesis of β-Ketonitriles and Trifunctionalized Building Blocks from Esters and Lactones. *Beilstein J Org Chem* **2019**, *15*, 2930–2935.

(127) Date, N. S.; Hengne, A. M.; Huang, K. W.; Chikate, R. C.; Rode, C. v. One Pot Hydrogenation of Furfural to 2-Methyl Tetrahydrofuran over Supported Mono- and Bi-Metallic Catalysts. *ChemistrySelect* **2020**, *5* (31), 9590–9600.

(128) Anastas, P.; Eghbali, N. Green Chemistry: Principles and Practice. *Chem Soc Rev* **2010**, *39*, 301–312.

(129) Ghatak, H. R. Biorefineries from the Perspective of Sustainability: Feedstocks, Products, and Processes. *Renew Sustain Energy Rev* **2011**, *15* (8), 4042–4052.

(130) Khoo, H. H.; Wong, L. L.; Tan, J.; Isoni, V.; Sharratt, P. Synthesis of 2-Methyl Tetrahydrofuran from Various Lignocellulosic Feedstocks: Sustainability Assessment via LCA. *Resour Conserv Recycl* **2015**, *95*, 174–182.

(131) Stewart Slater, C.; Savelski, M. J.; Hitchcock, D.; Cavanagh, E. J.; Slater, S. Environmental Analysis of the Life Cycle Emissions of 2-Methyl Tetrahydrofuran Solvent Manufactured from Renewable Resources. *J Environ Sci Health A* **2016**, *51* (6), 487–494.

(132) Treptow, R. S. Chatelier's Principle A Reexamination and Method of Graphic Illustration. *J Chem Educ* **1980**, *57* (6), 417–420.

(133) Lagoja, I. M. Pyrimidine as Constituent of Natural Biologically Active Compounds. *Chem Biodivers* **2005**, *2* (1), 1–50.

(134) Ahmed, N. M.; Youns, M.; Soltan, M. K.; Said, A. M. Design, Synthesis, Molecular Modelling, and Biological Evaluation of Novel Substituted Pyrimidine Derivatives as Potential Anticancer Agents for Hepatocellular Carcinoma. *J Enzyme Inhib Med Chem* **2019**, *34* (1), 1110–1120.

(135) Madhu Sekhar, M.; Nagarjuna, U.; Padmavathi, V.; Padmaja, A.; Reddy, N. V.; Vijaya, T. Synthesis and Antimicrobial Activity of Pyrimidinyl 1,3,4-Oxadiazoles, 1,3,4-Thiadiazoles and 1,2,4-Triazoles. *Eur J Med Chem* **2018**, *145*, 1–10.

(136) Jin, K. J.; Yin, H.; de Clercq, E.; Pannecouque, C.; Meng, G.; Chen, F. E. Discovery of Biphenyl-Substituted Diarylpyrimidines as Non-Nucleoside Reverse Transcriptase Inhibitors with High Potency against Wild-Type and Mutant HIV-1. *Eur J Med Chem* **2018**, *145*, 726–734.

(137) Dhillon, S.; Clark, M. Ceritinib: First Global Approval. *Drugs* **2014**, *74* (11), 1285–1291.

(138) della Corte, C. M.; Viscardi, G.; Liello, R. di; Fasano, M.; Martinelli, E.; Troiani, T.; Ciardiello, F.; Morgillo, F. Role and Targeting of Anaplastic Lymphoma Kinase in Cancer. *Mol Cancer* **2018**, *17* (30), 1–9.

(139) Shaw, A. T.; Kim, D.-W.; Mehra, R.; Tan, D. S.; Felip, E.; Chow, L. Q.; Ross Camidge, D.; Vansteenkiste, J.; Sharma, S.; de Pas, T.; Riely, G. J.; Solomon, B. J.; Wolf, J.; Thomas, M.; Schuler, M.; Liu, G.; Santoro, A.; Lau, Y. Y.; Goldwasser, M.; Boral, A. L.; Engelman, J. A.; Massachusetts General Hospital, F.; Ats, B.; National, S. Ceritinib in ALK-Rearranged Non–Small-Cell Lung Cancer. *N Engl J Med* **2014**, *370* (13), 1189–1197.

(140) Sluis-Cremer, N.; Tachedjian, G. Mechanisms of Inhibition of HIV Replication by Non-Nucleoside Reverse Transcriptase Inhibitors. *Virus Res* **2008**, *134* (1–2), 147–156.

(141) *The Pyrimidines, Volume 16, Supplement 2 - Google Books*. https://books.google.co.za/books?hl=en&lr=&id=J92YIS3ZOIEC&oi=fnd&pg=PP1&dq=pyrimidines+Chapter+II&ots=CriT7Eghrs&sig=WsMjAqp6rLQmAlgYPDsDAxGEgQs&redir_esc=y#v=onepage&q=pyrimidines%20Chapter%20II&f=false (accessed 2022-06-11).

(142) Grimaux, E. Synthesis of Uric Derivatives of the Alloxan Series,. *J Am Chem Soc* **2004**, *1* (7), 275–276.

(143) Falco, E. A.; Du, S. B.; Hitchings, G. H. 2,4-Diaminopyrimidines as Antimalarials. II. 5-Benzyl Derivatives. *J Am Chem Soc* **1951**, *73* (8), 3758–3762.

(144) Russell, P. B.; Hitchings, G. H. 2,4-Diaminopyrimidines as Antimalarials. III. 5-Aryl Derivatives. *J Am Chem Soc* **1951**, *73* (8), 3763–3770.

(145) Ahmad, S.; Ngu, K.; Combs, D. W.; Wu, S. C.; Weinstein, D. S.; Liu, W.; Chen, B. C.; Chandrasena, G.; Dorso, C. R.; Kirby, M.; Atwal, K. S. Aminoimidazoles as Bioisosteres of Acylguanidines: Novel, Potent, Selective and Orally

Bioavailable Inhibitors of the Sodium Hydrogen Exchanger Isoform-1. *Bioorg Med Chem Lett* **2004**, *14* (1), 177–180.

(146) Létinois, U.; Schütz, J.; Härter, R.; Stoll, R.; Huffschmidt, F.; Bonrath, W.; Karge, R. Lewis Acid-Catalyzed Synthesis of 4-Aminopyrimidines: A Scalable Industrial Process. *Org Process Res Dev* **2013**, *17* (3), 427–431.

(147) El-Hamamsy, M. H. R. I.; Smith, A. W.; Thompson, A. S.; Threadgill, M. D. Structure-Based Design, Synthesis and Preliminary Evaluation of Selective Inhibitors of Dihydrofolate Reductase from Mycobacterium Tuberculosis. *Bioorg Med Chem* **2007**, *15* (13), 4552–4576.

(148) Ito, I.; Oda, N.; Kato, T.; Ota, K. Synthesis of Compounds Related to Antitumor Agents. II. Studies on the Synthesis of Oxazolo [4, 5-d] Pyrimidine Nucleoside Derivatives. *Chem Pharm Bull (Tokyo)* **1975**, *23* (9), 2104–2108.

(149) Goswami, S.; Jana, S.; Dey, S.; Kumar Adak, A. Microwave-Expedited One-Pot, Two-Component, Solvent-Free Synthesis of Functionalized Pyrimidines. *Aust. J. Chem* **2007**, *60*, 120–123.

(150) Kappe, C. O.; Dallinger, D. The Impact of Microwave Synthesis on Drug Discovery. *Nat Rev Drug Discov* **2006**, *5* (1), 51–63.

(151) *1,4-Dioxane - American Chemical Society*. https://www.acs.org/content/acs/en/molecule-of-the-week/archive/d/dioxane.html (accessed 2022-07-06).

(152) Sonogashira, K.; Tohda, Y.; Hagihara, N. A Convenient Synthesis of Acetylenes: Catalytic Substitutions of Acetylenic Hydrogen with Bromoalkenes, Iodoarenes and Bromopyridines. *Tetrahedron Lett* **1975**, *16* (50), 4467–4470.

(153) Johansson Seechurn, C. C. C.; Kitching, M. O.; Colacot, T. J.; Snieckus, V. Palladium-Catalyzed Cross-Coupling: A Historical Contextual Perspective to the 2010 Nobel Prize. *Angew Chem Int Ed* **2012**, *51* (21), 5062–5085.

(154) Jira, R. Acetaldehyde from Ethylene - A Retrospective on the Discovery of the Wacker Process. *Angew Chem Int Ed* **2009**, *48* (48), 9034–9037.

(155) Colacot, T. J. *New Trends in Cross-Coupling*; Colacot, T., Ed.; Catalysis Series; Royal Society of Chemistry: Cambridge, 2014.

(156) Fujiwara, Y.; Moritani, I.; Danno, S.; Asano, R.; Teranishi, S. Aromatic Substitution of Olefins. VI. Arylation of Olefins with Palladium (II) Acetate. *J Am Chem Soc* **1969**, *91* (25), 7166–7169.

(157) Dieck, H. A.; Heck, F. R. Palladium Catalyzed Synthesis of Aryl, Heterocyclic and Vinylic Acetylene Derivatives. *J Organomet Chem* **1975**, *93* (2), 259–263.

(158) Cassar, L. Synthesis of Aryl- and Vinyl-Substituted Acetylene Derivatives by the Use of Nickel and Palladium Complexes. *J Organomet Chem* **1975**, *93* (2), 253–257.

(159) Beierlein, J. M.; Frey, K. M.; Bolstad, D. B.; Pelphrey, P. M.; Joska, T. M.; Smith, A. E.; Priestley, N. D.; Wright, D. L.; Anderson, A. C. Synthetic and Crystallographic Studies of a New Inhibitor Series Targeting Bacillus Anthracis Dihydrofolate Reductase. *J Med Chem* **2008**, *51*, 7532–7540.

(160) Beesu, M.; Salyer, A. C. D.; Brush, M. J. H.; Trautman, K. L.; Hill, J. K.; David, S. A. Identification of High-Potency Human TLR8 and Dual TLR7/TLR8 Agonists in Pyrimidine-2,4-Diamines. *J Med Chem* **2017**, *60* (5), 2084–2098.

(161) Chinchilla, R.; Nájera, C. The Sonogashira Reaction: A Booming Methodology in Synthetic Organic Chemistry. *Chem Rev* **2007**, *107* (3), 874–922.

(162) Jones, M. L.; Baccanari, D. p.; Tansik, R. L.; Boytos, C. M.; Rudolph, S. K.; Kuyper, L. F. Inhibitors of Dihydrofolate Reductase Design Synthesis and Antimicrobial Activities of 2,4-Diamino-6-Methyl-5-Ethynylpyrimidines. *J Heterocycl Chem* **1999**, *36*, 145–148.

(163) Roberts, J. D.; Caserio, M. C. *Modern Organic Chemistry*; W.A. Benjamin , Inc: New York, 1967.

(164) Böhm, V. P. W.; Herrmann, W. A. Coordination Chemistry and Mechanisms of Metal-Catalyzed CC Coupling Reactions, 13 [‡] A Copper-Free Procedure for the Palladium-Catalyzed Sonogashira Reaction of Aryl Bromides with Terminal Alkynes at Room Temperature. *European J Org Chem* **2000**, *11* (12), 3679–3681.

(165) Henning, H. Novel Synthetic Methodology for the Assembly of α-Carbolines and 7-Azaindoles, 2018.

(166) Elangovan, A.; Wang, Y.-H.; Ho, T.-I. Sonogashira Coupling Reaction with Diminished Homocoupling. *J. Photochem. Photobiol. A: Chem* **1998**, *120* (2), 1841–1844.

(167) Liu, Q.; Burton, D. J. A Facile Synthesis of Diynes. *Tetrahedron Lett* **1997**, *38* (25), 4371–4374.

(168) Clayden Jonathan; Greeves, N.; Warren, S. *Organic Chemistry*, second.; Oxford university press: New York, 2012.

(169) Liu, X. *10.5 Reaction of Alkenes: Hydrogenation*.

(170) Holy, N. L.; Shelton', S. R. Hydrogenation of Alkynes with a Palladium Anchored Polystyrene Catalyst. *Tetrahedron* **1981**, *37* (1), 25–26.

(171) Tarnchompoo, B.; Chitnumsub, P.; Jaruwat, A.; Shaw, P. J.; Vanichtanankul, J.; Poen, S.; Rattanajak, R.; Wongsombat, C.; Tonsomboon, A.; Decharuangsilp, S.; Anukunwithaya, T.; Arwon, U.; Kamchonwongpaisan, S.; Yuthavong, Y. Hybrid Inhibitors of Malarial Dihydrofolate Reductase with Dual Binding Modes That Can Forestall Resistance. *ACS Med Chem Lett* **2018**, *9* (12), 1235–1240.

(172) Nzila, A.; Mwai, L. In Vitro Selection of Plasmodium Falciparum Drug-Resistant Parasite Lines. *J Antimicrob Chemother* **2010**, *65* (3), 390–398.

(173) Adewusi, E. A.; Steenkamp, P.; Fouche, G.; Steenkamp, V. Isolation of Cycloeucalenol from Boophone Disticha and Evaluation of Its Cytotoxicity. *Nat Prod Commun* **2013**, *8* (9), 1213–1216.

(174) Liu, S.; Su, M.; Song, S. J.; Jung, J. H. Marine-Derived Penicillium Species as Producers of Cytotoxic Metabolites. *Mar Drugs* **2017***,* 15 (10), 329–372.

(175) Finiuk, N. S.; Hreniuh, V. P.; Ostapiuk, Y. v.; Matiychuk, V. S.; Frolov, D. A.; Obushak, M. D.; Stoika, R. S.; Babsky, A. M. Antineoplastic Activity of Novel Thiazole Derivatives. *Biopolym Cell* **2017**, *33* (2), 135–146.

(176) Oliveira, F. A.; Pinto, A. C. S.; Duarte, C. L.; Taranto, A. G.; Lorenzato Junior, E.; Cordeiro, C. F.; Carvalho, D. T.; Varotti, F. P.; Fonseca, A. L. Evaluation of Antiplasmodial Activity in Silico and in Vitro of N-Acylhydrazone Derivatives. *BMC Chem* **2022**, *16* (1), 1–13.

(177) Katsuno, K.; Burrows, J. N.; Duncan, K.; van Huijsduijnen, R. H.; Kaneko, T.; Kita, K.; Mowbray, C. E.; Schmatz, D.; Warner, P.; Slingsby, B. T. Hit and Lead Criteria in Drug Discovery for Infectious Diseases of the Developing World. *Nat Revs Drug Discov 2015 14:11* **2015**, *14* (11), 751–758.

(178) Ko, T. Y.; Youn, S. W. Cooperative Indium(III)/Silver(I) System for Oxidative Coupling/Annulation of 1,3-Dicarbonyls and Styrenes: Construction of Five-Membered Heterocycles. *Adv Synth Catal* **2016**, *358* (12), 1934–1941.

(179) Sun, J.; Ge, H.; Zhen, X.; An, X.; Zhang, G.; Zhang-Negrerie, D.; Du, Y.; Zhao, K. TBHP/AIBN-Mediated Synthesis of 2-Amino-Thioazoles from Active Methylene Ketones and Thiourea under Metal-Free Conditions. *Tetrahedron* **2018**, *74* (17), 2107–2114.

(180) Garg, U.; Azim, Y.; Kar, A.; Pradeep, C. P. Cocrystals/Salt of 1-Naphthaleneacetic Acid and Utilizing Hirshfeld Surface Calculations for Acid–Aminopyrimidine Synthons. *CrystEngComm* **2020**, *22* (17), 2978–2989.

(181) Tang, X. Y.; Zhang, Y. S.; He, L.; Wei, Y.; Shi, M. Intramolecular Annulation of Aromatic Rings with N-Sulfonyl 1,2,3-Triazoles: Divergent Synthesis of 3-Methylene-2,3-Dihydrobenzofurans and 3-Methylene-2,3-Dihydroindoles. *ChemComm* **2014**, *51* (1), 133–136.

(182) Schimler, S. D.; Hall, D. J.; Debbert, S. L. Anticancer (Hexacarbonyldicobalt)Propargyl Aryl Ethers: Synthesis, Antiproliferative Activity, Apoptosis Induction, and Effect on Cellular Oxidative Stress. *J Inorg Biochem* **2013**, *119*, 28–37.

(183) Chen, Y. Y.; Chen, K. L.; Tyan, Y. C.; Liang, C. F.; Lin, P. C. Synthesis of Substituted 3-Methylene-2,3-Dihydrobenzofurans and 3-Methylbenzofurans by Rhodium (II)-Catalyzed Annulation. *Tetrahedron* **2015**, *71* (36), 6210–6218.

(184) Lau, V. M.; Pfalzgraff, W. C.; Markland, T. E.; Kanan, M. W. Electrostatic Control of Regioselectivity in Au(I)-Catalyzed Hydroarylation. *J Am Chem Soc* **2017**, *139* (11), 4035–4041.

(185) Lasányi, D.; Tolnai, G. L. Copper-Catalyzed Ring Opening of [1.1.1]Propellane with Alkynes: Synthesis of Exocyclic Allenic Cyclobutanes. *Org Lett* **2019**, *21* (24), 10057–10062.

(186) Palakhachane, S.; Ketkaew, Y.; Chuaypen, N.; Sirirak, J.; Boonsombat, J.; Ruchirawat, S.; Tangkijvanich, P.; Suksamrarn, A.; Limpachayaporn, P. Synthesis of Sorafenib Analogues Incorporating a 1,2,3-Triazole Ring and Cytotoxicity towards Hepatocellular Carcinoma Cell Lines. *Bioorg Chem* **2021**, *112*.

(187) Zhu, D.; Wu, Z.; Luo, B.; Du, Y.; Liu, P.; Chen, Y.; Hu, Y.; Huang, P.; Wen, S. Heterocyclic Iodoniums for the Assembly of Oxygen-Bridged Polycyclic Heteroarenes with Water as the Oxygen Source. *Org Lett* **2018**, *20* (16), 4815–4818.

(188) Kamchonwongpaisan, S.; Vanichtanankul, J.; Tarnchompoo, B.; Yuvaniyama, J.; Taweechai, S.; Yuthavong, Y. Stoichiometric Selection of Tight-Binding Inhibitors by Wild-Type and Mutant Forms of Malarial (Plasmodium Falciparum) Dihydrofolate Reductase. *Anal Chem* **2005**, *77* (5), 1222–1227.

(189) Vanichtanankul, J.; Taweechai, S.; Uttamapinant, C.; Chitnumsub, P.; Vilaivan, T.; Yuthavong, Y.; Kamchonwongpaisan, S. Combined Spatial Limitation around Residues 16 and 108 of Plasmodium Falciparum Dihydrofolate Reductase

Explains Resistance to Cycloguanil. *Antimicrob Agents Chemother* **2012**, *56* (7), 3928–3935.

(190) Kamchonwongpaisan, S.; Vanichtanankul, J.; Taweechai, S.; Chitnumsub, P.; Yuthavong, Y. The Role of Tryptophan-48 in Catalysis and Binding of Inhibitors of Plasmodium Falciparum Dihydrofolate Reductase. *Int J Parasitol* **2007**, *37* (7), 787–793.

(191) Hoarau, M.; Suwanakitti, N.; Varatthan, T.; Thiabma, R.; Rattanajak, R.; Charoensetakul, N.; Redman, E. K.; Khotavivattana, T.; Vilaivan, T.; Yuthavong, Y.; Kamchonwongpaisan, S. Assay Development and Identification of the First Plasmodium Falciparum 7,8-Dihydro-6-Hydroxymethylpterin-Pyrophosphokinase Inhibitors. *Molecules* **2022**, *27* (11).

(192) Vichai, V.; Kirtikara, K. Sulforhodamine B Colorimetric Assay for Cytotoxicity Screening. *Nature Protocols 2006 1:3* **2006**, *1* (3), 1112–1116.

8 Appendices

^{1}H and ^{13}C NMR spectra for compound **34a** in $CDCl_3$

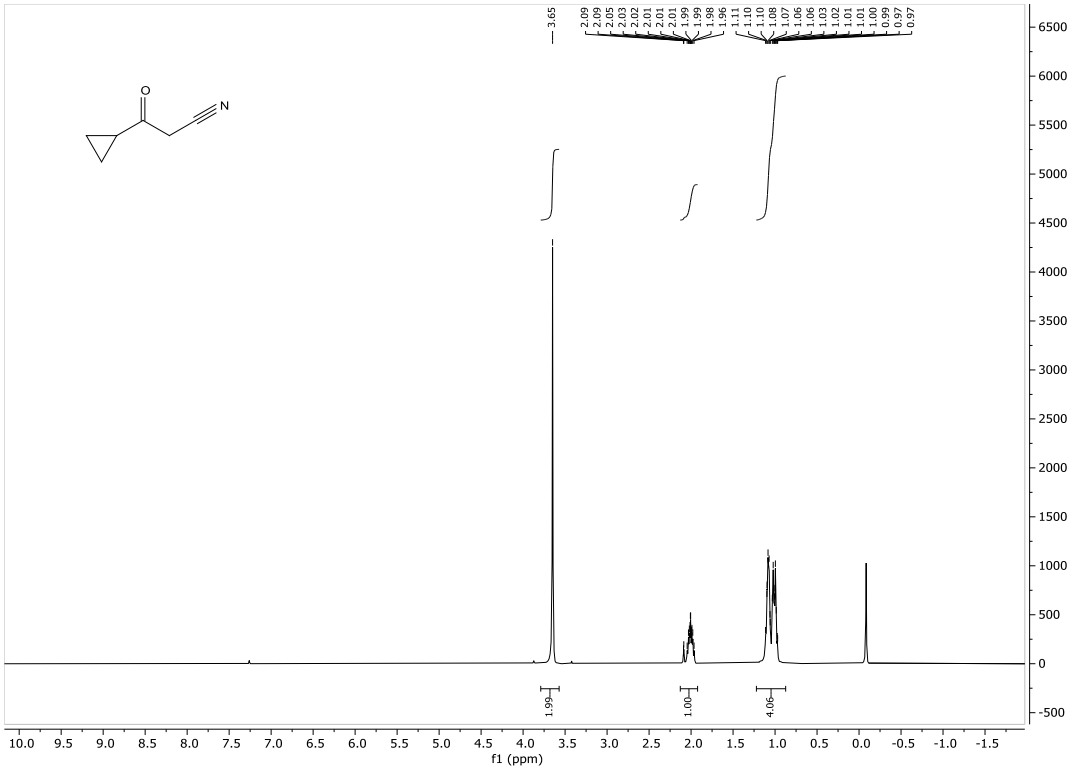

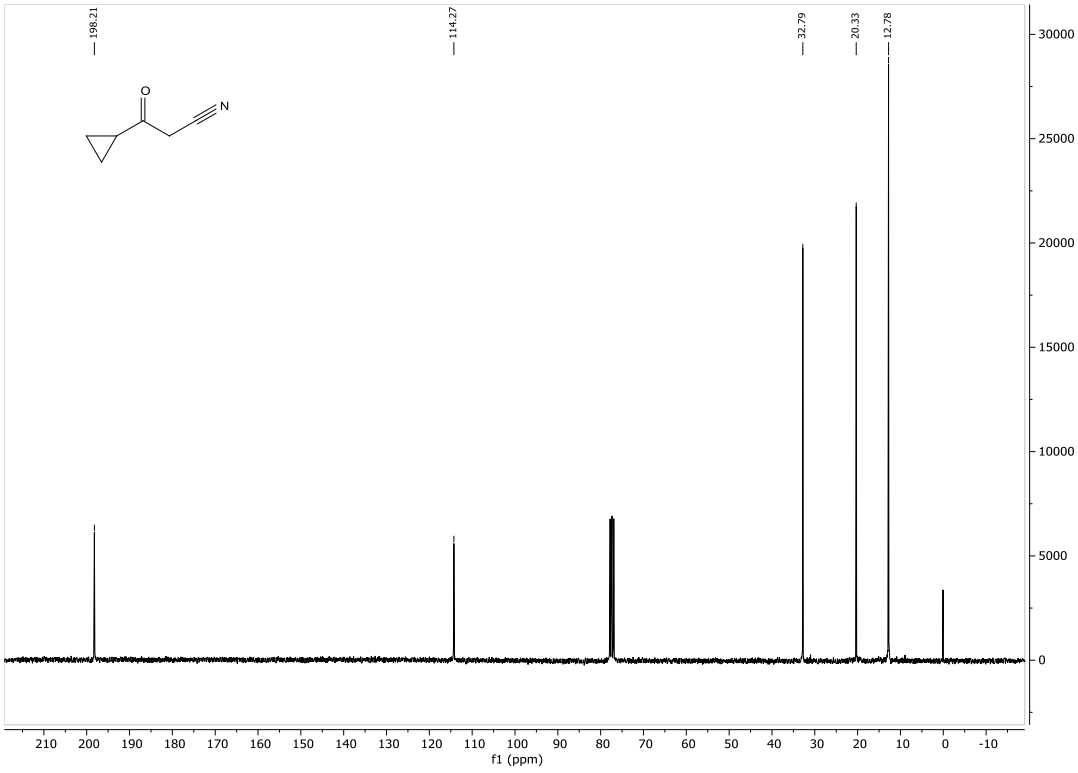

^{1}H and ^{13}C NMR spectra for compound **34c** in $CDCl_3$

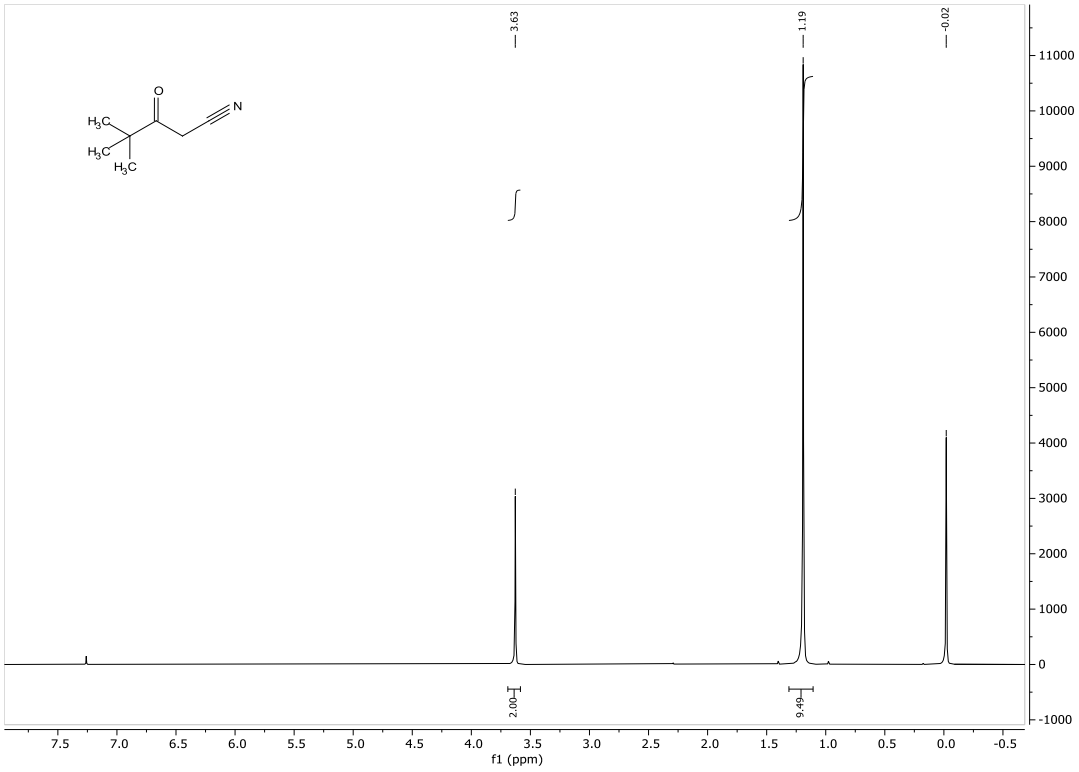

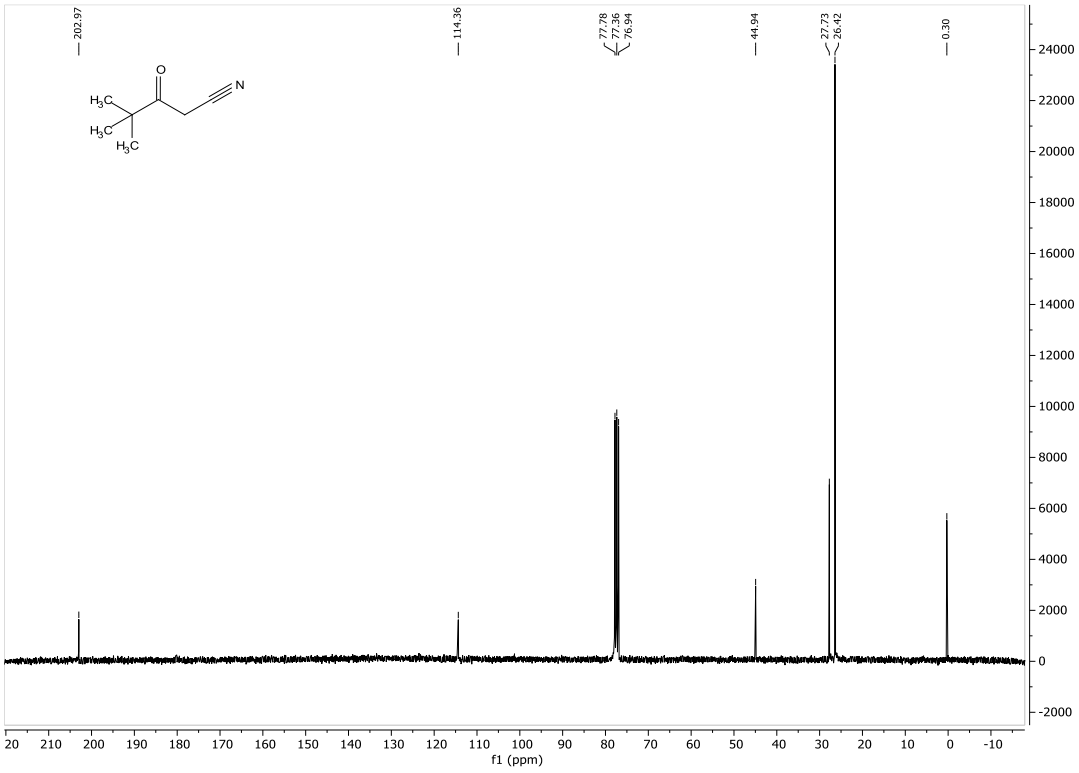

^{1}H and ^{13}C NMR spectra for compound **34d** in $CDCl_3$

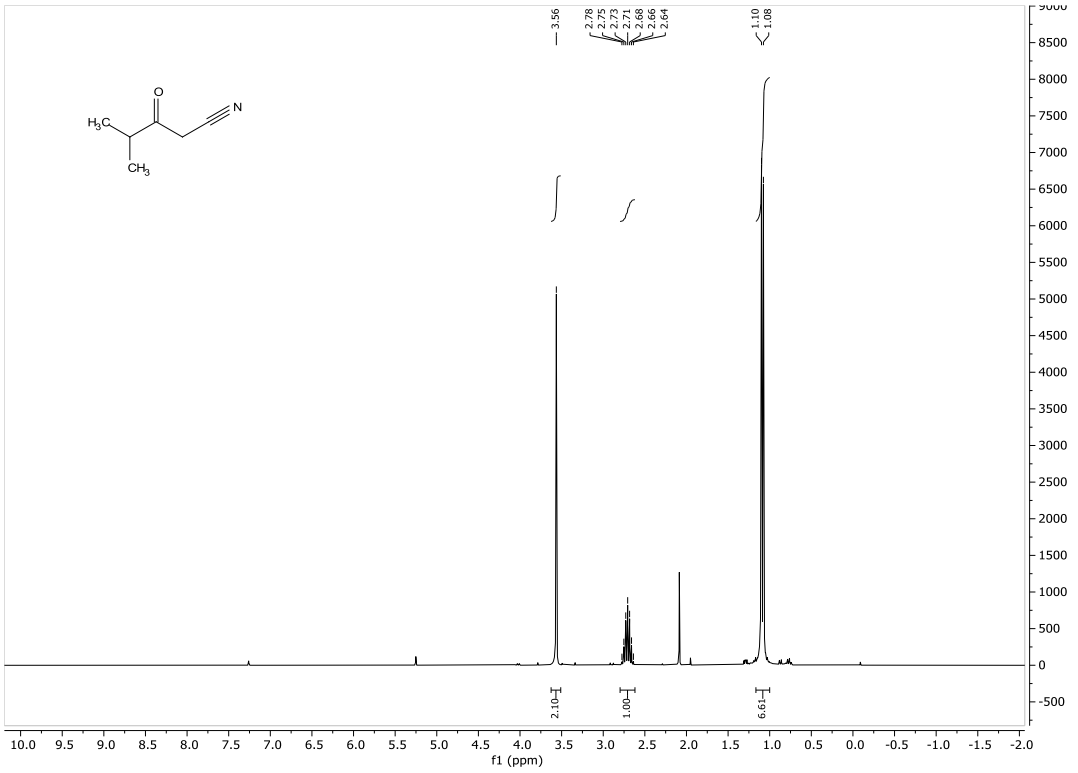

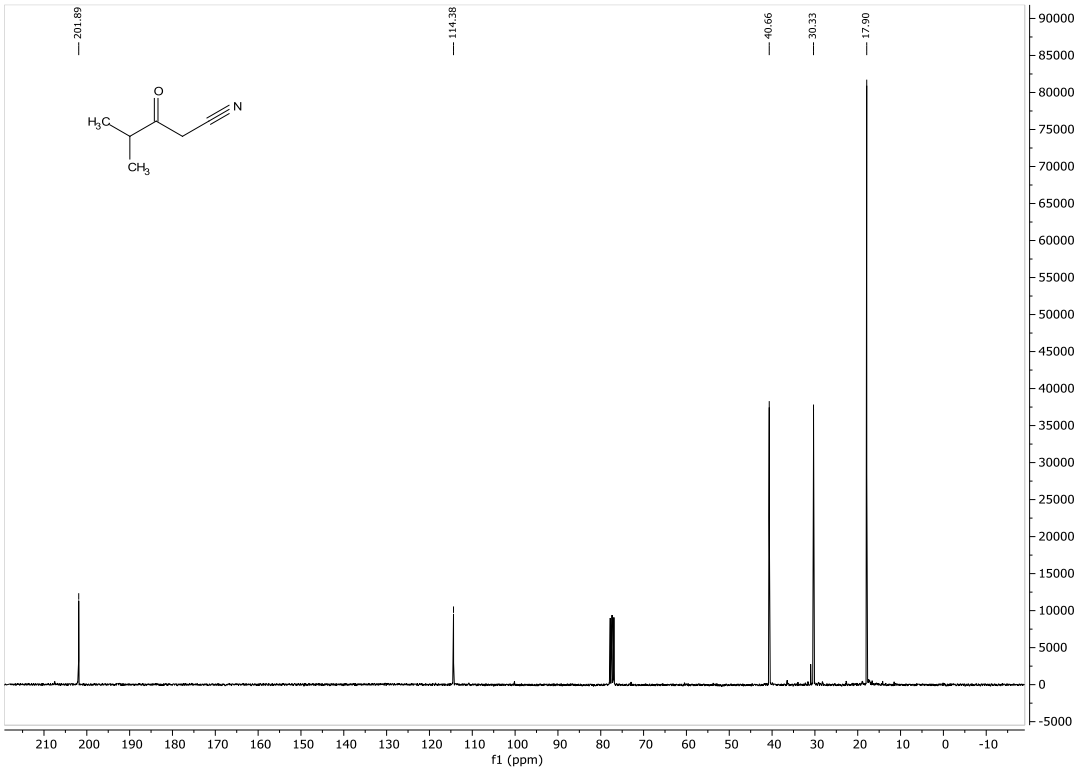

^{1}H and ^{13}C NMR spectra for compound **46a** in DMSO

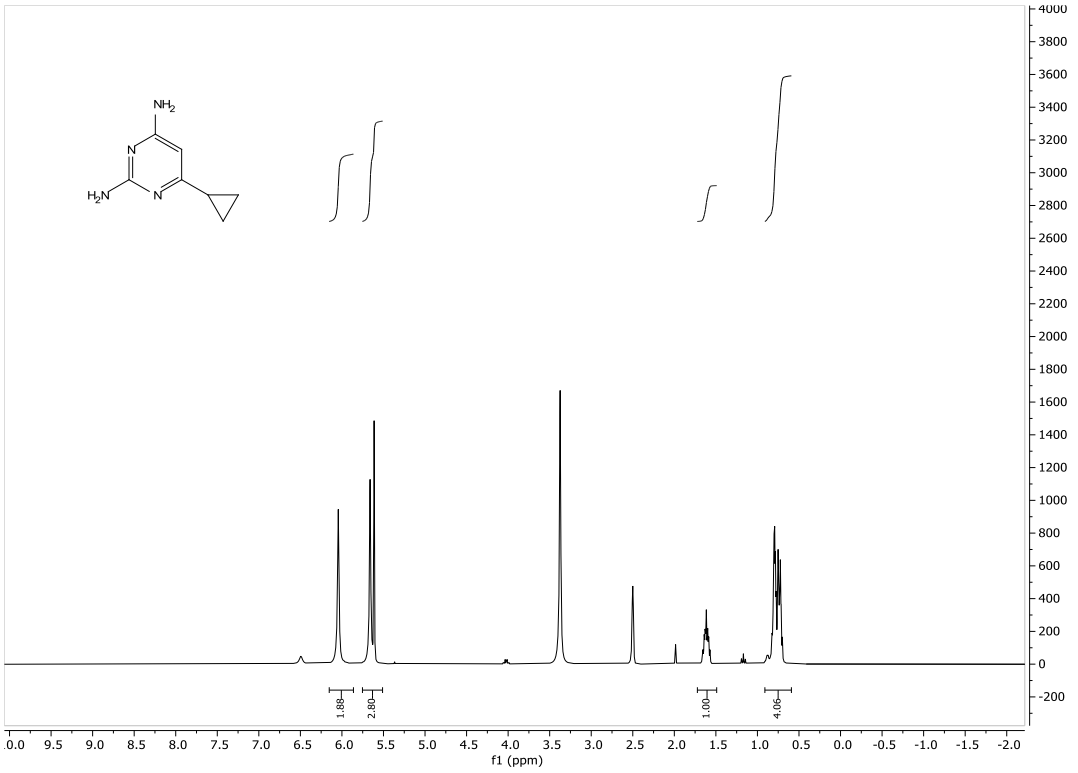

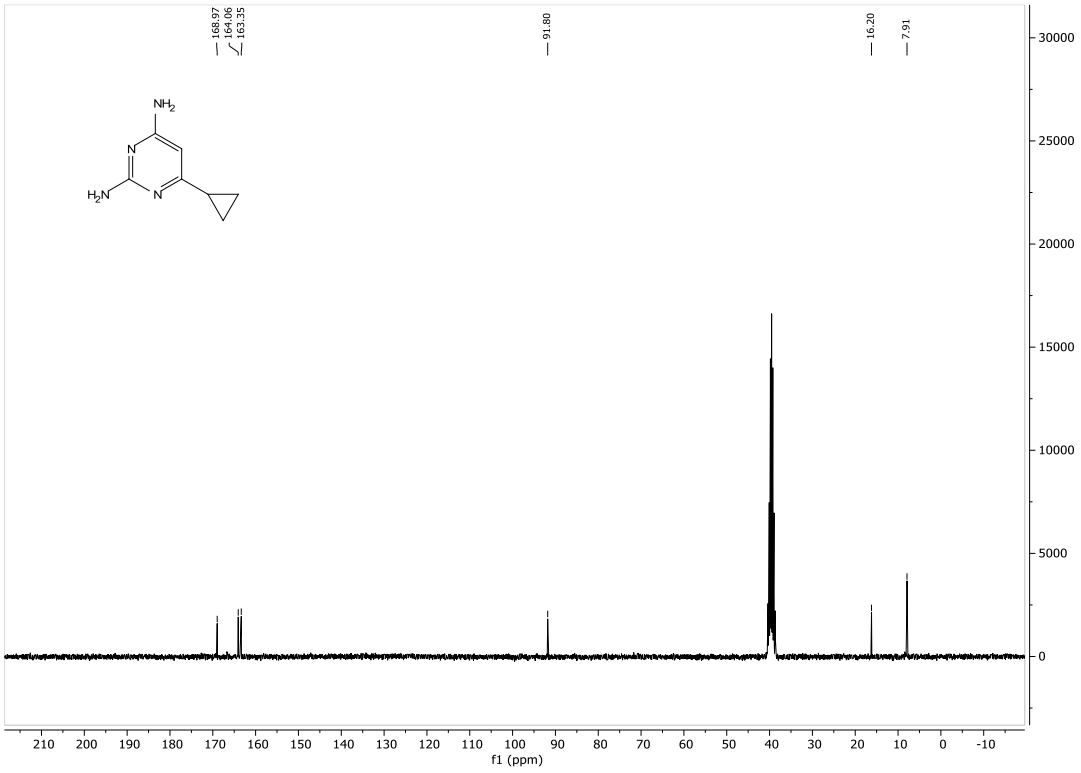

^{1}H and ^{13}C NMR spectra for compound **46c** IN DMSO

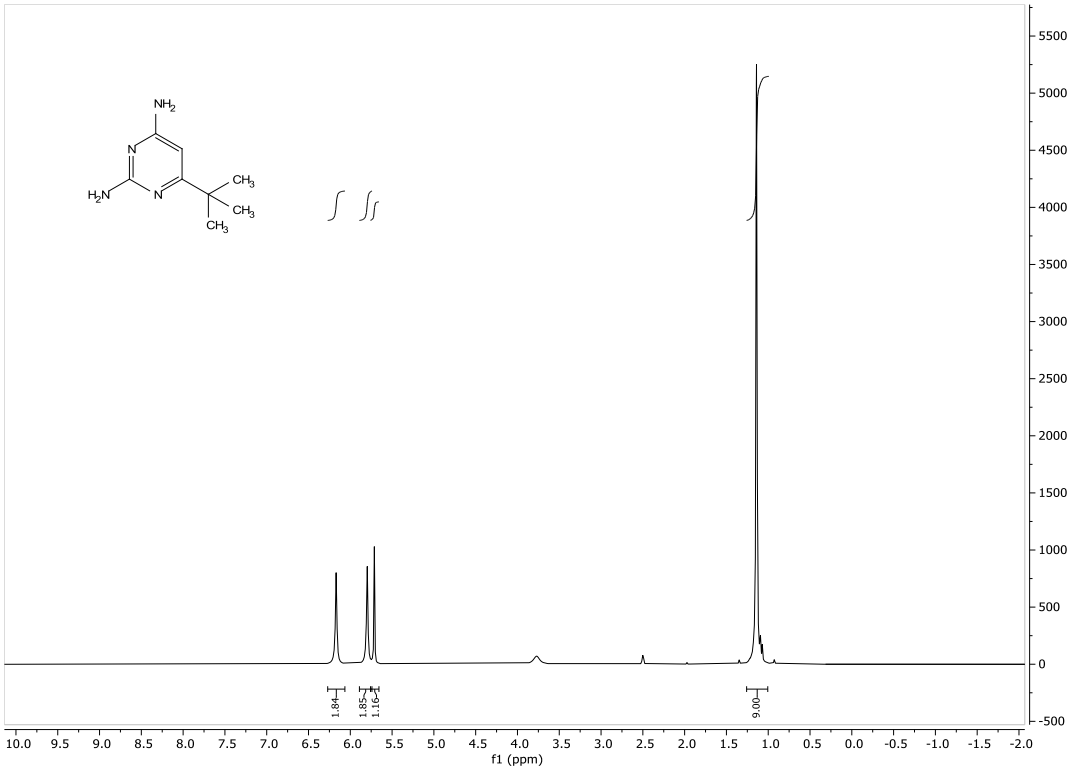

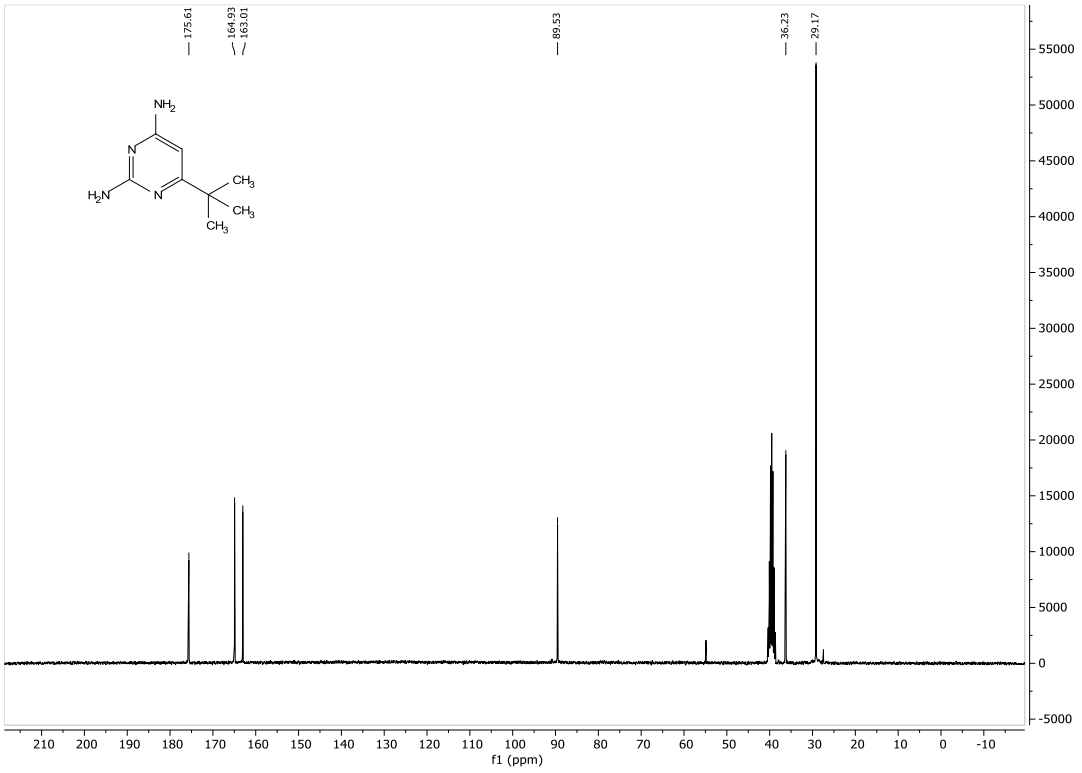

^{1}H and ^{13}C NMR spectra for compound **46d** in $CDCl_3$

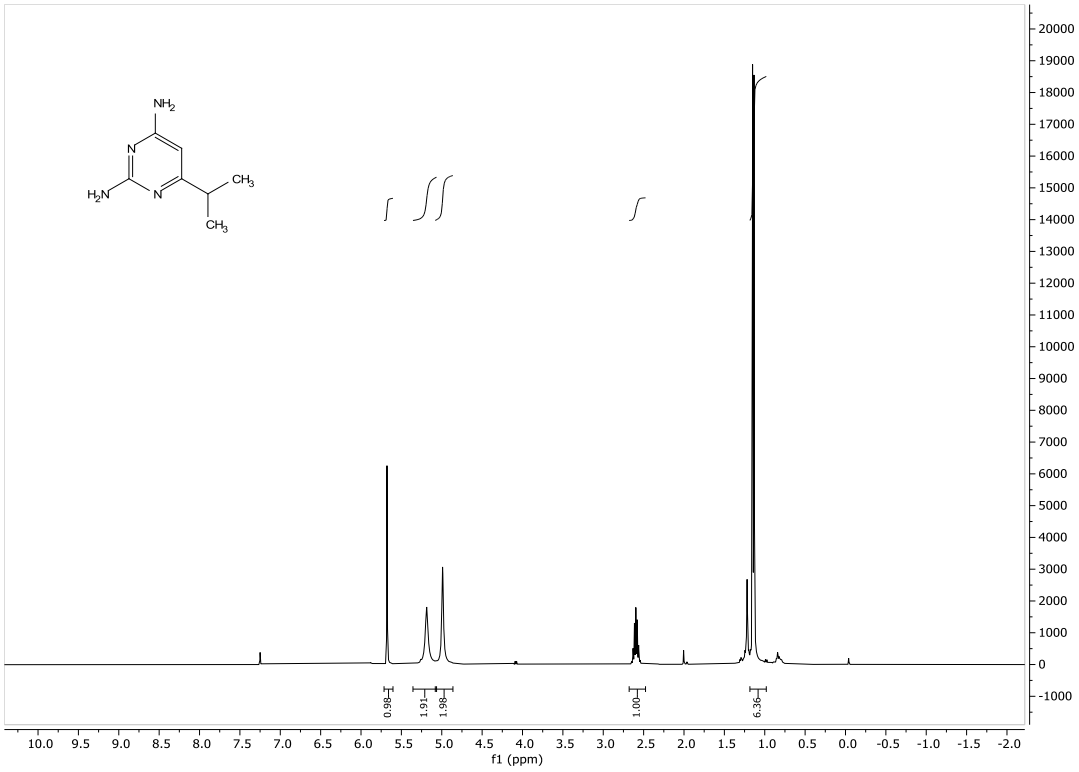

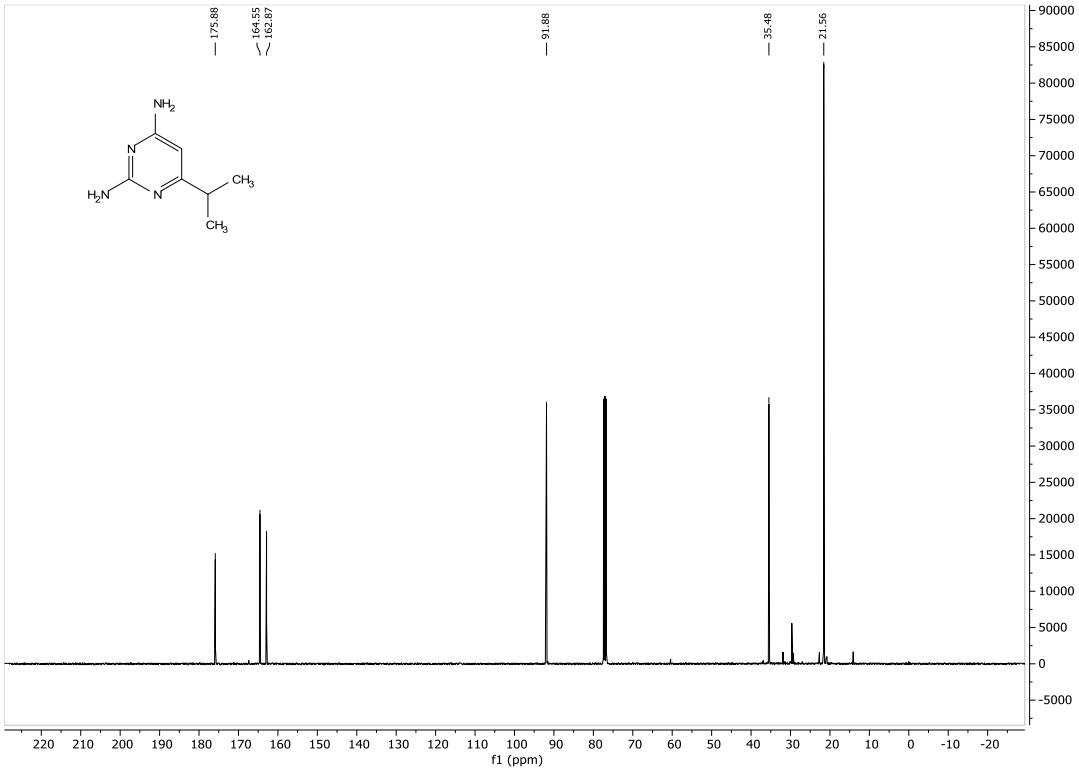

^{1}H and ^{13}C NMR spectra for compound **49a** in DMSO

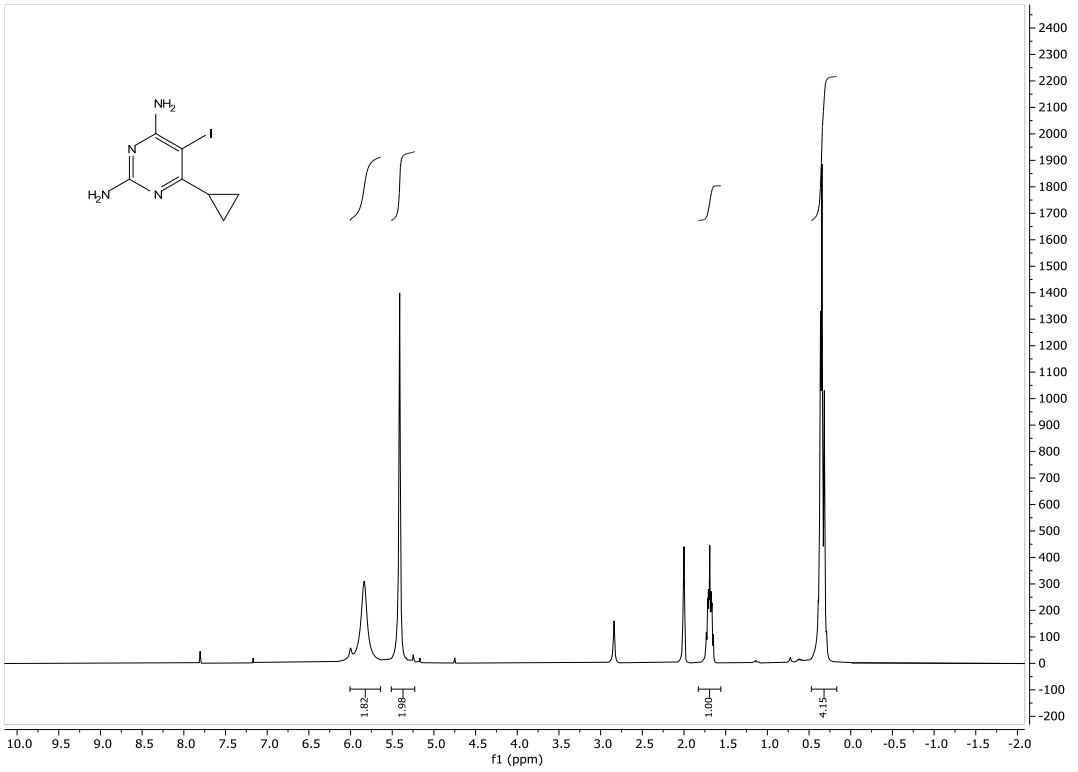

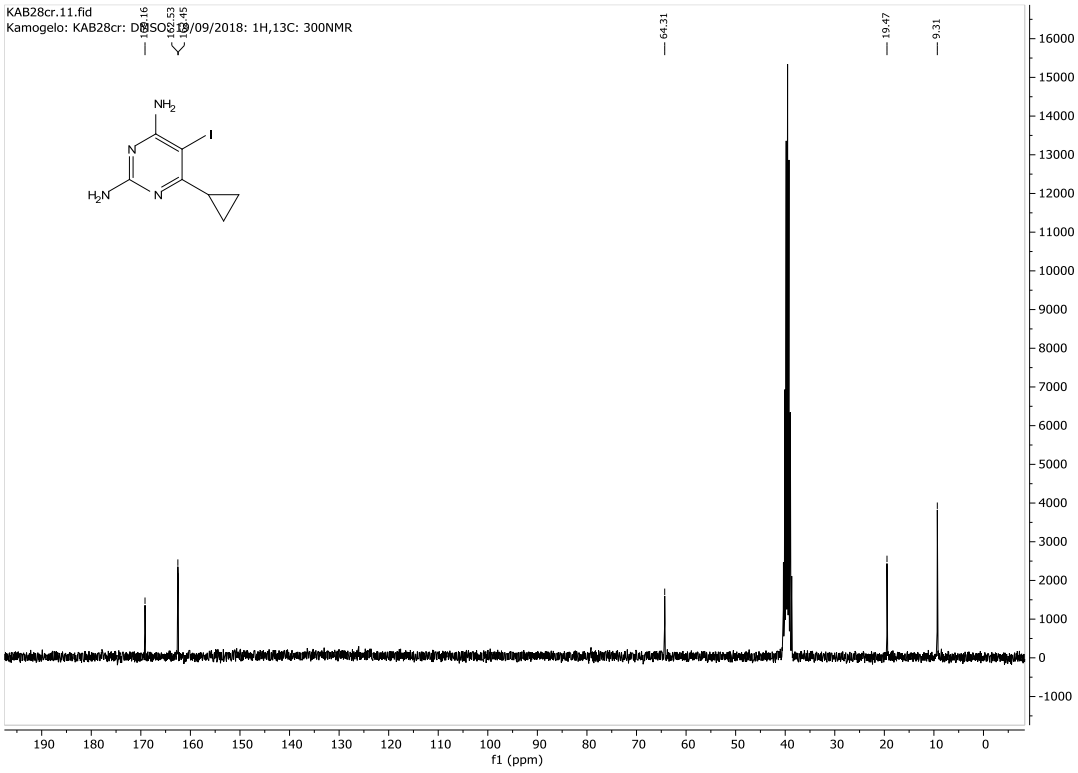

^{1}H and ^{13}C NMR spectra for compound **49c** in $CDCl_3$

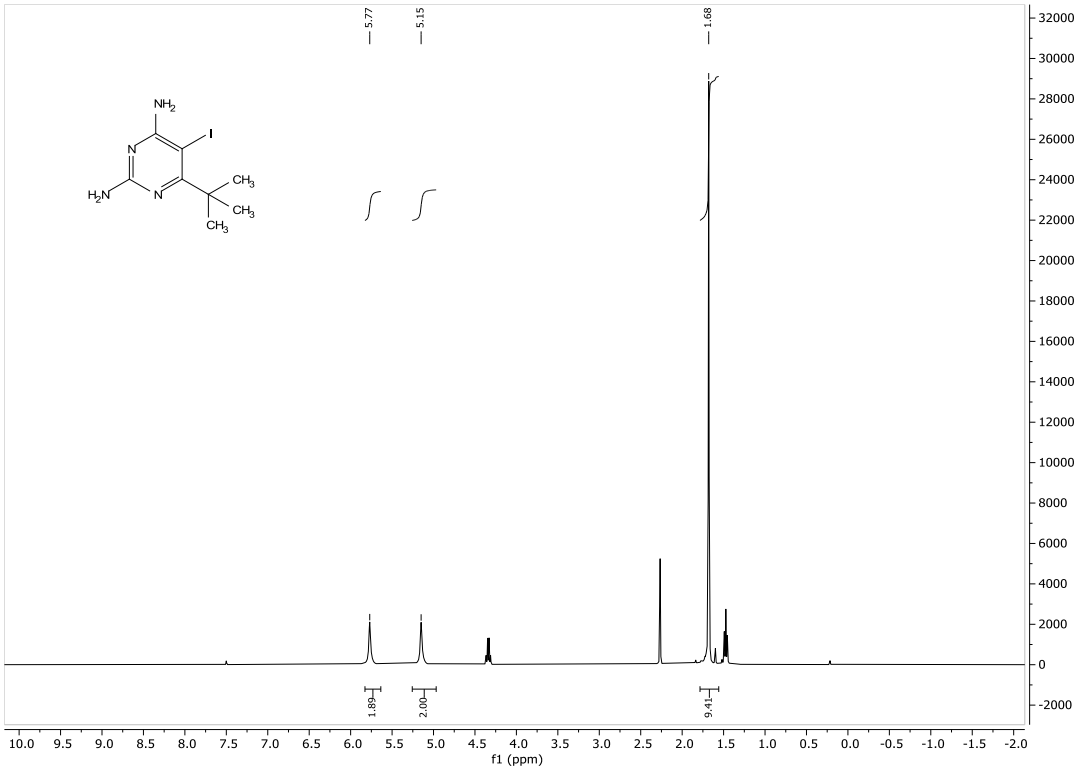

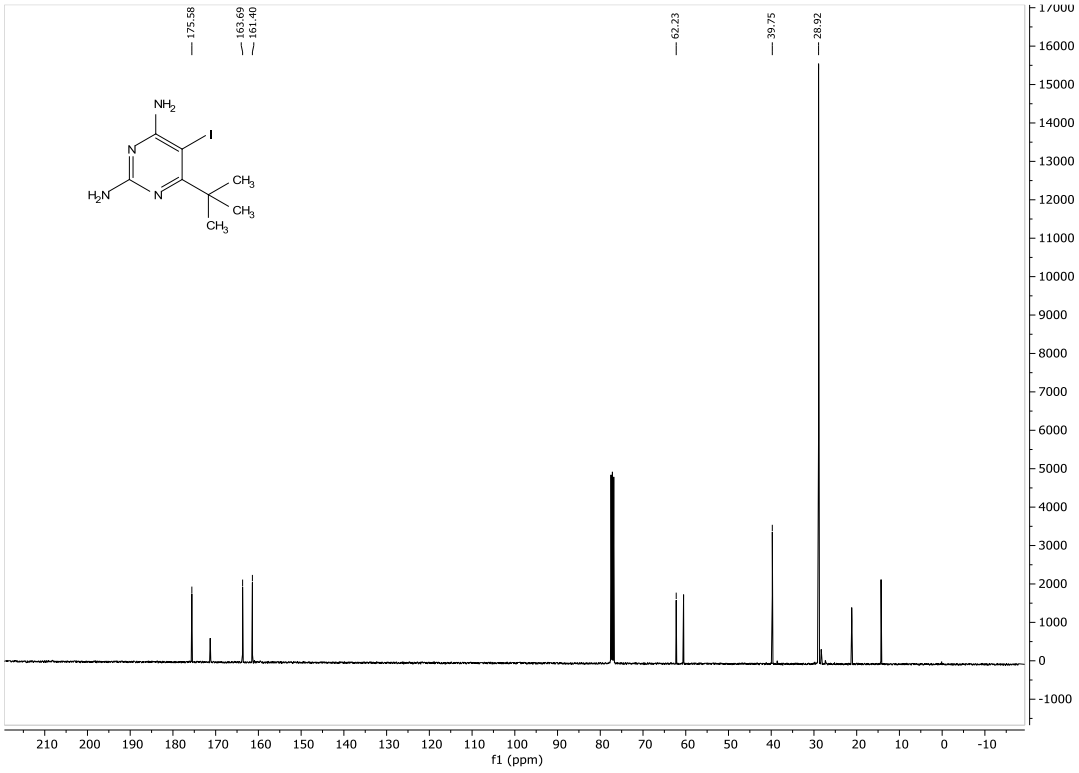

^{1}H and ^{13}C NMR spectra for compound **49d** in $CDCl_3$

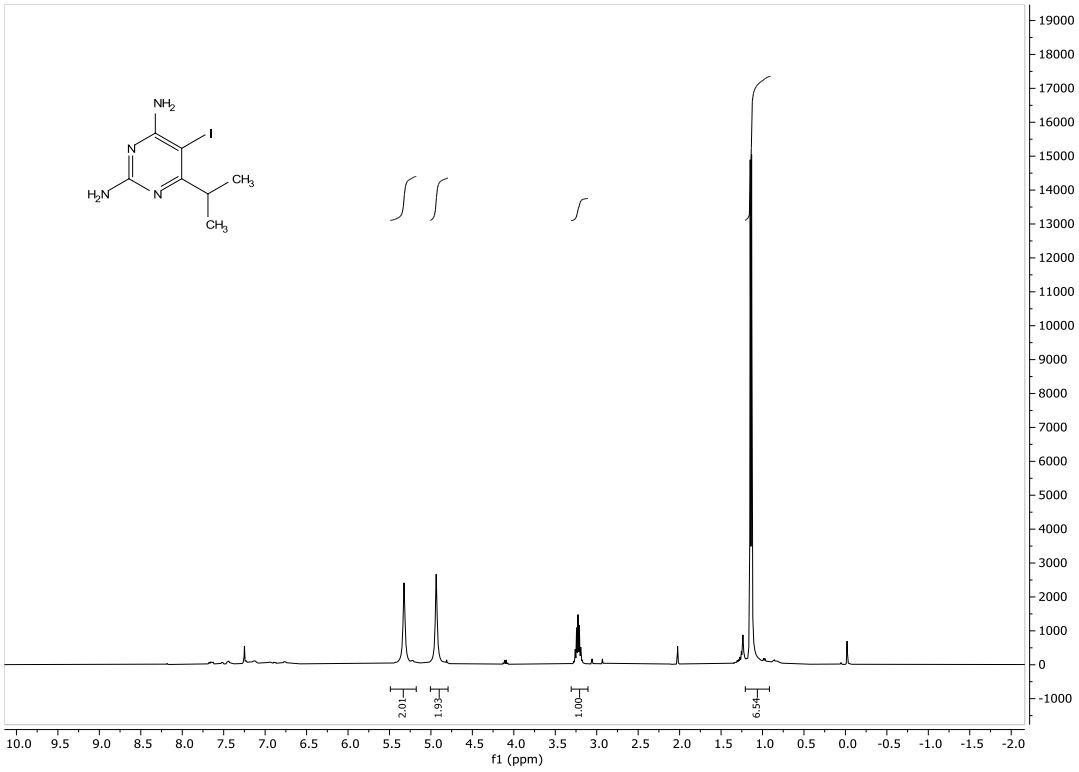

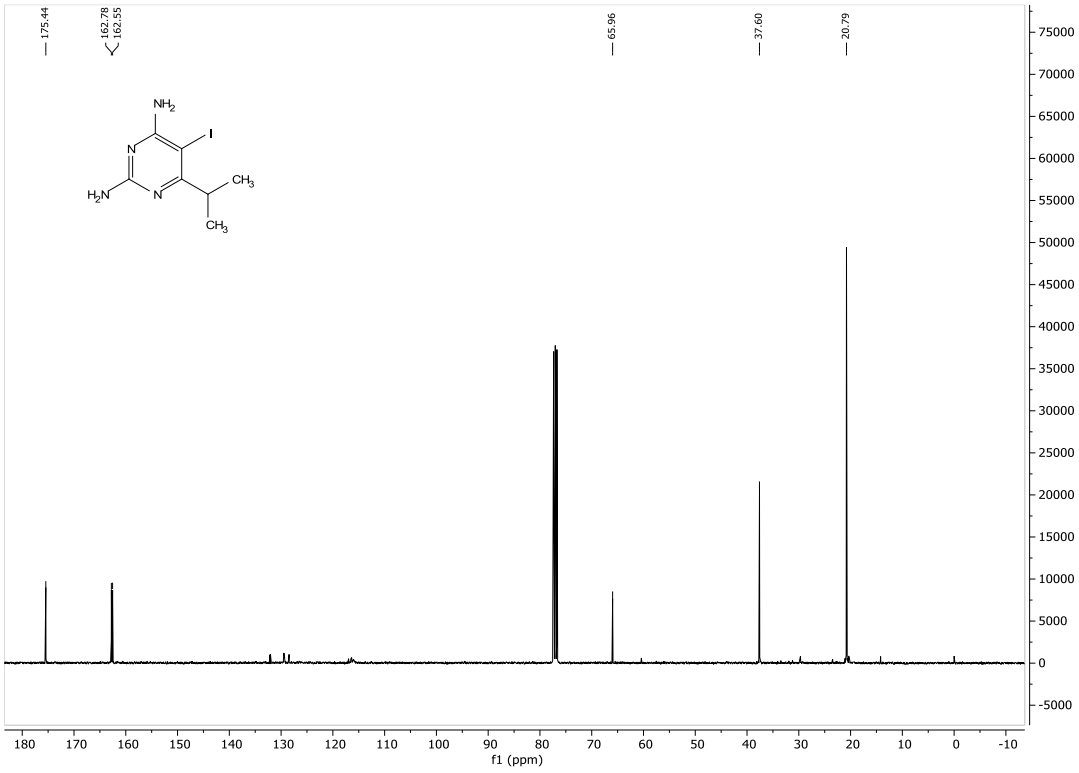

^{1}H and ^{13}C NMR spectra for compound **57b** in $CDCl_3$

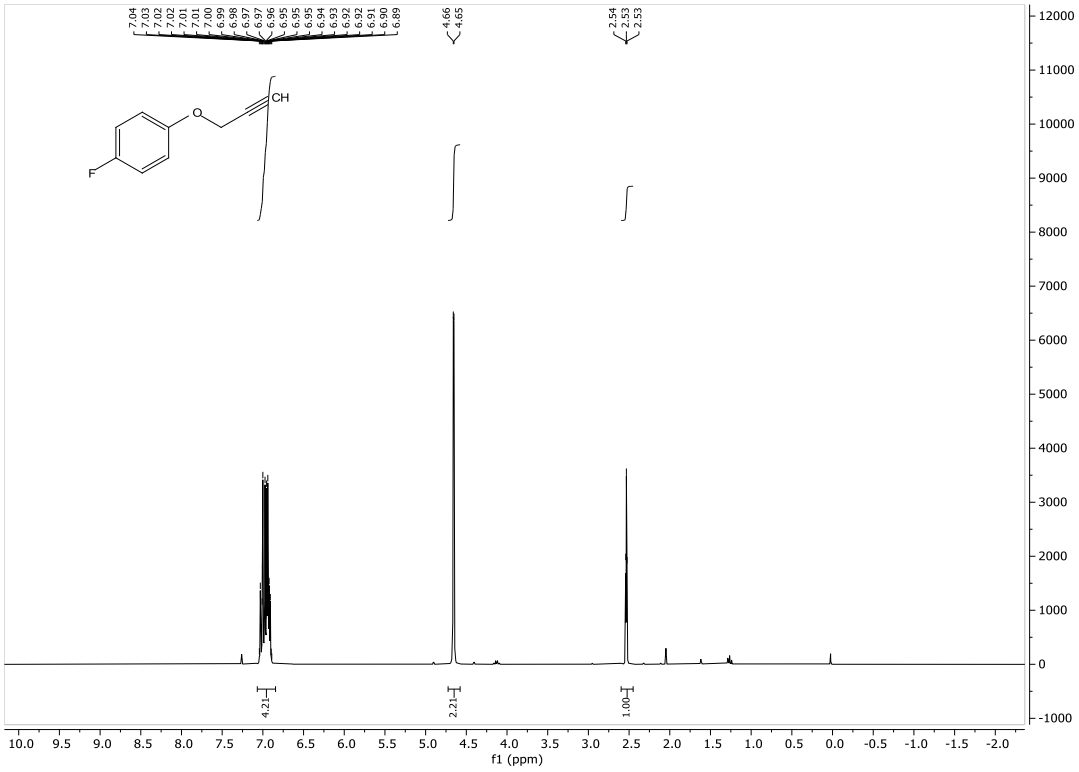

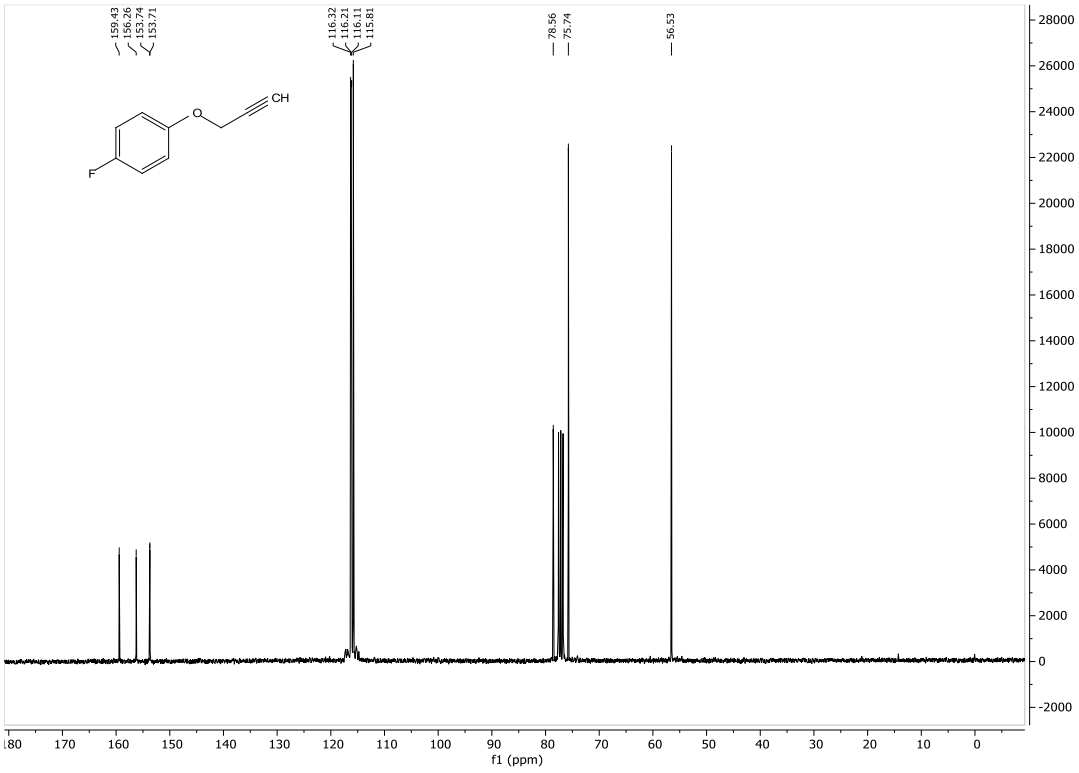

^{1}H and ^{13}C NMR spectra for compound **58a** in $CDCl_3$

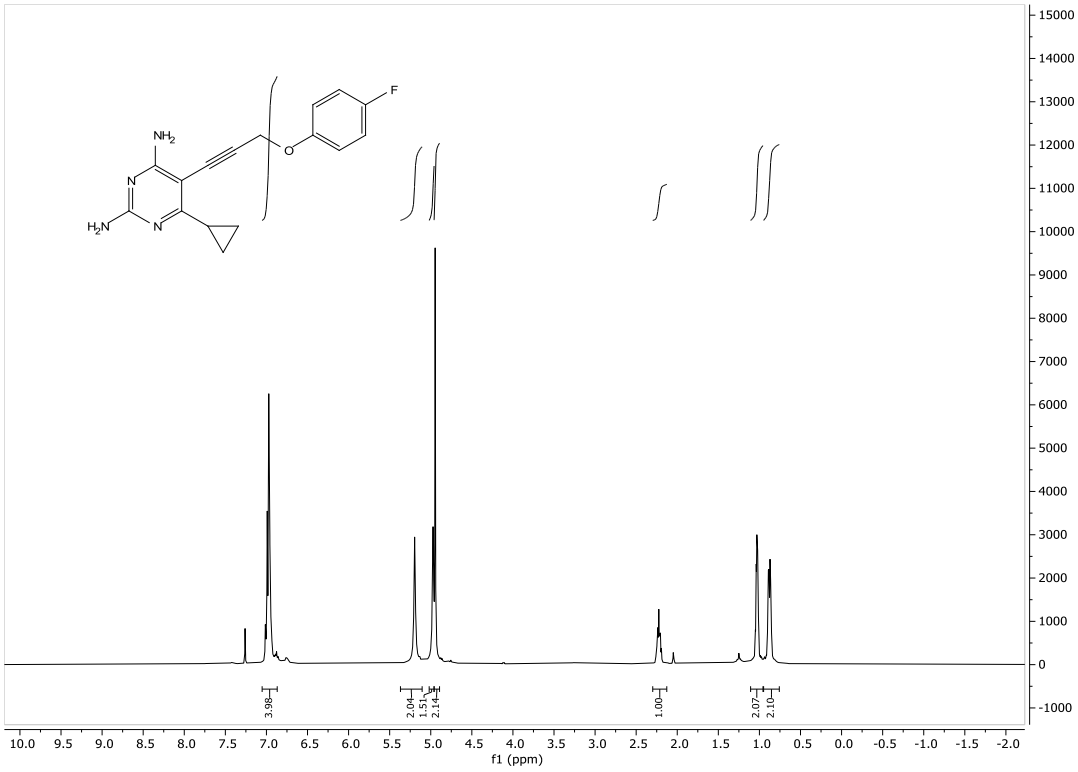

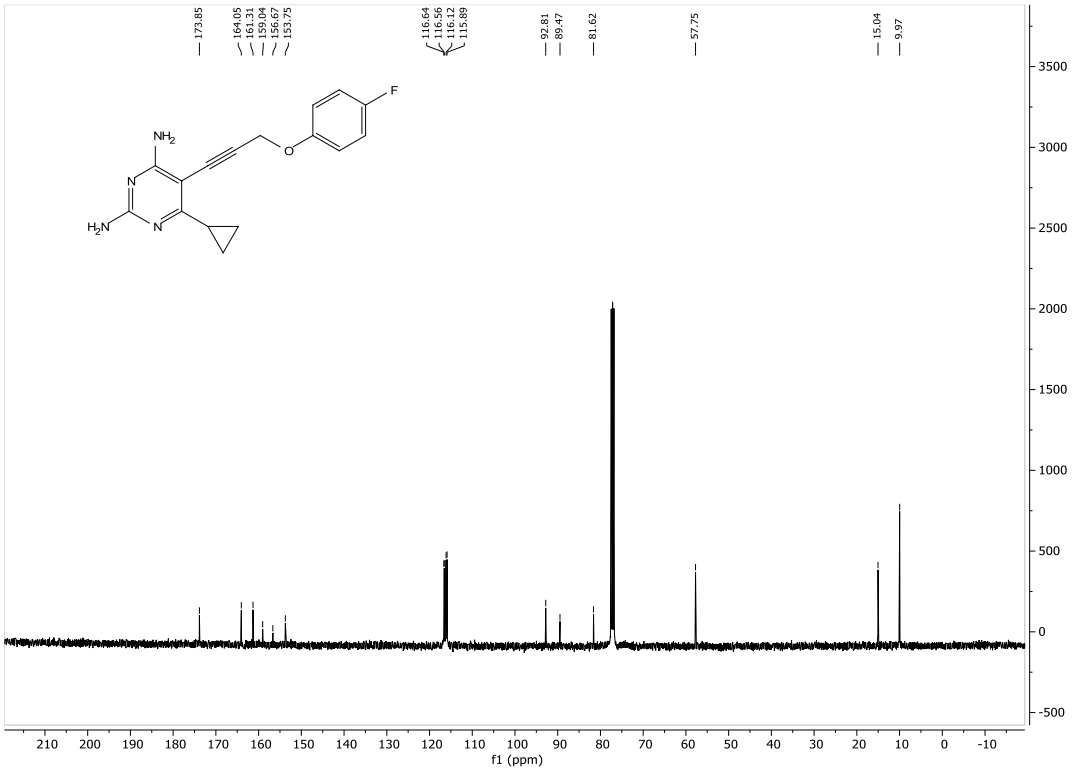

^{1}H and ^{13}C NMR spectra for compound **58b** in $CDCl_3$

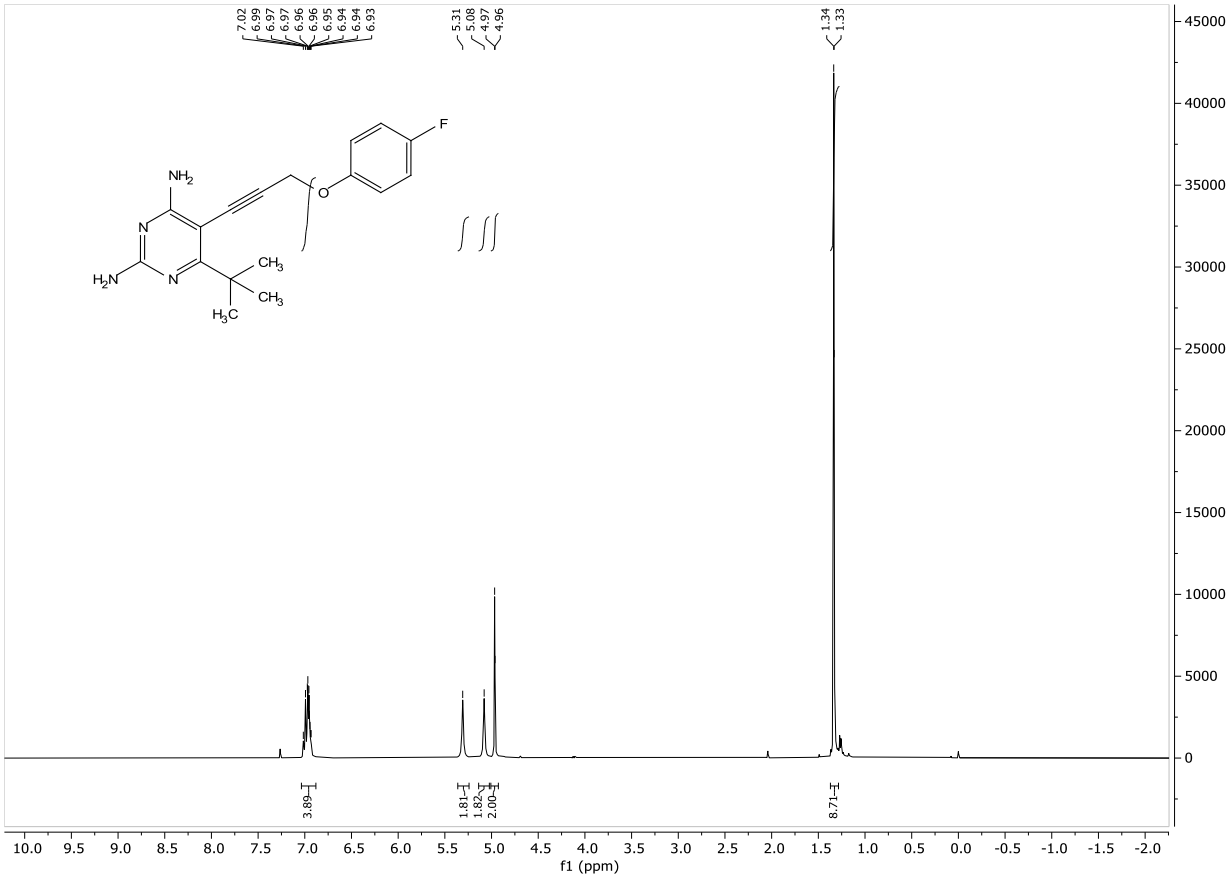

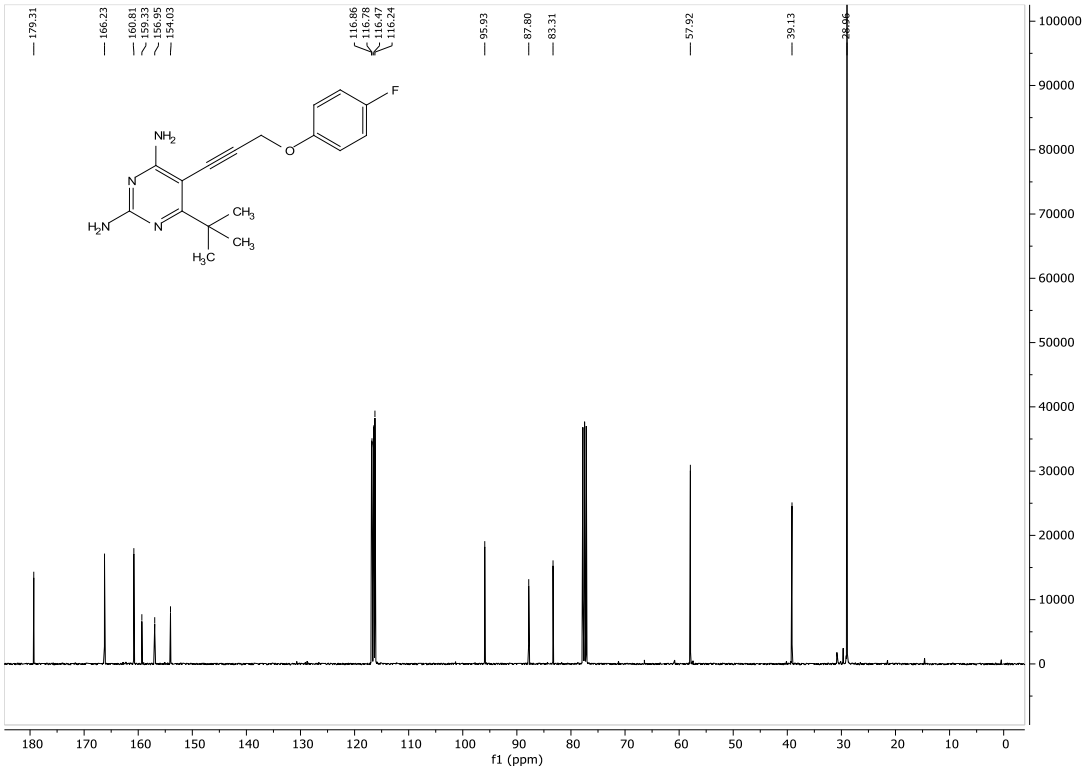

^{1}H and ^{13}C NMR spectra for compound **59b** in $CDCl_3$

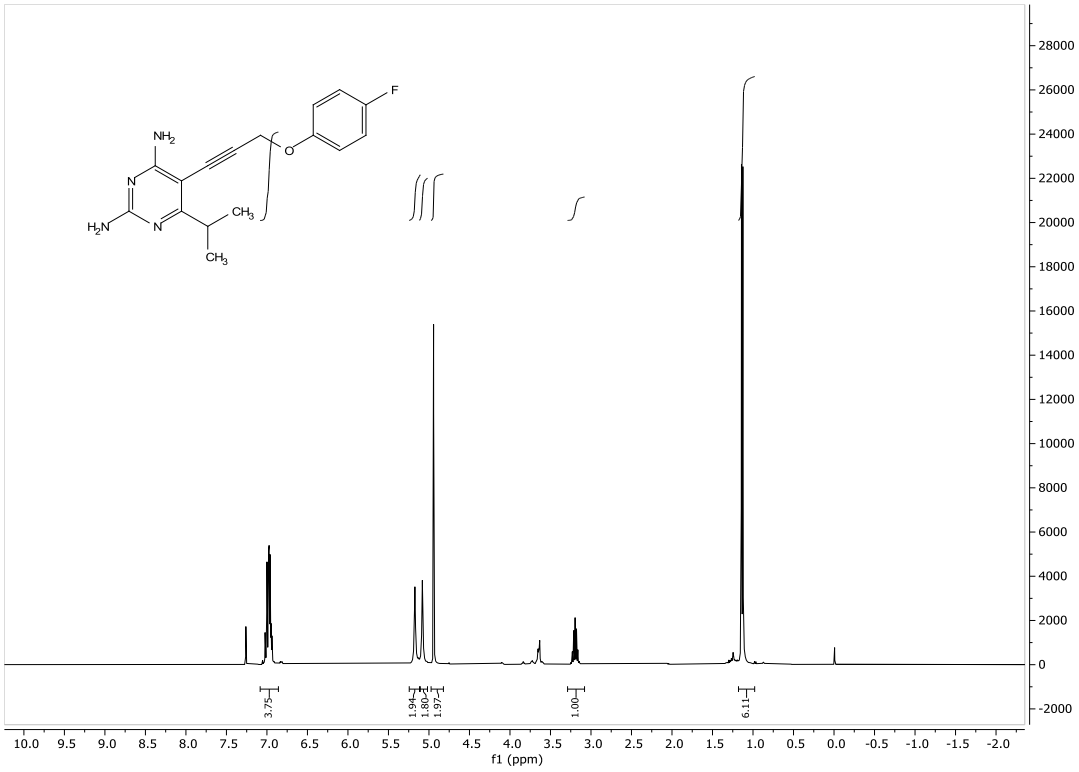

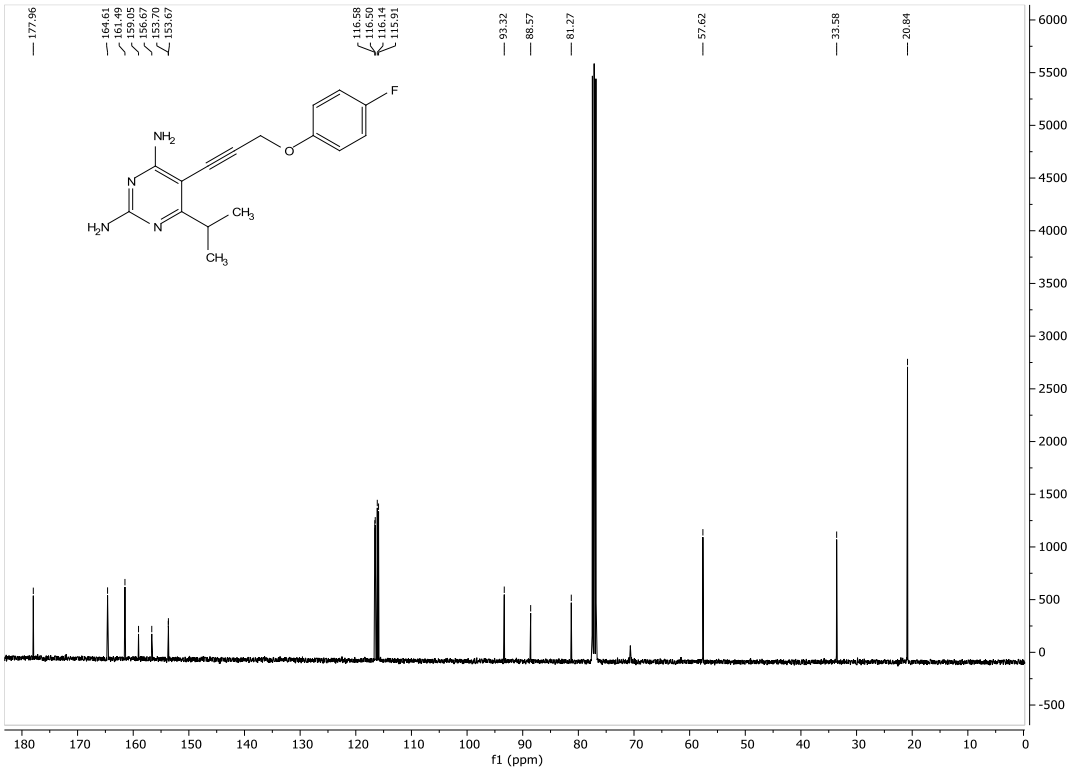

^{1}H and ^{13}C NMR spectra for compound in $CDCl_3$

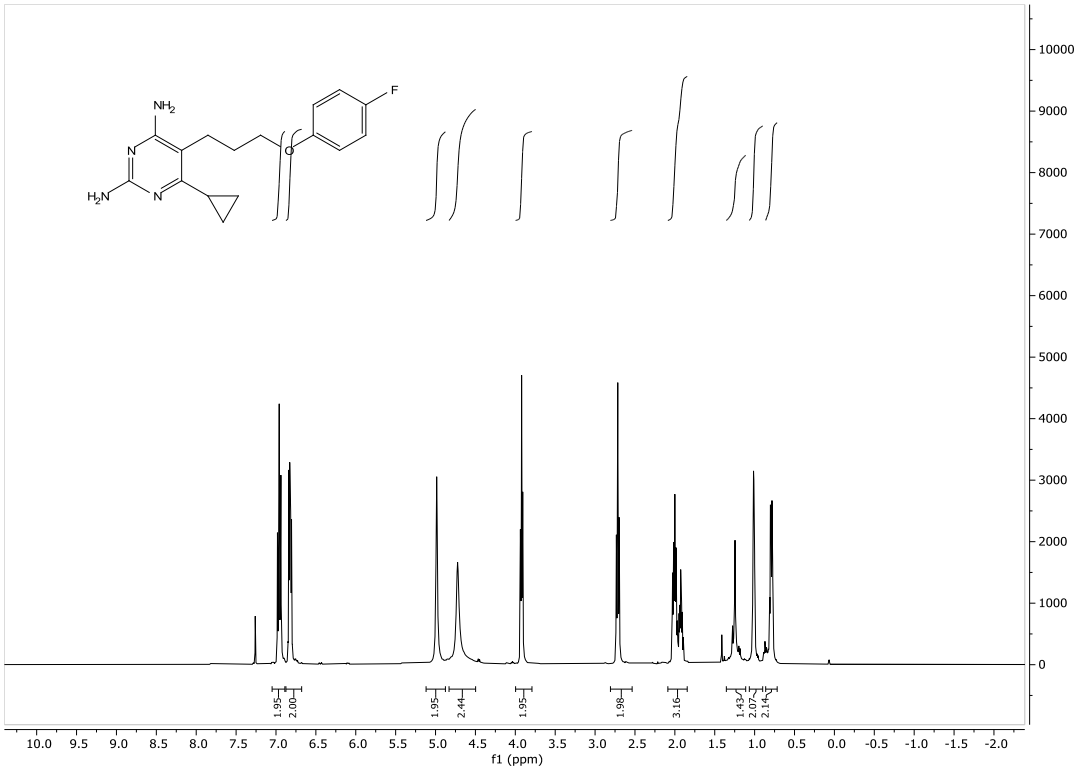

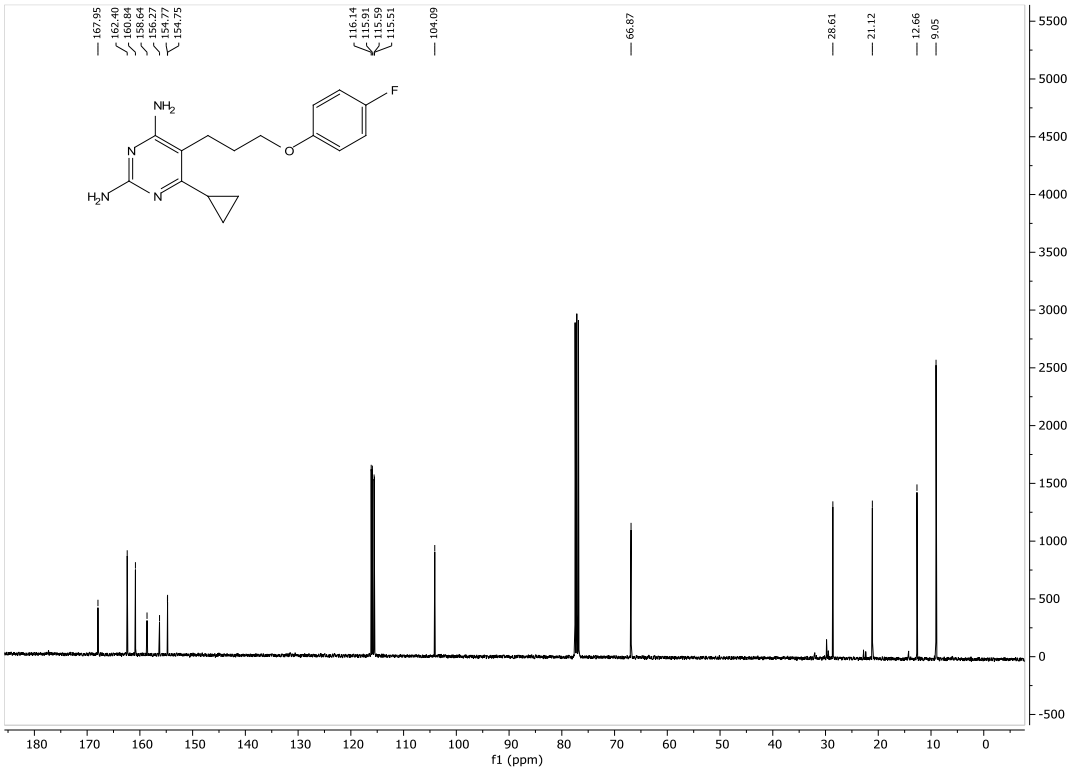

^{1}H and ^{13}C NMR spectra for compound **60b** in $CDCl_3$

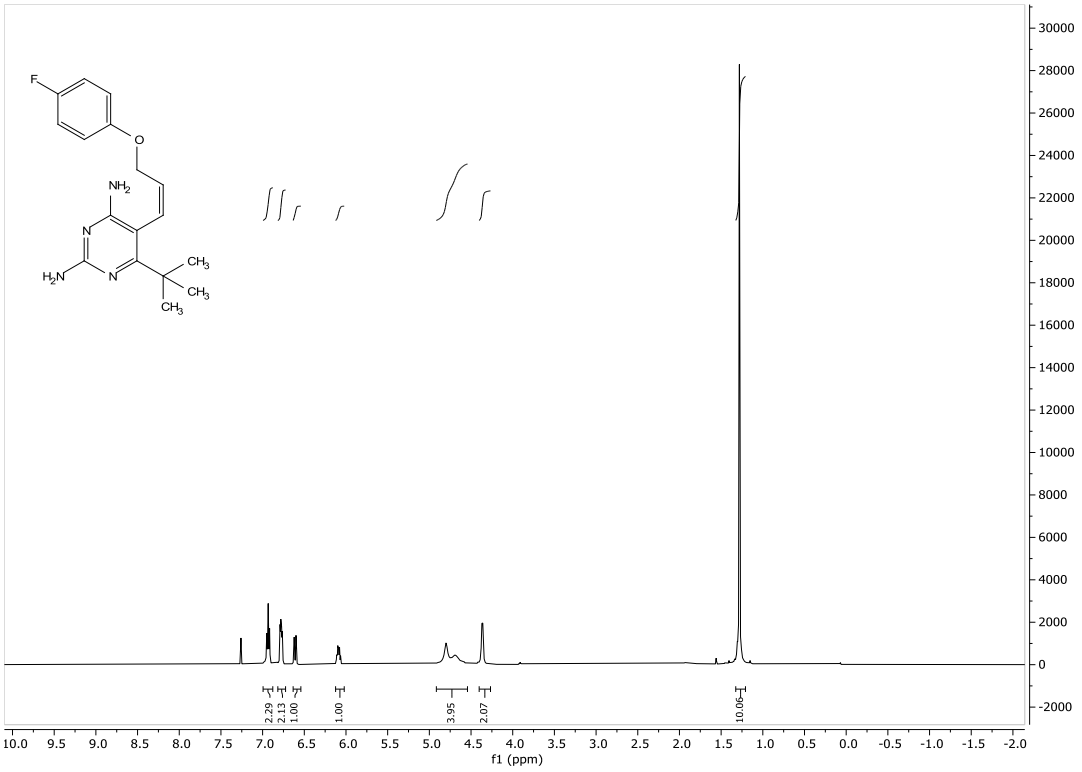

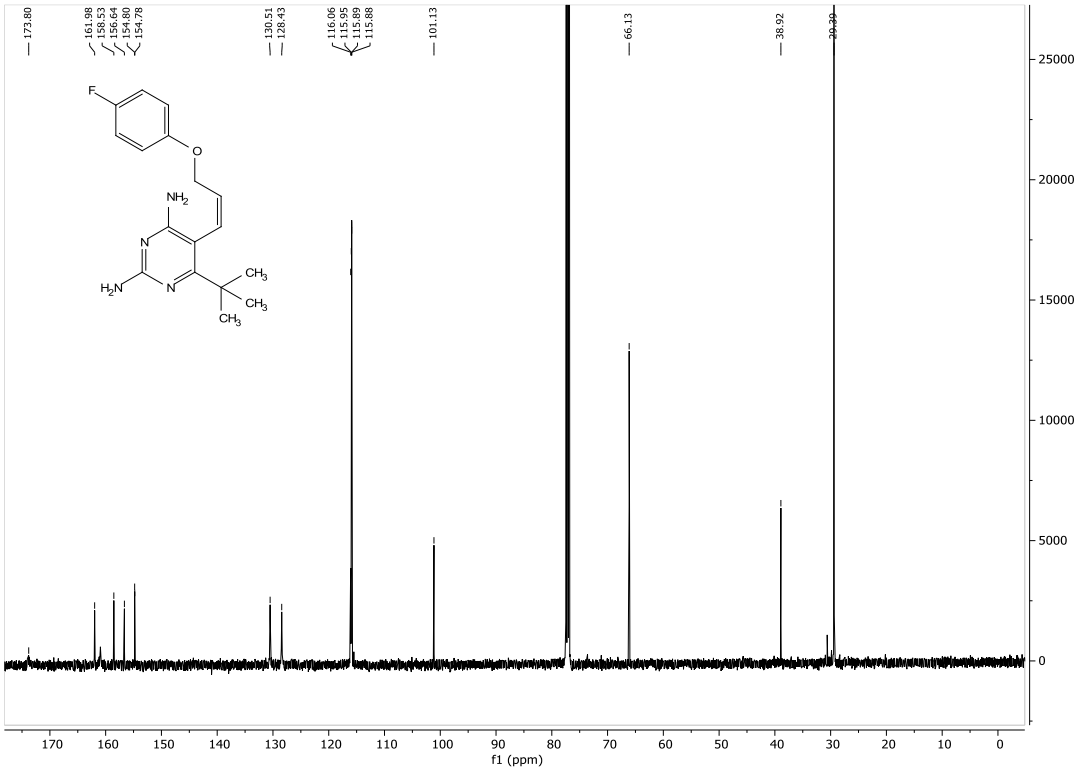

^{1}H and ^{13}C NMR spectra for compound **61b** in $CDCl_3$